INFORMATION TO USERS

This manuscript has been reproduced from the microfilm master. UMI films the text directly from the original or copy submitted. Thus, some thesis and dissertation copies are in typewriter face, while others may be from any type of computer printer.

The quality of this reproduction is dependent upon the quality of the copy submitted. Broken or indistinct print, colored or poor quality illustrations and photographs, print bleedthrough, substandard margins, and improper alignment can adversely affect reproduction.

In the unlikely event that the author did not send UMI a complete manuscript and there are missing pages, these will be noted. Also, if unauthorized copyright material had to be removed, a note will indicate the deletion.

Oversize materials (e.g., maps, drawings, charts) are reproduced by sectioning the original, beginning at the upper left-hand corner and continuing from left to right in equal sections with small overlaps. Each original is also photographed in one exposure and is included in reduced form at the back of the book.

Photographs included in the original manuscript have been reproduced xerographically in this copy. Higher quality 6" x 9" black and white photographic prints are available for any photographs or illustrations appearing in this copy for an additional charge. Contact UMI directly to order.

UMI

A Bell & Howell Information Company
300 North Zeeb Road, Ann Arbor MI 48106-1346 USA
313/761-4700 800/521-0600

Université d'Ottawa · University of Ottawa

MICROTUBULE-ASSOCIATED PROTEIN 1a: ANALYSIS OF ITS MICROTUBULE BINDING DOMAIN AND ITS FUNCTION IN DIFFERENTIATING P19 NEURONS

By

Andrew R. Vaillant

A thesis submitted to the School of Graduate Studies and Research, University of Ottawa, in partial fulfillment of the requirements for the degree of Doctor of Philosophy, Ottawa-Carleton Institute of Biology

For Cyrla and mom

ACKNOWLEDGMENTS

I would like to thank my thesis supervisor, Dr. David L. Brown, for his mentorship throughout my thesis research. I am grateful for the many instances when he has provided useful insight and helpful suggestions. I also appreciate his providing me with many opportunities to present my research at several scientific meetings and, last but not least, for introducing me to calamari!

I thank the members of my advisory committee for their input into this thesis research and to the many members of the Department of Biology at the University of Ottawa (especially Dr. Doug Johnson) for their invaluable expertise and advice.

My thanks to Dr. Martin Tenniswood at the W. Alton Jones Cell Science Center, Lake Placid, NY and all the members of his lab for their support.

No thesis work is really accomplished alone and I would like to acknowledge the members of Dr. Brown's lab, past and present, for their contributions and friendship:

Beatrice Valentine, for her patience and good humour.
Nicole Laferrière, for the many discussions, support and inspiration she provided.
Judy Little for teaching me to be neat(er).
Srabani Banarjee for her friendship and advice.
Josée Dufresne, Allison Hunter and Mikolaj Ostroski for making lab work more bearable.

Finally, I would like to thank my mother, who helped me get through the difficult stages of this degree and Cyrla, for her concern, patience and support at all times.

TABLE OF CONTENTS

ABBREVIATIONS

aa	amino acid
BES	N,N´-bis;(2-hydroxyethyl)-2-aminoethanesulfonic acid
BSA	bovine serum albumin
CaMK	Ca^{2+} -calmodulin dependent protein kinase
CCD	charge-cooled device
CNS	central nervous system
cs	coverslip
CY2	carboxymethylindocarbocyanine
CY3	indocarbocyanine
ddH_2O	double distilled, deionized water
dpi	dots per inch
EC	embryonal carcinoma
ECL	enhanced chemiluminescence
HMW	high molecular weight
IR	immunoreactivity
LB-broth	Luria Bertani broth
LC	light chain
LMW	low molecular weight
MAB	microtubule assembly buffer
mAb	monoclonal antibody
MAP	microtubule-associated protein
MAPK	mitogen activated protein kinase
MDB	microtubule depolymerizing buffer
mRNA	messenger ribonucleic acid
MSB	microtubule stabilizing buffer
MT	microtubule
MTOC	microtubule organizing center
MW	molecular weight
NC	nitrocellulose
NMDA	N-methyl-D-aspartate

NTT	non-tyrosinatable tubulin
ON	overnight
pAb	polyclonal antibody
PEFA	p-aminoethylbenzenesulfonyl fluoride
PEM	PIPES / EGTA / $MgCl_2$ buffer
PGK	phosphoglycerate kinase
PHF	paired helical filament
PKA	cAMP dependent protein kinase
PNS	peripheral nervous system
RA	retinoic acid
RT	room temperature
STOP	stable tubule only protein
T-broth	terrific broth
TIFF	tagged image file format
α-mem	α-modified Eagle's minimal essential media

N.B.: Standard abbreviations as defined in The Journal of Cell Biology are not included.

LIST OF FIGURES

ABSTRACT

The expression of several microtubule-associated proteins (MAPs), including MAP1a, was examined in RA-induced P19 embryonal carcinoma (EC) neurons. Immunofluorescence microscopy revealed that MAP1a and MAP1b were detected associated with microtubules (MTs) in undifferentiated cells while MAP2 was absent. At day 2, cells spontaneously formed aggregates and in these aggregates, MAP2 and increased amounts of MAP1b were detected in some cells. By day 4 of differentiation, neurite outgrowth was observed from these aggregates and MAP1a, MAP1b and MAP2 were colocalized with MTs in all neurites, including growth cones. HMW-MAP2 was restricted to the proximal regions of neurites and cell bodies. By day 8, substantial neurite outgrowth had occurred and MAP1a, MAP1b and MAP2 were seen in all processes. HMW-MAP2 was restricted to cell aggregates and largely absent from processes. At day 12, no further neurite outgrowth was evident and existing neurites were organized into fascicles, which were MAP1a, 1b and MAP2 positive but weaker than at day 4. Also, the restriction of HMW-MAP2 to aggregates was even more marked. Western blotting and ELISA showed that MAP1a, 1b and LMW-MAP2 protein levels increased during differentiation. Peak accumulation occurred no later than day 8, coinciding with the period of neurite outgrowth, and then decreased after day 8. HMW-MAP2 was absent in undifferentiated cells and increased steadily as development progressed. Juvenile tau appeared at day 4, and adult tau appeared at day 6. Both tau forms increased during development. These results show that MAP expression in serum-free differentiating P19 EC cells is similar to that seen in brain development, with the exception of MAP1a, which mirrors expression patterns seen only in axons. These observations suggest that MAP1a may modulate microtubule dynamics during neurite outgrowth.

To determine how MAP1a interacts with MTs, several myc-tagged MAP1a fragments were expressed in P19 EC and HeLa cells. Confocal immunofluorescence microscopy showed that the fragment consisting of amino acids (aa) 1-281 of MAP1a did not bind while the fragment consisting of aa 1-630 could bind, indicating that the region of MAP1a between aa 281-630 contains the MT binding domain. This region of MAP1a contains a series of basic repeats thought to be the MT binding domain. However, deletion of the basic repeats from

aa 336-540 did not prevent MT binding, suggesting that the regions flanking the basic repeats also bind MAP1a to MTs. In P19 EC cells expressing 6myc1A, process outgrowth was observed. Compared to MAP2c, MAP1a was less effective in making MTs resistant to colchicine-induced depolymerization. MAP1a increased the levels of acetylation and detyrosination of tubulin, but its effect was weaker than MAP2c and was only observed with the full-length MAP1a cDNA expression construct. The amount of MT-bound 6mycN1a-2ΔBR per unit microtubule length was greater than for any other fragment, suggesting it may have a greater affinity for MTs. These data show that aa 281-336 and / or 540-630 of MAP1a are involved in MT binding and may represent high affinity MT-binding regions. Additionally, MAP1a stabilized MTs, but to a lesser extent than MAP2c, supporting the hypothesis that MAP1a functions in the growth and / or plasticity of neurons.

To investigate the role of LCs in MAP1a function during development, the expression of LC3 during the differentiation of P19 EC cells was characterized. Western blotting and quantitative dot blotting showed that while the heavy chains for LC3 (i.e. MAP1a and 1b) peaked during the growth phase of development and then fell, the levels of LC3 steadily increased during development. The density of MAP1a bound to MTs was highest in undifferentiated cells and gradually decreased during differentiation, reaching a plateau at day 6. The decrease in MAP1b was more rapid, and it was not detected bound to MTs after day 6. The density of MT-bound LC3 exhibited a biphasic increase with a small peak at day 4 and a much larger peak at day 12, when MAP1a levels were the lowest. These observations suggest that MAP1a contains increasingly higher amounts of LC3 as differentiation progresses. This increase in LC3 association may serve to confer properties on MAP1a required for it to function properly in the adult. Myc-tagged LCs expressed in P19 EC and HeLa cells displayed a diffuse cytoplasmic distribution and never colocalized with MTs. These observations suggest that LC1 and LC2 association may be dependent on the processing event that forms these LCs and that factors present only during differentiation are required for LC3 binding.

The results of this study suggest a potential role for MAP1a during neuronal differentiation. The pattern of expression and effects on MT stability compared with MAP2 suggest that MAP1a is a weak stabilizer that functions in the growth of neurites

and in the adult may function to mediate MT stabilization by other adult MAPs. LC3 may also play a role in the regulation of MAP1a function during neuronal differentiation.

FOREWARD

A typical eukaryotic cell contains a network of polymerized protein filaments consisting of microfilaments, intermediate filaments and microtubules. This network of filaments is generally referred to as the cytoskeleton. The interaction of these cytoskeletal elements is responsible for several cellular functions including the regulation of cell shape. One of the hallmarks of neuronal development is a change in cellular morphology. Developing neurons form processes (neurites) which become specialized into axons and dendrites. The interaction of the various cytoskeletal elements is known to be an important factor in the changes in shape seen during neuronal differentiation (for review see Heidemann, 1996). This study is focused on one of these cytoskeletal elements, microtubules (MTs).

In undifferentiated cells, MTs form a radial array extending from an organizing center (MTOC). The change in neuronal shape is accompanied by changes in MT organization. In axons and dendrites, MTs are found in non-MTOC associated bundles that are present in all processes. MTs are dynamic structures growing and shrinking from the MTOC in undifferentiated cells. The MT bundles found in neurons are much less dynamic and are thought be the primary structural element in growing neurites (for review see Kirschner and Mitchison, 1988). The dynamics of MTs are regulated by many factors including tubulin isotype sorting, posttranslational modifications of tubulin, and the association of microtubule-associated proteins (MAPs) with MTs.

The research conducted in this study focuses on MAP1a, however there are many other MAPs which are present in developing neurons. The function of one particular MAP cannot be considered in isolation as the overall regulation of MT dynamics results from the interaction of many MAPs (Matus, 1994) and also from the isotype composition and posttranslational modifications of MTs.

The introduction that follows provides some basic information on tubulin isotype sorting, posttranslational modifications of tubulin, and the role that they play in MT dynamics in differentiating neurons. Because of many similarities and differences that exist between MAPs regarding their effect on MT dynamics, MT binding, and developmental expression in neurons, a comprehensive literature

review is provided for not only MAP1a, but also for the other neuronal MAPs: MAP1b, MAP2, MAP3, MAP4, tau and STOP.

INTRODUCTION

MT ORGANIZATION AND DYNAMICS

The cytoskeleton of eukaryotic cells consists of an internal, fibrous network composed of microfilaments, intermediate filaments and microtubules (MTs). MTs are polymers assembled from obligate heterodimers of α- and β-tubulin. These two 55 kDa subunits assemble into 110 kDa dimers that interact in a head to tail fashion to form protofilaments. Thirteen of these protofilaments assemble laterally to form a tube 24 nm in diameter (Fig. 1A). In undifferentiated cells, MTs are arranged in a radial array that has its origin in a MTOC located near the nucleus (Fig. 1B).

MTs are dynamic polymers that undergo cycles of assembly and disassembly. The addition and removal of dimers occurs preferentially at the plus end of MTs while the minus end is less dynamic and is associated with the MTOC (Fig. 1C). The current model for MT dynamics was proposed by Mitchison and Kirschner (1984). Each tubulin subunit can bind one molecule of GTP; however, only GTP bound to the β-tubulin subunit is hydrolyzed to GDP (Burns and Farrell, 1996). GTP hydrolysis leads to a conformational change in the β-tubulin subunit (Vale *et al.*, 1994), promoting the dissociation of the dimer from the MT. If GTP-bound tubulin is continuously added to the growing end of a MT, assembly continues, but if there is no GTP-dimer addition, the bound GTP will be hydrolyzed, destabilizing the MT lattice. This destabilization results in the depolymerization of the MT (Fig. 2A). Thus, the assembly of MTs is dependent on both the amounts of GTP and free tubulin present in the cytoplasm. The dynamic properties of MTs are essential for many cellular processes including cell division, organelle movement, maintenance of cell shape, cell motility and morphogenesis of differentiated cells (for review see Kirschner and Mitchison, 1986; Kreis, 1990; Ingber, 1993; Joshi and Baas, 1993)

THE ROLE OF MTS IN NEURONAL MORPHOGENESIS

A striking example of morphogenesis is seen in the formation of axons and dendrites during neuronal differentiation (see Fig. 2B). As neurons differentiate, the normal radial interphase array of MTs present in the cytoplasm is joined by non-MTOC associated bundles of MTs that run along the lengths of the axons and dendrites. The polarity of MTs in dendrites is mixed, while in axons MTs are all arranged with their +

Figure 1

Schematic showing: A) organization of tubulin dimers in MTs, B) organization of MTs within a typical eukaryotic cell and C) polarity of MTs with respect to the MTOC.

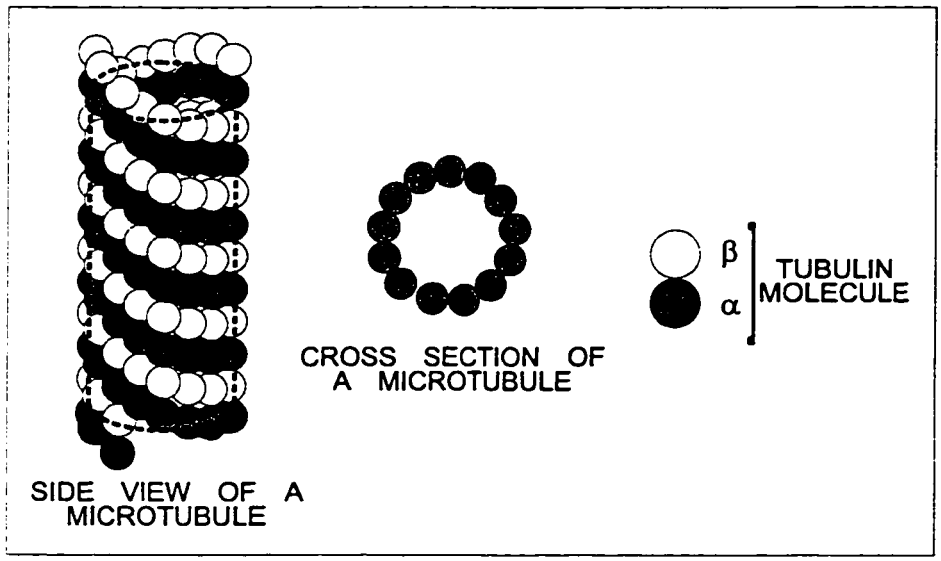
A
SIDE VIEW OF A MICROTUBULE
CROSS SECTION OF A MICROTUBULE
β
α
TUBULIN MOLECULE

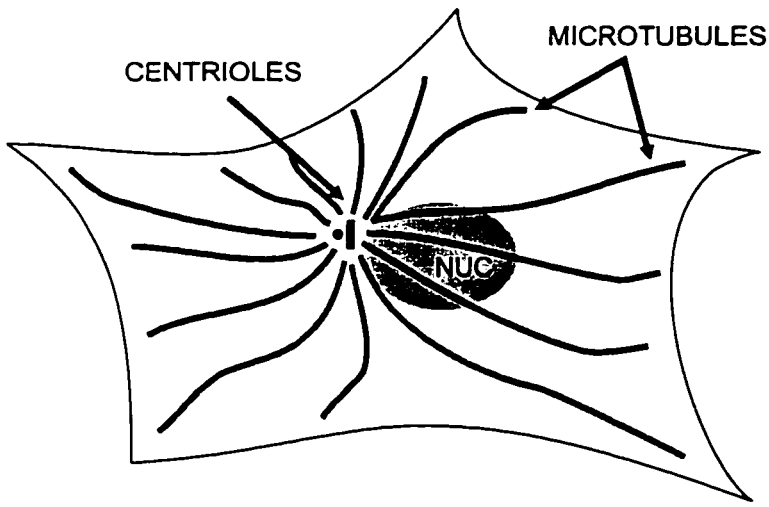
B
CENTRIOLES
MICROTUBULES
NUC

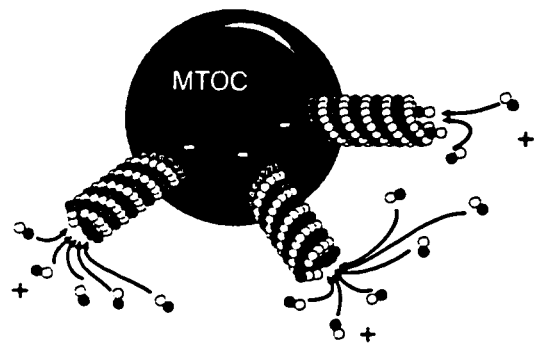
C
MTOC
-
-
-
+
+
+

Figure 2

A) A model for the regulation of MT dynamics by GTP hydrolysis (from Kirschner and Mitchison, 1986). B) Illustration of the changes in MT organization observed following neuronal differentiation.

A

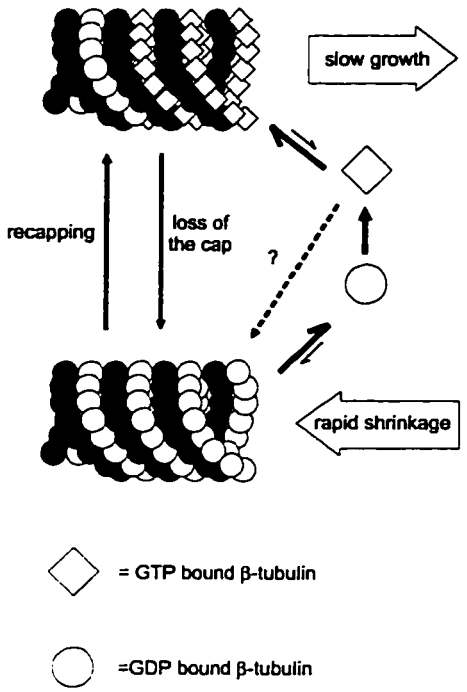
slow growth
recapping
loss of
the cap
?
rapid shrinkage
= GTP bound β-tubulin
=GDP bound β-tubulin

B

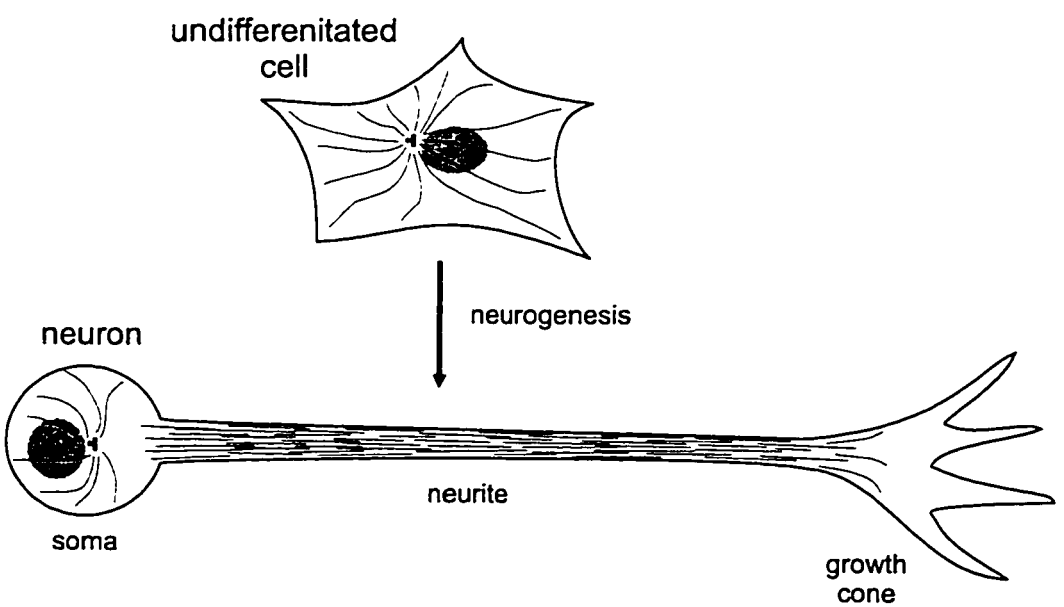
undifferenitated
cell
neurogenesis
neuron
neurite
soma
growth
cone

ends distal to the cell body (Heidemann *et al.*, 1981; Baas *et al.*, 1988). In neurons, MTs function in many processes including formation of axons and dendrites, vesicle transport, synaptic plasticity and long term potentiation involving learning and memory (for review see Mitchison and Kirschner, 1988; Falconer *et al.*, 1994 and Heidemann, 1996). The change in MT organization seen in differentiating neurons is accompanied by a change in MT dynamics. While MTs in undifferentiated cells have a half-life of approximately 5 min (Schulze and Kirschner, 1986), MTs in neurons have a half-life of approximately 2.2 h (Li and Black, 1996). During the differentiation of neurons, MTs become increasingly resistant to MT depolymerizing drugs (Black and Greene, 1982; Laferrière and Brown, 1996) and less dynamic (Lim *et al.*, 1989). This increasing stability of MTs is believed to be necessary for neuronal morphogenesis. Mechanisms thought to contribute to the increased stability of MTs include tubulin isotype sorting, post-translational modifications of tubulin, and the attachment of microtubule-associated proteins (MAPs).

TUBULIN ISOTYPE SORTING

In mouse, α- and β-tubulins are encoded by a multigene family which results in the expression of many different isotypes of tubulin (Villasante *et al.*, 1986; Lopata and Cleveland, 1987). These isotypes are distinguished by their heterogeneity in the last 15 aa of the tubulin peptide (Sullivan and Cleveland; 1986, Villasante *et al.*, 1986). An additional tubulin isotype, γ-tubulin, is found in the MTOC and functions in the nucleation of MTs (Oakley, 1994; Moritz *et al.*, 1995). The α- and β-tubulin isotypes display different levels of expression in different tissues (for review see Laferrière *et al.*, 1997). Given that MTs are assembled from the available pool of α- and β-tubulin isotypes (Raff, 1994), different isotype expression patterns in different tissues results in MTs with differing tubulin isotype compositions. The varying isotype composition of MTs may confer tissue-specific properties on them (Laferrière *et al.*, 1997). In brain, αI, αII and βII are the major isotypes expressed (Frankfurter *et al.*, 1986; Villasante *et al.*, 1986; Miller *et al.*, 1987). βIII tubulin is a neuron-specific, but lower abundance isotype in brain (Frankfurter *et al.*, 1986; Banerjee *et al.*, 1988). Panda *et al.* (1994) have shown that MTs assembled from purified dimers containing only the βIII isotype are more dynamic than MTs assembled from all brain isotypes or MTs assembled from αβII

or αβIV. However, MTs assembled from 20% αβIII and 80% αβII are less dynamic than MTs assembled from αβII alone, suggesting that isotype composition of MTs and co-operative interactions between isotypes may influence MT dynamics. In differentiating neurons, the amounts of βIII-tubulin and its incorporation into MT polymer increase concomitantly with an increase in MT stability, suggesting a role for the βIII isotype in stabilizing neuronal MTs (Laferrière and Brown, 1996).

POSTTRANSLATIONAL MODIFICATIONS OF TUBULIN

Several posttranslational modifications occur on tubulin and all except for one occur within the 15 aa isotype-defining region (Fig. 3). This region is known to be a site for interactions with MAPs (see Fig. 5) and with the exchangeable GTP site in β-tubulin (Padilla *et al.*, 1993). Since most of the modifications increase the negative charge of the already acidic c-terminus, these modifications may regulate ionic MAP-MT interaction or GTP interaction with β-tubulin, thus influencing MT dynamics. Posttranslational modifications of tubulin include detyrosination, acetylation, glycylation, glutamylation and phosphorylation.

Detyrosination of α-tubulin is a reversible modification that involves the removal of the c-terminal tyrosine residue by a tubulin carboxy-peptidase, exposing the penultimate glutamate residue. A tubulin-tyrosine ligase adds the tyrosine back on to the c-terminus (MacRae, 1997). Detyrosination preferentially occurs on polymerized tubulin whereas tyrosination occurs preferentially on depolymerized tubulin. Within neurons, MTs which turn over the slowest and display the greatest stability are found in the proximal regions of neurites. MTs in this region are most heavily detyrosinated while tyrosinated tubulin is most abundant in MTs in the proximal neurite and growth cone, which are the most dynamic and least stable (Lim *et al.*, 1989). While there is a correlation between the presence of detyrosinated tubulin and MTs with a low rate of turnover (Li and Black, 1996), there is evidence suggesting that detyrosination does not influence stability directly (Webster *et al.*, 1990; Robinson and Vandré, 1995).

An additional detyrosinated form of tubulin, called Δ2-tubulin is formed by the irreversible removal of the 2 c-terminal aa of α-tubulin (Paturle-Lafanechère *et al.*, 1991). This non-tyrosinatable form of tubulin (NTT) is neuron-specific, comprises 35–50% of brain tubulin, and is developmentally regulated. NTT is expressed early in

differentiation and is found in developing growth cones and dendrites, regions where detyrosinated tubulin is absent (Paturle-Lafanechère *et al.*, 1994). This modification may represent the final maturation of α-tubulin in MTs.

Acetylation involves the addition of an acetyl group to lysine 40 of α-tubulin by an acetyltransferase (Piperno and Fuller, 1985; Lloyd *et al.*, 1994). Acetylation occurs preferentially on assembled MTs, but also occurs on soluble tubulin (Maruta *et al.*, 1986; MacRae and Langdon, 1989). The acetyl group can be removed by a tubulin deacetylase. Acetylated tubulin shows the same distribution among MTs in neurons as detyrosinated tubulin (Li and Black, 1996). Any direct effect acetylation has on MT dynamics has yet to be determined. It has been suggested that acetylated tubulin may act as a localized MTOC in axons (Baas and Ahmad, 1992).

Glycylation involves the addition of 1-34 glycyl residues to glutamate residues within the 15 aa isotype defining region of both α- and β-tubulin (Redeker *et al.*, 1994; Mary *et al.*, 1996). Glycylation decreases the acidity of the c-terminus of tubulin and may serve to modify MAP binding and MT dynamics and perhaps anchor MTs to the cytoplasmic membrane (Laferrière *et al.*, 1997). This modification has yet to be characterized in neurons.

Both α- and β-tubulin undergo the reversible addition of 1 – 6 glutamates to a glutamate residue in their c-terminus (Redeker *et al.*, 1991; Wolf *et al.*, 1994). Glutamylation is found on tubulin that is also detyrosinated, acetylated or phosphorylated (Laferrière *et al.*, 1997). Glutamylation of tubulin occurs preferentially on MTs while deglutamylation can occur on MTs or soluble tubulin dimers (Audebert *et al.*, 1993). During neuronal differentiation, the extent of α-tubulin glutamylation is constant at high levels while β-tubulin glutamylation steadily increases (Audebert *et al.*, 1994), concomitant with the increase in MT stability seen in neurons (Laferrière and Brown, 1996). There is some evidence that posttranslational modifications of tubulin can affect MAP binding. The affinity of tau for tubulin is greatest when there is an intermediate level of polyglutamylation (i.e., 3 glutamyl residues). This affinity drops when there are either more or less than 3 glutamyl residues present (Boucher *et al.*, 1994).

Although both α- and β-tubulin can be phosphorylated *in vitro* (Wandosell *et al.*, 1986), the functionally significant phosphorylation of tubulin is thought to occur in the

Figure 3

Location of posttranslational modifications of tubulin.

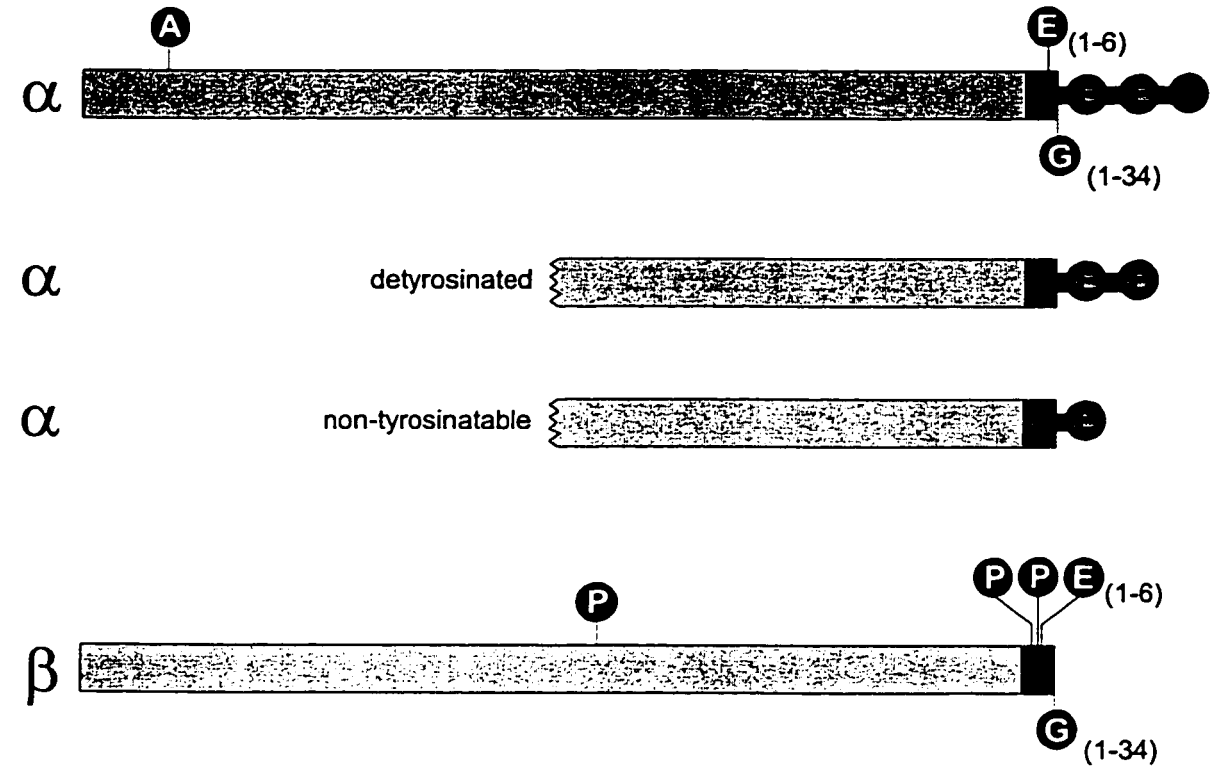

A = acetylation

E = glutamylation

G = glycylation

P = phosphorylation

■ = isotype defining region

isotype defining region of βIII-tubulin (Khan and Ludueña, 1996). The sites of phosphorylation affect the ability of the tubulin to assemble. Tubulin phosphorylated by Ca^{2+} / calmodulin kinases assembles inefficiently (Wandosell *et al.*, 1986) while tubulin modified by casein kinase II, the probable *in vivo* kinase for tubulin (Serrano *et al.*, 1987; Díaz-Nido *et al.*, 1990), is readily assembled (Serrano *et al.*, 1987). βIII-tubulin can be phosphorylated on ser239, ser444 and tyr437 (the latter two being in the isotype defining region) (Díaz-Nido *et al.*, 1990; Khan and Ludueña, 1996). Phosphorylated β-tubulin increases 4-fold during neuronal differentiation (Gard and Kirschner, 1985) and phosphorylated βIII-tubulin is always found in the assembled MT fraction (Denoulet *et al.*, 1989), suggesting that phosphorylation influences MT dynamics in neurons. It is thought that phosphorylation of βIII-tubulin increases the acidic charge of its c-terminal domain, increasing the strength of the partially ionic MT-MAP interaction (Laferrière *et al.*, 1997)

MICROTUBLE-ASSOCIATED PROTEINS

MAPs are proteins that associate with MTs. MAPs can be divided into two groups: motor MAPs which utilize nucleotide hydrolysis to move along MTs, and structural MAPs which can affect the assembly, stability, and organization of MTs. Motor MAPs include the dynein and kinesin families of proteins which interact with MTs to function in mitosis, organelle movement and flagellar-based motility (for review see Collins, 1994; Pereira and Goldstein, 1994; Scholey and Vale, 1994; Smith and Sale, 1994). The structural MAPs consist of groups of related proteins that include MAP1, MAP2, MAP3, MAP4, tau and STOP (stable tubule only protein).

THE MAP – MT INTERACTION

In all well characterized structural MAPs, there are two functional regions, a projection domain and a highly basic domain that binds MTs. Early studies demonstrated the periodic association of MAPs along MTs (Murphy and Borisy, 1975; Cleveland *et al.*, 1977; De Brabander *et al.*, 1981). More recent studies have shown that the association of MAPs along the MT results in projections extending from the microtubule wall (Fig. 4) (Murofushi *et al.*, 1986; Shiomura and Hirokawa, 1987; Hirokawa *et al.*, 1988; Sato-Yoshitake *et al.*, 1989). Several studies have shown that

Figure 4

A model of MAP association with MTs.

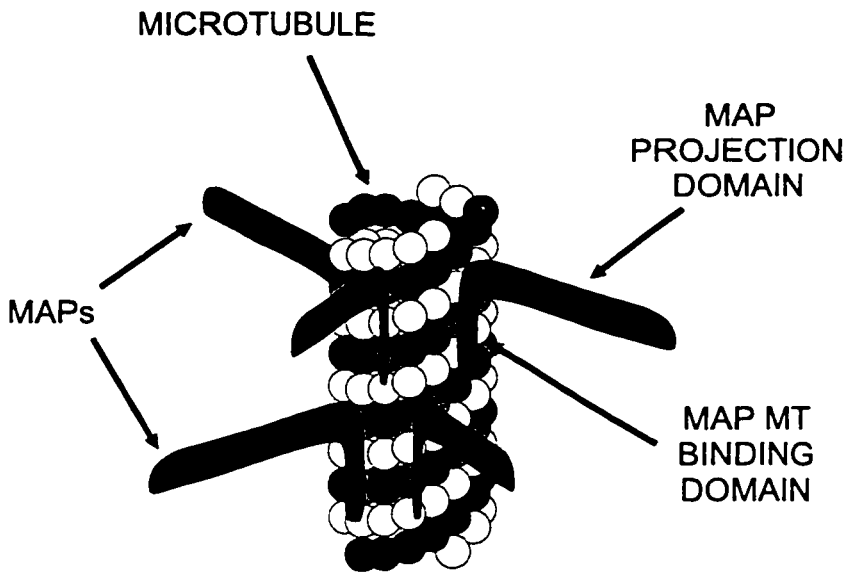
MICROTUBULE
MAP
PROJECTION
DOMAIN
MAPs
MAP MT
BINDING
DOMAIN

Figure 5

Location of MAP binding sites on tubulin.

TAU *

MAP1A *
MAP1B *
MAP2 *
MAP4 *
TAU *

■ = isotype defining region

MAP2, MAP4 and tau bind to the extreme c-terminal region of both tubulin subunits (Fig. 5.) (Serrano *et al.*, 1984; Aizawa *et al.*, 1987; Maccioni *et al.*, 1986, 1988). Tau also shows some affinity for the n-terminus of α-tubulin (Littauer *et al.*, 1986). MAP1a and MAP1b interact with the same region as MAP2 and tau on β-tubulin (Serrano *et al.*, 1985; Rivas *et al.*, 1988; Cross *et al.*, 1991). The region of tubulin binding to STOP has not been determined.

JUVENILE AND ADULT MAPS

Structural MAPs can be classified into two broad classes of MAPs based on the patterns of their expression during development. Juvenile MAPs are expressed at their highest levels during early development and then decrease or disappear in the adult (Fig. 6). These MAPs are considered to be involved in growth related functions during neuronal development. Adult MAPs are absent during early differentiation and found at their highest levels in the adult (Fig. 6). The increase in adult MAP expression is correlated with increased MT stability, suggesting that these MAPs are involved in the stabilization of MTs and in the transition of neurons from a growing state to their mature form (Matus, 1990a; 1990b).

STOP

STOP is a 952 aa polypeptide with a predicted molecular mass of 100.5 kD however, its apparent molecular mass as determined by SDS-PAGE is 145 kD. This aberrant migration is seen for all MAPs (see below). Several distinct regions exist on this protein (Fig. 7) (Bosc *et al.*, 1996). At the n-terminus there is a proline rich region containing two putative SH3 binding domains. In the middle of the protein, there is a region of 5 repeats of 46 aa which are highly homologous to each other. Within this repeated region are 4 P-loop motifs which can bind ATP. At the c-terminus, there is another region of 28 imperfect repeats of 11 aa. The functions of these domains are not yet understood, although both repeat domains bear similarity to functional domains in other MAPs (see below). Although the pattern of expression of this MAP has not been determined in detail, it is expressed in many tissues including brain (Pirollet *et al.*, 1988). STOP has been localized to MTs in neurons and the mitotic spindles of non-neuronal cells (Margolis and Job, 1994). STOP-bound MTS are resistant to cold

Figure 6

Expression patterns of MAPs in developing brain.

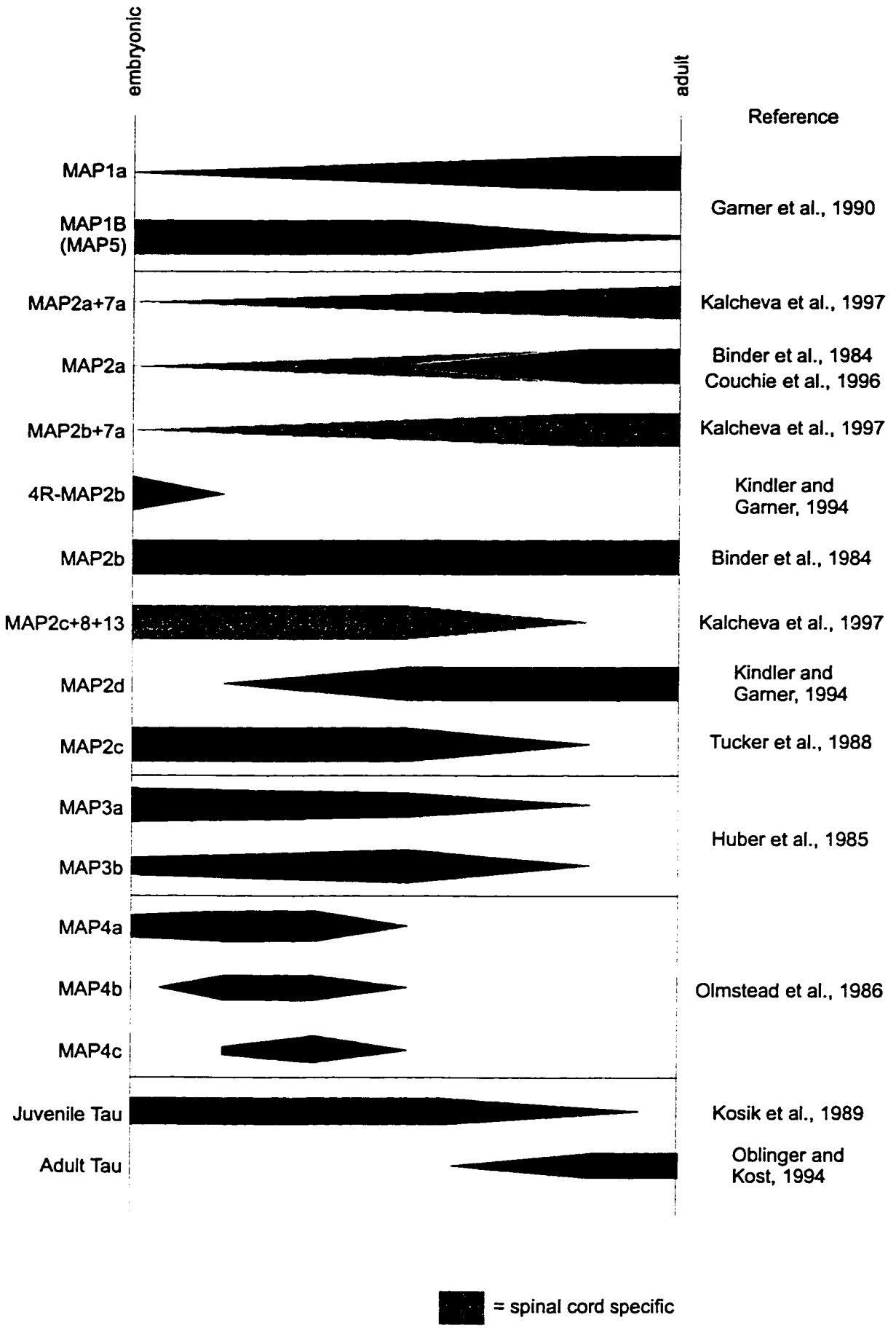
embryonic
adult
Reference
MAP1a
MAP1B (MAP5)
Garner et al., 1990
MAP2a+7a
Kalcheva et al., 1997
MAP2a
Binder et al., 1984
Couchie et al., 1996
MAP2b+7a
Kalcheva et al., 1997
4R-MAP2b
Kindler and Garner, 1994
MAP2b
Binder et al., 1984
MAP2c+8+13
Kalcheva et al., 1997
MAP2d
Kindler and Garner, 1994
MAP2c
Tucker et al., 1988
MAP3a
MAP3b
Huber et al., 1985
MAP4a
MAP4b
Olmstead et al., 1986
MAP4c
Juvenile Tau
Kosik et al., 1989
Adult Tau
Oblinger and Kost, 1994
= spinal cord specific

induced depolymerization, dilution and Ca^{2+} induced disassembly at room temperature (Margolis *et al.*, 1986a; Pirollet *et al.*, 1988; Margolis *et al.*, 1990). These properties are inhibited by Ca^{2+} -calmodulin, which binds directly to STOP (Pirollet *et al.*, 1988; 1992) and by arginylation at its n-terminus (Bongiovanni *et al.*, 1994). Although STOP is able to protect MTs against cold-induced depolymerization, it does not interfere with MT dynamics at room temperature (Margolis *et al.*, 1986b). STOP can move along MTs under normal physiological conditions, but when challenged by cold temperatures, it is immoblilized on the MT. This may explain the bifunctional nature of STOP (Pabion *et al.*, 1984; Margolis *et al.*, 1986b). This ability of STOP to move along MTs may also play a role in MT dynamics at the kinetochore during mitosis (Garel *et al.*, 1987).

MAP3

MAP3 is an approximately 180 kD protein that displays widespread expression in a variety of tissues (Huber and Matus, 1990). In brain, it is found in glia and axons where it colocalizes with MTs (Huber *et al.*, 1985). Two forms of MAP3 (MAP3a and 3b) slightly different in size exist in brain (Huber *et al.*, 1985). MAP3a is more prevalent in the late embryo and MAP3b is barely detectable. After birth, MAP3b increases until P10 when its levels are equal to MAP3a. MAP3a and 3b levels then drop dramatically and in the adult brain they are absent, except in Bergmann astroglia (Bernhardt *et al.*, 1985; Reiderer and Matus, 1985) and regions of the brain where neuronal growth still persists (Tucker *et al.*, 1988a). Although little is known about the function of this MAP, the expression of MAP3 during the neuronal differentiation of PC12 cells correlates with neurite outgrowth (Brugg and Matus, 1988). There is some evidence to suggest that MAP3 may be part of the MAP 4 family (Huber and Matus, 1990; Bulinski, 1994)

MAP4

MAP4 comprises MAPs previously identified as 190kD MAP, 210 kD MAP, HeLa MAP and 255kD MAP (Bulinski, 1994). MAP4 consists of several isoforms generated from a single gene by alternative splicing of the primary transcript (West *et al.*, 1991). MAP4 is found in many tissues and cell lines where it associates with interphase MTs and mitotic spindles (Bulinski and Borisy, 1980a; 1980b; De Brabander *et al.*, 1981; Olmsted *et al.*,

Figure 7

Schematic of microtubule-associated protein STOP. Numbers correspond to aa position.

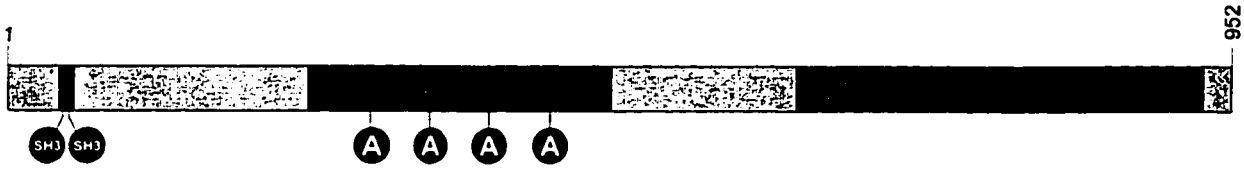

= repeated aa sequences

= proline rich

A = putative ATP binding site

SH3 = putative SH3 site

1986; Aizawa *et al.*, 1990; Chapin *et al.*, 1995). In brain, MAP4 distribution is limited to glial cells (Olmsted *et al.*, 1986). MAP4 consists of several domains (Fig. 8). There is a region of 17 acidic repeats of 14 aa in the n-terminus of the protein which is thought to form a flexible, rod-like structure (West *et al.*, 1991). In the c- terminus, there are 3-5 basic repeats of 18 aa (although repeat 2 appears degenerate)(Chapin *et al.*, 1995). These repeats are flanked on the n-terminal side by two domains, a proline rich domain and a serine / proline rich domain (West *et al.*, 1991).

During neuronal differentiation, MAP4 is expressed mainly in the late embryonic or early post-natal stages. Three forms, MAP4a, 4b and 4c (240-220 kD) have been identified in neurons. MAP4a and 4b are both present in the early embryo, with 4b appearing 4 days later in development. 4c is only detectable after birth and all MAP4 isoforms disappear as development progresses. (Olmsted *et al.*, 1986). A muscle-specific MAP4 has also been characterized which contains a large insertion in its projection domain (Fig. 8) (Mangan and Olmsted, 1996). Four splice variants of MAP4 have been cloned that differ by the presence of 3, 4 or 5 basic repeats in their c-terminus (Fig. 8) (Chapin *et al.*, 1995). The 5 repeat version is most abundant in lung, liver, kidney, spleen and testis and is the only form detectable in cell lines while the 3 repeat version is found only in heart, brain, skeletal muscle and lung. The 4 repeat MAP4 isoform appears to be brain specific. The relationship of these isoforms to MAP4 isoforms expressed during brain development is unknown at this time.

The MT binding region of MAP4 consists of the basic repeat domains and the serine / proline-rich domain flanking the repeats on the n-terminal side. The binding of MAP4 is markedly reduced in the absence of the serine / proline-rich domain and the successive deletion of the repeats also results in a successive decrease in MT binding. (Aizawa *et al.*, 1991; Chapin and Bulinksi, 1991; Olson *et al.*, 1995). Additionally, removal of the acidic c-terminus weakens the binding of MAP4 to MTs (Olson *et al.*, 1995). The serine / proline rich region and the basic repeats together increase the rate of MT assembly and stabilize MTs to drug-induced depolymerization. However, in the absence of the repeats, there is no stabilization and the MTs formed have an abnormal morphology (Aizawa *et al.*, 1991, Olson *et al.*, 1995). Although the projection region of MAP4 (from the n-terminus to the proline rich domain) does not directly bind to MTs (Aizawa *et al.*, 1991), it does exert some influence on MT binding (Olson *et al.*, 1995).

Figure 8

Schematic of MAP4 isoforms. Numbers represent aa position.

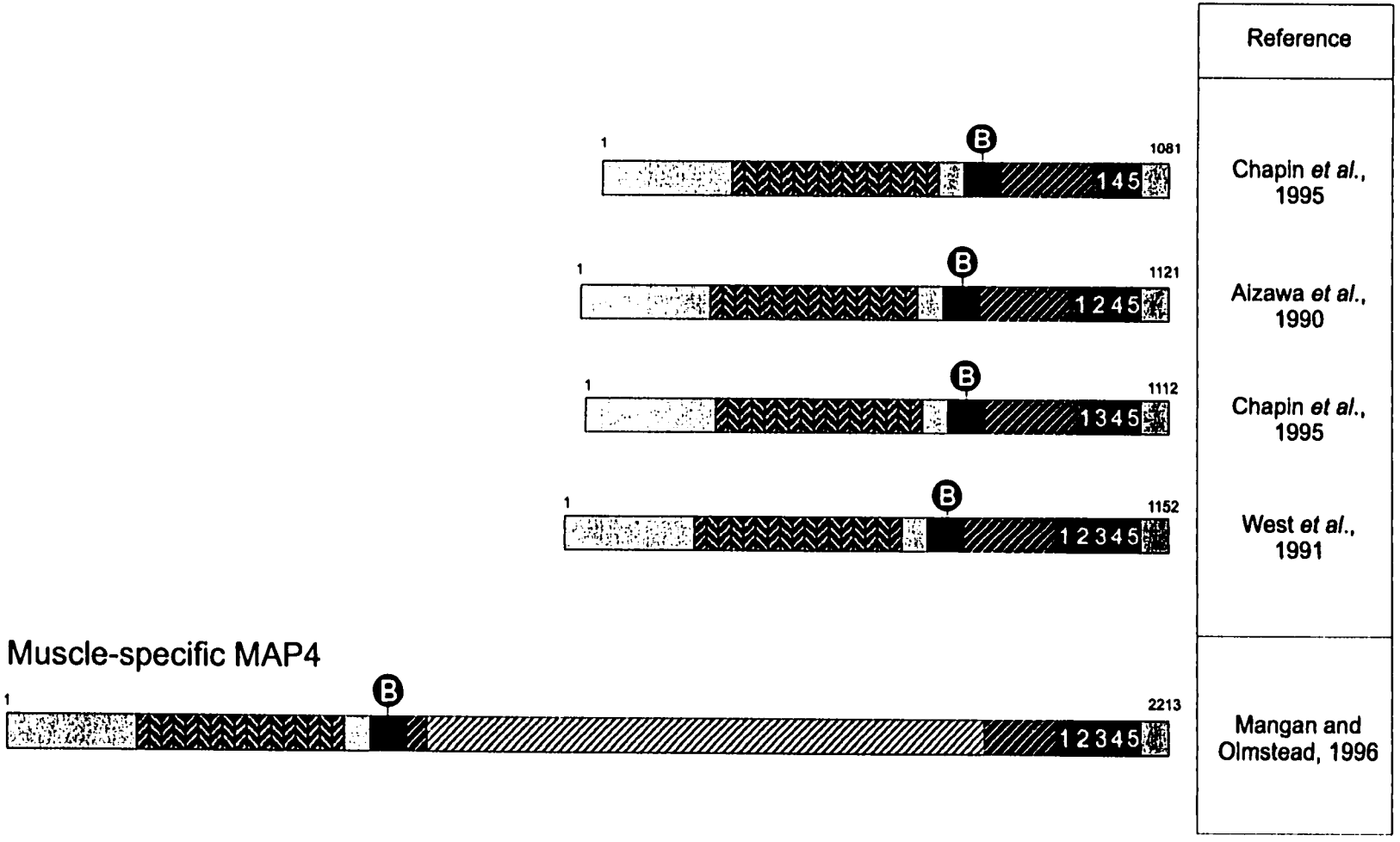
Reference
1
1081
B
1 4 5
Chapin et al., 1995
1
1121
B
1 2 4 5
Aizawa et al., 1990
1
1112
B
1 3 4 5
Chapin et al., 1995
1
1152
B
1 2 3 4 5
West et al., 1991
Muscle-specific MAP4
1
2213
B
1 2 3 4 5
Mangan and Olmstead, 1996
B = cyclin B binding domain
= basic repeat
= acidic repeat
= serine / proline rich domain
= proline rich domain
= projection domain insertion

The binding of MAP4 to MTs is also inhibited by $p110^{mark}$ phosphorylation (Illenberger *et al.*, 1996).

Although Olson *et al.* (1995) have shown that GFP-MAP4 can stabilize MTs to drug-induced depolymerization, stable transfection of MAP4 into CHO cells causes no detectable change in MT organization or dynamics (Barlow *et al.*, 1994). Antibody inhibition of MAP4-MT interactions has no detectable effect on MTs during either interphase or mitosis (Wang *et al.*, 1996), suggesting MAP4's functions are redundant. Inhibition of muscle-specific MAP4 expression during muscle development has a disruptive effect on muscle differentiation. Normal myotube fusion does not occur and myoblasts contain abnormal myofibrils. Also, the MTs in these cells are disorganized (Mangan and Olmsted, 1996). MAP4 interacts with cyclin B at its proline rich domain. Although $p34^{cdc2}$ / cyclin B phosphorylation of MAP4 has no effect on MT organization or dynamics, this interaction suggests a possible mechanism for targeting $p34^{cdc2}$ kinase to MTs during the cell cycle (Ookata *et al.*, 1995).

TAU

Tau isoforms are also generated by alternative splicing of the primary transcript from a single gene (Fig. 9) (Lee *et al.*, 1988). In general, tau is restricted to axons in brain (Tucker *et al.*, 1988; Dotti *et al.*, 1987; Viereck *et al.*, 1988). However, it can be detected in dendrites in some instances (Dotti *et al.*, 1987; Papasozomenos and Binder, 1987). The axonal localization is thought to result from a localization of tau mRNA to the proximal axon and a selective stabilization of tau due to its binding to MTs only in axons (Litman *et al.*, 1993; Kanai and Hirokawa, 1995; Hirokawa *et al.*, 1996).

All tau isoforms share similar domain structures (Fig. 9), with 3 – 4 imperfect basic repeats of 18 aa near their c-terminus, flanked by a fifth but degenerate repeat on the c-terminal side, and a proline rich domain on the n-terminal side. Some isoforms also contain insertions in their n-terminal projection domain (Fig. 9) (Geodert and Jakes, 1990; Geodert *et al.*, 1992). These isoforms can be classified into two groups: juvenile and adult isoforms. Juvenile tau is comprised of the three repeat (3R) isoforms. These are found at their highest levels in the early embryo and rapidly decline as maturation progresses (Kosik *et al.*, 1989). However, juvenile isoforms are still expressed in the olfactory system, where neuronal growth persists in the adult (Veireck *et al.*, 1989). The

Figure 9

Schematic of tau isoforms. Numbers indicate aa position.

Juvenile tau

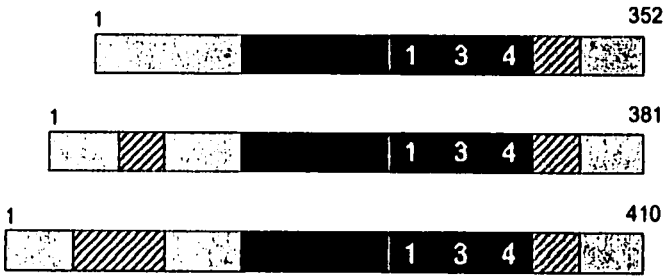

Adult tau

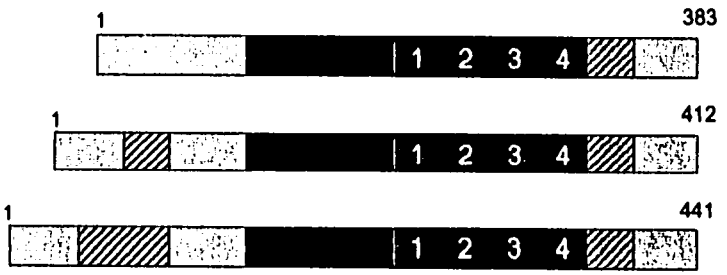

PNS-specific tau

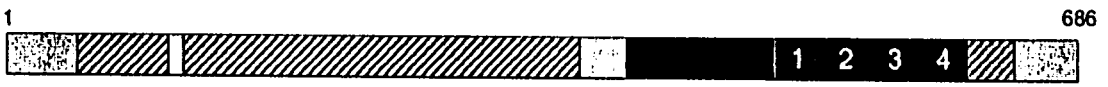

Predicted molecular weight	Observed molecular weight	Reference
36760	48000	Goedert and Jakes, 1990
39720	54000	
42603	62000	
40007	52000	Goedert and Jakes, 1990
42967	59000	
45850	67000	
71783	110000	Goedert *et al.*, 1992

= basic repeat

= degenerate repeat (c-terminal flanking region)

= proline rich domain (n-terminal flanking region)

= projection domain insertions

four repeat (4R) adult isoforms are only detectable post-natally at which point their levels continually increase throughout development (Bahr *et al.*,1994; Oblinger and Kost, 1994). The mRNA levels for adult and juvenile tau mirror the protein levels seen during development (Kosik *et al.*, 1989). In the central nervous system (CNS), juvenile and adult isoforms also display cell type-specific expression. 3R tau is detected in pyramidal and granule cells while 4R tau is found only in pyramidal cells (Goedert *et al.*, 1989b). A large 4R tau isoform, characterized by a large insertion in the projection domain (Fig. 9), is expressed only in the adult peripheral nervous system (PNS) (Georgieff *et al.*, 1991; Couchie *et al.*, 1992; Goedert *et al.*, 1992). The expression of this large tau isoform decreases during development (Oblinger *et al.*, 1991).

Tau has also been detected in the nucleus of HeLa, LA-N-5 and CHO cells where it colocalizes with the nucleolar organizing region (Lu and Wood, 1993; Greenwood and Johnson, 1995; Thurston *et al.*, 1996). Nuclear tau is encoded by a 2 kb transcript which is detectable in the frontal cortex of the brain (Andreadis *et al.*, 1996; Wang *et al.*, 1993). Microinjection of this tau form into CHO cells results in its transport into the nucleus (Lu and Wood, 1993). Thurston *et al.* (1996) have suggested that nuclear tau may function in ribosomal biogenesis and / or rRNA transcription.

The MT binding domain of tau consists of the basic repeats and flanking regions (Himmler *et al.*, 1989; Gustke *et al.*, 1994). The binding of tau to MTs is cooperative, with the affinity being much stronger in the presence of the flanking regions compared to the basic repeats alone (Kanai *et al.*,1992; Gustke *et al.*, 1994). The basic repeats have also been reported to serve as an actin-binding region *in vitro* (Correas *et al.*, 1990). The n-terminal projection domain is thought to act as a spacer between MTs (Chen *et al.*, 1992; Frappier *et al.*, 1994). The regulation of MT dynamics by tau is related to its MT binding domains. In the presence of both flanking domains and the basic repeats, there is a strong stabilization of MTs. Loss of any flanking region or repeat region leads to a reduction in stabilization (Leger *et al.*, 1994; Trinczek *et al.*, 1995). In the absence of the basic repeats, tau still binds MTs but its nucleating and stabilizing ability is lost (Gustke *et al.*, 1994; Trinczek *et al.*, 1995). The functions of these domains are also reflected in the differences between juvenile (3R) and adult (4R) tau. Adult tau is more efficient at binding and stabilizing MTs and forming processes in transfected cells than juvenile tau (Goedert and Jakes, 1990; Brandt and Lee, 1993;

Montejo de Garcini *et al.*, 1994). The increased affinity of 4R tau is due to strong specific electrostatic interactions between tubulin and the 14 aa inter-repeat region that accompanies the inserted repeat in adult tau (Goode and Feinstein,1994).

The function of tau has been heavily investigated. Severai studies have shown that expression of tau in non-neuronal cell lines causes MT bundling and stabilization (Drubin and Kirschner, 1986; Kanai *et al.*,1989; Takemura *et al.*,1992; Barlow et al,1994; Brandt and Lee, 1994) and formation of thin processes reminiscent of axons (Knops *et al.*, 1991; Lo *et al.*, 1993; Esmaeli-Azad *et al.*, 1994; Montejo de Garcini *et al.*, 1994). MT bundles formed *in vitro* exhibit a random polarity orientation suggesting that the uniform orientation of MTs in axons is generated by some other mechanism (Brandt and Lee, 1994).

Inhibition of tau expression in neurons, either by the introduction of tau antisense oligodeoxynucleotides or tau antibodies, resulted in the retraction of growing neurites or the inhibition of further neurite growth (Cáceres and Kosik, 1990; Cáceres *et al.*, 1992b; Shea and Beermann, 1994). Interestingly, the inhibition of tau expression after neurite specialization only affects axons, while dendrites continue to grow normally suggesting tau has a specific role in axonal specification (Cáceres *et al.*, 1992b). Tau is also upregulated after axonal injury, indicating a role for tau in regeneration (Yin *et al.*, 1995). Some of these functions may be partially redundant *in vivo* as transgenic tau knockout mice show normal neuronal development with only a limited reduction in MT stability seen in small-caliber axons (Harada *et al.*, 1994). Tau interactions may not be limited to MTs. In growing neurons, Black *et al.* (1996) have demonstrated an increasing gradient of tau concentration towards the growth cone that is weakly associated with MTs. Tau's presence in the growth cone may be due to an interaction with microfilaments (Di Tella *et al.*, 1994; Knowles *et al.*, 1994). Tau-actin interaction is inhibited by the binding of calmodulin (Lee and Wolff, 1984; Kotani *et al.*, 1985).

Tau has been implicated in pathologies seen in Alzheimer's and liver disease. In Alzheimer neurons, tau self assembles into paired helical filaments (PHFs) which are an integral part of the neurofibrillary tangles found in the soma of these cells (Goedert *et al.*, 1989a; for review see Mandelkow and Mandelkow, 1993; Goedert *et al.*, 1994). Tau has also been detected in Mallory bodies of livers from alcoholics, implying a role for tau in liver dysfunction (Kenner *et al.*, 1994).

Tau is posttranslationally modified by phosphorylation and glycation. Tau is phosphorylated by several kinases including cAMP-dependent protein kinase (pKA), Ca^{2+} -calmodulin-dependent protein kinase (CaMK), casein kinase I and II and glycogen synthase kinase-3 (GSK-3) (Pierre and Nuñez, 1983; Yamamoto *et al.*, 1983; Steiner *et al.*, 1990; Mandelkow *et al.*, 1992). Developmentally, tau is most heavily phosphorylated early in development but this modification disappears rapidly as differentiation progresses (Goedert *et al.*, 1993). Phosphorylation causes a change in the conformation of tau from a short, elastic form to a long stiff form (Hagestedt *et al.*, 1989). Additionally, phosphorylation of tau within the flanking regions causes a decrease in its ability to stabilize MTs and phosphorylation within the basic repeats abolishes MT binding (Yamamoto *et al.*, 1988; Trinczek *et al.*, 1995). Glycation of tau has been shown to decrease MT binding and enhance the self-aggregation of tau *in vitro* (Ledesma *et al.*, 1994). Interestingly, tau in PHFs is heavily phosphorylated and glycated (Lee *et al.*, 1991; Goedert *et al.*, 1993; Ledesma *et al.*, 1994) and these modifications may contribute to the abnormal organization of tau in Alzheimer neurons.

MAP2

Like tau, MAP2 consists of a large family of isoforms generated from a single gene by alternative splicing of the primary transcript (Fig. 10) (Lewis *et al.*, 1986; Garner and Matus, 1988; Papandrikopoulou *et al.*, 1989). All MAP2 isoforms share similar domain structure (see Fig. 10). They have 3 – 4 imperfect basic repeats of 18 aa near their c-terminus, flanked by a proline rich domain on the n-terminal side and a 5^{th} repeat on the c-terminal side which shows only partial similarity with the other repeats (Kindler *et al.*, 1990; Doll *et al.*, 1993; Ferralli *et al.*, 1994; Kindler and Garner, 1994; Chung *et al.*, 1996; Couchie *et al.*, 1996; Kalcheva *et al.*, 1997). They also contain several different insertions in their amino terminal projection domain that in the high-molecular weight forms contains a binding site for calmodulin (Kindler *et al.*, 1990a). In the extreme n-terminus there is a binding domain for the RII regulatory subunit of type II cAMP-dependent protein kinase (PKA) (Rubino *et al.*, 1989; Obar *et al.*, 1989).

MAP2 isoforms are also developmentally regulated. The juvenile forms of MAP2, MAP2c and a variant of MAP2b (4R-2b, see Fig. 10), are expressed at their highest levels in the embryo and decrease as development progresses (Tucker *et al.*,

Figure 10

Schematic of MAP2 isoforms. Numbers indicate aa position.

Juvenile MAP2

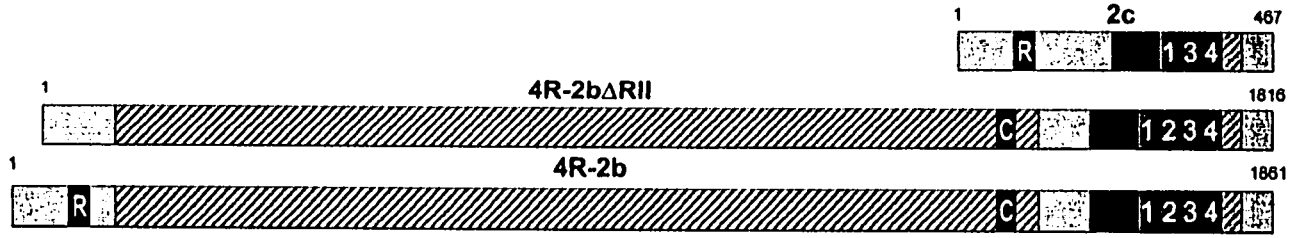

Adult MAP2

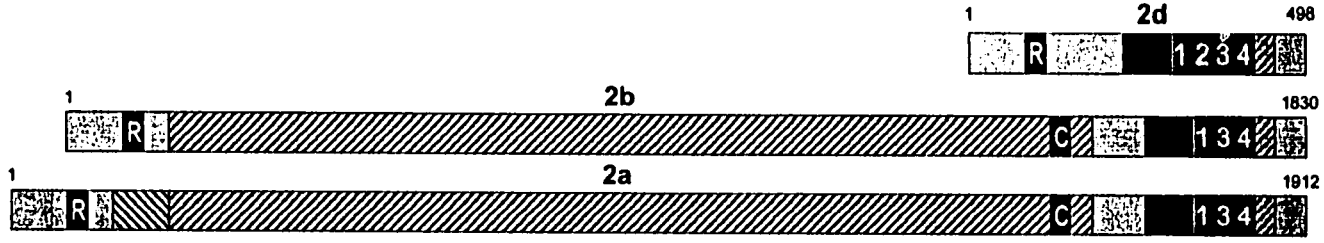

Spinal cord-specific MAP2

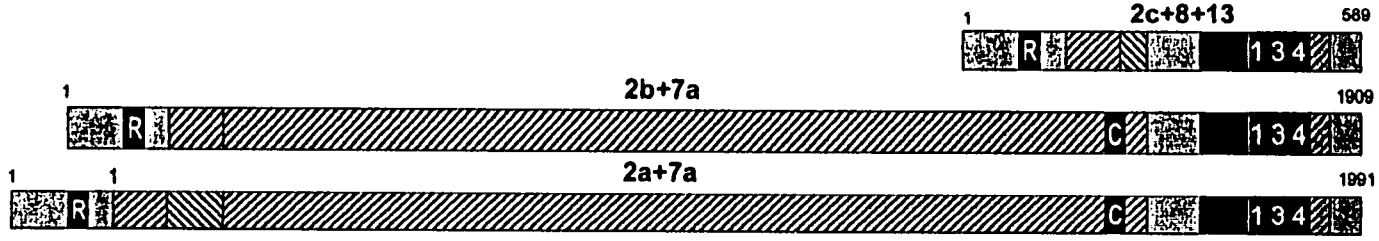

Predicted molecular weight	Observed molecular weight	Reference
49200	70000	Doll *et al.*, 1990
nr	nr	Langkopf *et al.*, 1994
nr	nr	Kindler and Garner, 1994
nr	74000	Kindler and Garner, 1994
199100	280000	Kindler *et al.*, 1990
nr	288000	Chung *et al.*, 1996
nr	nr	Kalcheva *et al.*,1997
nr	nr	Couchie *et al.*, 1996
nr	nr	

nr = not reported

C = calmodulin binding domain

= basic repeat

= degenerate repeat (c-terminal flanking region)

R = RII subunit binding domain

= proline rich domain (n-terminal flanking region)

= projection domain insertions

1988a; 1988c; Crandall and Fischer, 1989; Charrière-Bertrand *et al.*, 1991; Kindler and Garner, 1994). However, MAP2c can be found in adult brain in areas where neuronal growth persists in the adult (Tucker *et al.*, 1988b, Viereck *et al.*, 1989). MAP2c is found in neurons where it is present in both axons and dendrites (Tucker *et al.*, 1988a) and a variant of MAP2c is specifically expressed in fetal spinal cord (2c+8+13) (Kalcheva *et al.*, 1997). The adult forms of MAP2 include several HMW-MAP2 forms, generally termed MAP2a and MAP2b, and a low molecular weight form, MAP2d. MAP2b is present throughout development where its expression is constant while MAP2a is absent early in development and its level increases as differentiation progresses (Binder *et al.*, 1984; Przyborski and Cambray-Deakin, 1995). All HMW-MAP2 forms are restricted to dendrites. They are also found in post-synaptic densities and dendritic spines, regions of dendrites devoid of MTs (Cáceres *et al.*, 1984; Niinobe *et al.*, 1988; Tucker *et al.*, 1988a; Veireck *et al.*, 1988). The localization of MAP2a is more restricted than MAP2b. In the cerebellum, MAP2b is found in all cells while MAP2a is restricted to granule cells. In the retina, MAP2a is only found in ganglion cells while MAP2b is found in both amacrine and ganglion cells (Chung *et al.*, 1996). Additionally, there are spinal cord-specific variants of MAP2a and 2b (2a+7a, 2b+7a) which localize to specific cell types in the lumbar region (Couchie *et al.*, 1996, Kalcheva *et al.*, 1997; Shafit-Zagardo *et al.*, 1997). These variants are expressed much earlier during development in the spinal cord than in brain (Kalcheva *et al.*, 1997). MAP2d is restricted to glial cells and it is found only at later developmental stages (Doll *et al.*, 1993). In ND 7/23 cells, a novel splice variant of 4R-MAP2b (4R-2bΔRII) has been identified lacking the binding site for the RII subunit of PKA (Langkopf *et al.*, 1994).

MAP2 mRNA exists as either a 6 kb species encoding LMW isoforms or a 9 kb species encoding HMW isoforms (Garner and Matus, 1988). Messenger RNA levels for MAP2 isoforms generally reflect the levels of protein during development, except for MAP2a / 2b mRNA which, during the latter stages of development, decrease while MAP2a / 2b protein levels continue to increase. This is attributed to a sequestering of HMW-MAP2 on microtubules, preventing it from being degraded (Safei and Fischer, 1989a; Przyborski and Cambray-Deakin, 1995).

The specific localization of HMW-MAP2 isoforms in dendrites is thought to be due to mRNA targeting and differential turnover of MAP2 forms in axons and dendrites.

In situ hybridization has localized the mRNA for HMW-MAP2 to the cytoskeleton in dendrites (Garner *et al.*, 1988; Bruckenstein *et al*, 1990). HMW-MAP2 introduced by microinjection in spinal cord neurons is initially found in all processes but after 3 days, it is completely removed from the axon. (Okabe and Kirokawa, 1989) while MAP2c introduced by transfection is retained in both axons and dendrites (Meichsner et al, 1993). The dendritic sorting of HMW-MAP2 may be due in part to its association with MTs only in the dendrite (Okabe and Hirokawa, 1989; Kanai and Hirokawa, 1995). This might lead to a more rapid turnover of HMW-MAP2 in the axon. It has also been suggested that the larger projection domain of HMW-MAP2 prevents it from entering the axon (Kanai and Hirokawa, 1995). In transgenic mice overexpressing MAP2c, Marsden *et al.* (1996) observed that MAP2c was found only in dendrites. They have suggested that MAP2 may be transported into dendrites on – end proximal MTs, which are only found in dendrites.

The microtubule binding and bundling domains of MAP2 consist of the 3-4 imperfect basic repeats of 18 aa found in the c-terminus as well as domains flanking the basic repeats. The repeats are very similar to those found in MAP4 and tau (Lewis *et al.*, 1988; Aizawa *et al.*, 1989; Chapin and Bulinski, 1991). In fact, each individual repeat shares higher homology with the same repeat on the other MAP species than with the other repeats in its own MT binding domain (West *et al.*, 1991; Ludin *et al.*, 1996). The flanking region on the n-terminal side consists of the proline-rich domain and on the c-terminus contains a degenerate repeat (Doll *et al.*, 1990; Lewis *et al.*, 1989; Lewis and Cowan, 1990; Ferralli *et al.*, 1994). While the role of the MAP2 flanking domains in MT binding does not appear to be as pronounced as in tau, they are required for bundling activity (Lewis *et al.*, 1989, Ferralli *et al.*, 1994). It appears that while the strength of MT binding increases with the number of repeats (Ferralli *et al.*, 1994), only one repeat can bind at any one time (Coffey and Purich, 1995). Of these repeats, the 3rd repeat exhibits the greatest ability to bind and bundle MTs and to stimulate their assembly, suggesting that it is the most important (Joly *et al.*, 1989; Joly and Purich, 1990; Ludin *et al.*, 1996). The projection domain of MAP2, like that in tau, acts as a spacer between MTs (Chen *et al.*, 1992). However, there is some evidence to suggest that the presence of the projection domain of MAP2 also influences MT interaction (Fellous *et al.*, 1994). The effect of 3 versus 4 repeats on the binding and

bundling ability of MAP2 is unclear. While Doll *et al.* (1993) showed that the MT binding and bundling caused by either MAP2c or MAP2d is the same, it appears that the assembly rate of tubulin in the presence of MAP2d is twice that seen in the presence of MAP2c (Olesen, 1994). The bundling of MTs by MAP2 has been suggested to be caused by a dimerization of MAP2 molecules (Lewis and Cowan, 1990). The dimerization of MAP2c *in vitro* can occur (Wille *et al.*, 1992) but does not appear to occur *in vivo* (Burgin *et al.*, 1994). Another protein factor may act to link MAP2 molecules together (Lewis and Cowan, 1990; Chapin *et al.*, 1991).

Although binding of MAP2 to tubulin has been well documented it also associates with actin and intermediate filaments (Hirokawa *et al.*, 1988; Cunningham *et al.*, 1997). The binding of MAP2 to actin occurs in the MT-binding region, but this interaction appears to be much weaker than the MAP2 – MT interaction (Sattilaro, 1986; Correas *et al.*, 1990; Pedrotti *et al.*, 1994a). Like tau-actin interactions, actin binding by MAP2 is inhibited by the interaction of calmodulin (Lee and Wolff, 1984: Kotani *et al.*,1985). Interestingly, MAP2d (4R) is capable of stabilizing actin microfilaments while MAP2c (3R) is not (Ferhat *et al.*, 1996). The interaction of MAP2 with both vimentin and neurofilaments has been demonstrated in neuronal cells however, this interaction seems to be weaker than the MAP2-MT interaction (Bloom and Vallee, 1983; Hirokawa *et al.*, 1988; Bigot and Hunt, 1991).

Several studies have shed light on MAP2 function. Expression of MAP2 forms in non-neuronal cells and association with MTs *in vitro* lead to stabilization and bundling of MTs (Lewis *et al.*, 1988; Weisshar and Matus, 1993; Umeyama *et al.*, 1993; Takemura *et al.*, 1992; 1995; Gamblin *et al.*, 1996). MAP2 can also induce process formation (Langkopf *et al.*, 1995; LeClerc *et al.*, 1996). HMW-MAP2 and MAP2c induce different processes in SF9 cells. MAP2c induces processes that are short, thin and have a uniform spacing and MT number similar to tau-induced processes. HMW-MAP2 induces processes that are thicker but with a proximo-distal taper with a reduced number of MTs compared to MAP2c (LeClerc *et al.*, 1996). Although tau and MAP2 both stabilize and bundle MTs, there are differences in their effects. In SF9 cells, tau induces a single process while MAP2c induces multiple processes (LeClerc *et al.*, 1993). In ND 7/23 cells, tau and MAP2c both induce MT bundles but only MAP2c induces process formation (Langkopf *et al.*, 1995). This enhanced ability to induce

process formation is attributed to an increase in MT stiffness caused by MAP2 (Weisshaar *et al.*, 1992; Dye *et al.*, 1993; Edson *et al.*, 1993). The polarity of bundles formed by MAP2c is uniform and MTs are aligned with their + ends distal to the nucleus (Umeyama *et al.*, 1993; Takemura *et al.*, 1995), while tau induced bundles display random MT polarity (Brandt and Lee, 1994).

Inhibition of MAP2 in cortical neurons using antisense oligonucleotides causes a reduction in the size and length of neurites. Within these neurites, MTs appear disorganized and are fewer in number (Sharma *et al.*, 1994). In cultured cerebellar macroneurons, suppression of MAP2 leads to a complete inhibition of process formation (Cáceres *et al.*, 1992a).

MAP2 is implicated in several diseases. It is found in neurofibrillary tangles in Alzheimer neurons (Kosik *et al.*, 1988; Dammerman *et al.*, 1989) and is markedly reduced in the hippocampus and entorhinal cortex in brains of schizophrenics (Arnold *et al.*, 1991). MAP2 is also extremely sensitive to ischemia and it is lost from the hippocampus and other regions of the brain following occlusion of the carotid artery (Kitagawa *et al.*, 1989, Ye *et al.*, 1997). However, synthesis of the embryonic form of MAP2 (MAP2c) is upregulated following ischemia and in regenerating neurons following spinal cord transection (Saito *et al.*, 1995; Yin *et al.*, 1995).

MAP2 is heavily phosphorylated and can contain up to 50 mol of phosphate per mol of MAP2 *in vivo* (Tsuyama *et al.*,1986). MAP2 is phosphorylated by several kinases including PKA, CaMK, p110^{mark}, mitogen-activated protein kinase (MAPK), and GSK-3 (Theurkauf and Vallee, 1983; Yamamoto *et al.*, 1983; Adavi *et al.*, 1985; Berling *et al.*, 1994; Illenberger *et al.*, 1996; Morishima-Kawashima and Kosik, 1996). During development, phosphorylation of MAP2 occurs concomitantly with dendritic extension in hippocampal neurons (Díez-Guerra and Avila, 1995). In general, phosphorylation of MAP2 decreases its affinity for MTs while dephosphorylation strengthens MT binding. This in turn serves to increase and decrease MT dynamics (Murthy and Flavin, 1983; Yamamoto *et al.*, 1988; Illenberger *et al.*, 1996). However, Brugg and Matus (1991) have demonstrated that the association of MAP2 with MTs is also regulated by the location of the phosphorylation on the MAP2 molecule. Phosphorylation also lowers the affinity of MAP2 for actin (Selden and Pollard, 1983; Sattilaro, 1986; Yamauchi and Fujisawa, 1988). This regulation of MAP2-MT / MAP2-actin interaction and MT

dynamics by phosphorylation is thought to be a mechanism involved in synaptic plasticity in neurons (Friedrich and Aszódi, 1991). Quillan and Halpain (1996) have shown a specific increase in phosphorylation of MAP2 following glutamate receptor activation and a specific decrease in MAP2 phosphorylation mediated by NMDA receptors. Additionally, exposure of dark reared kittens to light causes an increase in the *in vivo* phosphorylation of MAP2 concomitant with synaptic reorganization in the visual cortex (Aoki and Siekevitz, 1985).

MAP1

MAP1 consists of two closely related members based on charge and aa distribution, MAP1a and MAP1b, each being derived from its own unique gene (Fig. 11) (Garner *et al.*, 1990). Historically, MAP1b has been identified as MAP1X, MAP5 and MAP1.2 (Calvert and Anderton, 1985; Riederer *et al.*, 1985; Aletta *et al.*, 1988) which were thought to be distinct proteins due to their differing mobility by SDS-PAGE. It has since been shown that these are the same proteins but that their mobilities differ because of differential phosphorylation (Harrison *et al.*, 1993). MAP1a and 1b have predicted molecular masses of 299 and 255 kD respectively, but their apparent mobility as determined by SDS-PAGE is 350 and 330 kD (Noble *et al.*, 1989; Langkopf *et al.*, 1992). MAP1a and MAP1b share a similar domain structure (Fig. 11). In the n-terminus both MAPs contain several repeats of a basic KKE motif which are randomly spaced (11 in MAP1a, 21 in MAP1b). The regions flanking these repeats in MAP1a and 1b are also highly homologous (Noble *et al.*, 1989; Langkopf *et al.*, 1992). MAP1b has an additional repeat region in its c-terminus not found in MAP1a. This region consists of 12 imperfect acidic repeats of 15 aa (Noble *et al.*, 1989). MAP1a and 1b are found in many tissues and cell lines where they are associated with MTs (Bloom *et al.*, 1984a, 1984b; Tanaka *et al.*, 1992). However, MAP1a and 1b expression is most prominent in brain (Bloom *et al.*, 1985; Díaz-Nido and Avila, 1989; Fink *et al.*, 1996). Both MAP1 forms are developmentally regulated. Analysis of MAP1a and MAP1b levels in whole brain extracts shows that MAP1a increases and MAP1b decreases during brain development (Riederer *et al.*, 1986; Safei and Fischer, 1989b; Schoenfeld *et al.*, 1989; Garner *et al.*, 1990). In both cases, protein levels are mirrored by mRNA levels (Safei and Fischer, 1989b; Garner *et al.*, 1990). The localization of MAP1a and 1b during

Figure 11

Schematic of MAP1a, MAP1b and associated LCs. Numbers indicate aa position.

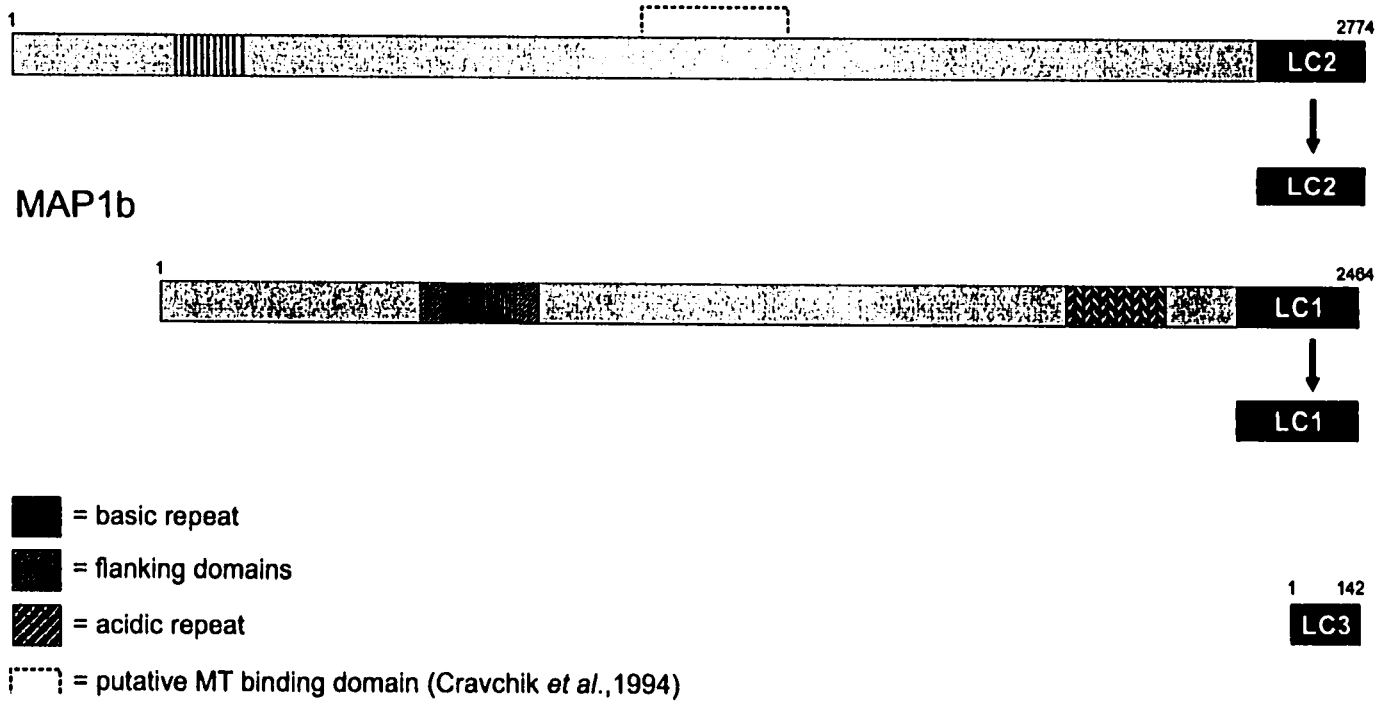

Predicted molecular weight	Observed molecular weight	Reference
299221	350000	Langkopf *et al.*, 1992
	28000	Schoenfeld *et al.*, 1989
255534	330000	Noble *et al.*, 1989
	30000	Schoenfeld *et al.*, 1989
16400	18000	Mann and Hammarback, 1994

brain development is more complex (Tucker and Matus, 1988; McKerracher *et al.*, 1989; Schoenfeld *et al.*, 1989; Viereck *et al.*, 1989). In the developing cerebellum, MAP1a is present at P5 in proximal dendrites and soma while MAP1b is found in axons and dendrites. As differentiation progresses, MAP1a is transiently expressed in axons and occupies both proximal and distal dendrites while MAP1b decreases in axons and is expressed at low levels in dendrites. In the olfactory bulb and retina, both MAP1a and 1b are expressed at high levels throughout development with MAP1a present in dendrites and MAP1b in axons. In the cortico-spinal tract, MAP1a is transiently expressed in axons and no MAP1b expression is detectable during development. In the hippocampus, MAP1a is found in dendrites throughout development while MAP1b, initially only in axons, is also found in dendrites by P20. Although the expression of MAP1a and 1b is primarily in neurons, they can also be detected in oligodendrocytes and astrocytes (Bloom *et al.*, 1984b; Fischer *et al.*, 1990). A MAP1b related antigen has also been localized to the centrosome (Domínguez *et al.*, 1994).

The MT binding domain of MAP1b consists of both the basic repeats and the regions flanking these repeats (Noble *et al.*, 1989). The affect of these regions on MT binding and stabilization is not known. The basic repeat region of MAP1b may form α-helices which are amphipathic in nature, one side being positively charged and the other negative (Avila, 1991). It has been suggested that MAP1b interacts with tubulin through the positively charged surfaces of these α-helices and negatively charged α-helices present in the c-terminus of tubulin (Avila, 1991). Although the MT binding site of MAP1a has not been well characterized, Cravchik *et al.* (1994) have suggested that the basic repeats in MAP1a do not bind MTs and that the MT binding domain is an acidic self-similar region in the middle of the protein (Fig. 11). MAP1a and 1b have also been shown to interact with actin (Asai *et al.*, 1985, Fujii *et al.*, 1993; Pedrotti *et al.*, 1994b; Pedrotti and Islam, 1996).

There are some insights into the function of MAP1a and 1b. MTs assembled in the presence of MAP1a or MAP1b show increased rates of assembly. The rates of assembly observed are higher than those observed for MAP2 (Pedrotti and Islam, 1994b; 1995b). Interestingly, the rate of MT assembly is greater in the presence of MAP1b than MAP1a. The ability of MAP1b to stabilize MTs to drug-induced depolymerization *in vitro* is much weaker than MAP2 (Vandecandelaere *et al.*, 1996).

The morphology of MTs is also affected by MAP1a and 1b. MTs assembled in the presence of MAP1a are short and straight while those assembled in the presence of MAP1b are long and "bendy" (Pedrotti *et al.*, 1996a). In growing axons, MAP1b is concentrated distally, where MTs are most labile (Black *et al.*, 1994). Overexpression of MAP1b in non-neuronal cells does not cause bundling of MTs as seen for MAP2 and tau but an increase in resistance to drug induced MT depolymerization and tubulin acetylation is noted (Takemura *et al.*, 1992). However, the stabilization and acetylation of MTs in cells expressing MAP1b is weaker than in cells expressing MAP2c. Inhibition of MAP1b expression in cultured neurons using antisense oligodeoxynucleotides or microinjection of antibodies leads to the loss of neurite outgrowth (Brugg *et al.*, 1993; Shea and Beermann, 1994). In adult brain, MAP1a and 1b are found in regions where growth and plasticity still occur (Tucker and Matus, 1988; Sato-Yoshitake *et al.*, 1989, Viereck *et al.*, 1990), suggesting they are essential for neuronal growth and in regenerating axons, the levels of MAP1b are upregulated (Fawcet *et al.*, 1994; Tonge *et al.*, 1996). The levels of MAP1a in regenerating axons do not change, but it is rapidly degraded from ganglion cells following axotomization (McKerracher *et al.*, 1989; Fawcett *et al.*, 1994) illustrating its importance in the maintenance of neuronal processes. It has also been shown that MAP1a and MAP1b are sensitive markers for neuronal injuries such as ischemia and seizures. In axons challenged by focal ischemia, the MAP1a and 1b staining in axons changes from a uniform distribution along the axon to an irregular, punctate staining (Fischer *et al.*, 1995; Deware and Dawson, 1997). In MAP1b mutant transgenic mice, homozygotes for the MAP1b mutation are lethal. Heterozygotes have malformed dendrites that contain no MAP1b, demonstrating that MAP1b plays a role in normal development (Edelmann *et al.*, 1996). In tau deficient transgenic mice, MAP1a levels are elevated in small caliber axons where tau levels are reduced and the MTs in these cells are less resistant to drug induced depolymerization (Harada *et al.*, 1994). This suggests that MAP1a cannot complement the MT stabilization induced by tau.

MAP 1a and 1b are both phosphorylated *in vivo* by casein kinase II and other as yet unidentified kinases (Díaz-Nido *et al.*, 1988; Ulloa *et al.*, 1993a; Fujii *et al.*, 1996). The phosphorylation of MAP1a and 1b is regulated spatially and developmentally. Phosphorylated MAP1a is only detectable in late development (Schoenfeld *et al.*, 1989;

Díaz-Nido *et al.*, 1990). Two types of MAP1b phosphorylation can be distinguished by SDS-PAGE. Type I is probably catalyzed by casein kinase II and causes an upward shift in MAP1b's mobility by SDS-PAGE. Type II phosphorylation (probably catalyzed by a proline-directed kinase) has no effect on the mobility of SDS-PAGE (Ulloa *et al.*, 1993a). Type I phosphorylation of MAP1b is highest early in development and disappears in the adult (Fischer and Romano-Clarke, 1990; Bush and Gordon-Weeks, 1994; Ulloa *et al.*, 1993b) except in regions where neuronal growth continues (Nothias *et al.*, 1996). Type I phosphorylation is also upregulated in regenerating axons (Bush *et al.*, 1996; Tonge *et al.*, 1996). Type II phosphorylated MAP1b is present throughout development (Ulloa *et al.*, 1993b). Type I phosphorylated MAP1b is present exclusively in axons, and within the axon it is most heavily phosphorylated in the distal axon and growth cone (Sato-Yoshitake *et al.*, 1990; Mansfield *et al.*, 1992; Boyne *et al.*, 1995). In contrast, mode II phosphorylated MAP1b can be found in axons, dendrites and the soma (Ulloa *et al.*, 1993b). In the adult brain, MAP1a and 1b are most heavily phosphorylated in the corpus callosum while levels in other regions of the brain are lower (Díaz-Nido *et al.*, 1990).

The effect of phosphorylation on the MT binding ability of MAP1a and 1b is opposite to that of MAP2. Phosphorylated MAP1a and MAP1b are preferentially bound to MTs while phosphorylated MAP2 is preferentially excluded (Díaz-Nido *et al.*, 1990). Also, MAP1b interaction with actin is inhibited by phosphorylation (Pedrotti and Islam, 1996). Axons of Trembler mice show abnormal morphology, and also show reduced phosphorylation of MAP1a and MAP1b. This may link the phosphorylation state of MAP1a and 1b to normal neuronal development (Kirkpatrick and Brady, 1994).

MAP1 LIGHT CHAINS

MAP1a and MAP1b exist in a complex with three light chains (LC1 - LC3) with respective molecular weights of 34, 28 and 18 kD (Vallee and Davis, 1983; Kuznetsov *et al.*, 1986; Kuznetsov and Gelfand, 1987; Schoenfeld *et al.*, 1989). LC1 is encoded in the 3′ end of the open reading frame of MAP1b (see Fig. 11) (Hammarback *et al.*, 1991) and is thought to be cleaved during or after translation to yield a heavy chain (MAP1b) and LC1. Similarly, LC2 is encoded in the 3' end of the open reading frame of MAP1a and is probably produced by a similar mechanism (Langkopf *et al.*, 1992). LC3 is

encoded by a separate gene and is expressed only in neurons where its expression increases during development (Mann and Hammarback, 1994; 1996). LC2 is found predominantly associated with MAP1a whereas LC1 and LC3 associate with both MAP1a and MAP1b (Schoenfeld *et al.*, 1989; Pedrotti *et al.*, 1995c). All three LCs associate at or near the MT binding domain of MAP1a and MAP1b (Kuznetsov *et al.*, 1986; Schoenfeld *et al.*, 1989). Although the exact stoichiometry is not known, the MAP1 heavy chains can bind more than one copy of a particular light chain (Schoenfeld *et al.*, 1989). It is thought that the association of these light chains with MAP1a and MAP1b alters their ability to bind MTs and alter MT dynamics during development (Schoenfeld *et al.*, 1989, Mann and Hammarback, 1996).

P19 EC CELLS AS A MODEL FOR NEURONAL DIFFERENTIATION

P19 EC cells were isolated from a teratocarcinoma generated by the grafting of a 7 day mouse embryo to the testis of a mouse (McBurney and Rogers, 1982). These cells can be cultured and remain undifferentiated when kept in an exponentially growing state. Unlike other embryonal carcinoma cell lines, which spontaneously differentiate when allowed to aggregate or grow at high densities, P19 EC cells undergo very little differentiation when cultured under these conditions (McBurney, 1993).

The developmental pathway of P19 EC cells can be controlled by the use of different morphogens. When P19 EC cells are incubated in the presence of 0.5 – 1% DMSO, they differentiate into cardiac muscle and incubation in 2-3% DMSO causes the formation of smooth muscle (McBurney *et al.*, 1982). When incubated in the presence of 10^{-6}M RA, P19 EC cells differentiate in a mosaic culture composed of neurons, glia and fibroblast-like cells (Jones-Villeneuve *et al.*, 1982). The neurons formed in this culture system express neuronal antigens found in brain and display similar morphology to neurons *in vivo* (McBurney *et al.*, 1988).

The isotype composition, dynamics, and organization of MTs have been examined in P19 EC cells during RA-induced neuronal differentiation and all these parameters of MTs are similar to those seen in brain (Falconer *et al.*, 1989; 1992; 1994; Laferrière and Brown, 1996). In addition, the developmentally regulated expression of HMW-MAP2, MAP2c and tau during the early stages of P19 EC cell differentiation mimic patterns seen in brain (Fig. 12) (Falconer *et al.*, 1992; 1994). These studies

Figure 12

Expression of several cytoskeletal antigens during RA-induced, serum-free neuronal differentiation. From Falconer *et al.* (1994).

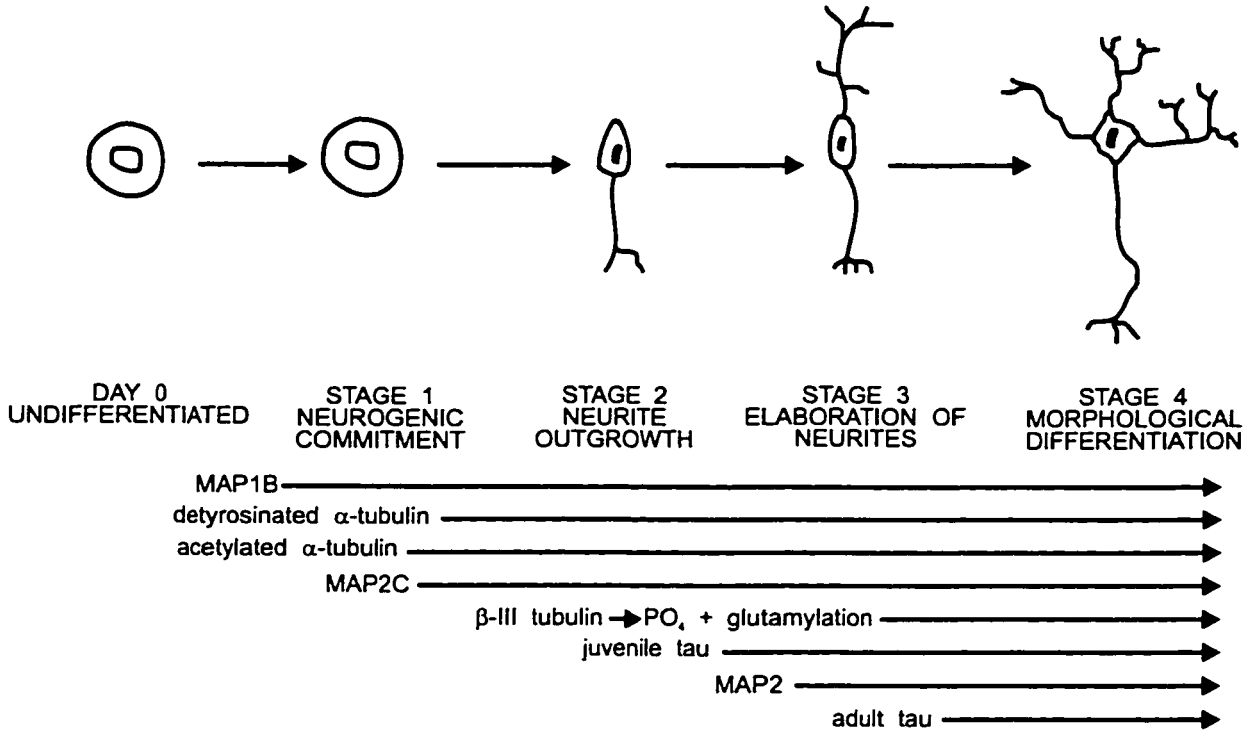
DAY 0
UNDIFFERENTIATED
STAGE 1
NEUROGENIC
COMMITMENT
STAGE 2
NEURITE
OUTGROWTH
STAGE 3
ELABORATION OF
NEURITES
STAGE 4
MORPHOLOGICAL
DIFFERENTIATION
MAP1B
detyrosinated α-tubulin
acetylated α-tubulin
MAP2C
β-III tubulin → PO4 + glutamylation
juvenile tau
MAP2
adult tau

show that the RA-induced neuronal differentiation of P19 EC cells is a good *in vitro* model for neuronal differentiation *in vivo*. Recently, MacPherson and McBurney, (1995) have developed a serum-free method of differentiating P19 EC cells into neurons. Traditionally, P19 EC cells were differentiated in the presence of low concentrations of FCS (2-3%). The serum-free method uses a defined medium with no FCS to culture the cells following RA induction. One advantage of this new method are cultures containing larger proportions of neurons during differentiation. P19 EC neurons cultured using the serum-free method also live longer, making the investigation of more mature P19 EC neurons possible. P19 EC cells are also amenable to genetic manipulation by transfection (MacPherson and McBurney, 1995), making it an ideal cell system to investigate the function of MAPs and other cytoskeletal proteins during neuronal differentiation.

RATIONALE FOR EXPERIMENTS

MAP1a is one of the most abundant MAPs in the adult brain yet little is known about its function. The correlation of its expression with increasing MT stability during brain development has led to the suggestion that MAP1a functions like other adult MAPs, such as HMW-MAP2 and tau, to stabilize MTs (Matus, 1990a; 1990b). However, the regional expression of MAP1a during brain development suggests that its postulated role as a MT stabilizer is too simplistic.

MAP1a is only transiently expressed during axonal formation (Schoenfeld et al., 1989) while MT stability continually increases (Black and Green, 1982). It is present in the olfactory bulb and retina throughout development (McKerracher *et al.*, 1989; Schoenfeld *et al.*, 1989) and these regions contain neurons which grow throughout development. Finally, dendrites, the primary location of MAP1a in the adult, can undergo plastic rearrangements, suggesting that MTs in these processes are more labile than those in axons (Frederich and Asódi, 1991). While these observations are not inconsistent with a stabilizing role for MAP1a, they suggest that it may function in neuronal growth, when MTs are more labile.

Little is known about the MAP1a-MT interaction or how LCs affect the ability of MAP1a to bind to or affect MT dynamics. Cravchik *et al.* (1994) have suggested that an acidic domain centrally located in MAP1a binds MTs. However, in MAP1b, a closely

related protein with similar charge and aa composition (Langkopf *et al.*, 1992), the basic repeats and flanking domains are the MT binding region (Noble *et al.*, 1989). In addition, all other MAP MT-binding domains contain repeats of basic aa.

Schoenfeld *et al.* (1989) and Pedrotti and Islam (1995a) have shown a preferential association of LC2 with MAP1a. MAP1a bound MTs are less dynamic than MAP1b-bound MTs (Pedrotti and Islam, 1994; 1995b) suggesting that LC2 may be required for MT-stabilization by MAP1a. LC3 is neuron specific and its expression in developing brain is correlated with increased MT stability (Mann and Hammarback, 1996). LC3 may also affect MT stability on MAP1a-bound MTs

The goal of this thesis research was to answer questions about how MAP1a binds to MTs, how it effects MT organization and dynamics and how LCs effect the role it plays in the morphological development of neurons. The following hypotheses were proposed:

1. Does MAP1a expression in P19 EC cells increase during development?
2. Does MAP1a binds to MTs via its basic repeats and regions flanking these repeats?
3. Are MAP1a-associated MTs weakly stabilized?
4. Does the interaction of light chains, especially neuron-specific LC3, with MAP1a affect the stabilization of MTs mediated by MAP1a?

MATERIALS AND METHODS

EXPRESSION CONSTRUCTS

Three overlapping rat cDNA clones (p19a, p14 and p19) spanning the entire mRNA for MAP1a (Langkopf *et al.*, 1992) were obtained from Drs A. Langkopf (Institut Jacques Monod, France) and Dr. R. Muller (University of Bremen, Germany). The cDNA for light chains 1, 2, and 3 (pCR3-LC1, pCR3-LC2 and pCR3-LC3) were obtained from Dr. J. Hammarback (Bowman Gray School of Medicine, NC). These cDNAs were used to make all expression constructs (Fig. 13). pKJ1ΔF-6myc and pPOP (a gift from Dr. M. McBurney, University of Ottawa) are pUC19-based vectors containing the constitutively active mouse phosphoglycerate kinase (PGK) promoter. This vector drives the efficient expression of proteins in undifferenitated P19 EC cells (Pratt *et al.*, 1993; Morasutti *et al.*, 1994; Skerjanc *et al.*, 1994). PKJ1ΔF-6myc drives the expression of 6 repeats of a 9 aa epitope from the human *c-myc* protein (Fig.14). These vectors were used to express proteins epitope tagged at the n-terminus (Fig. 15). When necessary, sequencing was performed to ensure all proteins were expressed in frame with the 6-myc tag, to confirm ligations, and to determine the location of in frame stop codons in the cDNA. All sequencing reactions were performed using the ABI Prism Dye Terminator Cycle Sequencing Kit (with Amplitaq DNA polymerase, FS) (Perkin Elmer). All sequencing reactions were cycled using a Perkin Elmer PCR machine and run on an ABI model 373A automated sequencer. PGK-MAP2cmyc was provided by C. Addison.

PGK-6myc

This is the unmodified pKJ1ΔF-6myc vector. It expresses the 6myc tag followed by a 25 aa tail (NSCSPGDPLVLERPPPRYSSDPCRN)

PGK-6mycN1a-1

A Nco I – Hind III fragment from clone p19a was blunt-end ligated into Sma I – Sac I cut pKJ1ΔF-6myc. This vector expresses the 6myc tag followed by 5 aa (NSCSP), followed by aa 1-281 from MAP1a terminating with a 6 aa tail (TDPCRN).

Figure 13

Schematic showing the cDNAs used in the design of expression constructs in this study. Nucleotide positions in the MAP1a cDNAs (p19, p14 and p19a) are according to Langkopf *et al.*, 1992. Vectors containing the cDNA are indicated to the left of the cDNA and construct sizes to the right. Restriction sites used in construct synthesis are indicated.

p19a

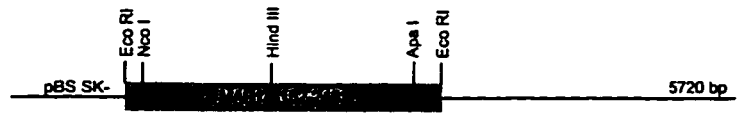

p14

p19

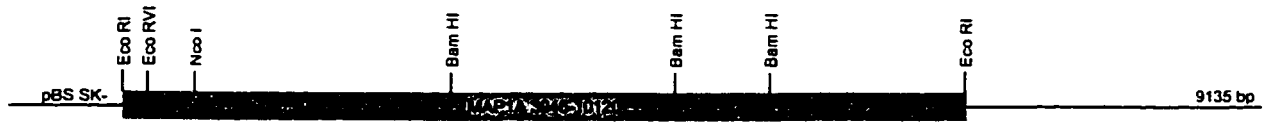

pCR3-LC1

pCR3-LC2

pCR3-LC2

Figure 14

Schematic showing the expression vectors used in the design of expression constructs. Sites used in construct synthesis are indicated.

pPOP

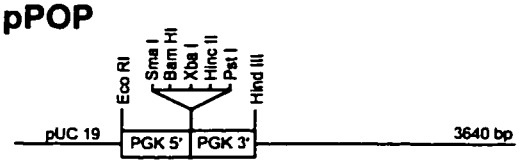

pKJ1ΔF-6myc

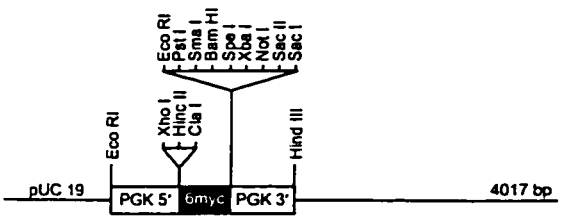

PGK-6mycN1a-2

A Nco I – Apa I fragment from clone p19a was blunt-end ligated into Sma I – Sac I cut pKJ1ΔF-6myc. This vector expresses the 6myc tag, the NSCSP linker, aa 1-630 of MAP1a followed by a 6 aa tail (ADPCRN).

PGK-6mycN1a-3

A partial Nco I – Bam HI fragment (7800 bp) from PGK-6mycN1a-4 (see below) was blunt-ended and religated. The expressed protein contains the 6myc tag, a 7 aa linker (NSREFLH), aa 1-1310 of MAP1a and a 2 aa tail (IL).

PGK-6mycN1a-4

A Cla I – Bam HI fragment from PGK-6myc1a (see below) was blunt-end ligated into Sma I cut pPOP. The expressed protein contains the 6myc tag, a 7 aa linker (NSREFLH), aa 1-2016 of MAP1a and a 14 aa tail (RGSSRVDLQLFMIY).

PGK-6myc1a

A Nco I – Eco RI fragment from clone p19a was blunt-end ligated into Sma I – Hind III cut pKJ1ΔF-6myc. A partial Apa I fragment (1959 bp) from clone p14 was then ligated into this vector at the ApaI site. In to this vector a 6070 bp Eco RI – Eco RV fragment from clone p19 was blunt-end ligated into the Eco RV site. Finally a short oligonucleotide containing a SmaI site (5'-AATTCCCGGG-3', New England Biolabs) was inserted into the Eco RI site between the 6myc tag and the MAP1a cDNA to bring the cDNA for MAP1a into frame with the 6myc tag. The expressed protein contains the 6myc tag, a 7 aa linker (NSREFLH) and the full length cDNA for MAP1a. The predicted molecular weight for the tagged protein is based on the predicted molecular weight for the MAP1a heavy chain as reported in Langkopf *et al.*, (1992).

PGK-6mycN1a-2ΔBR

PGK-6myc1a was digested with Xho I and Hae II to yield two fragments (1514 and 1223 bp) A 1357 bp fragment was PCR amplified from the 1514 bp fragment using the primers PCR-1 and PCR-2 (phosphorylated) (see appendix 3). A 279 bp fragment was PCR amplified from the 1223 bp fragment using the primers PCR-3

(phosphorylated) and PCR-4. The 1357 and 279 bp PCR products were ligated and then further cut with ClaI and Apa I. This fragment was ligated into Cla I – Apa I cut pKJ1ΔF-6myc. Both strands of the entire PCR product were then completely sequenced to ensure the fidelity of the PCR reaction and to check the joint between the two PCR products. The expressed protein contains the 6myc tag, a 7aa linker (NSREFLH), aa 1-335 and 541-631 of MAP1a followed by a 29 aa tail (GGSTSSRAAATAVEN-LIPYRENMYLGRLR).

PGK-6mycLC1

A 753 bp Nco I – Eco RI fragment from pCR3-LC1 was blunt end ligated into Sma I cut pKJ1ΔF-6myc. This vector expresses the 6myc tag, the NSCSP linker, aa 2215-2464 of rat MAP1b which corresponds to the region reported to be light chain 1 (Hammarback *et al.*, 1991) and a 7 aa tail (KPNWGMH).

PGK-6mycLC2

A 666 bp Nco I – Eco RI fragment from pCR3-LC2 was blunt end ligated into Sma I cut pKJ1ΔF-6myc. This vector expressed the 6myc tag, the NSCSP linker, aa 2554-2774 of rat MAP1a which corresponds to the region reported to be light chain 2 (Langkopf *et al.*, 1992).

PGK-6mycLC3

A 818bp Nde I – Eco RI fragment from pCR3-LC3 was blunt end ligated in to Sma I cut pKJ1ΔF-6myc. This vector expresses the 6myc tag, the NSCSP linker and the complete open reading frame of rat LC3 (Mann and Hammarback, 1994).

SCREENING OF BACTERIAL COLONIES

Ligation products were transformed by heat shock into chemically competent DH5αF′ *E.coli* (Hanahan, 1983). Transformed *E.coli* were then plated onto LB plates supplemented with 100 μg / ml of ampicillin (Sigma) and incubated ON at 37°C. Colonies were used to innoculate 5 ml cultures of T-broth (Maniatis et al, 1982) with ampicillin as above and grown ON at 250 rpm and 37°C. Plasmid DNA was harvested from each culture using the alkaline-lysis method (Maniatis et al,

Figure 15

Expression constructs used in this study. The full length cDNA and MAP1a protein are provided for comparison. * This molecular weight does not include LC2, see Materials and Methods.

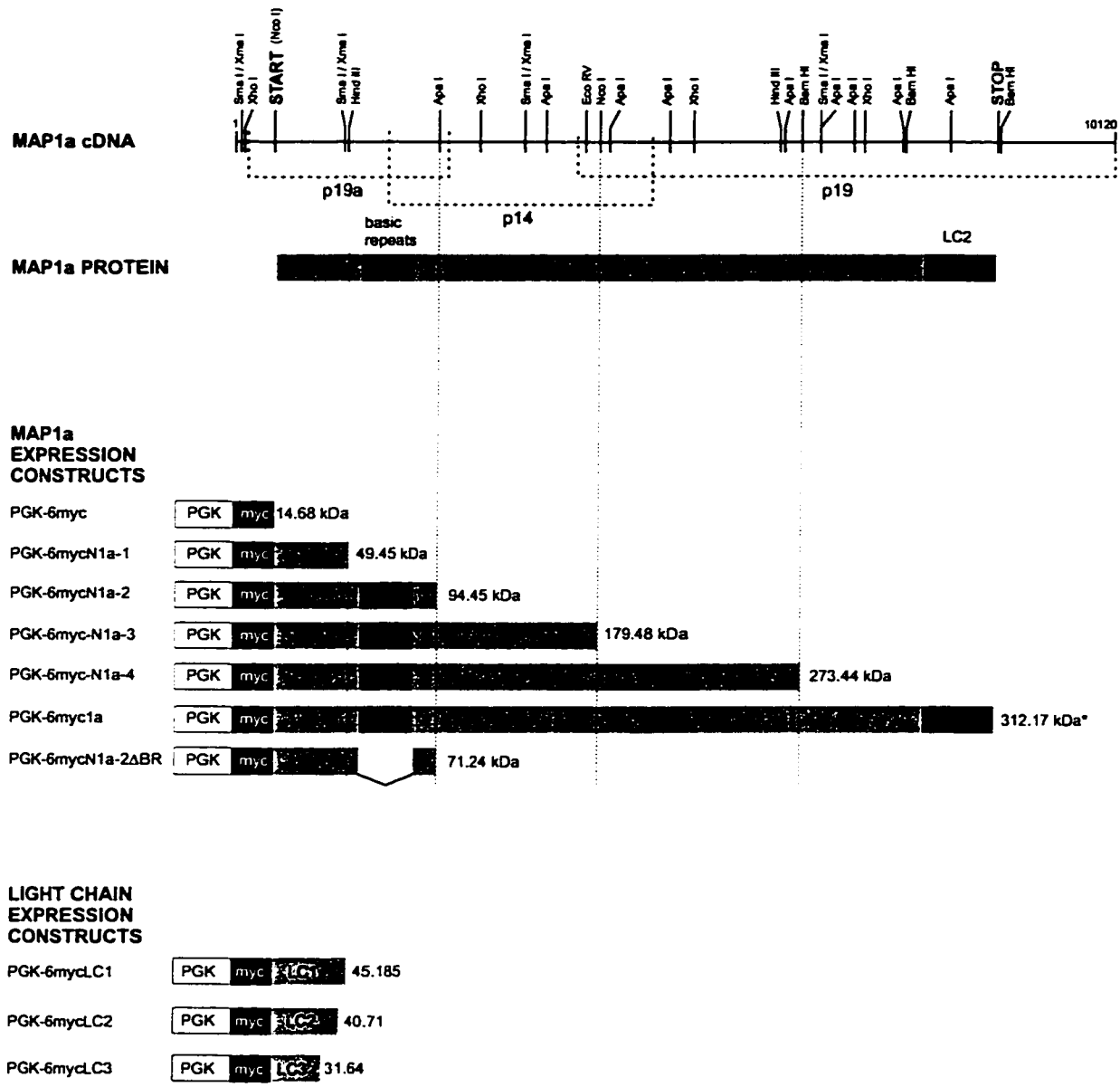
MAP1a cDNA
START (Nco I)
STOP
10120
p19a
p14
p19
basic repeats
MAP1a PROTEIN
LC2
MAP1a EXPRESSION CONSTRUCTS
PGK-6myc
PGK
myc
14.68 kDa
PGK-6mycN1a-1
49.45 kDa
PGK-6mycN1a-2
94.45 kDa
PGK-6myc-N1a-3
179.48 kDa
PGK-6myc-N1a-4
273.44 kDa
PGK-6myc1a
312.17 kDa*
PGK-6mycN1a-2ΔBR
71.24 kDa
LIGHT CHAIN EXPRESSION CONSTRUCTS
PGK-6mycLC1
45.185
PGK-6mycLC2
40.71
PGK-6mycLC3
31.64

1982) and screened by restriction digest. Positive clones were further purified using the Geneclean procedure (Bio 101) prior to sequencing.

LARGE SCALE PRODUCTION OF PLASMID DNA FOR TRANSFECTION

Plasmid DNA was transformed in to competent DH5αF′ *E. coli* as above. Colonies were used to inoculate 5 ml T-broth cultures as above. The following day, small cultures were diluted 1:100 in LB broth (500 ml) with ampicillin and grown ON as above. Plasmid DNA was harvested from large cultures using Qiagen megaprep silica resin columns (Qiagen), resuspended in ddH_2O and stored at –20°C. DNA concentration and purity was determined by absorbance at 260 and 280nm using a Genequant® spectrophotometer (Pharmacia).

TISSUE CULTURE AND DRUG TREATMENTS

P19 EC cells (McBurney and Rogers, 1982) and HeLa CCL-2 cells (ATCC) were kept semiconfluent in α-modified Eagle's minimal essential medium (α-MEM) (GIBCO BRL) supplemented with 10% FCS (Flow Labs), and antibiotics (Gibco). Cells were grown in a humidified incubator at 37°C and 5% CO_2 and passed every two days. To differentiate cells into neurons, the serum-free method of MacPherson and McBurney (1995) was used with some modifications. Cells were plated as a semiconfluent monolayer on 22 X 22mm glass coverslips (VWR) or 100 mm culture dishes (Corning) and allowed to recover for 24 h in α-MEM containing 10% FCS and antibiotics. The medium was then changed and supplemented with 10^{-6} M RA (SIGMA). 24 h later, the medium was replaced with a defined, serum free medium (without retinol) Half of the medium was changed each day until cells were ready for processing. Taxol (obtained from the National Cancer Institute) was kept as a 10 mM stock in DMSO at -20°C. This stock was then diluted to 10^{-6} M in α-MEM, 10% FCS and antibiotics to treat cell cultures for 24 h. Colchicine (SIGMA) was kept as a 1mg / ml stock in ddH_2O and diluted to 1μg/ml to treat cells.

TRANSFECTION OF P19 AND HELA CELLS

Expression vectors were introduced into P19 EC and HeLa cells by calcium phosphate mediated transfection (Chen and Okayama, 1987). For protein extraction,

cells were plated onto 100 / 60mm dishes (Corning) at 1.25 $x10^5$ / $7.5X10^4$ cells / dish (P19 EC) or $2X10^5$ / $1X10^5$ cells / dish (HeLa) in 10 / 5ml of medium (see above). For microscopy, cells were plated onto 18 mm round cs (Corning) at 1.25 $x10^4$ cells / cs (P19 EC) or $2X10^4$ cells / cs (HeLa) in 1 ml of media. Cells were allowed to settle for 24 h. 40 µg of DNA in 500 µl of 0.25 M $CaCl_2$ was then gently mixed with 500 µl 2X BES buffer (50 BES, pH 6.86, 280 mM NaCl, 1.5 mM Na_2HPO_4) to a final volume of 1 ml and allowed to sit for 20 min. The solution of calcium phosphate-DNA precipitate was then gently added to the cells (2 ml for 100 mm dishes, 1 ml for 60 mm dishes, 200 µl for cs) without removing the media and allowed to sit for 8 h in the incubator. The DNA solution was then aspirated and replaced with fresh medium. Cells were incubated a further 48 h before processing.

PROTEIN EXTRACTION

Cells were extracted by one of the following methods:

SDS-WHOLE CELL (Fig. 16)

This method was used for preparing extracts for SDS-PAGE and dot-blot analysis. Protein was extracted from cells using the method described in Drubin *et al.*, (1985), but using higher concentrations of protease inhibitors in the extraction buffer. Dishes were rinsed briefly in rinse buffer (0.13 M NaCl, 2 mM KCl, 8 mM Na_2HPO_4, 2 mM KH_2PO_4, pH 7.2) and then 250 – 500 µl of extraction buffer [25 mM Na_2HPO_4, pH 7.2, 400 mM NaCl, 0.5% (w/v) SDS, 40 µM benzamidine HCl (SIGMA), 4 mM PEFA (Centrichem), 1 mM 1,10-phenanthroline (Sigma), 40 µg / ml each of aprotinin, pepstatin A and leupeptin (all from Sigma)] was added, depending on the size of the dish. The viscous lysate was immediately scraped into an eppendorf tube and placed in a boiling water bath for 10 min and then spun for 10 min at 10000 rpm and 4°C. The supernatant was removed and stored at –80°C

WHOLE CELL EXTRACTION (Fig. 17)

This method was used for preparing extracts for in vitro assembly. Cells were rinsed briefly in cold MAB2 (0.1 M MES pH 6.4, 2.5 mM EGTA, 0.1 mM EDTA, 0.5 mM $MgCl_2$, Pedrotti *et al.*, 1993) and then 250 – 500 µl of extraction buffer [MAB2 +

4 mM PEFA, 1 mM 1,10-phenanthroline and 40 µg/ml each of aprotinin, pepstatin A and leupeptin] was added. Cells were immediately scraped into an eppendorf and sonicated 15 sec at 94 W, then immediately spun for 10 min at 10000 rpm and 4°C. The supernatant was removed and stored at -80°C.

SDS-POLYMER / SOLUBLE EXTRACTION (Fig. 18)

This method was used for SDS-PAGE analysis of MAP1a. To prepare soluble and cytoskeletal (polymer) protein fractions, cells were briefly rinsed in RT PBS then extracted with 0.2% Triton X-100 in PEM [80 mM PIPES (Sigma), pH 6.8, 5 mM EGTA (SIGMA), 1 mM $MgCl_2$,] containing the above protease inhibitors at RT for 2 min. The soluble fraction was removed from the dish, SDS added to 0.5% (w/v), and placed in a boiling water bath for 10 min. The sample was then centrifuged 10 min at 10000 rpm and 4°C, and the supernatant removed and stored at –80. The remaining cytoskeletal fraction was solubilized and stored as in the SDS-whole cell extraction.

POLYMER / SOLUBLE EXTRACTION (Fig 19)

This method was used to prepare extracts for tubulin and MAP analysis. Dishes were washed briefly with PEM at 37°C. Cells were then incubated for 5 min and 37°C in 250 – 500 µl of MSB [0.1 M MES, pH 6.75, 1 mM $MgSO_4$, 2 mM EDTA (SIGMA), 0.1 mM EGTA (SIGMA), 4 M glycerol, 0.5% Triton X-100 (Pierce), Joshi and Cleveland, 1989] with addition of 4 mM PEFA, and 40 µg / ml of aprotinin, pepstatin A and leupeptin. The extraction buffer was then pipetted from the dish and spun for 2 min at 10000 rpm at RT and the supernatant was removed. Then 250 – 500 µl of MDB [0.1 M MES (Boehringer), 1 mM $MgSO_4$, 10 mM $CaCl_2$, pH 6.9, 1 mM DTT (BRL) and 5 mM GTP (type IIS, Sigma), Thrower *et al.*, 1991], including inhibitors as above, was added to the dish and the cells were scraped into the eppendorf containing the pellet from the soluble fraction. The cells were then sonicated 15 sec at 94 W using a Braun sonicator, incubated for 1 h on ice and spun 10 min at 10000 rpm and 4°C. The supernatant was removed and stored at -80°C.

Figure 16

Protocol for SDS-whole cell extraction.

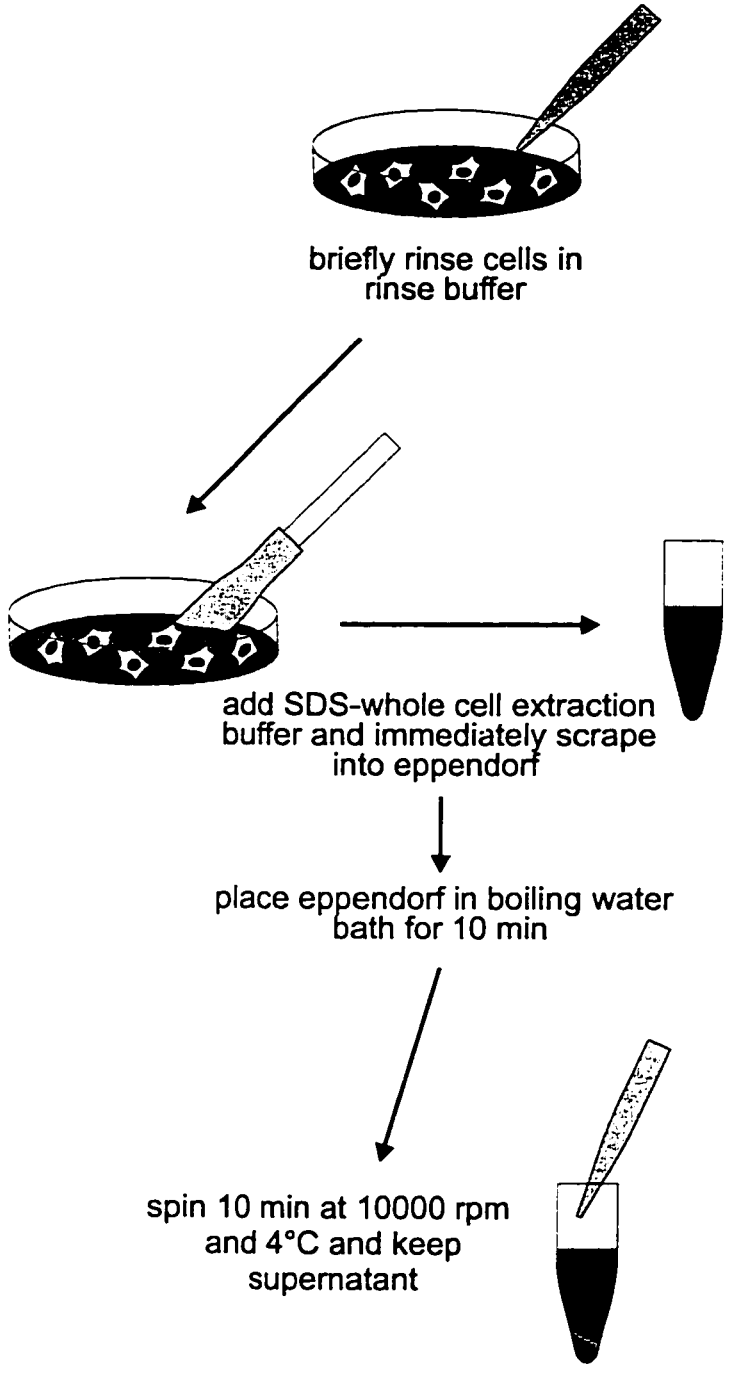
briefly rinse cells in rinse buffer
add SDS-whole cell extraction buffer and immediately scrape into eppendorf
place eppendorf in boiling water bath for 10 min
spin 10 min at 10000 rpm and 4°C and keep supernatant

Figure 17

Protocol for whole cell extraction.

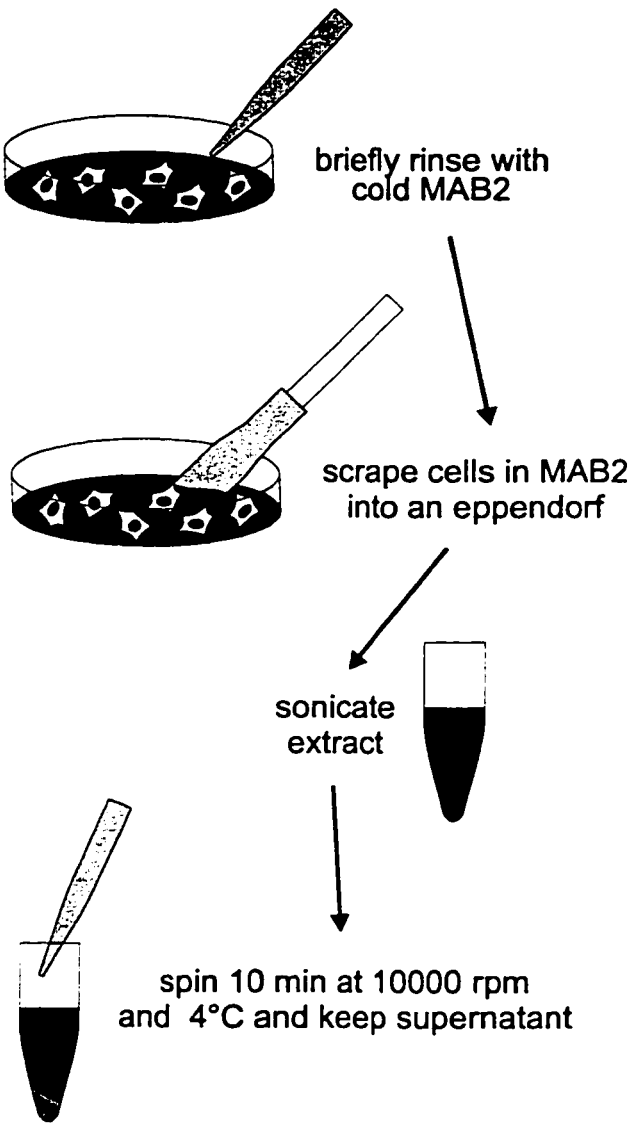
briefly rinse with
cold MAB2
scrape cells in MAB2
into an eppendorf
sonicate
extract
spin 10 min at 10000 rpm
and 4°C and keep supernatant

Figure 18

Protocol for SDS-polymer /soluble extraction.

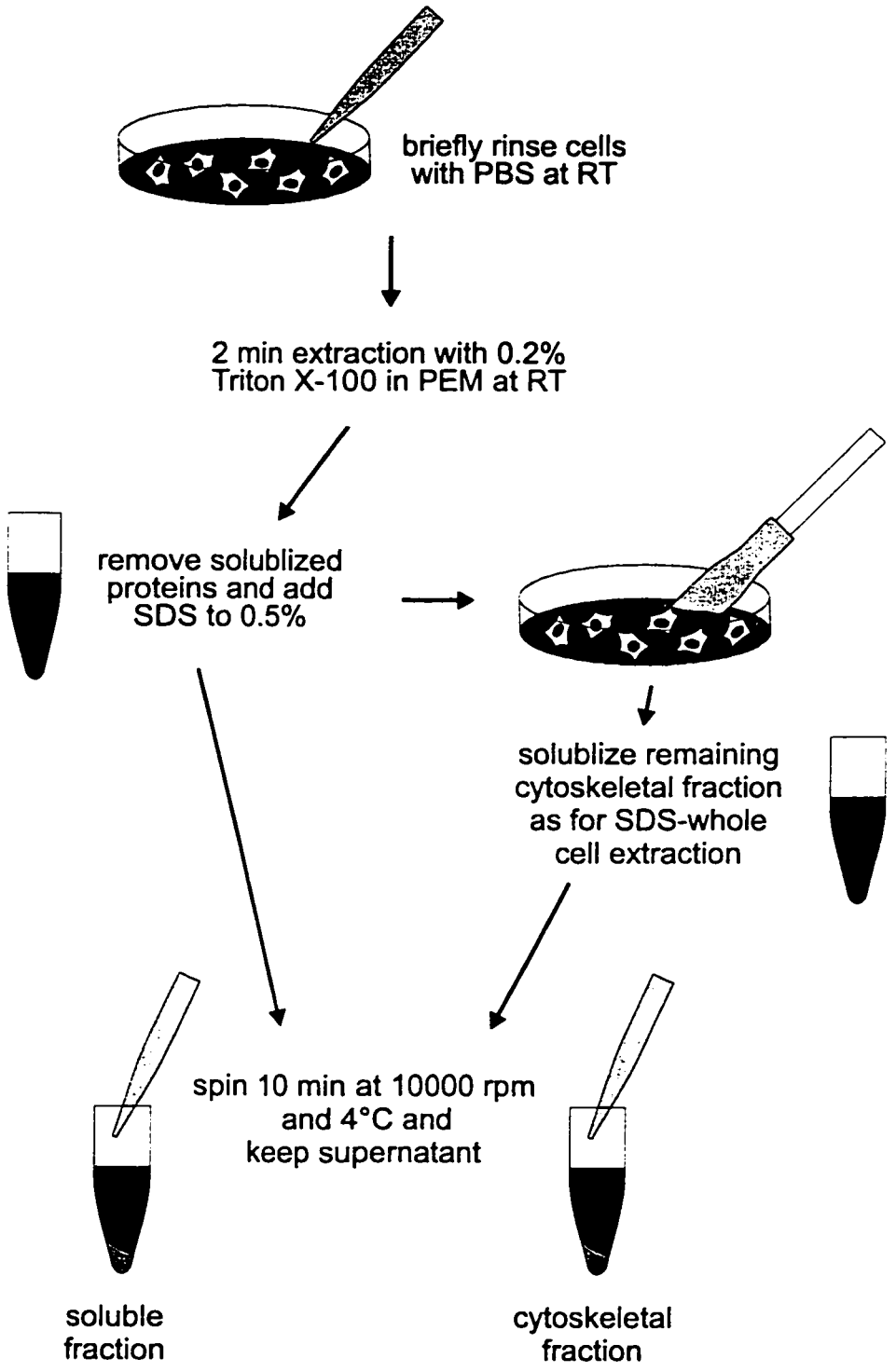
briefly rinse cells with PBS at RT
2 min extraction with 0.2% Triton X-100 in PEM at RT
remove solublized proteins and add SDS to 0.5%
solublize remaining cytoskeletal fraction as for SDS-whole cell extraction
spin 10 min at 10000 rpm and 4°C and keep supernatant
soluble fraction
cytoskeletal fraction

Figure 19

Protocol for polymer /soluble extraction.

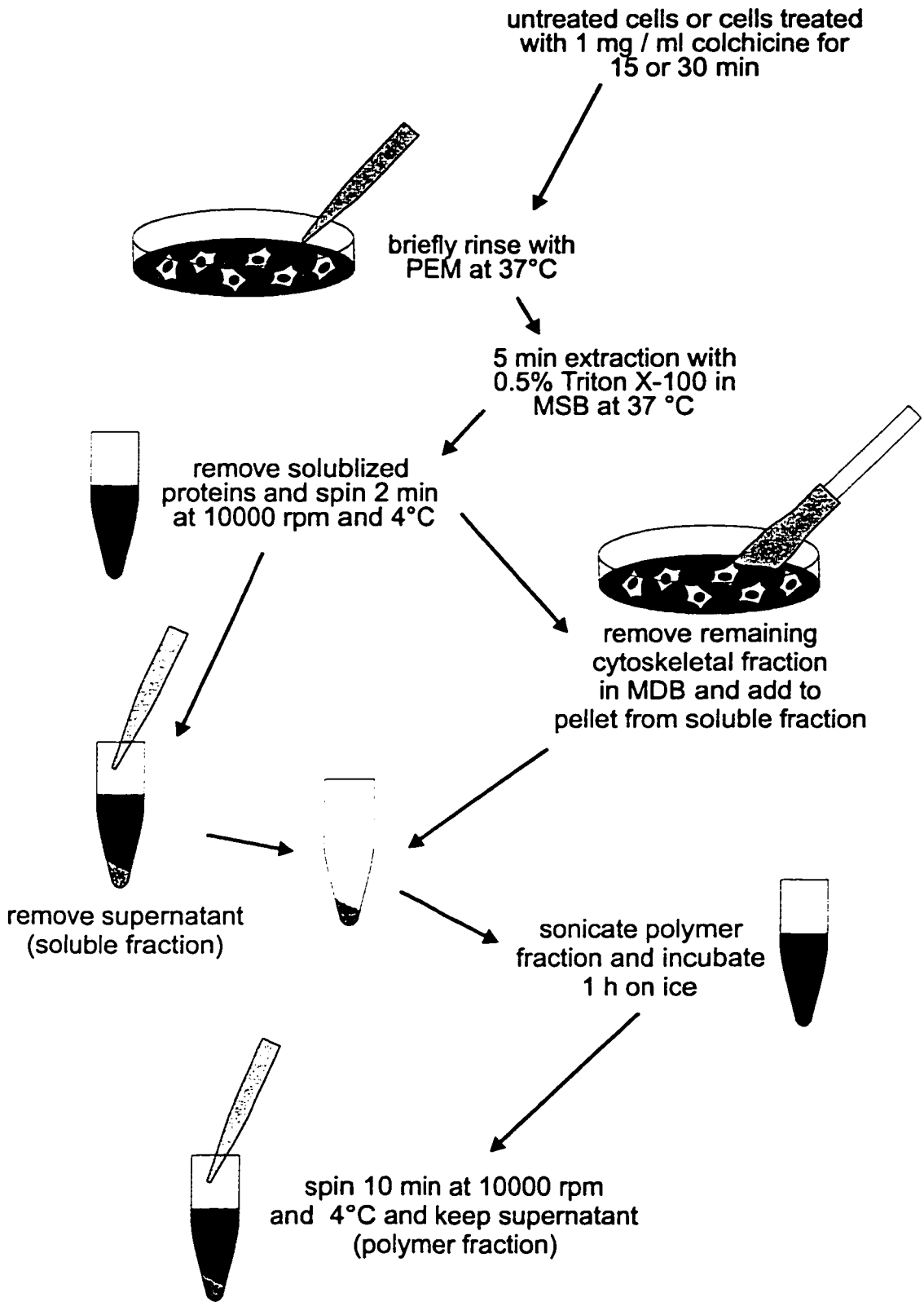
untreated cells or cells treated with 1 mg / ml colchicine for 15 or 30 min
briefly rinse with PEM at 37°C
5 min extraction with 0.5% Triton X-100 in MSB at 37 °C
remove solublized proteins and spin 2 min at 10000 rpm and 4°C
remove remaining cytoskeletal fraction in MDB and add to pellet from soluble fraction
remove supernatant (soluble fraction)
sonicate polymer fraction and incubate 1 h on ice
spin 10 min at 10000 rpm and 4°C and keep supernatant (polymer fraction)

For all samples, protein concentrations were determined using the BCA protein assay (PIERCE) using BSA (PIERCE) as a standard diluted in ddH_2O. Controls were included using buffer alone.

CYCLING OF TUBULIN AND MAPS FROM BOVINE BRAIN (FIG 20)

This procedure is derived from Weingarten *et al.* (1975) and Collins and Vallee (1987). Two fresh adult bovine brains were obtained from the C.H. Thomas slaughter house (Nepean, Ontario) and kept submerged in ice water while the connective tissues and meninges were removed. The brains were then homogenized in a Waring blender for 45 sec in 70% (v/w) chilled MAB1 (0.1 M PIPES, pH 6.4, 1 mM EGTA, 1 mM $MgCl_2$, 4 M glycerol and 0.1 mM GTP) and transferred to pre-chilled centrifuge bottles. The homogenate was then spun 10 min at 18000 g and 4°C (10000 rpm using a Sorval GSA rotor). The supernatant was transferred to new, pre-chilled centrifuge tubes and spun 30 min at 36000g and 4°C (18000 rpm using a Sorval SS-34 rotor). To this supernatant (designated S1) GTP was added to a final concentration of 1.8 mM and then incubated 30 min and 37°C. The now viscous S1 extract was spun 30 min at 36000g and 37°C. The pellet was resuspended in chilled MAB1 (15% of the volume used to homogenize whole brain tissue) and homogenized in a Dounce homogenizer on ice for 30 – 40 min. This homogenate was then spun 30 min at 36000g and 4°C. The supernatant (designated S2) was again brought to 1.8 mM GTP and incubated 30 min and 37°C. After spinning this supernatant (as for S1), the pellet was resuspended in 7 ml of chilled MAB1 and homogenized as for the S1 pellet. The S2 homogenate was then spun 30 min at 36000g and 4°C. The resulting supernatant was designated S3. Protein concentrations of S1, S2 and S3 were determined using the BCA assay and aliquots stored at -80°C for further use.

PHOSPHOCELLULOSE PURIFICATION OF TUBULIN (FIG. 21)

(Weingarten et al., 1975; Lee *et al.*, 1978) This procedure was used to provide a tubulin standard for the tubulin measurements performed in this study. A small volume of S3 (8 ml) was spun 20 min at 36000g and 4°C. The supernatant was then brought to 1.8 mM GTP and incubated 30 min and 37°C and then spun for

Figure 20

Protocol for cycling of tubulin and MAPs from bovine brain.

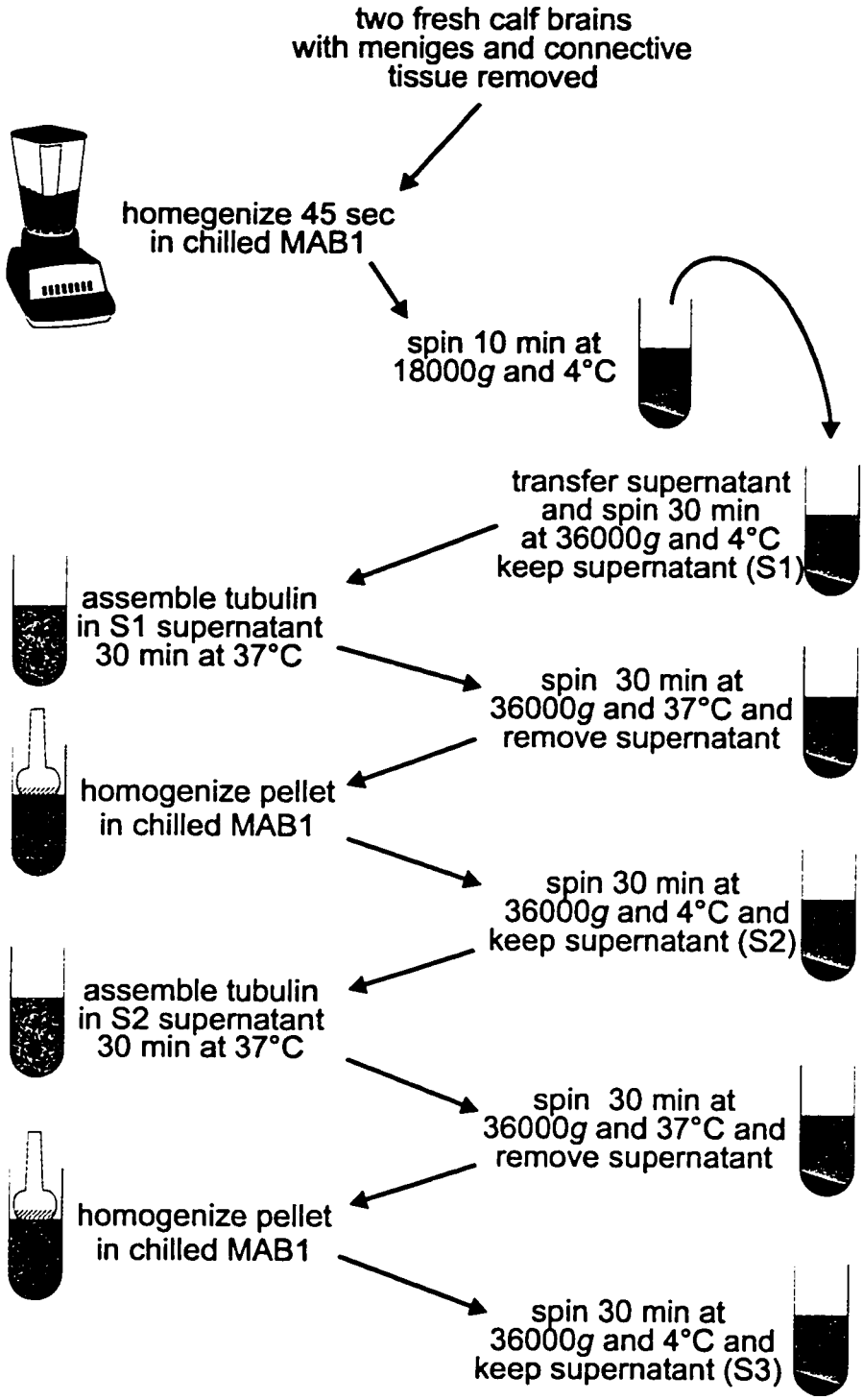
two fresh calf brains
with meniges and connective
tissue removed
homegenize 45 sec
in chilled MAB1
spin 10 min at
18000g and 4°C
transfer supernatant
and spin 30 min
at 36000g and 4°C
keep supernatant (S1)
assemble tubulin
in S1 supernatant
30 min at 37°C
spin 30 min at
36000g and 37°C and
remove supernatant
homogenize pellet
in chilled MAB1
spin 30 min at
36000g and 4°C and
keep supernatant (S2)
assemble tubulin
in S2 supernatant
30 min at 37°C
spin 30 min at
36000g and 37°C and
remove supernatant
homogenize pellet
in chilled MAB1
spin 30 min at
36000g and 4°C and
keep supernatant (S3)

Figure 21

Protocol for phosphocellulose purification of tubulin.

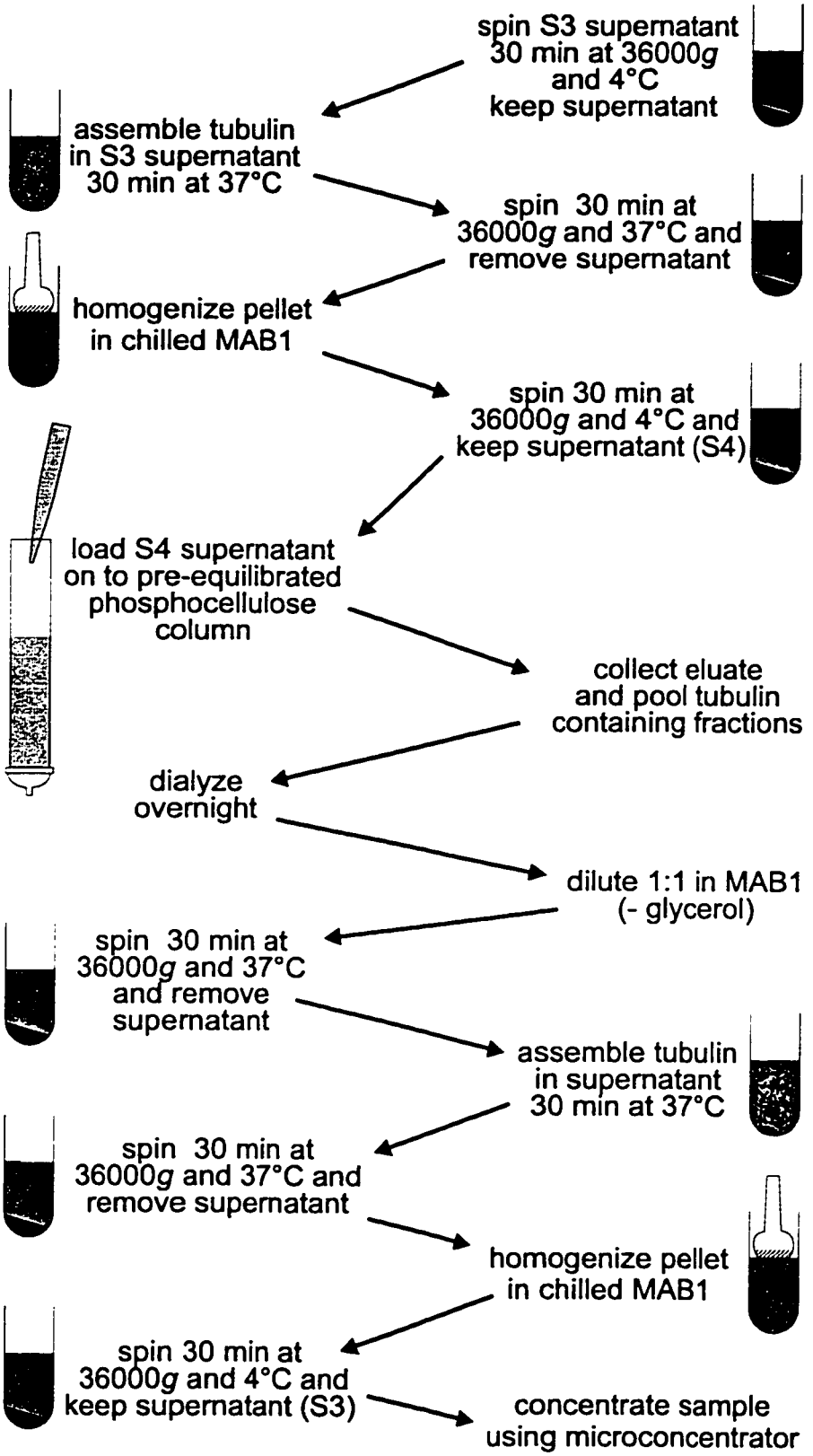
spin S3 supernatant
30 min at 36000g
and 4°C
keep supernatant
assemble tubulin
in S3 supernatant
30 min at 37°C
spin 30 min at
36000g and 37°C and
remove supernatant
homogenize pellet
in chilled MAB1
spin 30 min at
36000g and 4°C and
keep supernatant (S4)
load S4 supernatant
on to pre-equilibrated
phosphocellulose
column
collect eluate
and pool tubulin
containing fractions
dialyze
overnight
dilute 1:1 in MAB1
(- glycerol)
spin 30 min at
36000g and 37°C
and remove
supernatant
assemble tubulin
in supernatant
30 min at 37°C
spin 30 min at
36000g and 37°C and
remove supernatant
homogenize pellet
in chilled MAB1
spin 30 min at
36000g and 4°C and
keep supernatant (S3)
concentrate sample
using microconcentrator

30 min at 36000g at 37°C. The pellet was resuspended in 3.5 ml of MAB1 (- glycerol) on ice for 30 min and spun for 30 min at 36000g and 4°C. The supernatant (S4) was then loaded on to a phosphocellulose column (P-II, Whatman) preequilibrated with 5 column volumes of MAB (- glycerol) and eluted with MAB (- glycerol). The presence of tubulin in the collected fractions was analyzed by SDS-PAGE. Tubulin containing fractions were pooled and dialyzed overnight against 1 L of MAB1 (+ 8 M glycerol). The dialyzed tubulin was then diluted 1:1 with MAB1 (- glycerol) and spun for 20 min at 36000g and 4°C. The supernatant was brought to 1.8 mM GTP and 10 mM $MgCl_2$, incubated for 30 min and 37°C then spun 30 min at 36000g and 37°C. The resulting pellet was resuspended in MAB1 (-glycerol) and concentrated using a 30 kDa cutoff microconcentrator (Amicon). Protein concentration was determined using the BCA assay and aliquots were stored at -80°C.

IN VITRO MAP BINDING ASSAY (FIG 22)

Parts of this procedure are derived from the taxol-dependent purification of MAPs reported by Vallee (1982). 1 ml of S3 was brought to 1.8 mM GTP and 20 μm taxol, assembled for 30 min and 37°C and then spun 15 min at 36000g and 37°C (18000 rpm using a Sorval SS-20 rotor). The pellet was gently resuspended using a 1 ml pipetter in the same volume of MAB1 (+ 400 mM NaCl, 1.8 mM GTP and 20 μm taxol). The suspension was then spun for 15 min at 36000g and 37°C. The pellet was then resuspended in the same buffer and spun again as above. The supernatant was then spun through a 15% sucrose cushion in MAB1 (+ 1.8mM GTP and 20μm taxol) for 15 min at 36000g and 37°C. The pellet was then resuspended in MAB2 (+ 1.8 mM GTP and 20 μm taxol) and spun for 15 min at 36000g and 37°C. The pellet was then gently resuspended in MAB2 as above and to this suspension was added an equal volume of protein from transfected P19 EC cells, brought to 1.8mM GTP and 20μm taxol and incubated for 15 min and 37°C. The suspension was then spun 15 min at 36000g and 37°C. The resulting pellet was resuspended in MAB2 (+ 1.8mM GTP and 20μm taxol) and spun through a 15% sucrose cushion in MAB2 (+ 1.8 mM GTP and 20 μm taxol) for 15 min at 36000g and 37°C. The resulting pellet was resuspended in MAB2 (+ 1.8mM GTP and 20μm taxol).

Figure 22

Protocol for in vitro MAP binding assay. Steps are numbered for comparision with data in figures 43 and 44. Steps indicated with an * contain extracts from P19 EC cells expressing various MAP1a fragments..

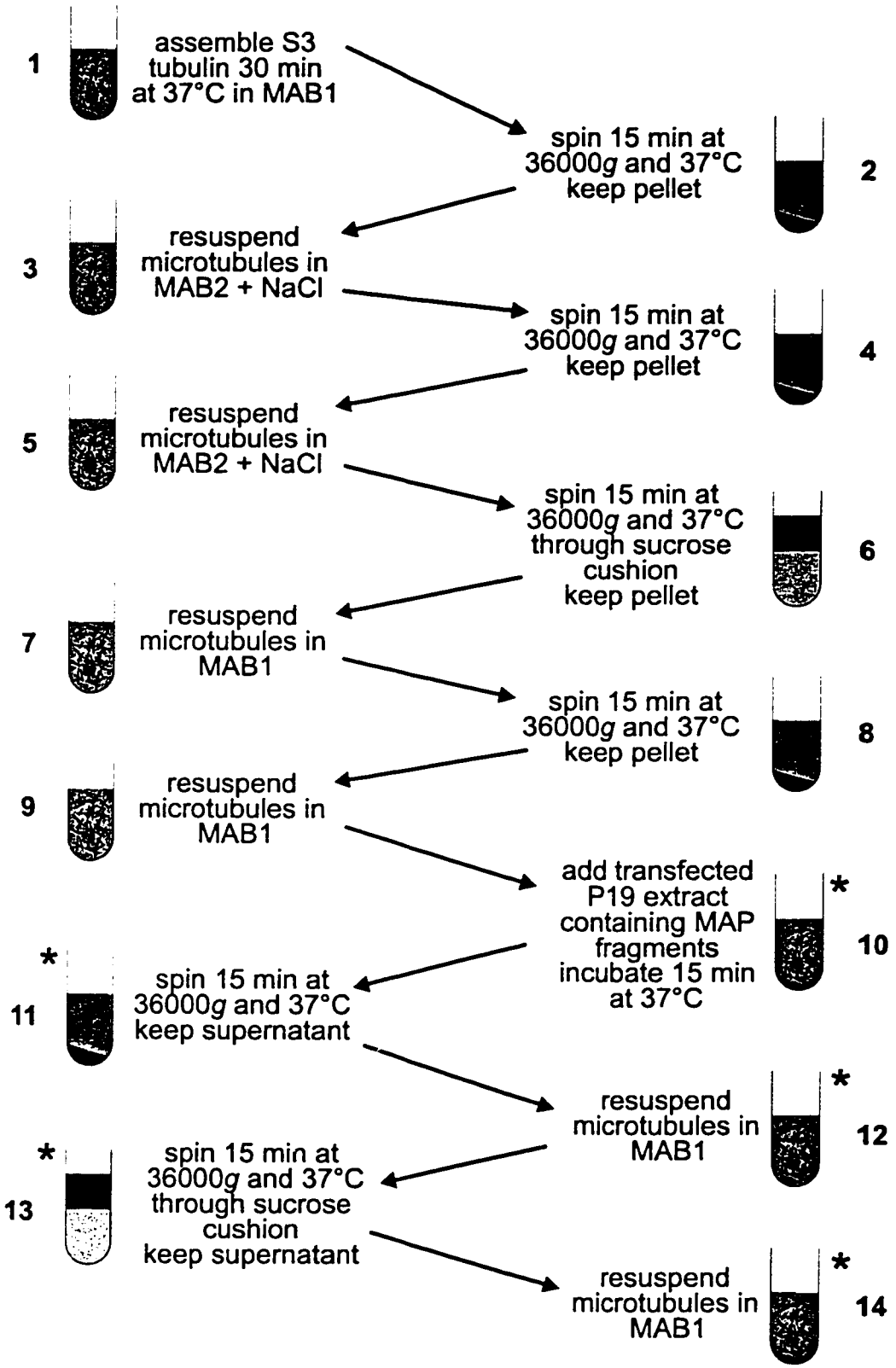
1
assemble S3 tubulin 30 min at 37°C in MAB1
spin 15 min at 36000g and 37°C keep pellet
2
3
resuspend microtubules in MAB2 + NaCl
spin 15 min at 36000g and 37°C keep pellet
4
5
resuspend microtubules in MAB2 + NaCl
spin 15 min at 36000g and 37°C through sucrose cushion keep pellet
6
7
resuspend microtubules in MAB1
spin 15 min at 36000g and 37°C keep pellet
8
9
resuspend microtubules in MAB1
add transfected P19 extract containing MAP fragments incubate 15 min at 37°C
*
10
*
11
spin 15 min at 36000g and 37°C keep supernatant
resuspend microtubules in MAB1
*
12
*
13
spin 15 min at 36000g and 37°C through sucrose cushion keep supernatant
resuspend microtubules in MAB1
*
14

Samples were taken throughout the procedure to determine the presence or absence of MAPs by western blotting. Volumes used to resuspend pellets were adjusted throughout the procedure to account for loss of volume due to sampling. Samples were processed for negative staining transmission electron microscopy from the first assembly step and after each spin through sucrose to ensure that MTs remained polymerized.

MICROAFFINITY PURIFICATION OF POLYCLONAL ANTIBODIES

LC1 and LC2 polyclonal antibodies (see below) were microaffinity purified as described in Xiang and MacRae (1995) prior to use.

10 μg / lane of S1 was separated by SDS –PAGE on 12% gels and transferred to nitrocellulose (NC, Schleicher & Schuell). 2 lanes of the blot were cut out and LC1 and LC2 were used to immunodetect light chains 1 and 2 by western blotting (see below). The location of these light chains was marked on the remaining blot and the region excised with a scalpel. The excised NC strips were washed 5 min in ddH_20 and then incubated in TBS-T [10 mM TRIS-HCl pH 7.4, 140 mM NaCl and 0.1% tween-20 (Sigma)] containing 5% skim milk (Carnation) for 2 h at RT. The strips were washed 3X10 min with TBS-T and then 1X5 min with TBS (without Tween 20). The blocked NC strips were then incubated in fresh TBS-T containing the antisera for light chain 1 or 2 diluted 1:500 for 3 h at RT with gentle agitation. The antibody solution was then decanted and the strips washed as above. NC-bound antibody was then eluted by washing 3X2 min in 350 μl of elution buffer (5 mM glycine, 500 mM NaCl, 0.5% tween-20, 100 μg / ml BSA, pH 1.8). The three eluted fractions were combined and neutralized with a 1 M TRIS solution.

ANTIBODIES

ANTI-MAP1a

Mouse monoclonal IgG_1 (clone 1A-1, Bloom *et al.*, 1984) provided by Dr. R. Vallee, Worcester Foundation, Mass. and used at 1:500 for immunofluorescence microscopy and 1:1000 for immunoblotting.

ANTI-MAP1b

Mouse monoclonal IgG (clone 6D4) provided by Dr. L. Binder and used at 1:30 for microscopy and 1:300 for immunoblotting.

Mouse monoclonal IgG (clone 1B-4, Bloom *et al.*, 1985) provided by Dr. R. Vallee and used at 1:1000 for immunoblotting

Anti-MAP2

Mouse monoclonal IgG [clone HM-2 (Sigma), Tucker *et al.*,1988) used at 1:400 for immunofluorescence microscopy and 1:1000 for immunoblotting.

ANTI-HMW-MAP2

Mouse monoclonal IgG (clone AP-14, Kalcheva *et al.*, 1994) provided by Dr. L. Binder (Molecular Geriatrics Corp, IL) and used at 1:200 for immunofluorescence microscopy and 1:1000 for immunoblotting.

ANTI-TAU

Mouse monoclonal IgG (clone Tau-2, Papasosomenos and Binder, 1987) provided by Dr. L. Binder and used at 1:1000 for immunoblotting.

ANTI-LIGHT CHAIN 1

Rabbit polyclonal Ig (LC-1) provided by Dr. J. Hammarback. Affinity purified (P-LC1) and used undiluted for immunoblotting.

ANTI-LIGHT CHAIN 2

Rabbit polyclonal Ig (LC-2) provided by Dr. J. Hammarback. Affinity purified (P-LC2) and used undiluted for immunoblotting.

ANTI-LIGHT CHAIN 3

Rabbit polyclonal Ig (LC-3, Mann and Hammarback, 1994) provided by Dr. J. Hammarback and used at 1:1000 for immunoblotting.

ANTI-β-TUBULIN

Mouse monoclonal IgG [clone DM1B (Amersham), Blose *et al.*, 1984], used at 1:1000 for immunoblotting.

ANTI-α-TUBULIN

Rat monoclonal IgG [clone $YOL^1/_{34}$ (Serotech), Kilmartin *et al.*, 1982] used at 1:10 for immunofluorescence microscopy.

ANTI-βIII-TUBULIN

Mouse monoclonal IgG (clone TuJ1, Moody *et al.*, 1989) provided by Dr. A. Frankfurter (University of Virginia, VA) and used at 1:50 for immunofluorescence microscopy and 1:500 for immunoblotting.

ANTI-ACETYLATED α-TUBULIN

Mouse monoclonal IgG [clone 6-11B-1 (Sigma) Piperno and Fuller, 1985] used at 1:100 for immunofluorescence microscopy and 1:1000 for immunoblotting.

ANTI-DETYROSINATED α-TUBULIN

Rabbit polyclonal Ig (anti-E, Xiang and MacRae, 1995) provided by Dr. T. MacRae (Dalhousie University, NB) and used at 1:250 for immunoblotting.

ANTI-6MYC TAG

Mouse monoclonal IgG (clone 9E10, Evan *et al.*, 1985) provided by Dr. C. Garner (Universitry of Albama, AL) and used undiluted for immunofluorescence microscopy and diluted 1:1 for immunoblotting.

ANTI-MOUSE IgG

Polyclonal donkey IgG conjugated to CY3 (Jackson) used at 1:400 for immunofluorescence

Biotinylated polyclonal horse IgG (Vector) used at 1:1000 for immunoblotting.

Biotinylated polyclonal goat IgG (Amersham) used at 1:1000 for ELISA.

ANTI-RAT IgG

Polyclonal donkey IgG conjugated to CY2 (Jackson) used at 1:100 for immunofluorescence microscopy.

Polyclonal donkey IgG conjugated to FITC (Sigma) used at 1:150 for immunofluorescence microscopy.

ANTI-RABBIT IgG

Biotinylated polyclonal goat IgG (Dimension) used at 1:1000 for immunoblotting

SDS-PAGE AND WESTERN BLOTTING

Protein samples were diluted 1:1 in 2X sample buffer (Laemmli, 1970) and were placed in a boiling water bath for 5 min, loaded onto 7.5, 12 or 4 - 20% gradient polyacrylamide gels and separated using the BIORAD minigel apparatus. Proteins were electroblotted onto NC according to Towbin *et al.* (1979) and the NC blots were rinsed in PBS (130 mM NaCl, 5 mM Na_2HPO_4, 1.5 mM KH_2PO_4, pH 7.4). Immunodetection of western blots was performed as follows: block ON in 5% skim milk (Carnation) in PBS and 4°C, 1 h incubation in primary antibody diluted in 2% skim milk in PBS, 1 h incubation in biotinylated secondary antibody in 2% skim milk in PBS, and 1 h incubation in biotinylated streptavidin-HRP (Amersham) diluted 1:5000 in PBS. A 3X5 min PBS wash was done between all antibody incubations (with 2% milk added between the primary and secondary). Antibody binding was detected by enhanced chemiluminescence (ECL) (Amersham) using Hyperfilm-ECL (Amersham). Except where noted, all steps were performed at room temperature. Exposed films were digitized at 400 dpi with a 12-bit dynamic range (interpolated to 8 bits) using a Hewlett-Packard 4c flatbed scanner. Digitized TIFF images were processed using Adobe Photoshop v4.0 and prepared for publication using Powerpoint 97 (Microsoft)

ENZYME-LINKED IMMUNOSORBENT ASSAY (ELISA)

The method of Voller *et al.* (1979) was used with several modifications. Equal amounts of SDS-whole cell extracted protein were diluted 6 to 8-fold in PBS to give a final protein concentration of 0.3 μg / μl and 100 μl / well of this solution was dried overnight onto Xenobind (Xenopore) 96 well plates. Antibody incubations were as described for western blotting followed by biotinylated streptavidin-HRP diluted 1:750. Antibody binding was detected using colour development with o-phenylenediamine (SIGMA). Absorbance was read at 490 nm using a Ceres UV 900 HDI microplate reader. A standard curve for mAb 1A-1 was established using serial dilutions of S1 supernatant.

QUANTITATIVE DOT BLOTTING

Protein samples were diluted in PBS and 200 μl / well was passed through NC in a 96 well Minifold apparatus (Schleicher & Schuell) which had been pre-wetted with 200 μl / well of PBS. After the entire sample had been passed through the nitrocellulose by a gentle vacuum, an additional 400 μl of PBS / well was passed through the NC. The NC was then removed from the apparatus, rinsed briefly in PBS and then fixed for 10 min in transfer buffer (25 mM TRIS, 190 mM glycine, 20% (v/v) MeOH). The blot was then re-equilibrated in PBS and processed as for western blotting. The resulting films were scanned at 200 dpi as above. The chemiluminescent signal from each dot in the digitized image was quantified using SigmaGel v1.0 (Jandel Scientific). These values were then imported into Excel 97 (Microsoft) and Sigmaplot v4.0 (Jandel Scientific) for analysis. Standard curves for all primary antibodies used were established either with S1 supernatant or with PC-tubulin to ensure that sample measurements fell within the linear response of the antibody used.

CELL FIXATION

Cells plated on glass coverslips were briefly rinsed in PEM and fixed at room temperature by three different protocols:

METHANOL

Cells were immersed in MeOH at –20°C for 20 min. Coverslips were then re-equilibrated with 3 X 20 min PBS washes.

PRECIPITATION

(Stefanini *et al.*, 1967) Coverslips were incubated for 1 h in Zamboni's fixative [14% picric acid (FISHER), 4% paraformaldehyde (JB EM Services Inc.) in 0.5 M Na_2HPO_4, 0.5 M NaH_2PO_4, pH 7.1] followed by a 3X5 min PBS wash, 5 min extraction with 0.5% Triton X-100 in PBS and a final 3X5 min PBS wash.

EXTRACTION / FIXATION

(Falconer *et al.*, 1992) Coverslips were rinsed briefly in PEM followed by 2 min pre-extraction with 0.2% Triton X-100 in PEM followed by 10 min fixation with 3.7% formaldehyde (BDH), 0.25% glutaraldehyde (JB EM Services Inc.) and 0.5% Triton X-100 in PEM, followed by 3X5 min PBS wash.

CRYOSECTIONING

Newborn and adolescent (120 g) Sprague-Dawley male rats were anethestized with a 0.088 ml / g intramuscular injection of Somnotol (MPC Pharmaceuticals). Rats were then perfused with 60 ml of PBS followed by 120 ml of fixative (see precipitation fixation method). Brains were removed, post-fixed for a further 90 min in the same fixative and then immersed in 10% sucrose (w / v) in PBS. After storage for at least 1 h at 4°C, sucrose-immersed brains were frozen using liquid CO_2 and 12 µm cryosections were taken at –14 to -19°C using a cyrotome (Microm). Sections were mounted on coated cs (0.5% gelatin, 0.005% chromium potassium sulfate) and stored at -80°C.

IMMUNOFLUORESCENCE MICROSCOPY

Following fixation, samples were quenched 3X4 min in 1 mg / ml $NaBH_4$ (BDH) in PBS followed by a 3X5 min PBS wash. All antibody incubations were for 1 h in PBS at room temperature with 3X5 min PBS washes after each incubation. For all labeling,

sequential primary and secondary incubations were used. Samples were visualized by one of three following methods:

IMMUNOFLUORESCENCE MICROSCOPY

Stained cells were visualized with a Zeiss Axophot epifluorescence microscope equipped with a 50 W Hg burner. Images were recorded on Ilford 400 ASA B&W film and printed on Ilford multigrade III paper. Prints were digitized at 400 dpi and processed and prepared for publication as above.

CONFOCAL IMMUNOFLUORESCENCE MICROSCOPY

Stained cells were visualized through a 63X Plan Apochromat (NA 1.4) and 40X objective on a Leica Upright Confocal Laser Scanning Microscope equipped with a 50 mW Ar / Kr mixed gas laser. Serial optical sections were digitally recorded every 1μm in TIFF files 512 pixels X 512 pixels with an 8 bit dynamic range. The pinhole was adjusted so that the FWHM function yielded a section thickness no greater than 850 nm. Serial sections were processed using the simulated fluorescence algorithm which projects highlights and shadows on the image stack, emphasizing depth cues. TIFF images were processed and prepared for publication as above.

DIGITAL FLUORESCENCE MICROSCOPY

Stained cells were visualized on a Zeiss Universal epifluorescence microscope equipped with a 50 W Hg burner. Images were digitally recorded with a Hammatsu integrating CCD camera using Metamorph v2.75 (Universal Imaging). TIFF images were processed and prepared for publication as above.

ELECTRON MICROSCOPY

Samples were fixed 1 min at 37°C in a equal volume of fixative (4% paraformaldehyde, 0.2% glutaraldehyde in MAB1 or MAB2, depending when the sample was taken). 5 μl of the sample was allowed to settle onto parlodion-coated 400 mesh copper grids (J.B. EM Services Inc) for 1 min. Grids were then washed with 5 drops of Photoflo solution [2 drops of Photoflo (Kodak) in 100 ml of ddH_2O], 5 drops of ddH_2O and then stained with 4 drops of 1% uranyl acetate. Samples were

then visualized on a Philips 201 transmission electron microscope. Images were recorded on KODAK Electron Image Film SO-163 and printed on Ilford multigrade III paper. Prints were digitized at 600 dpi and processed and prepared for publication as above.

EXPRESSION AND DISTRIBUTION OF MAPS IN DIFFERENTIATING P19 NEURONS

RESULTS

MAP EXPRESSION IN DIFFERENTIATING P19 NEURONS

To see if MAP expression patterns in differentiating P19 neurons matched those found in brain, the expression of MAP1b, MAP2 and tau was characterized, using βIII-tubulin to monitor neuronal differentiation. Figure 23 illustrates the time course of MAP expression during RA-induced P19 EC cell differentiation. Detection of MAP1b showed a single polypeptide at all stages that co-migrated with MAP1b from adult bovine brain. MAP1b was present in undifferentiated cells and during differentiation, MAP1b levels increased until day 6 after which its levels dropped. Three forms of LMW-MAP2 were detected during differentiation. The smallest form was first detected at day 4, reached its highest levels at day 8 and decreased afterwards. The intermediate form, while detectable at day 4, was less abundant than the smaller form. Its levels also increased, reaching a peak at day 10 and then declining. The largest form co-migrated with the single LMW-MAP2 form from adult bovine brain. It was first detectable at day 6, increased until day 10 and then dropped slightly afterwards. HMW-MAP2 was present as a single peptide that co-migrated with adult bovine HMW-MAP2. It was first detectable at day 6 and continually increased during differentiation. Two forms of tau were detected in P19 extracts. The smaller form was first detected at day 6 and increased steadily. The larger form co-migrated with the smallest tau form seen in adult bovine brain. It was detected at day 6, but was much lower in abundance than the smaller form and increased slightly during differentiation. βIII-tubulin was present as a single polypeptide that co-migrated with adult bovine βIII-tubulin. In undifferentiated cells βIII-tubulin was absent, but was first detected at day 4 after which it levels steadily increased.

The localization of these MAPs and tubulin in differentiating culture was determined by immunofluorescence microscopy. Control experiments showed no non-specific 2° Ab interaction (Fig. 24). In undifferentiated cells fixed with methanol, MAP1b colocalized with MTs (Fig. 25a, a'). In undifferentiated cells fixed by precipitation, MAP1b colocalized with MTs but a diffuse cytoplasmic staining was also observed

Figure 23

Expression of various MAPs during differentiation of P19 EC cells. SDS-whole cell extracts of differentiating P19 EC cells at days 0 to 12 following RA induction were separated by SDS-PAGE on 7.5% gels. MAPs and βIII-tubulin were immunodetected on western blots using monoclonal antibodies 6D4 (MAP1B), HM-2 (LMW- and HMW-MAP2), Tau-2 (juvenile and adult tau) and TuJ1 (βIII-tubulin). S1 denotes bovine brain extract as described in Materials and Methods.

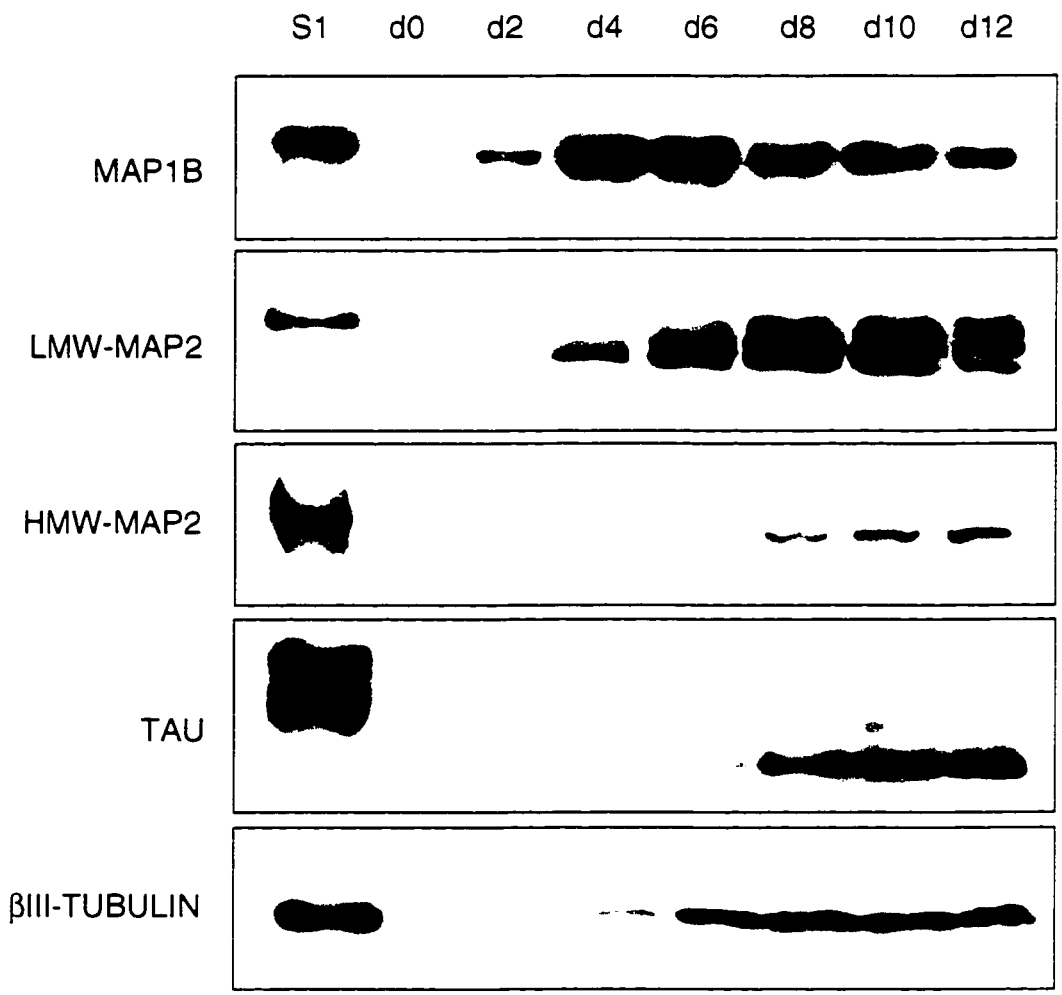
S1
d0
d2
d4
d6
d8
d10
d12
MAP1B
LMW-MAP2
HMW-MAP2
TAU
βIII-TUBULIN

Figure 24

Controls for non-specificity of secondary antibodies for MAP detection in differentiating P19 EC cells. Cells at day0 (a - a′) and day 12 (b - b′) were fixed by precipitation, quenched and then incubated with the secondary antibodies donkey anti-rat FITC (a, b) and donkey anti-mouse CY3 (a′ - b′). Scale bar = 20μm.

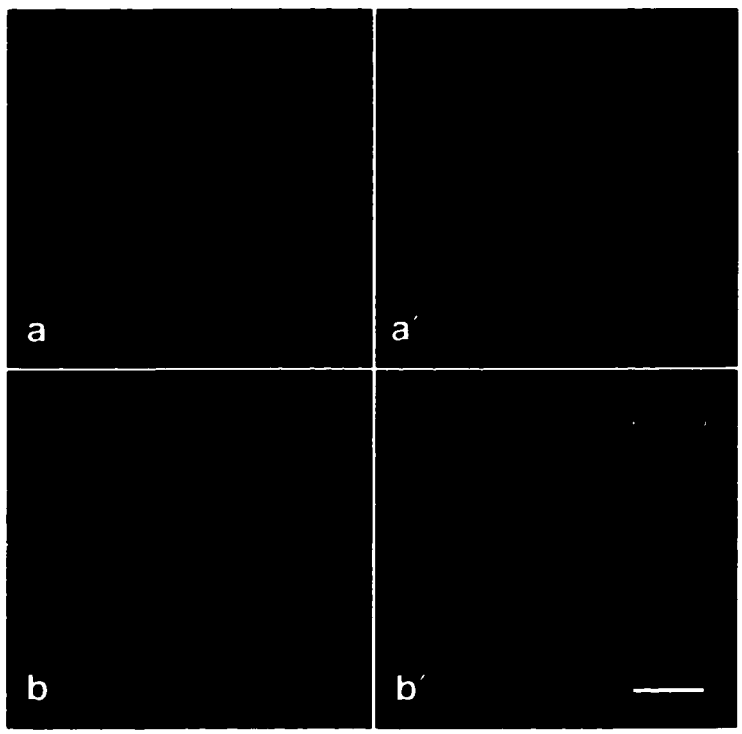
a
a´
b
b´

Figure 25

Detection of tubulin (m Ab YOL1/34, a – g) and MAP1b (mAb 6D4, a′ - g′) in differentiating P19 EC cells by double immunofluorescence microscopy. Cells at day 0 were fixed by methanol (a - a′) and precipitation (b - b′). Differentiating cells were fixed by precipitation. MAP1b is present on MTs (a – a′) and cytoplasmically (b – b′) in undifferentiated cells. MAP1b is present in spontaneously forming aggregates by day2 (c – c′) and is found in growth cones and colocalized with MTs in neurites by day 4 (d – d′). MAP1b remains present in neurites at day 6 (e – e′) and day 8 (f – f′) however, MAP 1b staining decreases by day 12 (g – g′). Scale bar for day 0 – 8 (f′) = 20μm and for day 12 (g′) = 100μm

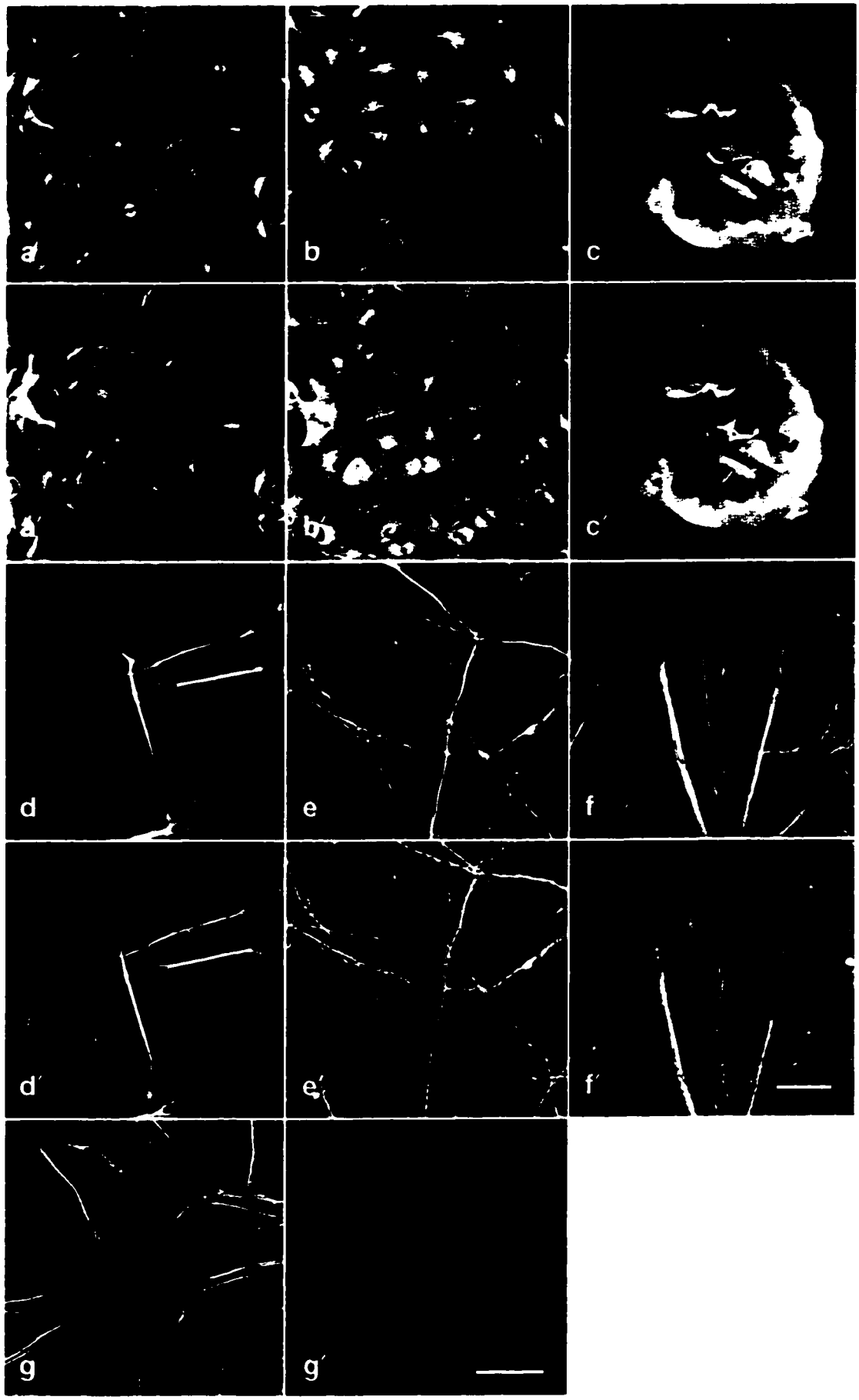
a
b
c
a'
b'
c'
d
e
f
d'
e'
f'
g
g'

Figure 26

Detection of tubulin (mAb YOL1/34, a – f) and MAP2 (mAb HM-2, a´ - f´) in differentiating P19 EC cells by double immunofluorescence microscopy. Cells were fixed by precipitation. MAP2 is absent in undifferentiated cells (a – a´) but is detectable in spontaneously forming aggregates by day2 (b – b´). By day 4 MAP2 is found in growth cones and colocalizes with MTs in neurites (c – c´). MAP2 remains present in neurites at day 6 (e – e´) and day 8 (f – f´) by day 12 (g – g´) MAP2 can be detected in all processes. Scale bar for day 0 – 8 (f´) = 20μm and for day 12 (g´) = 100μm

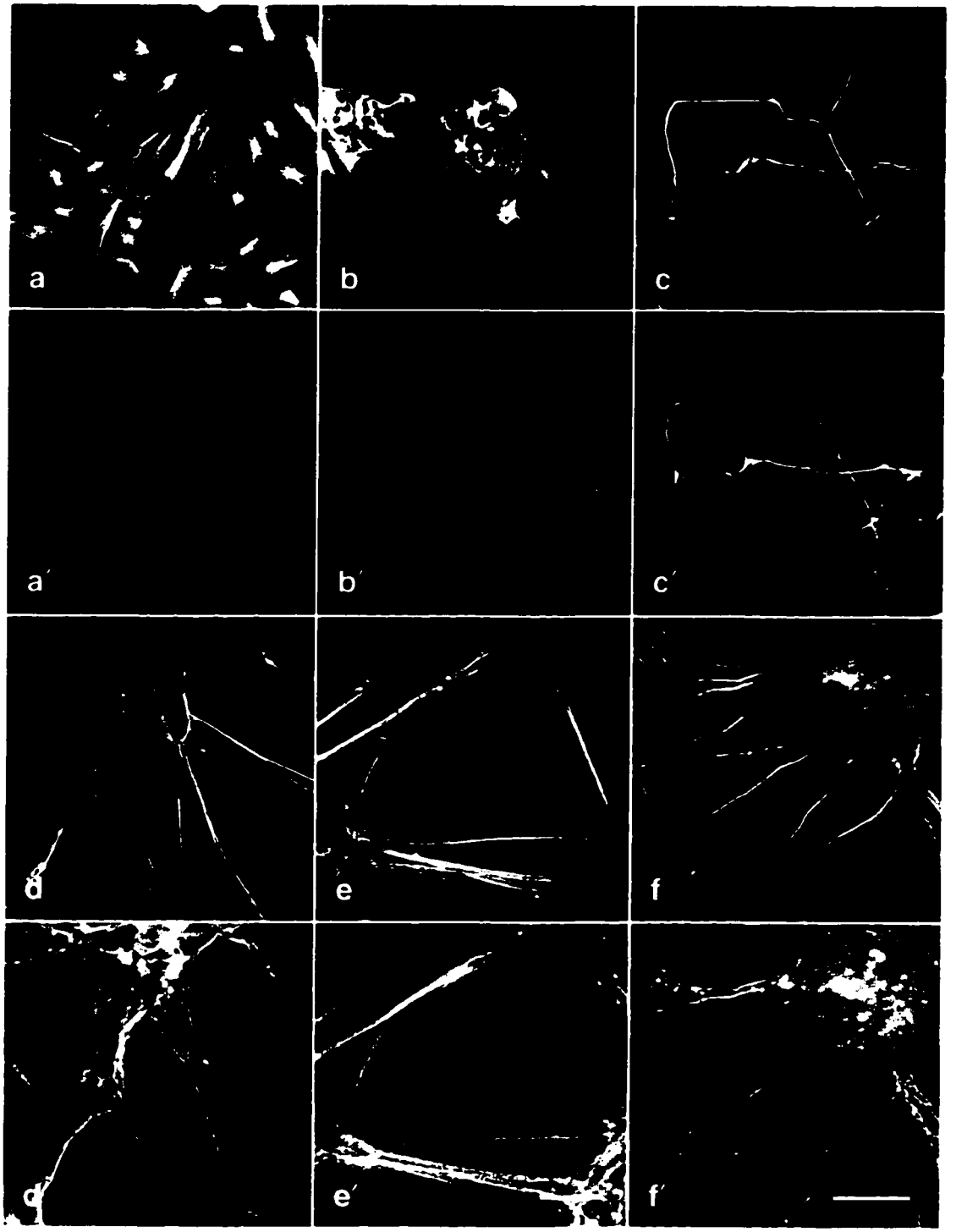
a
b
c
a'
b'
c'
d
e
f
d'
e'
f'

Figure 27

Detection of tubulin (mAb YOL1/34, a – f) and HMW-MAP2 (mAb AP14, a′ - f′) in differentiating P19 EC cells by double immunofluorescence microscopy. Cells were fixed by precipitation. HMW-MAP2 is absent in undifferentiated cells (a – a′) but is detectable in spontaneously forming aggregates by day 2 (b – b′). By day 4 HMW-MAP2 is restricted to proximal neurites where it colocalizes with MTs (c – c′). HMW-MAP2 is restricted to processes in aggregates at day 6 (e – e′) and day 8 (f – f′). By day 12 (g – g′) HMW-MAP2 staining is most prominent but is restricted to processes found in aggregates. Scale bar for day 0 – 8 (f′) = 20μm and for day 12 (g′) = 100μm

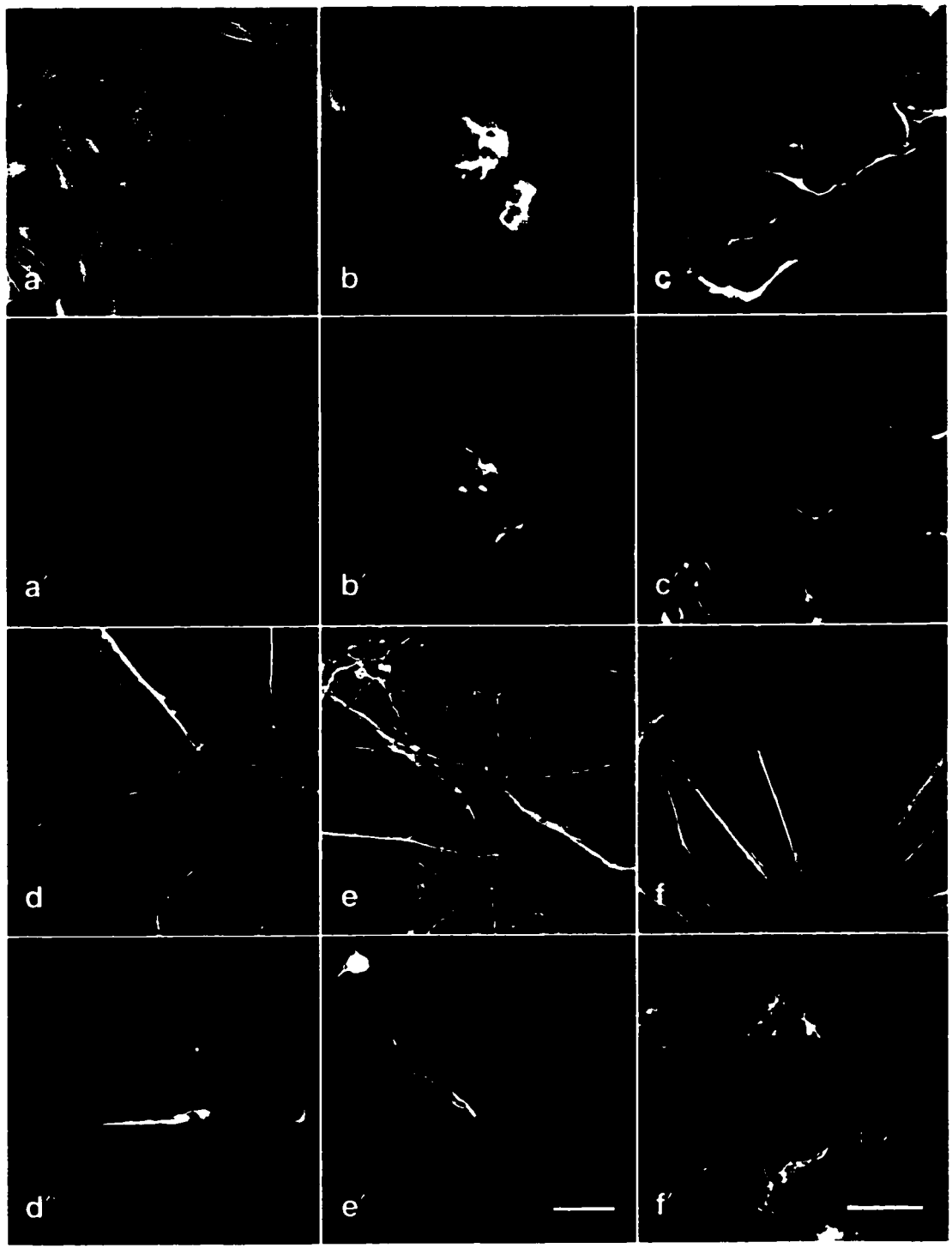
a
b
c
a'
b'
c'
d
e
f
d'
e'
f'

Figure 28

Detection of tubulin (mAb YOL1/34, a – f) and βIII-tubulin (mAb TuJ1, a′ - f′) in differentiating P19 EC cells by double immunofluorescence microscopy. Cells were fixed by precipitation. βIII-tubulin is absent in undifferentiated cells (a – a′) but is detectable in spontaneously forming aggregates by day2 (b – b′). By day 4 βIII-tubulin is found in growth cones and colocalizes with MTs in neurites (c – c′). βIII-tubulin remains present in neurites at day 6 (e – e′) and day 8 (f – f′) by day 12 (g – g′) βIII-tubulin can be detected in all processes. Scale bar for day 0 – 8 (f′) = 20μm and for day 12 (g′) = 100μm. From Vaillant and Brown, 1995 (Figure 1).

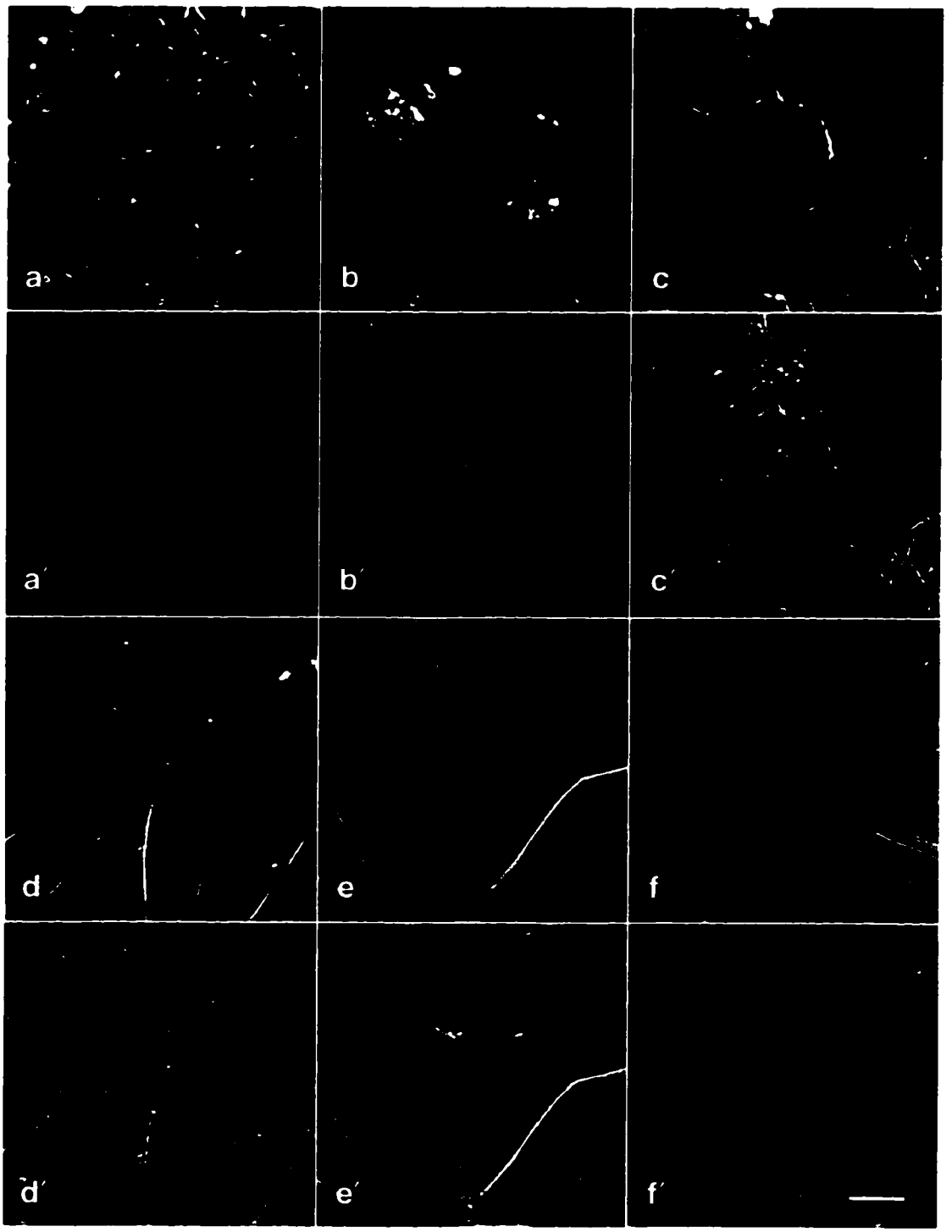
a
b
c
a′
b′
c′
d
e
f
d′
e′
f′

(Fig. 25b, b′). 2 days after RA-induction, cells spontaneously formed aggregates and within these aggregates, cells could be detected that displayed more intense α-tubulin labeling. These were the first cells in which an elevated level of MAP1b was detected (Fig. 25c, c′). After 4 days of differentiation, neurites with growth cones were detected. MAP1b was detected uniformly along the neurite shaft and in the growth cone in all neurites (Fig. 25d, d′). Between day 4 and day 8 of differentiation, there was a large increase in the number of processes present in the cultures. These processes were stained in a punctate fashion by MAP1b (Fig. 25e – f′). By day 12 no new neurite growth could be detected, but there was a reorganization of individual processes into fascicles. MAP1b labeled all fascicles, but the intensity of MAP1b was reduced compared to day 6 and day 8 (Fig. 25g, g′).

MAP2 was undetectable in undifferentiated cells (Fig. 26a, a′) but by day 2, MAP2 positive cells could be detected within aggregates (Fig. 26b, b′). At day 4 MAP2 was detected uniformly along the entire neurite shaft, and was also present in the growth cone (Fig. 26c, c′). At day 8 MAP2 was present in all neurites, but labeling was punctate along the neurite shaft (Fig. 26d – e′). At day 12 all processes were MAP2 positive (Fig. 26f, f′). HMW-MAP2 was also absent in undifferentiated cells (Fig. 27a, a′), and was first detectable within aggregates (Fig. 27b, b′) at day 2. However at day 4, HMW-MAP2 was most prevalent in proximal neurites, and was absent from growth cones (Fig. 27 c, c′). At day 6 and day 8 only a small proportion of cells were HMW-MAP2 positive, and these were restricted to aggregates (Fig. 27d – e′). By day 12 HMW-MAP2 labeling was most intense, but its restriction to aggregates was even more marked (Fig. 27f, f′).

βIII-tubulin also undetectable in undifferentiated cells (Fig. 28a, a′), but was present in cells within aggregates at day2 (Fig. 28b, b′). βIII-tubulin was detected in the entire neurite including the growth cone at day 4 (Fig. 28c, c′), and was present in all processes throughout differentiation (Fig. 28d – e′). Although more difficult to visualize, cell bodies within aggregates were also stained for βIII-tubulin. Almost all cells in the culture were βIII-tubulin positive by day 12.

MAP1A EXPRESSION IN UNDIFFERENTIATED P19 EC CELLS

Detection of MAP1a by immunofluorescence microscopy in undifferentiated cells was first attempted on cells fixed by methanol or precipitation (Fig. 29). In methanol-fixed cells, patchy immunoreactivity was observed in the nucleus. A diffuse cytoplasmic staining was observed in cells fixed by precipitation and no MT colocalization was observed. By confocal immunofluorescence microscopy of cells fixed by the extraction / fixation method, MAP1a was seen to colocalize with MTs in the mitotic spindle (Fig. 30b, b′). Faint MAP1a staining of MTs was detectable in the cytoplasm of some interphase cells, but in most cells it was not possible to see a definite colocalization (Fig. 30a, a′). A faint staining of the nucleus was also seen (Fig. 30a′). In an attempt to enhance the detection of MAP1a associated with MTs in interphase, cells were treated with 10^{-6} M taxol for 24 h to induce microtubule bundles. In the treated cells intense MAP1a reactivity colocalized with taxol-induced MT bundles (Fig. 30c, c′).

Western blotting of equal amounts of protein from SDS-whole cell, SDS-soluble and SDS-cytoskeletal fractions showed no effect of taxol treatment on MAP1a degradation (Fig. 31A, lanes 1-3). The partitioning of MAP1a into SDS-soluble and SDS-cytoskeletal fractions was identical in untreated and taxol-treated cells, with almost all the MAP1a present in the cytoskeletal fraction (Fig. 31A, lanes 4-7). To ensure that no MAP1a was lost due to precipitation from boiling, western blotting of the pellet fraction left after centrifugation was performed and showed no MAP1a was present in this fraction. ELISA showed no difference in the levels of MAP1a in SDS-whole cell protein in untreated cells, DMSO control cells and taxol treated cells (Fig. 31B) showing that taxol treatment did not increase the amount of MAP1a present in these cells.

MAP1A EXPRESSION IN DIFFERENTIATING P19 EC CELLS

After 4 days of RA-induced differentiation, MAP1a was seen in all growing neurites in the culture (Fig. 32a, a′). Labeling was observed uniformly along the entire neurite, colocalizing with MTs in the shaft of the neurite as well as in the proximal, but not in the distal, portions of the growth cones. At day 8, MAP1a was seen in all neurites (Fig. 32b, b′) and in fascicles at day 12 (Fig. 32c, c′), although the intensity of

Figure 29

Detection of tubulin (mAb YOL 1/34, a – b) and MAP1A distribution (mAb 1A-1, a′ - b′) in undifferentiated P19 EC cells by double immunofluorescence microscopy. Cells were fixed by methanol (a, a′) and precipitation (b, b′). In cells fixed by methanol MAP1a does not colocalize with MTs but is present in aggregates within nuclei (a′). In cells fixed by precipitation, MAP1a displays a diffuse cytoplasmic staining which does not colocalize with MTs (b′). Scale bar = 20μm.

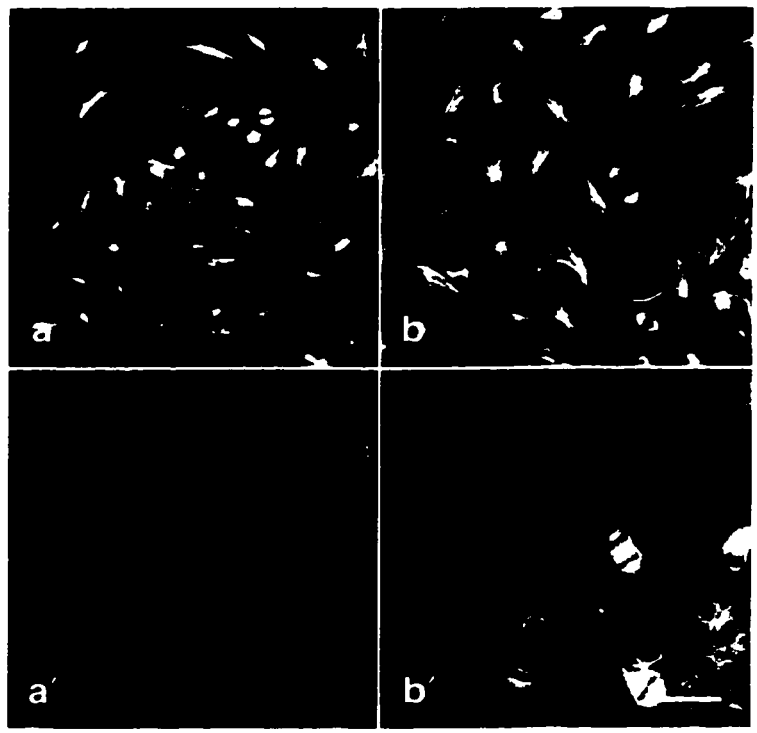
a
b
a´
b´

Figure 30

Detection of tubulin (mAb YOL1/34, a – c) and MAP1A (mAb 1A-1, a′ - c′) in undifferentiated P19 EC cells by confocal double immunofluorescence microscopy. Cells were fixed by extraction / fixation. A faint, non MT-colocalized cytoplasmic staining was detected in interphase cells (a – a′) but was colocalized with MTs in mitotic spindles (b - b′) and in 10^{-6}M taxol treated cells (c – c′). A faint nuclear MAP1a staining was observed in all cells (a′ - c′). Scale bar = 20μm. From Vaillant and Brown, 1995 (Figure 2).

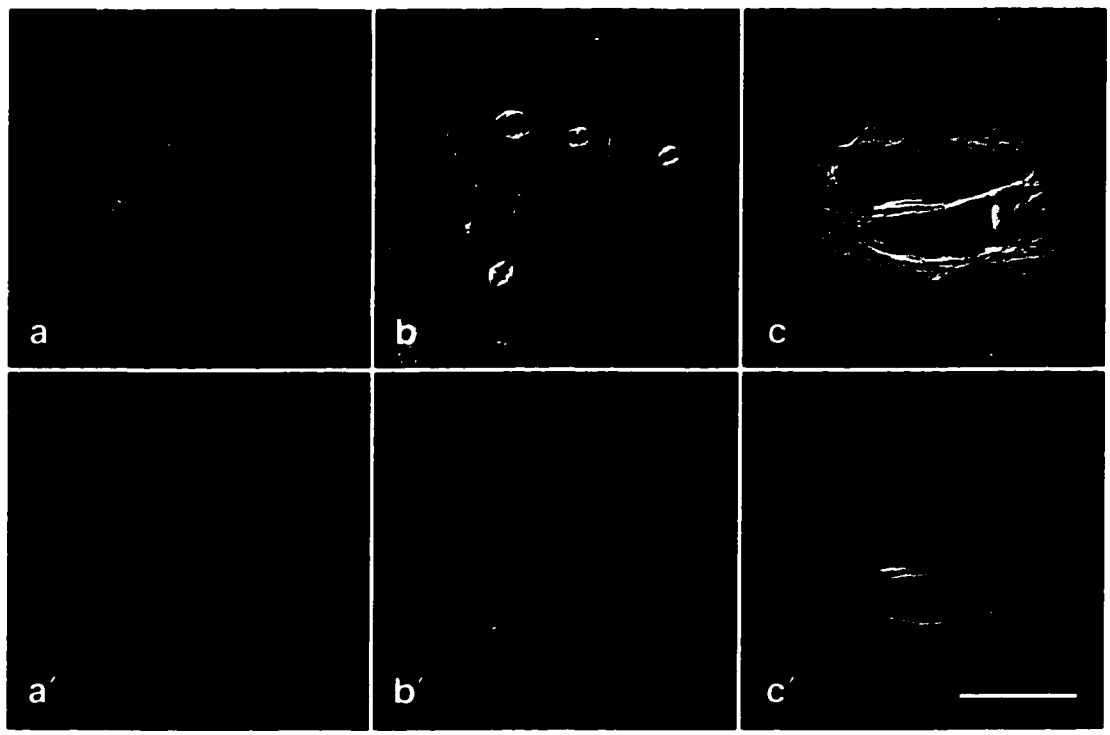
a
b
c
a´
b´
c´

Figure 31

MAP1A levels in undifferentiated cells. A) Protein extracts were separated by SDS-PAGE on 7.5% gels and MAP1A was immunodetected on western blots using mAb 1A-1. Lane 1: 30 μg of SDS-whole cell protein from untreated cells, lane2: DMSO control cells and lane 3: 10^{-6}M taxol-treated cells. Lane 4: 10 μg of untreated SDS-polymer and lane 5: SDS-soluble extracts. Lane 6: 10^{-6}M taxol-treated polymer and lane 7: soluble extracts. B) Quantification of MAP1A levels by ELISA of 30 μg of the same whole cell protein extracts as in (A) from untreated cells (U), DMSO control cells (D) and taxol-treated cells (T) using mAb 1A-1. Error bars represent the standard error of the averages of three measurements from three independent experiments. Effects of DMSO and taxol on MAP1a levels were not significantly different from untreated MAP1a levels as judged by the Student's t-test. From Vaillant and Brown, 1995 (Figure 3).

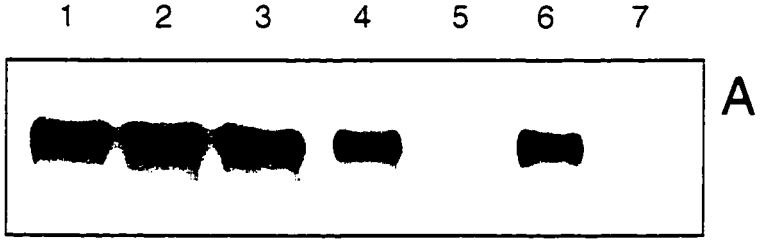
1
2
3
4
5
6
7
A

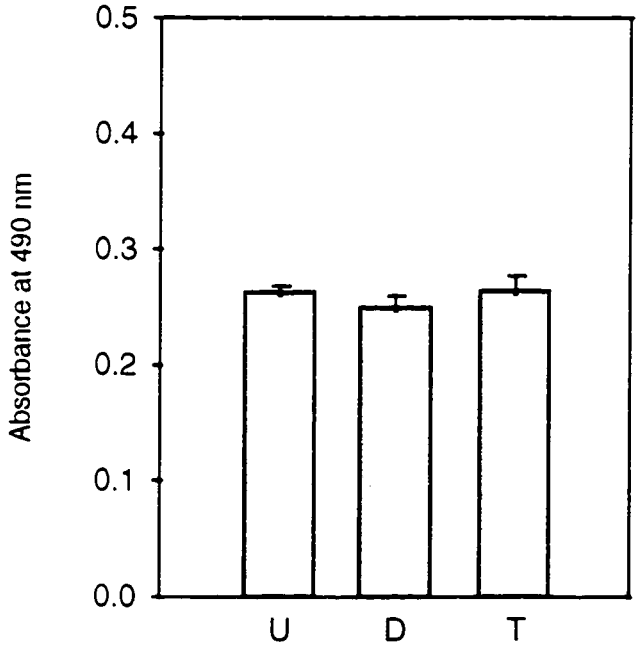
0.5
0.4
0.3
0.2
0.1
0.0
Absorbance at 490 nm
U
D
T

Figure 32

Detection of tubulin (mAb YOL 1/34, a – c) and MAP1A (mAb 1A-1, a´ - c´) in differentiating P19 EC cells by confocal double immunofluorescence microscopy. Cells were fixed by extraction / fixation. At day 4, MAP1a colocalizes with MTs along the entire neurite shaft and in the proximal growth cone (a, a´). By day 8 (b, b´) and day 12 (c, c´) MAP1a is still present in all neurites but staining is weaker than at day 4. Nuclear staining of MAP1a was detected at all days (a´ - c´). Scale bar = 20μm. From Vaillant and Brown, 1995 (Figure 4).

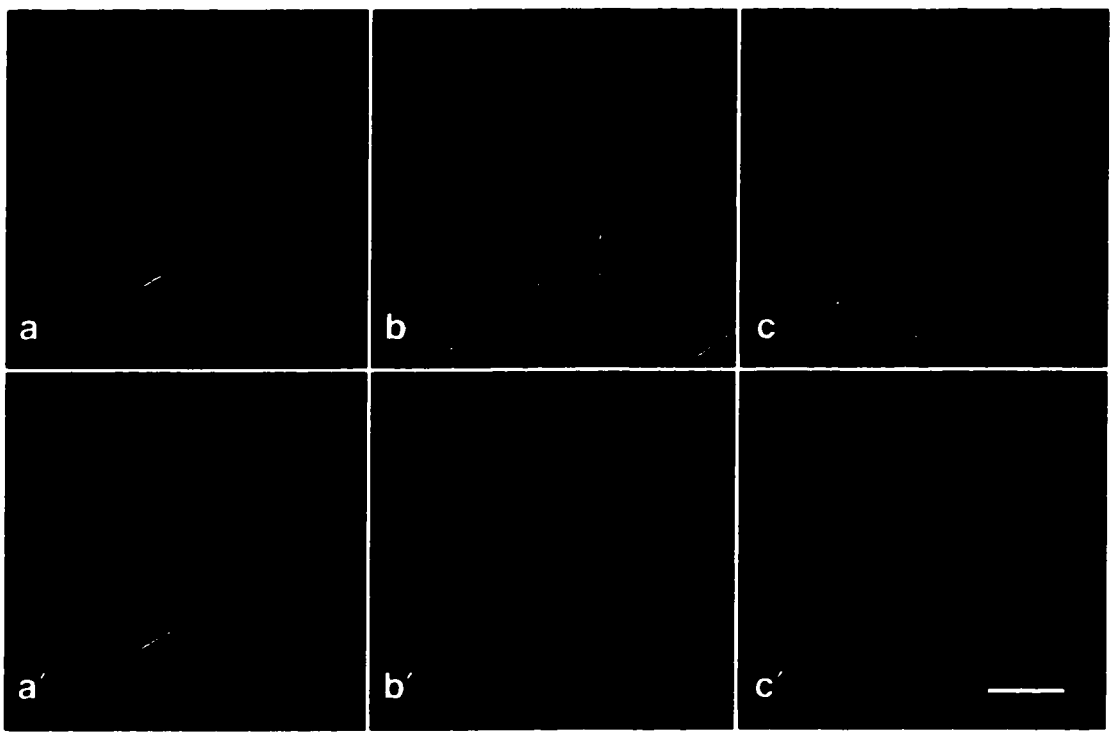
a
b
c
a′
b′
c′

Figure 33

MAP1A levels in differentiating P19 EC cells. 30μg of whole cell protein extract from cells at day 0 to 12 was separated by SDS-PAGE on 7.5% gels. MAP1A was immunodetected on western blots using mAb 1A-1. Results of 3 experiments are presented. From Vaillant and Brown, 1995 (Figure 5a).

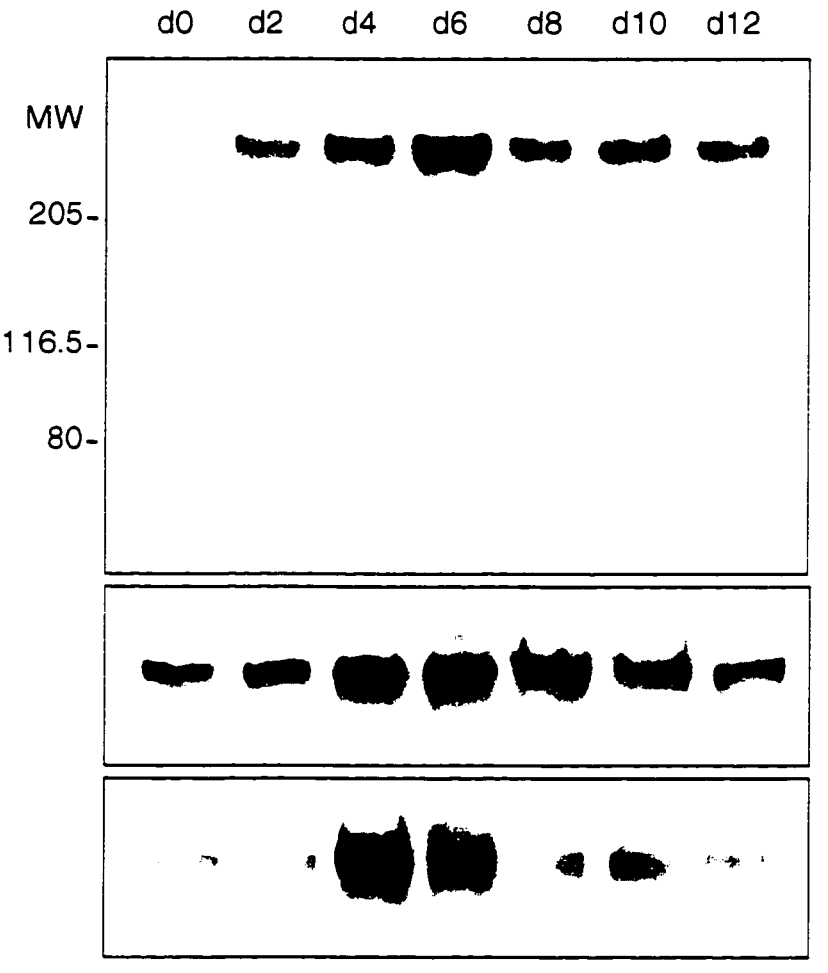
d0
d2
d4
d6
d8
d10
d12
MW
205-
116.5-
80-

Figure 34

Quantification of MAP1A levels in differentiating P19 EC cells. Detection of MAP1A by ELISA of 30μg of SDS-whole cell protein extract from cells at day 0 to 12 using mAb 1A-1. Results of 3 experiments are presented. Error bars represent the standard error of three measurements. *= values significantly different from day 0 ($p < 0.05$) as judged by the Student's t-test. From Vaillant and Brown, 1995 (Figure 5b).

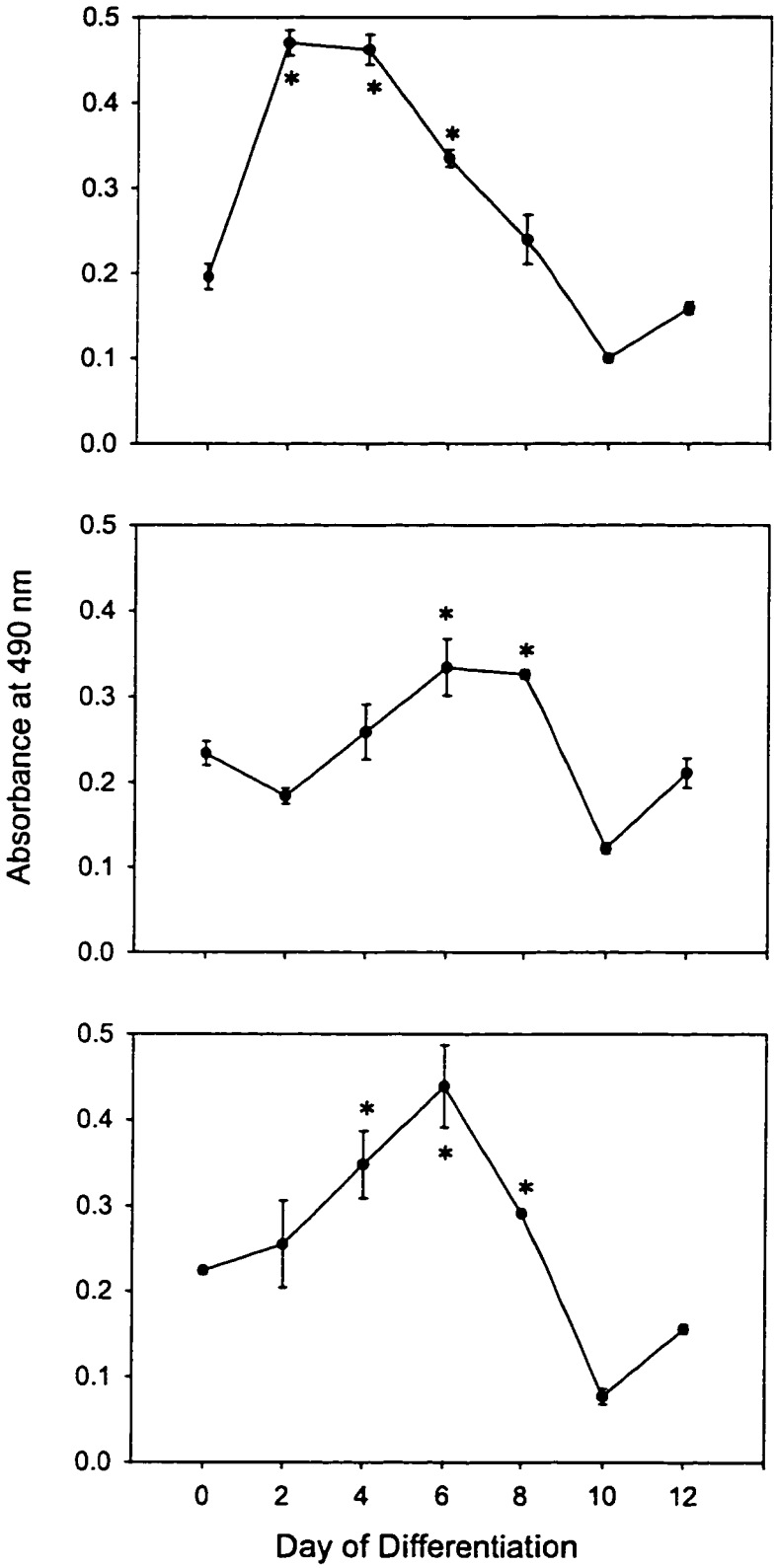
0.5
0.4
0.3
0.2
0.1
0.0
Absorbance at 490 nm
0 2 4 6 8 10 12
Day of Differentiation

staining was reduced compared to day 4. The faint nuclear staining observed in undifferentiated cells was also seen in differentiated cells.

Western blots of of whole cell protein from differentiating P19 EC cell cultures revealed a single band of approximately 350 kDa representing MAP1a (Fig. 33). The intensity of this reactive band increased and appeared to reach a peak no later than day 8, after which it became less intense. Similar results were obtained using an ELISA assay (Fig. 34) to determine the relative amounts of MAP1a present during differentiation. As seen in Figures 33 and 34 some variability in MAP1a accumulation was observed among trials, however, the highest levels of MAP1a accumulation always coincided with the period of neurite growth as assessed by phase contrast microscopy of live cultures (data not shown)

DISCUSSION

MAP EXPRESSION IN DIFFERENTIATING P19 EC CELLS

The general patterns of MAP1b, MAP2, tau and βIII-tubulin expression in P19 EC cells are similar to the established time course of expression of these MAPs in brain (Frankfurter et al, 1986; Tucker and Matus, 1988; Kosik *et al.*, 1989; Garner *et al.*, 1990; Oblinger and Kost, 1994). The presence of βIII-tubulin in almost all cells indicates that a large majority of differentiating P19 EC cells is neuronal by day 12. This is in agreement with MacPherson and McBurney (1995) who report that in serum-free differentiated P19 EC cultures, 90% of the cells are neuronal.

The various LWM-MAP2 forms observed during differentiation might be due to post-translational modification by phosphorylation or alternative splicing. Kindler and Garner (1994) observed the presence of an alternatively spliced form of MAP2c, MAP2d which contains an extra basic repeat and has an apparent molecular weight 4 kDa higher than MAP2c. MAP2d is glial cell specific and is present only in later stages of development (Doll *et al.*, 1993). In adult bovine brain only one LWM-MAP2 polypeptide was detected. Because MAP2c is a juvenile MAP and is largely absent in the adult (Crandall and Fischer, 1989) the single LMW-MAP2 form detected is probably MAP2d. The fact that that the largest form of LMW-MAP2 in differentiating P19 EC culture co-migrates with this single LMW-MAP2 form in adult bovine brain suggests that it is also MAP2d. This indicates the presence of glial

cells in differentiating P19 EC cells. This result is not surprising since the presence of glial cells in differentiating P19 EC cells has been previously noted (Jones-Villeneuve *et al.*, 1982; Cadrin *et al.*, 1988; Addison and Brown, unpublished data).

At day 12, neurites are present in fascicles that run between cell aggregates. These fascicles represent the bulk of processes in culture and contain βIII-tubulin and MAP2, indicating that they are neuronal. However, very few of these fascicles contain HMW-MAP2. The HMW-MAP2 present at day 12 is restricted to aggregates. HMW-MAP2 is found only in dendrites in developing brain (Tucker *et al.*, 1988c; Viereck *et al.*, 1988) while MAP2c is found in both axons and dendrites (Tucker *et al.*, 1988b, Viereck *et al.*, 1989). The differential localization of MAP2 and HMW-MAP2 at day 12 suggests that most of the processes observed at this time are axonal, with dendrites being confined to aggregates.

These observations demonstrate that serum-free differentiated P19 EC culture containing glial cells and a high proportion of neurons whose neurites undergo specialization into axons and dendrites. The similarities between MAP location and accumulation during developing P19 EC cells suggest that the underlying mechanisms responsible for neuronal morphogenesis in P19 EC cells and in brain are similar.

MAP1a IN UNDIFFERENTIATED P19 EC CELLS

Western blotting and immunofluorescence staining showed that MAP1a was expressed in undifferentiated P19 cells. These results agree with the observations of Bloom *et al.* (1984b) for a variety of other cell lines. The localization of MAP1a was dependent on the type of fixation used. Cells fixed by MeOH showed a sub-nuclear localization reminiscent of nucleoli while cells fixed by precipitation displayed a diffuse cytoplasmic localization. Fixation extraction of cells revealed a MT association in mitotic and taxol treated cells, and in interphase cells a weak diffuse nuclear staining was observed. The faint staining of MAP1a on interphase MTs in undifferentiated P19 cells might be due to extraction of the MAP1a by the detergent treatment for immunofluorescence staining, however the same protocol gave intense MAP1a staining of MTs in interphase 3T3 cells (data not shown). Bloom et al (1984b) also noted mitotic spindle and nuclear localization of MAP1a in HeLa cells. The fixation-

dependent localization in undifferentiated P19 EC cells suggests that MAP1a may also associate with cellular structures other than MTs. There is a precedent for nuclear MAPs. A tau isoform exists in the nucleolus and it may function in ribosomal biogenesis and rRNA transcription (Thurston *et al.*, 1996).

The association of MAP1a with the mitotic spindle may be a reflection of a cell cycle-dependent increase in MAP1a synthesis as suggested by Bloom *et al.* (1984b). Alternatively, the increased immunofluorescence staining may result from the higher concentration of MTs in the spindle. The effects of taxol treatment on undifferentiated P19 cells supports this explanation. MTs in taxol-induced bundles stained intensely for MAP1a. Western blotting and ELISA showed that the increased detection of MAP1a was not due to an increase in the amount of MAP1a present in the taxol-treated cells or to a shift in the partitioning of MAP1a between the soluble and cytoskeletal fractions.

MAP1a IN DIFFERENTIATING P19 EC CELLS

The pattern of MAP1a accumulation in differentiating P19 EC cells peaks during the growth of neurons and falls as differentiation progresses. This pattern is different from the steadily increasing levels of MAP1a obtained from extracts of developing whole brain (Schoenfeld *et al.*, 1989; Garner *et al.*, 1990. However, MAP1a levels in differentiating P19 EC cells are comparable to those in axons of the cerebellum and corticospinal tract during brain development (Schoenfeld *et al.*, 1989). Since the majority of processes in differentiating P19 EC cells appear to be axonal (see above), this pattern of MAP1a expression may reflect an axon-specific profile.

The peak in MAP1a levels during neurite outgrowth and the presence of MAP1a in all neurites during the growth phase in these cultures suggests a growth-related function. The stability of MTs in differentiating P19 EC cultures increases during differentiation (Laferrière and Brown, 1996) even after the peak in MAP1a occurs. *In vitro* assembly studies have shown that MTs assembled with MAP1a are more dynamic than those assembled with MAP2 (Pedrotti and Islam, 1994). These observations suggest MAP1a is not a large contributor to the stabilization of MTs during the later stages of neuronal differentiation and that MAP1a functions to antagonize the MT stability induced by MAP2 and tau in mature neurons. The specific

localization of MAP1a in dendrites may play a role in the plasticity observed in these processes (Frederich and Asódi, 1991).

HETEROLOGOUS EXPRESSION OF MAP1a IN P19 EC and HeLa CELLS

RESULTS

EXPRESSION OF MAP1a FRAGMENTS IN P19 EC AND HeLa CELLS

All MAP1a fragments used in this study are shown in Figure 35. To ensure that all fragments were being expressed correctly, their expression was analyzed by western blotting using mAb 9E10 to detect myc tagged proteins. In P19 EC (Fig. 36A) and HeLa (Fig. 36B) cells all of the fragments displayed mobilities within 5-10 kDa of their predicted molecular weights, except for PGK-6myc1a, which had an apparent mobility of ~360 kDa (compared to its predicted size of 312 kDa). However, this is not unexpected since endogenous MAP1a migrates at ~350 kDa and has a predicted molecular weight of 299 kDa (Langkopf *et al.*, 1992). The amounts of individual fragments decreased as the size of the fragments increased. The bands seen in all lanes (P19 and HeLa cells) at 118 and 70 kDa represent non-specific, get artifacts (data not shown) and immunoreactive bands from 52 – 30 KDa represent MAP1a fragment degredation. In HeLa cell extracts, endogenous human c-myc was detected by the 9E10 antibody (see Fig 35B *).

DETECTION OF MAP1a FRAGMENTS WITH mAb 1A-1

To see if any of the expressed fragments could be detected with mAb 1A-1, western blots from transfected P19 EC were probed with mAb 9E10 (Fig. 37A) and mAb 1A-1 (Fig. 37B). In all lanes, the endogenous MAP1a could be detected. A second band was detected in the extract from PGK-6mycN1a-4 transfected cells which displayed a mobility identical to the MAP1a fragment present (see Fig. 37A).

Confocal immunofluorescence microscopy was used to detect MAP1a in P19 EC and HeLa cells expressing 6myc1a. In all P19 EC cells, a weak diffuse staining was seen (Fig 38a′) which represents the normal staining pattern of endogenous MAP1a in undifferentiated cells. In P19 EC cells expressing 6myc1a, there was an increase in the signal compared to untransfected cells and MT colocalization was easily seen (Fig 38a′). In HeLa cells no MAP1a was detected, except in 6myc1a

Figure 35

Schematic showing the various MAP1a fragments used in this study. The cDNA (with important restriction enzymes and cDNA clones used) and the wildtype MAP1a protein are provided for comparison. The predicted molecular weights for each fragment are provided. *This predicted weight does not include LC2, see Materials and Methods.

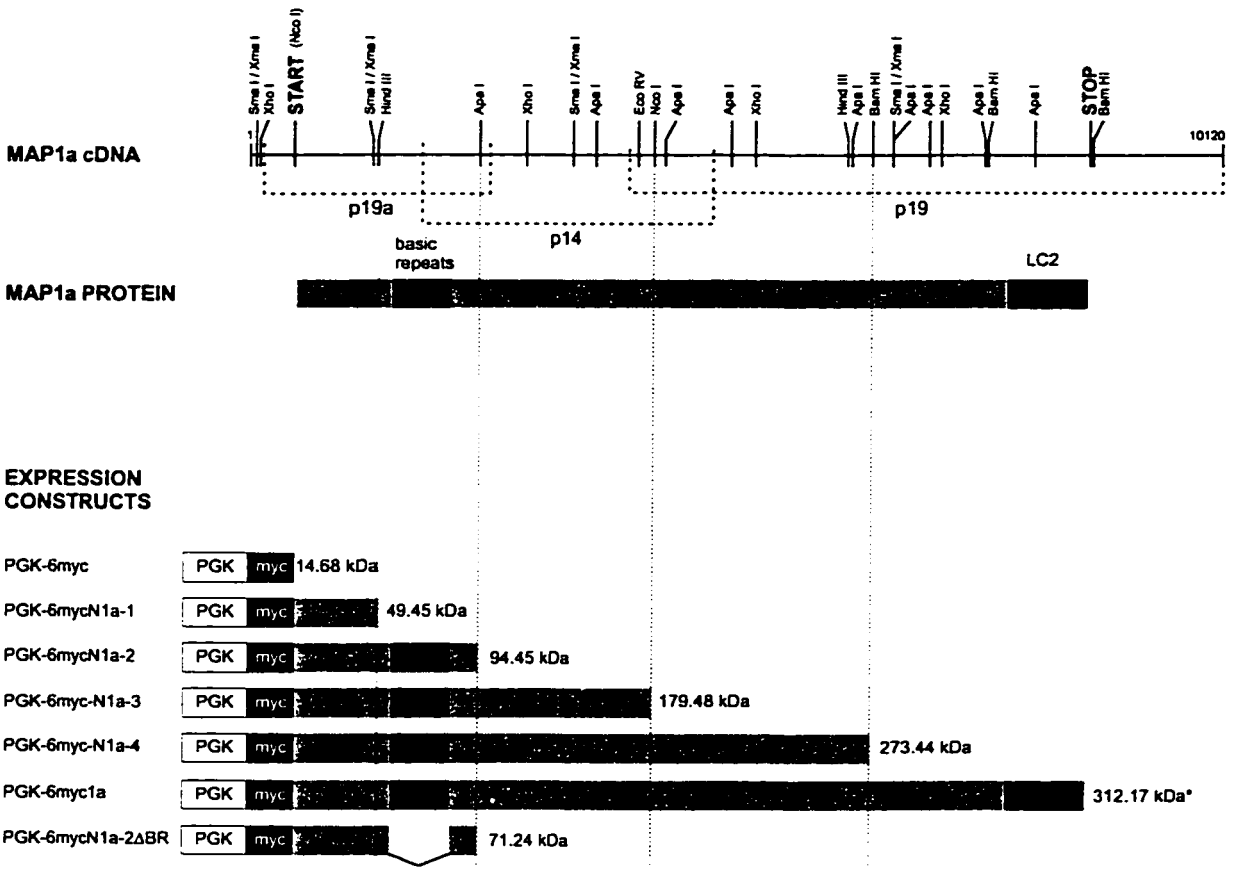
MAP1a cDNA
Sma I / Xma I
Xho I
START (Nco I)
Sma I / Xma I
Hind III
Ape I
Xho I
Sma I / Xma I
Ape I
Eco RV
Nco I
Ape I
Ape I
Xho I
Hind III
Apa I
Bam HI
Sma I / Xma I
Ape I
Ape I
Xho I
Ape I
Bam HI
Ape I
STOP
Bam HI
10120
p19a
p14
p19
basic repeats
LC2
MAP1a PROTEIN
EXPRESSION CONSTRUCTS
PGK-6myc
PGK
myc
14.68 kDa
PGK-6mycN1a-1
49.45 kDa
PGK-6mycN1a-2
94.45 kDa
PGK-6myc-N1a-3
179.48 kDa
PGK-6myc-N1a-4
273.44 kDa
PGK-6myc1a
312.17 kDa*
PGK-6mycN1a-2ΔBR
71.24 kDa

Figure 36

Detection of 6myc – tagged MAP1A fragments in transfected P19 EC (A) and HeLa (B) cells. 20μg (P19) or 10μg (HeLa) of transfected SDS-whole cell extracts were separated by SDS-PAGE on 12% gels. 6myc-tagged fragments were immunodetected on western blots using mAb 9E10. * Indicates endogenous human c-myc expression in HeLa cells. Molecular weight markers (MW) are in kD.

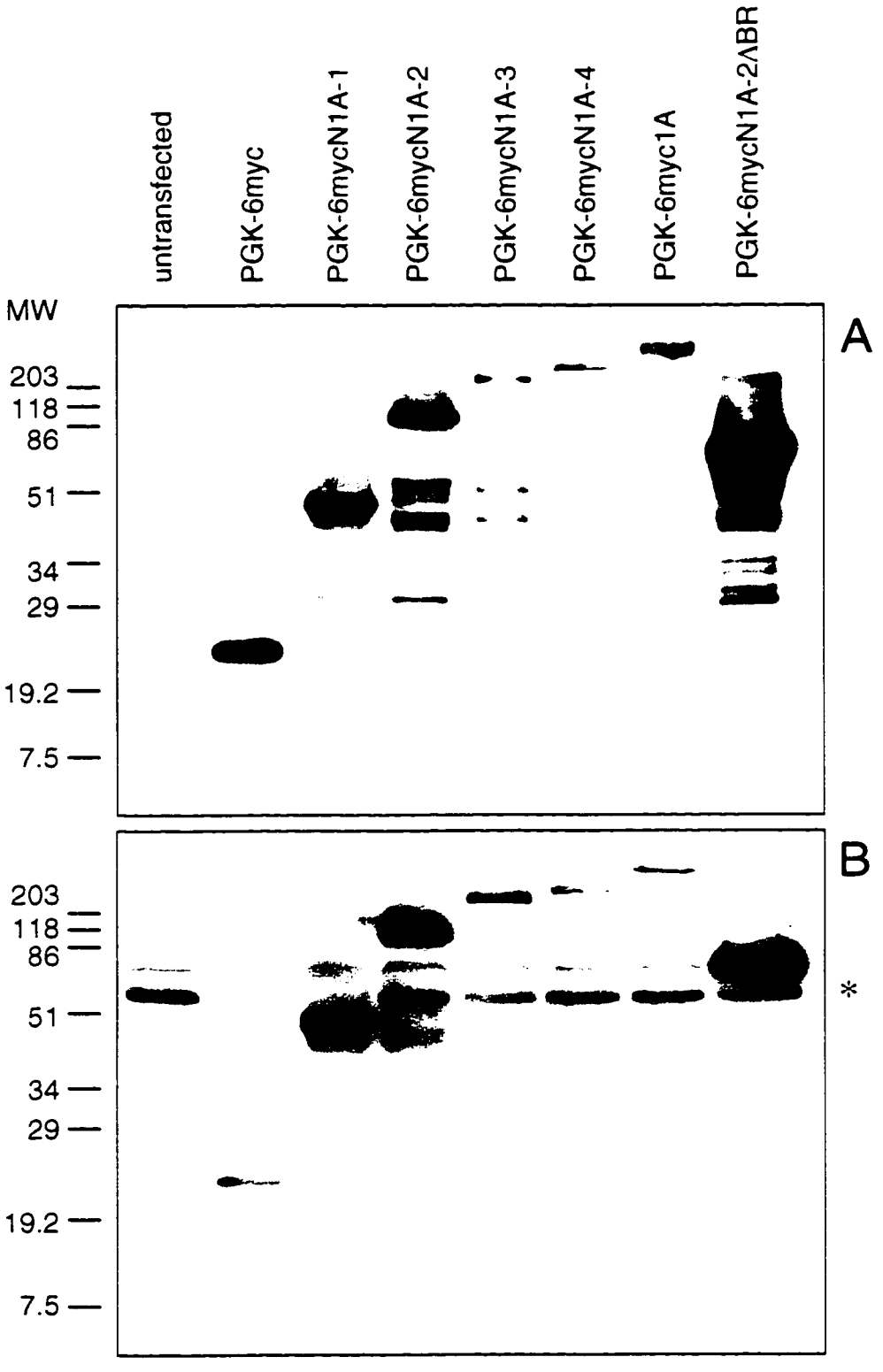
untransfected
PGK-6myc
PGK-6mycN1A-1
PGK-6mycN1A-2
PGK-6mycN1A-3
PGK-6mycN1A-4
PGK-6myc1A
PGK-6mycN1A-2ΔBR
MW
203
118
86
51
34
29
19.2
7.5
A
B
*

Figure 37

Detection of 6myc-tagged MAP1A fragments expressed in P19 EC cells. 20μg of transfected whole cell extracts were separated by SDS-PAGE on 7.5% gels. 6myc-tagged fragments were immunodetected on western blots using mAb 9E10 (A) and MAP1A was immunodetected using mAb 1A-1 (B). Molecular weight markers (MW) are in kD.

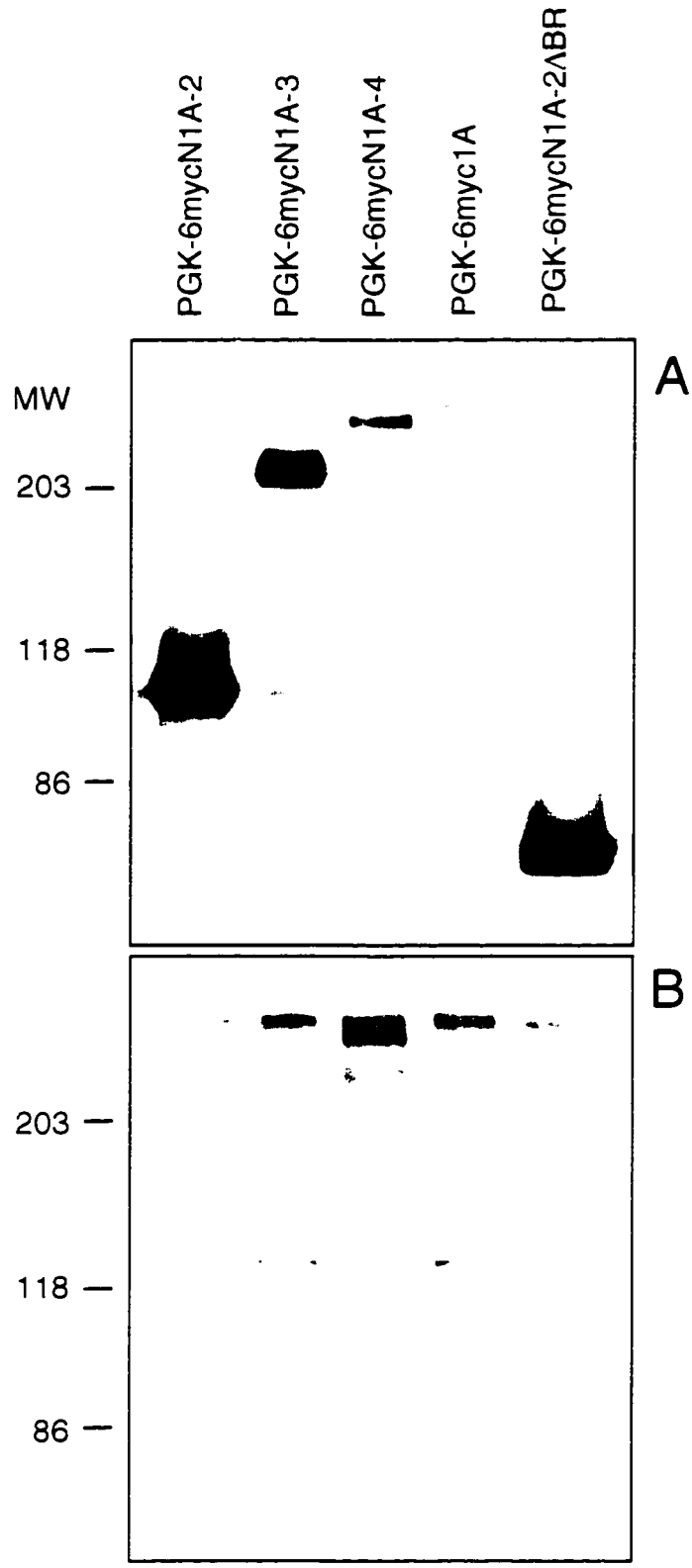
PGK-6mycN1A-2
PGK-6mycN1A-3
PGK-6mycN1A-4
PGK-6myc1A
PGK-6mycN1A-2ΔBR
MW
203
118
86
A
B
203
118
86

Figure 38

Detection of tubulin (mAb YOL1/34, a - b) and MAP1a (mAb 1A-1, a´ - b´) in 6myc1A expressing P19 EC (a, a') and HeLa cells (b, b') by confocal double immunofluorescence microscopy. Cells were fixed by the extraction / fixation method. Endogenous MAP1a is detected in P19 cells and 6myc1A expressing cells show a more intense staining that colocalizes with MTs (a, a´). In HeLa cells, no MAP1a is detected except in 6myc1A expressing cells, where it colocalizes with MTs (b, b´). Scale bar = 20μm

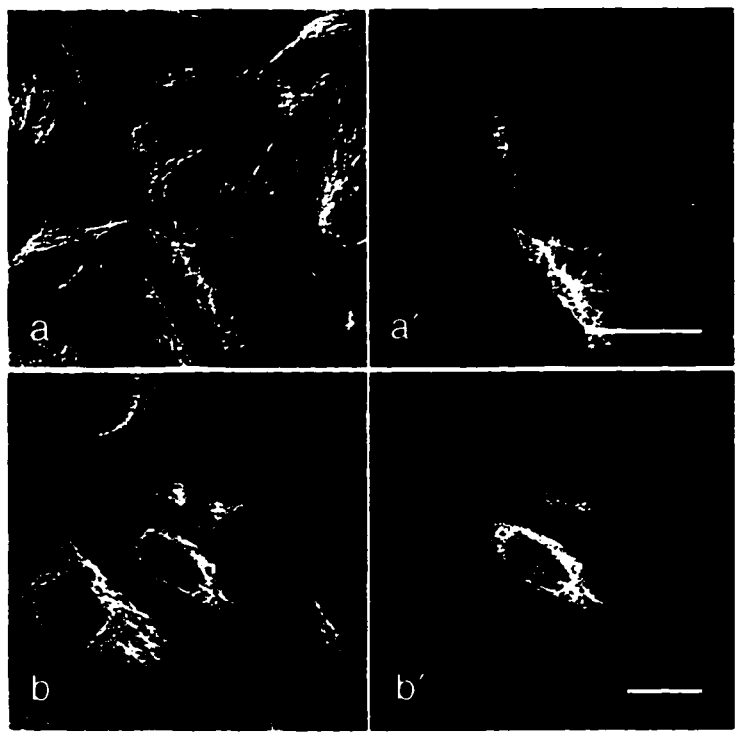
a
a'
b
b'

transfected cells where MAP1a colocalized with MTs (Fig. 38b′). This shows that the full length MAP1a was expressed in frame and suggests that MAP1a was in its native conformation in these cells.

ANALYSIS OF MYC-TAGGED MAP1a FRAGMENT BINDING

To determine which fragments of MAP1a bound to MTs, transfected P19 EC and HeLa cells were observed by confocal immunofluorescence microscopy. Cells were fixed by precipitation so that expression of myc-tagged MAP1a fragments could be monitored even if they did not bind MTs. The extraction \ fixation method was used to determine if a particular fragment was bound to MTs.

Cells expressing 6myc prepared by precipitation showed a diffuse myc staining in the cytoplasm (Fig. 39a′, 40a′). The MTs in the transfected cells showed a normal cytoplasmic interphase organization and appeared identical to that of untransfected cells (Fig. 39a, 40a). Extraction / fixation of cells expressing 6myc, showed no myc labeling (Fig. 39h′, 40h′) and similar results were obtained for cells expressing 6mycN1a-1 (Fig. 39b, b′, i, i′, 40b, b′, i, i′) showing that the tagged protein did not remain bound to MTs.

6mycN1a-2 expressing cells prepared by precipitation showed diffuse cytoplasmic staining, similar to 6myc and 6mycN1a-1 (Fig. 39c′, 40c′). MTs in these cells were also unaffected (Fig. 39c, 40c). However, extraction / fixation of 6mycN1a-2 expressing cells showed the myc tag colocalized with MTs (Fig. 39j, j′, 40j, j′). Similar results were obtained for cells expressing 6mycN1a-3 (Fig 39d, d′, k, k′, 40d, d′, k, k′), 6mycN1a-4 (Fig. 39e, e′, l, l′, 40e, e′, l, l′), 6myc1a (Fig. 39f, f′, m, m′, 40f, f′, m, m′) and 6mycN1a-2ΔBR (Fig. 39g, g′, n, n′, 40g, g′, n, n′) showing that all of these fragments bound to MTs and that the MT distribution was unchanged compared to untransfected cells. These results are summarized in Table 1.

In a few P19 EC cells expressing high levels of the 6myc1a, as judged by the intensity of myc labeling, process outgrowth was observed (Fig. 41). No process outgrowth was observed in transfected HeLa cells with any of the fragments of MAP1a.

Figure 39

Detection of tubulin (YOL 1/34, a – n) and 6myc tagged MAP1A fragments (mAb 9E10, a´ - n´) in transfected P19 EC cells by confocal double immunofluorescence microscopy. Cells were fixed by precipitation (a - g') or by extraction / fixation (h - n'). 6myc and 6mycN1a-1 were present following precipitation (a, a´; b, b´) but absent after extraction / fixation (h, h´; i, i´), 6mycN1a-2 was present after precipitation (c, c´), but was also found colocalized with MTs following extraction / fixation (j, j´). Behavior similar to 6mycN1a-2 was observed for 6mycN1a-3 (d, d', k, k'), 6mycN1a-4 (e, e', l, l'), 6myc1a (f, f', m, m') and 6mycN1a-2ΔBR (g, g', n, n'). Scale bar = 20μm.

Figure 40

Detection of tubulin (YOL 1/34, a – n) and 6myc tagged MAP1A fragments (mAb 9E10, a´ - n´) in transfected HeLa cells by confocal double immunofluorescence microscopy. Cells were fixed by precipitation (a - g') or by extraction / fixation (h - n'). 6myc and 6mycN1a-1 were present following precipitation (a, a´; b, b´) but absent after extraction / fixation (h, h´; i, i´), 6mycN1a-2 was present after precipitation (c, c´), but was also found colocalized with MTs following extraction / fixation (j, j´). Behavior similar to 6mycN1a-2 was observed for 6mycN1a-3 (d, d', k, k'), 6mycN1a-4 (e, e', l, l'), 6myc1a (f, f', m, m') and 6mycN1a-2ΔBR (g, g', n, n'). Scale bar = 20μm.

Figure 41

Confocal immunofluorescence microscopy of process outgrowth in 6myc1a expressing P19 EC cells. Cells were fixed by extraction / fixation. Tubulin was detected using mAb YOL1/34 (a) and 6myc1a was detected using mAb 9E10 (a'). Scale bar = 20μm.

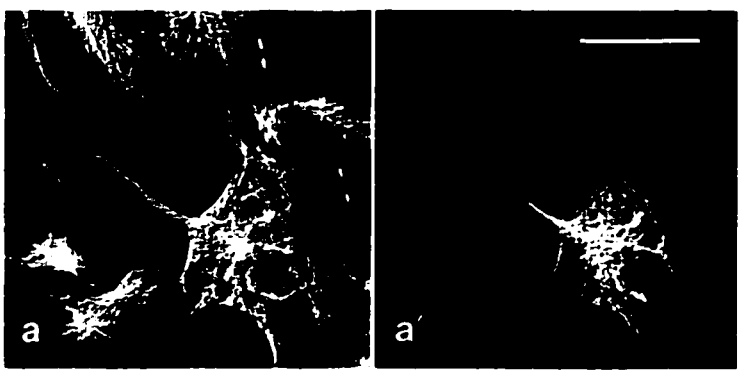
a
a'

TAXOL TREATMENT OF TRANSFECTED P19 EC CELLS

To see if the lack of detection of the 6myc tag and 6mycN1a-1 was due to low levels of fragments present after extraction / fixation, transfected P19 EC cells were treated with taxol to induce MT bundles. This has been shown to enhance the detection of low levels of MAP1a in undifferentiated P19 EC cells by concentrating the MT-bound protein (see previous section).

The MTs in taxol-treated cells were arrayed in thick bundles running through the cytoplasm (Fig. 42a, b). MT-associated 6myc or 6mycN1a-1 after extraction / fixation of taxol treated, transfected cells was never observed (Fig. 42a′, b′). As expected, extraction / fixation of cells expressing 6mycN1a-2 showed myc labeling which colocalized with the MT bundles present (Fig. 42c, c′). Similar results were obtained for 6mycN1a-3 (Fig. 42d, d′), 6mycN1a-4 (Fig. 42e, e′), 6myc1a (Fig. 42f, f′) and 6mycN1a-2ΔBR (Fig. 42g, g′).

IN VITRO MT BINDING OF MAP FRAGMENTS

To confirm the microscopic analysis of MAP fragment binding, an assay was devised to test the binding of MAP fragments to assembled MTs *in vitro* (see Materials and Methods and Fig. 22). In this procedure, two different sulfonate buffers were used (MAB1 and MAB2). Pedrotti *et al.*, 1993 showed that PIPES buffer (MAB1) resulted in loss of MAP1a from microtubules while MES buffer (MAB2) retained MAP1a bound to MTs. These buffers were used in succession to first remove as much endogenous MAP1a as possible and then, after exogenous fragments were added, keep all MAP1a present (exogenous and endogenous) bound to MTs. Immunoblot analysis indicated that tubulin was present throughout the procedure (Fig. 43A) and TEM showed this tubulin was assembled into MTs (Fig. 43c, d. e). Endogenous MAP1a, although at very high levels after the first assembly step (Fig. 43B, lane1), was mostly removed by the salt washes (Fig 43B, lanes 2 – 7). A small amount of MAP1a remained bound to MTs at the end of the procedure (Fig. 43B, lanes 9 - 14).

6myc and 6mycN1a-1 were absent from MTs following the final sucrose wash while6mycN1a-2, 6mycN1a-3 and 6mycN1a-2ΔBR were bound (Fig. 44, lane 14).

Figure 42

Detection of tubulin (YOL 1/34, a – g) and 6myc tagged MAP1A fragments (mAb 9E10, a´ - g´) in transfected, taxol treated P19 EC cells by confocal double immunofluorescence microscopy. Cells were fixed by extraction / fixation. 6myc and 6mycN1a-1 were not detectable after extraction / fixation (a, a´; b, b´) but 6mycN1a-2 was colocalized with MTs (c, c´). Behavior similar to 6mycN1a-2 was observed for 6mycN1a-3 (d, d´), 6mycN1a-4 (e, e´), 6myc1a (f, f') and 6mycN1a-2ΔBR (g, g'). Scale bar = 20μm.

Figure 43

In vitro MAP binding assay. Equal volumes of sample were taken from each step during the protocol (see Materials and Methods) and separated by SDS-PAGE on 12% (A) or 7.5% (B) gels. Immunodetection of tubulin with DM1B (A) or MAP1a with 1A-1 (B) on western blots shows the prevalence of tubulin and MAP1a during the procedure. Whole cell extracts from P19 EC cells expressing myc-tagged MAP1a fragments were added to MTs at step 10. Samples were negatively stained for transmission electron microscopy at steps 1 (c), 7 (d) and 14 (e) to show the presence of intact MTs throughout the entire procedure. Scale bar = 100nm. Figure 22 is reproduced here to facilitate comparison. * Steps that contain transfected P19 EC cell extract.

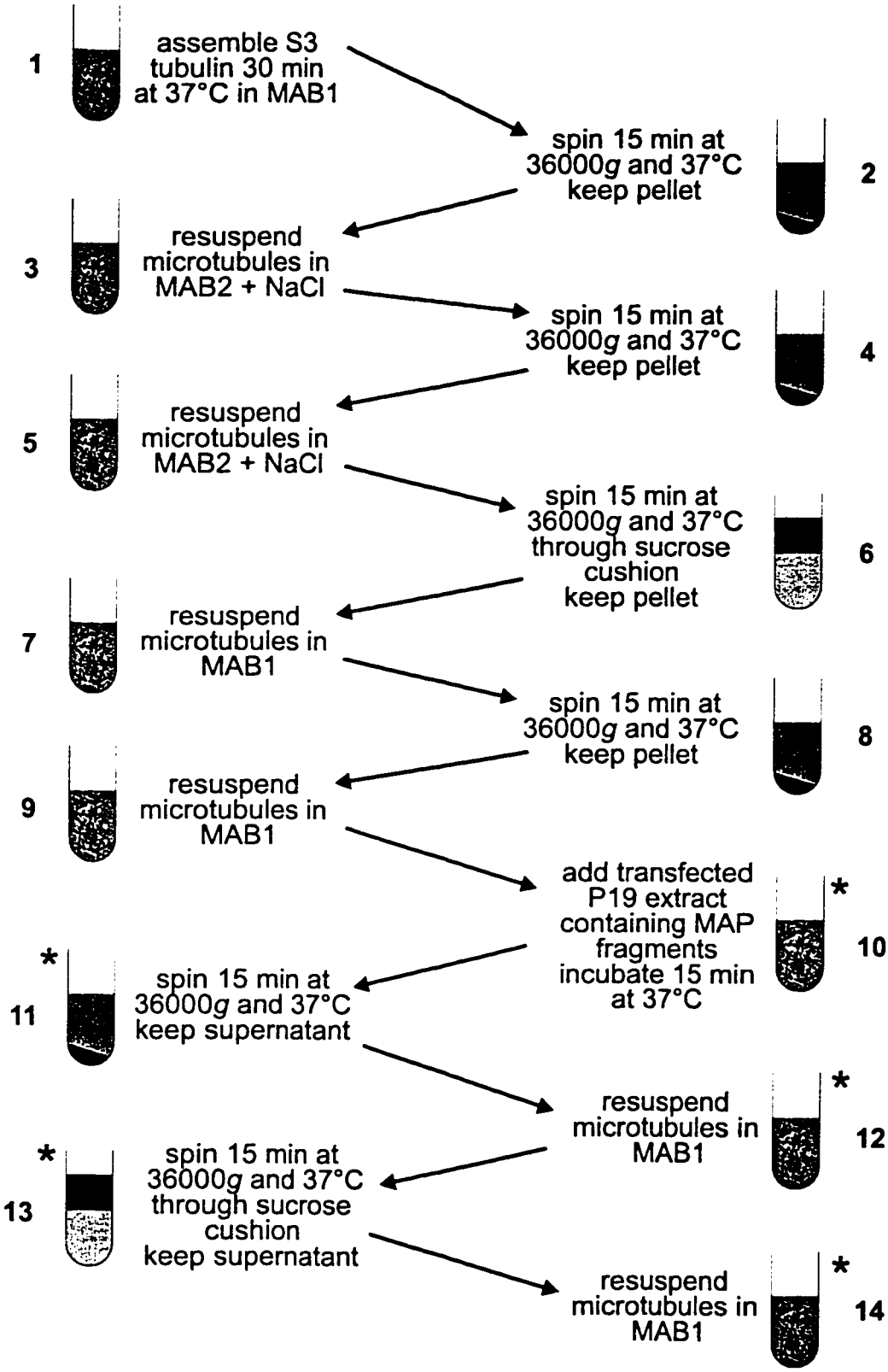
1
assemble S3 tubulin 30 min at 37°C in MAB1
spin 15 min at 36000g and 37°C keep pellet
2
3
resuspend microtubules in MAB2 + NaCl
spin 15 min at 36000g and 37°C keep pellet
4
5
resuspend microtubules in MAB2 + NaCl
spin 15 min at 36000g and 37°C through sucrose cushion keep pellet
6
7
resuspend microtubules in MAB1
spin 15 min at 36000g and 37°C keep pellet
8
9
resuspend microtubules in MAB1
add transfected P19 extract containing MAP fragments incubate 15 min at 37°C
*
10
*
11
spin 15 min at 36000g and 37°C keep supernatant
resuspend microtubules in MAB1
*
12
*
13
spin 15 min at 36000g and 37°C through sucrose cushion keep supernatant
resuspend microtubules in MAB1
*
14

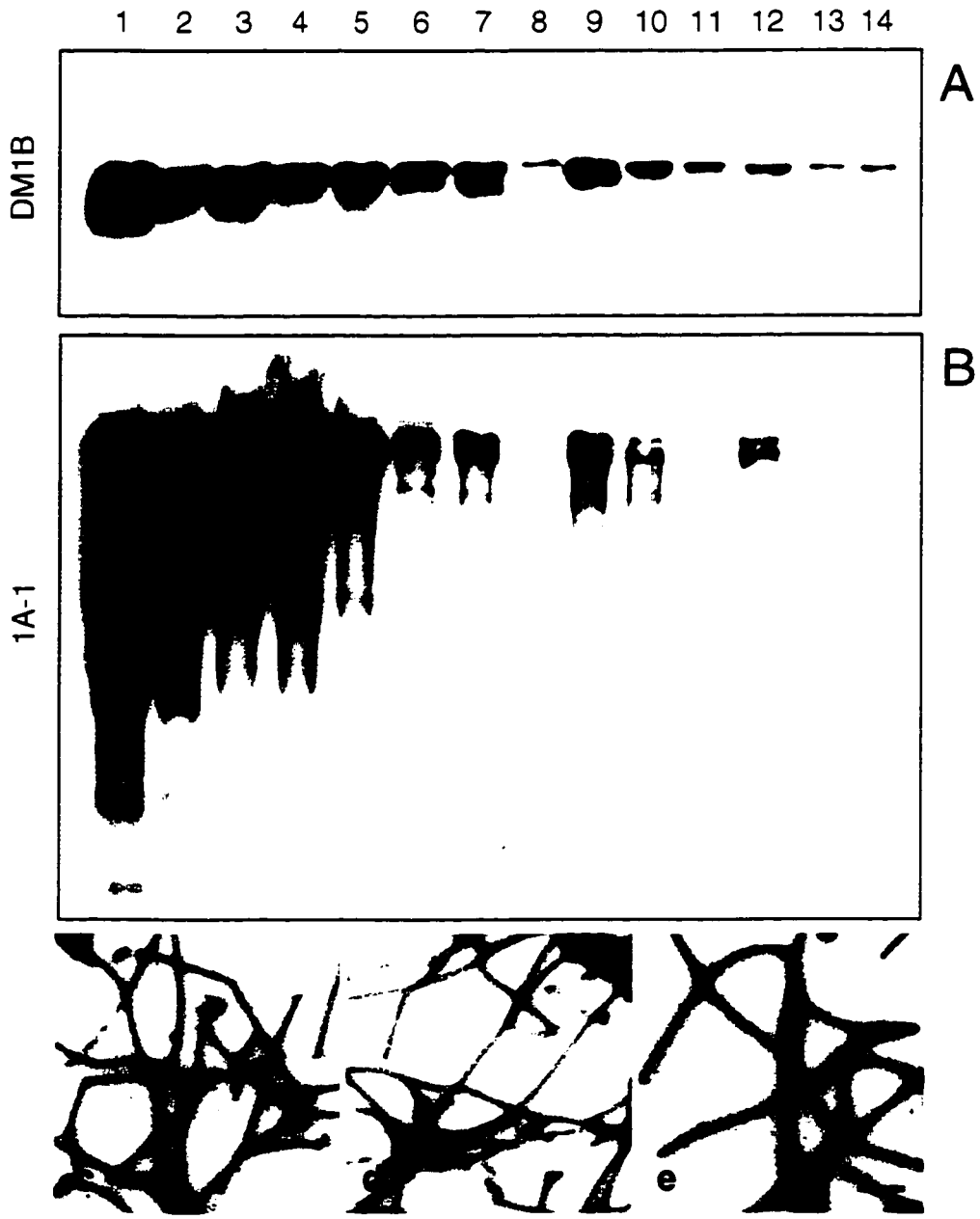
1 2 3 4 5 6 7 8 9 10 11 12 13 14
A
DM1B
B
1A-1

Figure 44

In vitro MAP binding assay. Equal volumes of sample were taken from steps 10 to 14 during the protocol (see materials and methods) and separated by SDS-PAGE on 12% or 7.5 gels. Immunodetection of myc-tagged MAP1A fragments (using mAb 9E10) on western blots shows the presence or absence of fragments at each step sampled. Molecular weight markers (MW) are in kD.

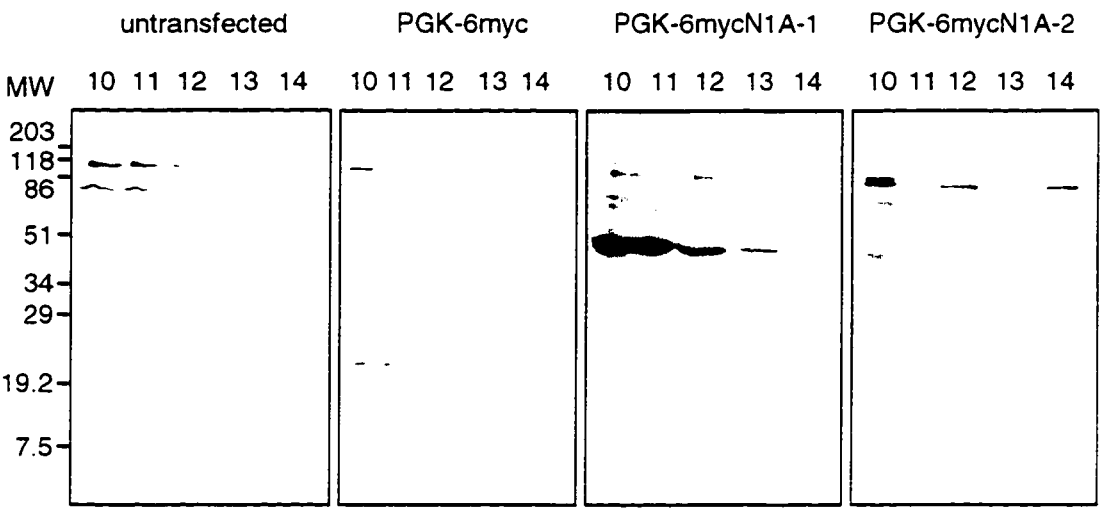
untransfected
PGK-6myc
PGK-6mycN1A-1
PGK-6mycN1A-2
MW
10 11 12 13 14
10 11 12 13 14
10 11 12 13 14
10 11 12 13 14
203
118
86
51
34
29
19.2
7.5

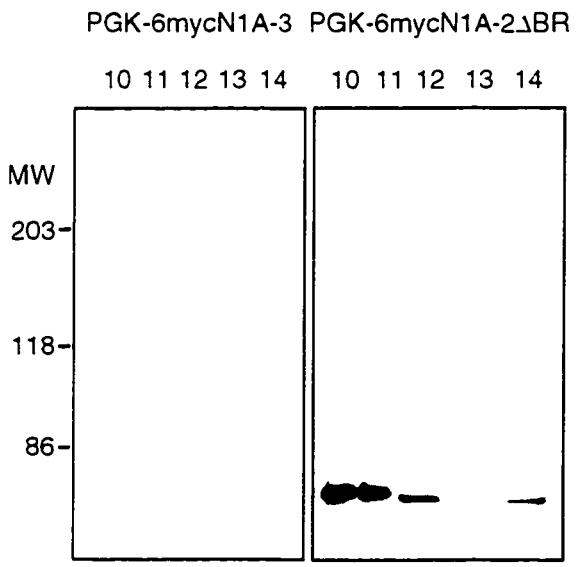
PGK-6mycN1A-3
PGK-6mycN1A-2ΔBR
10 11 12 13 14
10 11 12 13 14
MW
203
118
86

TABLE 1. Summary of MAP1A fragment transfection experiments.

	P19 EC Cells		HeLa Cells		
MAP1A FRAGMENT	**Present in cytoplasm**	**MT colocalization**	**Present in cytoplasm**	**MT colocalization**	**Binds MTs *in vitro***
6myc	yes	no	yes	no	no
6mycN1A-1	yes	no	yes	no	no
6mycN1A-2	yes	yes	yes	yes	yes
6mycN1A-3	yes	yes	yes	yes	yes
6mycN1A-4	yes	yes	yes	yes	ND
6myc1A	yes	yes	yes	yes	ND
6mycN1A-2ΔBR	yes	yes	yes	yes	yes

ND = not determined

6mycN1a-4 and 6mycN1a were not analyzed due to the very low levels of tagged protein available from culture extracts. These results are summarized in Table 1.

COLCHICINE TREATMENT OF TRANSFECTED P19 EC CELLS

Transfected P19 EC cells were treated with colchicine to ensure that the pattern of myc labeling in cells prepared by extraction / fixation was really due to an association with MTs and not with other cytoskeletal components, and also to see if the colchicine stability of MTs was altered by any of the MAP1a fragments. As a positive control, P19 EC cells were transfected with PGK-MAP2cmyc (provided by C. Addison). MAP2c is a juvenile form of MAP2 and, like HMW-MAP2, also has MT bundling and stabilizing abilities (Weissharr *et al.*, 1992).

MAP2cmyc expressing cells showed the presence of thick bundles of MTs in the cytoplasm (Fig. 45a.) The myc labeling was found colocalized with these bundles (Fig. 45a′). After 15min of colchicine treatment, the MTs in the untransfected cells were partially depolymerized. In MAP2cmyc transfected cells, some of the unbundled MTs began to depolymerize, but the bundled MTs appeared unaffected (Fig. 45b, b′). After 30min of colchicine treatment almost all MTs were completely depolymerized, except for the MAP2cmyc bundled MTs that remained polymerized (Fig. 45c, c′)

Untreated cells expressing 6mycN1a-2 show a normal distribution of MTs compared to untransfected cells. (Fig. 45d, d′). After 15min of colchicine, the MTs in transfected cells displayed some depolymerization but appeared to be slightly more resistant to colchicine than the MTs in untransfected cells (Fig. 45e, e′). After 30min of colchicine treatment, no myc labelling was seen colocalized with MTs. In a few cells, a weak, diffuse cytoplasmic staining was observed, but myc labeling was never colocalized with other cytoplasmic structures. In these samples, almost all MTs were completely depolymerized with the exception of midbodies and MTs closest to to the microtubule organizing center. (Fig. 45f, f′). Similar results were obtained for cells expressing 6mycN1a-3 (Fig. 45g-i′). In 6mycN1a-2ΔBR expressing cells, an increase in resistance to colchicine-induced MT disassembly was not detectable (Fig. 45j-l′).

Figure 45

Detection of tubulin (mAb YOL 1/34, a – l) and myc-tagged MAPs (mAb 9E10, a´ - l´) in transfected, colchicine-treated P19 EC cells by digital immunofluorescence microscopy. Cells were untreated (left column), treated for 15min (middle column) or treated for 30min (right column) with 1mg / ml colchicine and then fixed by extraction / fixation. MTs in MAP2cmyc expressing cells were resistant to colchicine even after 30 min of colchicine treatment (a - c'). 6mycN1a-2 and 6mycN1a-3 expressing cells were detected in untreated cells (d – d´; g – g´). MTs showed a slight resistance after 15 min of treatment compared to untransfected cells (e – e´; h – h´), and no MAP1a fragment expressing cells were detected after 30 min of colchicine(f – f´, i – i´). MTs in 6mycN1a-2ΔBR expressing cells did not display any detectable colchicine resistance (j – l´). Scale bar = 40μm.

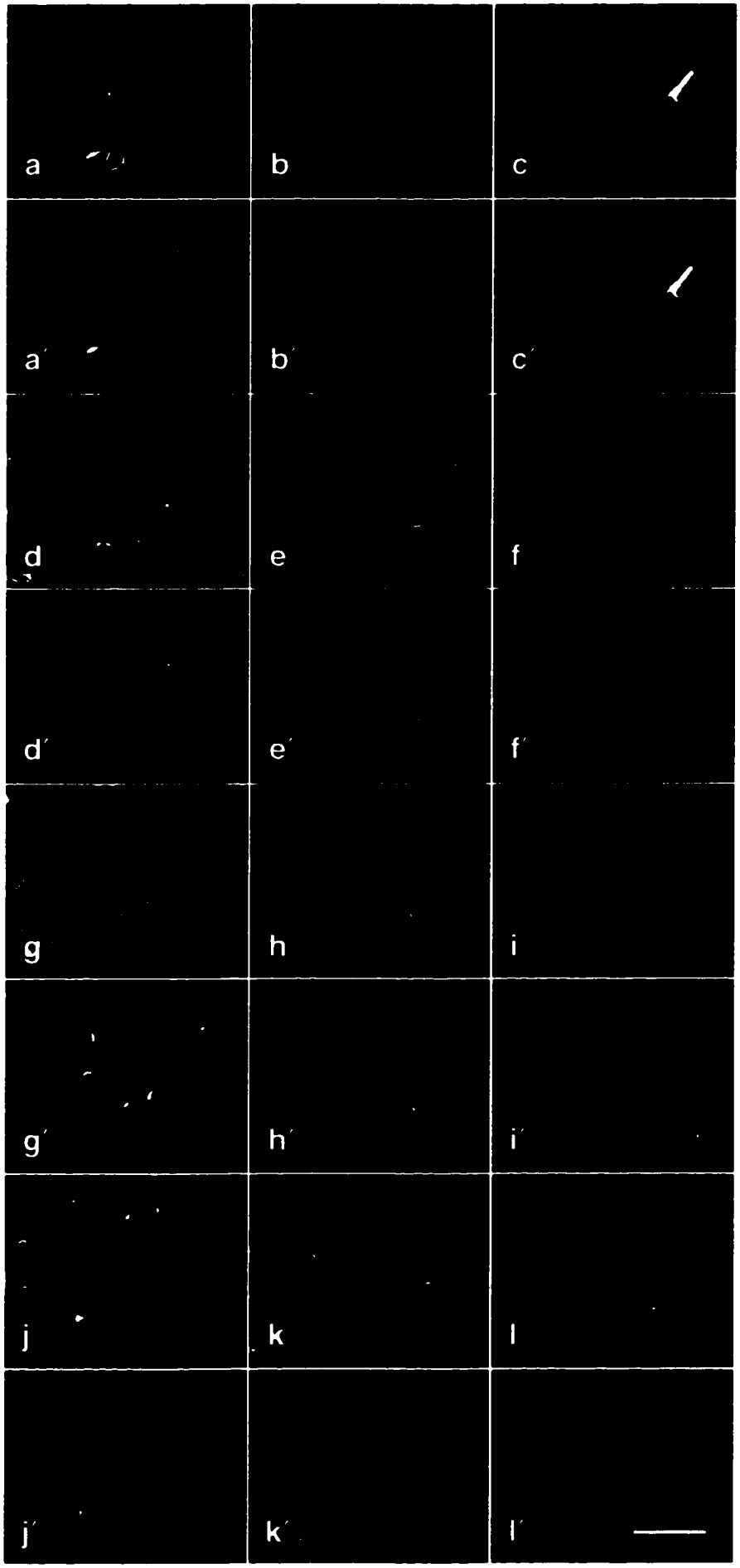
a
b
c
a′
b′
c′
d
e
f
d′
e′
f′
g
h
i
g′
h′
i′
j
k
l
j′
k′
l′

EFFECT OF MAP1a FRAGMENTS ON α-TUBULIN MODIFICATIONS

To test the effect of MAP1a fragments on MT dynamics, the extent of α-tubulin acetylation and detyrosination was determined in transfected cultures by quantitative dot blotting. These posttranslational modifications of tubulin have been shown to be biochemical markers of MTs that have a decreased rate of turnover (Li and Black, 1996). As positive controls, levels of α-tubulin acetylation and detyrosination were also determined in cultures expressing MAP2cmyc and in cultures treated with 10^{-6}M taxol.

The levels of acetylation and detyrosination were normalized to levels found in untransfected cells (Fig. 46 a, b). There was a marked increase in acetylation and detyrosination in cultures expressing 6myc1a. However, the amounts observed were less than that for MAP2cmyc-expressing and taxol-treated cultures. There were marked decreases in acetylation and detyrosination in cultures expressing 6mycN1a-4 and 6mycN1a-2ΔBR. The effects of 6mycN1a-2 and 6mycN1a-3 were not considered important, as the levels of acetylation and detyrosination were similar to 6mycN1a-1 and 6myc, which do not bind MTs.

By normalizing the amounts of acetylation and detyrosination to the amount of myc-tagged fragment bound to MTs, the effect of each fragment on acetylation and detyrosination can be compared on a per molecule basis (Fig. 46c, d). 6mycN1a-4 markedly reduced the acetylation and detyrosination of MTs compared to the other fragments. 6myc1a markedly enhanced the acetylation and detyrosination of MTs. 6mycN1a-3 also enhanced acetylation and detyrosination but its affect was weaker than 6myc1a. Finally, while 6mycN1a-2ΔBR-bound MTs had the lowest levels of acetylation and detyrosination it appeared to have a similar effect per molecule as 6mycN1a-2. Analysis of the levels of myc tagged fragments bound to MTs showed that there was a notable increase in the amount of MT-bound 6mycN1a-2ΔBR compared to the other fragments, including 6myc1a (Fig. 46E). This increased binding was not due to differential expression of different fragments as the proportion of 6mycN1a-2ΔBR bound to MTs was also significantly greater than all other fragments (Fig. 46F).

Figure 46

Effect of MAP1a fragments on α-tubulin modifications in P19 EC cells. The relative levels of acetylation (mAb 6-11B-1, A - C) and detyrosination (pAb anti-E, B – D) were analyzed in polymer extracts from transfected P19 EC cells by quantitative dot blotting (n=3). Quantification of myc tagged fragments in polymer and soluble extracts was performed using mAb 9E10. A and B represent the relative levels of acetylation and detyrosination per μg of tubulin. C and D represent the relative levels of acetylation and detyrosination for equivalent amounts of myc-tagged fragments per μg of tubulin. E represents the amounts of MT-bound myc-tagged fragment per μg of tubulin and F is fraction of total myc tag present that is bound to MTs. Error bars represent the standard errors of the averages of three measurements from three independent experiments.

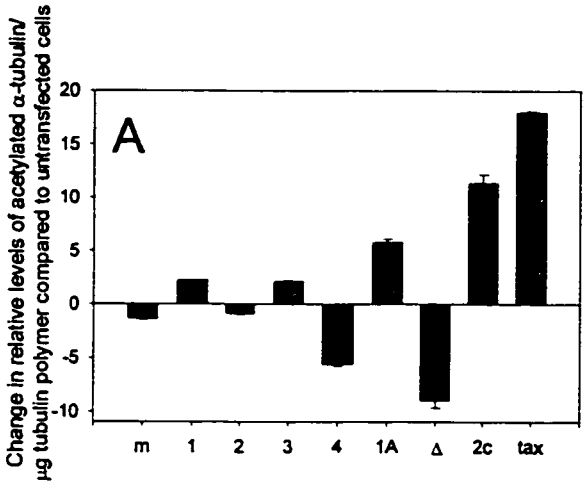
A
Change in relative levels of acetylated α-tubulin/ µg tubulin polymer compared to untransfected cells
20
15
10
5
0
-5
-10
m
1
2
3
4
1A
Δ
2c
tax

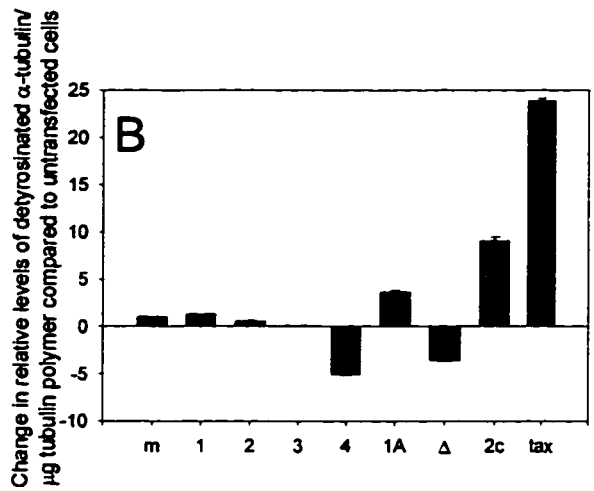
B
Change in relative levels of detyrosinated α-tubulin/ µg tubulin polymer compared to untransfected cells
25
20
15
10
5
0
-5
-10
m
1
2
3
4
1A
Δ
2c
tax

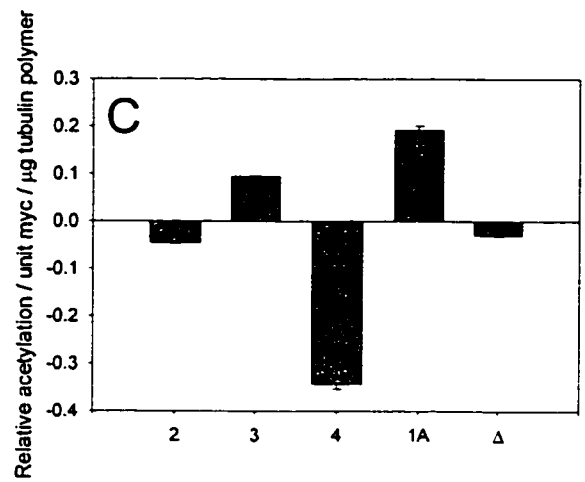
C
Relative acetylation / unit myc / µg tubulin polymer
0.3
0.2
0.1
0.0
-0.1
-0.2
-0.3
-0.4
2
3
4
1A
Δ

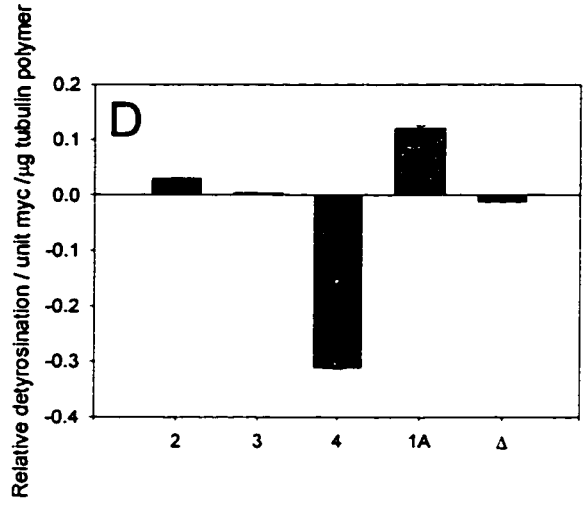
D
Relative detyrosination / unit myc /µg tubulin polymer
0.2
0.1
0.0
-0.1
-0.2
-0.3
-0.4
2
3
4
1A
Δ

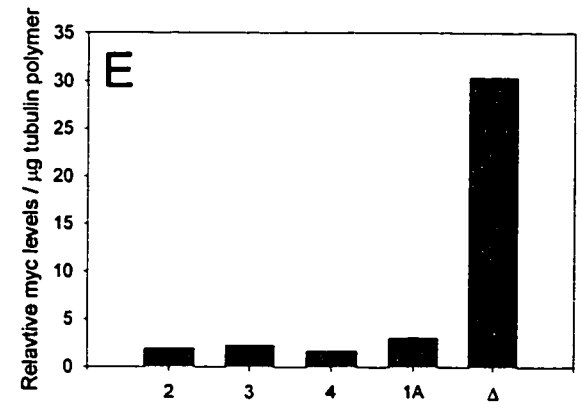
E
Relavtive myc levels / µg tubulin polymer
35
30
25
20
15
10
5
0
2
3
4
1A
Δ

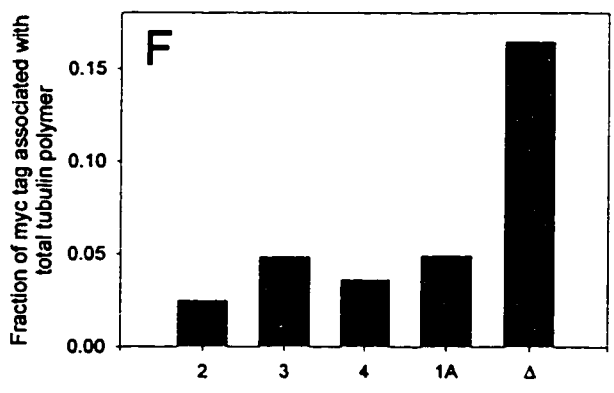
F
Fraction of myc tag associated with total tubulin polymer
0.15
0.10
0.05
0.00
2
3
4
1A
Δ

DISCUSSION

EXPRESSION OF MYC TAGGED MAP1a FRAGMENTS

All fragments (with the exception of 6myc1a) ran within 5 - 10 kDa of their predicted molecular weights. For 6myc1a, the apparent mobility (360 kDa) was close to the mobility of endogenous MAP1a (350 kDa, Langkopf *et al.*, 1992), given the extra 12 kDa present in the 6myc tag. This shows that the termination of translation was occurring as predicted for all the fragments. A decrease was observed in the amounts of myc tagged MAP1a fragments as their size increased, suggesting either that transfection of larger plasmids is less efficient or that expression of larger proteins is less efficient. This was consistent with microscopic observations showing that for the smaller fragments (6myc, 6mycN1a-1, 6mycN1a-2 and 6mycN1a-2ΔBR), 20 - 30% of the cells on a coverslip expressed the myc tag; whereas for the larger fragments (6mycN1a-4 and 6myc1a), only 5 - 10 expressing cells were visible on a cs (data not shown). The detection of MAP1a fragments with 1A-1 showed that the epitope for 1A-1 lies within aa 1310-2016 of MAP1a. This is in agreement with Schoenfeld *et al.* (1989) who failed to detect N-terminal MT-binding fragments of MAP1a with 1A-1.

MT BINDING OF MYC TAGGED MAP1a FRAGMENTS

In both P19 EC and HeLa cells the 6myc tag was expressed but did not bind to MTs, even in taxol-treated cells, demonstrating that this was a good tag for these studies. 6mycN1a-1 also did not bind MTs demonstrating that aa 1 - 281 of MAP1a were not sufficient for MT binding. 6mycN1a-2 did bind to MTs, suggesting that aa 282-630 of MAP1a are involved in MT binding. Removal of the basic repeats from 6mycN1a-2 (6mycN1a-2ΔBR) did not noticeably affect its ability to bind to MTs indicating the presence of MT binding domain(s) contained within aa 281-355 or aa 451-630 or both. Langkopf *et al*, (1992) have reported a region of protein similarity flanking the basic repeat domain in MAP1a and MAP1b. In MAP1b, these flanking domains bind MTs (Noble *et al.*, 1989). We also observed that larger fragments of MAP1a, 6mycN1a-3 and 6mycN1a-4, and the full length MAP1a (6myc1a) also bound to MTs. The morphology of MTs in cells expressing all MAP1a fragments was not detectable altered compared to untransfected cells. The ability of these fragments to

bind MTs *in vitro* was identical, except for 6mycN1a-4 and 6myc1a, which could not be tested *in vitro* due to the low levels of expression of these fragments (see above).

These results do not agree with those of Cravchik *et al.*, (1994) who, by microscopy of transfected HeLa cells, failed to detect a MAP1a fragment consisting of aa 1 - ~1300 of MAP1a (identical to 6mycN1a-3) bound to MTs. They also showed that a region near the middle of MAP1a (aa 1307-1606) consisting of self-similar acidic elements was the MT binding domain and that this domain induced the reorganization of normal interphase MTs into short-perinuclear MTs. In this study, the MAP1a fragments containing this region, 6mycN1a-4 and 6myc1a, bound to MTs but did not result in any of the rearrangements seen in their study. We suggest that this acidic domain, while having the capacity to bind MTs, is not a part of MAP1a which normally participates in binding. It may be folded inside the polypeptide, possibly participating in a structural aspect of MAP1a's projection domain. The presence of acidic repeats has been documented in STOP, MAP4 and MAP1b. These acidic domains are thought to form α-helices which contribute to the long rod shape of the protein (Noble *et al.*, 1989; West *et al.*, 1991 Bosc *et al.*, 1996).

In a few P19 EC cells expressing large amounts 6myc1a, we observed the formation of processes, indicating that MAP1a can induce process outgrowth. This observation is consistent with a role for MAP1a in neuronal growth.

EFFECT OF MAP1a FRAGMENTS ON COLCHICINE STABILITY OF MTS

In P19 EC cells expressing 6mycN1a-2, 6mycN1a-3, a slight increase in resistance to colchicine-induced MT depolymerization compared to untransfected cells was observed after 15 min. However, after 30 min, no MAP1a fragments could be detected in association with the few MTs left intact. In contrast, cells expressing MAP2cmyc displayed bundled arrays of MTs that were resistant to depolymerization even after 30min of treatment. These data suggest that while MAP1a may have some stabilizing ability, it is small in comparison to MAP2c and probably more similar to MAP1b. In MAP1b transfected cells MTs were also stabilized, but to a lesser extent than in cells transfected with MAP2c (Takemura *et al.*, 1992). These results are also consistent with those of Pedrotti and Islam (1994) who showed that the rates of

association and dissociation of dimers onto and from MT polymer were 2 -3 times higher for MAP1a than for MAP2

EFFECT OF MAP1a FRAGMENTS ON ACETYLATION AND DETYROSINATION

MTs in 6myc1a-expressing cells showed increases in acetylation and detyrosination that were greater than any MAP1a fragment, but these levels of acetylation and detyrosination were still smaller than in cells expressing MAP2cmyc. This suggests that overexpression of MAP1a induces MTs that turn over more slowly than in untransfected cells, but more rapidly than in MAP2cmyc expressing cells. These observations are also in agreement with the *in vitro* results of Pedrotti *et al.* (1994) (see above). Similar results were obtained for MAP1b by Takemura *et al.* (1992) who showed an increase in acetylation of MTs in MAP1b transfected cells but that the acetylation induced by MAP2c was stronger. The increase in acetylation and detyrosination seen for 6myc1a may be because the open reading frame in PGK-6myc1a also contains the LC2 sequence. This LC would be present in substoichiometric amounts in cultures expressing MAP1a fragments because LC2 is not present in the constructs transfected. This LC may serve to allow the proper folding of the MAP1a polypeptide so that it has normal activity in affecting MT dynamics or may be required to be present at the MT-binding domain for stabilizing activity.

6mycN1a-4, although bound to MTs, significantly reduced the acetylation and detyrosination of MTs. On a per molecule basis, the acetylation and detyrosination of MTs bound by 6mycN1a-4 were much lower than MTs bound by any other fragment. It is possible that this fragment is folded aberrantly during translation and that this abnormal folding, while allowing the molecule to bind to MTs, acts to destabilize the MT lattice, resulting in more rapid turnover of MTs bound by this fragment.

The changes in acetylation and detyrosination induced by 6mycN1a-2 and 6mycN1a-3 could not be considered significant because they were less than or equal to changes induced by 6mycN1a-1. Because 6mycN1a-1 could not be detected associated with MTs either microscopically or *in vitro*, the changes in acetylation and detyrosination observed with this fragment were assumed to be an increase attributable to some aspect of MAP1a fragment transfection other than MT-binding.

Acetylation and detyrosination induced by 6mycN1a-1 were treated as baselines for comparison with other fragments. However, the expression of 6mycN1a-2 and 6mycN1a-3 appeared to slightly increase the stability of MTs to colchicine-induced depolymerization. Although colchicine treatment of 6mycN1a-4 and 6myc1a transfected cells was attempted, the extremely small number of transfected cells present made it impossible to determine the effect of these fragments on colchicine stability. The colchicine stability induced by 6myc1a might be greater than that induced by 6myc N1a-1 or 6mycN1a-2.

REGULATION OF MAP1a AFFINITY FOR MTS.

6mycN1a-2 and 6mycN1a-2ΔBR appeared to have the same effect per molecule of fragment on acetylation and detyrosination. However, there was a decrease in the levels of these modifications per unit length of 6mycN1a-2ΔBR bound MTs compared with 6mycN1a-2. This suggests that these MTs turn over more rapidly. This is consistent with the lack of colchicine resistance of MTs in 6mycN1a-2ΔBR transfected cells. More 6mycN1a-2ΔBR was bound per unit length of MT than any other fragment. The increase in levels of MT-bound 6mycN1a-2ΔBR was not due to differential expression of fragments as the fraction of total fragment bound was much greater for 6mycN1a-2ΔBR when compared to all other fragments. MT bound 6mycN1a-2ΔBR may have a greater affinity for MTs than other fragments, allowing it to more efficiently compete for MT binding with endogenous MAP1a than other fragments. This competition would cause the loss of enough endogenous MAP1a from the MT to lose its stabilizing activity. The increase in MT-bound 6mycN1a-2ΔBR compared to other fragments appears to be due to a greater affinity for MTs than other fragments. This suggests that the MT-binding regions that flank the basic repeats have a high affinity for MTs. This affinity may be modulated by the presence of the basic repeats. This kind of co-operativity has already been demonstrated for tau, where the regions flanking the basic repeats have greater MT binding ability than in the presence of the basic repeats (Gustke *et al.*, 1994), and for MAP4 (Aizawa *et al.*, 1991).

The data presented here show that MAP1a is similar to MAP1b in terms of its stabilizing ability in comparison with MAP2 and that the mechanism of MAP1a binding to MTs may be similar to that of tau.

CONCLUDING REMARKS

FUNCTION OF MAP1A DURING NEURONAL DIFFERENTIATION

The expression patterns of MAP1b, MAP2 and tau in RA-induced, serum-free neuronal differentiation of P19 EC cells reflect the expression patterns of MAPs seen in brain (Binder *et al.*, 1984; Tucker *et al.*, 1988c; Kosik *et al.*, 1989; Garner *et al.*, 1990; Oblinger and Kost, 1994). In the case of MAP2 and tau, a shift from juvenile forms to adult forms was detected. This shift is considered integral to the development of more stable populations of MTs and to axonal and dendritic specialization in developing brain (Caceres *et al.*, 1984; Tucker *et al.*, 1988a; Goedert and Jakes, 1990). In addition, the differential localization of MAP2 and HMW-MAP2 in developing P19 EC cultures suggested that neurites were specializing into dendrites and axons and that most of the processes seen in these cultures were axonal in nature.

The pattern of MAP1a expression in P19 EC cells is similar to the axonal expression of MAP1a during brain development (Schoenfeld *et al.*, 1989). The apparent conflict between the patterns of MAP1a expression obtained from whole brain extracts and in differentiating P19 EC cells can be reconciled if the majority of MAP1a in whole brain extracts is derived from dendrites. The work of Schoenfeld *et al.* (1989) supports this hypothesis as they showed that throughout brain development, MAP1A is primarily found in dendrites.

A MT binding domain of MAP1A is contained within aa 281-335 and / or aa 451-630. These regions are similar to regions flanking the basic repeats in MAP1b (Langkopf *et al.*, 1992) which can bind MTs (Noble *et al.*, 1989). MAP1a also contains 11 repeats of the basic consensus sequence KKE that is also present in MAP1b. These basic repeats in MAP1b can bind MTs (Noble *et al.*, 1989) which suggests that this domain in MAP1a is also capable of binding to MTs. If the basic repeats in MAP1a can bind MTs, they may modulate the affinity of MAP1a for MTs. This interaction would be similar to the interactions of MT binding domains in tau, whose flanking regions demonstrate a higher affinity for MTs in the absence of the basic repeats (Gustke *et al.*, 1994).

The effects of MAP1a and MAP2 on acetylation, detyrosination, and colchicine-stability of MTs from this study and in vitro assembly results from Pedrotti and Islam (1994) shows that MAP1a stabilizes MTs, but is much less effective in stabilizing MTs compared to MAP2. Additionally, overexpression of MAP1a in P19 EC cells induces process outgrowth. This suggests that MAP1A-bound MTs are stable enough to support process outgrowth, but are still moderately dynamic so that growth is not inhibited.

LCs may contribute to these stabilizing properties of MAP1a. LC2 is preferentially bound to MAP1a (Schoenfeld *et al.*, 1989; Pedrotti and Islam, 1995a) and MTs appear more dynamic in the presence of MAP1b than MAP1a (Pedrotti and Islam, 1994a, 1995b). These observations suggest the increased ability of MAP1a to stabilize MTs compared to MAP1b may be due to the association of LC2 with MAP1a. Pedrotti and Islam (1994) noted that MAP1a purified from adult brain could stabilize MTs, but that this stabilization was weaker than that induced by MAP2. Overexpression of MAP1a in undifferentiated P19 EC cells demonstrated the same intermediate effect on MT stability compared with the MT stabilization seen in untransfected and MAP2-expressing cells. LC3 is present in whole cell extracts from undifferentiated cells but it is not found in the polymer fraction, indicating that MAP1a in undifferentiated P19 EC cells does not associate with LC3. This suggests that LC3 does not influence the ability of MAP1a to stabilize MTs. LC3 may serve to increase the affinity of MAP1a for MTs so that it can remain MT-associated in adult neurons. In differentiating P19 EC cells, the peak of MAP1a expression during differentiation coincides with a gradual reduction in the density of MAP1a present on MTs in these cells. However, the levels of MT-bound LC3 continually increase during development. This indicates that the association of LC3 with MAP1a increases during development. This increase in association of LC3 with MAP1a during differentiation may serve to increase the MT-affinity of MAP1a. Schoenfeld *et al.* (1989) have shown that more than one of a particular LC molecule can associate with MAP1a. Shiomura and Hirokawa (1987) have demonstrated the colocalization of MAP1a and MAP2 on neuronal MTs and in maturing brain, MAP1a is only found in dendrites (Schoenfeld et al., 1989). The MAP1a present during the later stages of P19 EC cell differentiation may represent a stable population of MAP1a associated

with many LC3 molecules, allowing it to successfully compete with MAP2 for MT binding sites in dendrites. If MAP1a is a weak stabilizer, but can compete with MAP2 for MT-binding sites, it would reduce the MT stability in dendrites by preventing the saturation of MTs by MAP2. This may also reflect the situation seen in neurons *in vivo*, as mature axons, deficient in MAP1a, are far less plastic than dendrites. This then begs the question: what is the role of MAP1a in dendrites? These structures have been shown to be plastic and respond morphologically in response to stimulation (Aoki and Siekevitz, 1985). MAP1a may contribute to this synaptic plasticity by preventing strong stabilizers (i.e. HMW-MAP2) from saturating dendritic MTs and reducing the plastic capabilities of dendritic MTs.

A MODEL FOR TEMPORAL AND SPATIAL REGULATION OF MT DYNAMICS BY MAPs DURING NEURONAL DEVELOPMENT

The interaction of MAPs with MTs during neuronal differentiation is very complex. Four aspects of MAPs which regulate neuronal morphogenesis and neuronal connections in the adult are developmental regulation, subcellular localization, the ability of a particular MAP species to stabilize MTs, and the effect of developmentally regulated posttranslational modifications on MAP-mediated MT stabilization. A model for MAP interactions during neuronal development is presented in figure 47. During differentiation, MAP1a and MAP2c are upregulated in both the dendrite and axon in immature neurons (Crandall and Fischer, 1989; Schoenfeld *et al.*, 1989). Both these MAPs can stabilize MTs, but MAP2c is much more efficient than MAP1a (Pedrotti and Islam, 1994). The combination of these two MAPs would yield MTs that are stable enough to support efficient process outgrowth, but still dynamic enough to allow further elongation. MAP1b, MAP3 and juvenile tau are primarily found in the immature axon (Huber *et al.*, 1985; Kosik *et al.*, 1989; Schoenfeld *et al.*, 1989). MAP1b has very little stabilizing ability at this stage and is present primarily in the growing distal axon and growth cone where it is most highly phosphorylated (Sato-Yoshitake *et al.*, 1990; Boyne *et al.*, 1995). As phosphorylated MAP1b binds MTs more efficiently (Díaz-Nido *et al.*, 1990), this specific phosphorylation may serve to promote efficient MAP1b association with MTs and prevent stabilization only in areas where active growth is occurring. Juvenile tau

is phosphorylated early in development (Goedert *et al.*, 1993), displays the same gradient as MAP1B in immature axons, and is weakly associated with MTs (Black *et al.*, 1996). The high level of tau phosphorylation present in early development may prevent MT-association of tau, allowing it to interact with actin and regulate microfilament dynamics in the growth cone. Additionally, phosphorylated MAP1b may be able to efficiently compete with phosphorylated tau for MT binding, preventing strong stabilization of MTs in actively growing regions of the neurite.

As maturation of neurons progresses changes occur in the subcellular localization of MAPs, as well as in the expression of adult MAP isoforms by developmentally regulated alternative splicing, that alter the characteristics of maturing neurons. MAP1a continues to be upregulated in dendrites, but is lost from axons (Schoenfeld *et al.*, 1989). MAP2c is lost from both axons and dendrites and is replaced by HMW-MAP2, but only in the dendrite (Tucker *et al.*, 1988c). A small amount of MAP1b can also be found in maturing dendrites (Schoenfeld *et al.*, 1989). The combination of these MAPs might yield populations of MTs that function to maintain dendritic organization in the adult, but are capable of supporting the plastic reorganizations that are seen in dendrites. In maturing axons, MAP3, juvenile tau and MAP1b are lost and are replaced by adult tau (Huber *et al.*, 1985; Garner *et al.*, 1990; Oblinger and Kost, 1994). Adult tau is a stronger stabilizer that juvenile tau (Montejo de Garcini *et al.*, 1994) and, due to the low levels of tau phosphorylation at this stage of development (Goedert et al., 1993), tau efficiently binds MTs and acts in the absence of MAPs "antagonistic" to its function (MAP1a and 1b) to produce a population of very stable MTs in the axon. It is interesting to note that the plasticity of axons may also be related to their inter-MT spacing. In mature dendrites, only MAPs with large projection domains are present, while in the axons MAPs have smaller projection domains. These serve to produce MTs which in dendrites are spaced further apart in than in axons. This spacing may have an impact on the structural characteristics of the MT cytoskeleton in axons and dendrites. MT bundles having large spacers would be more able to flex and bend than MT bundles with smaller spacings. The MAP composition seen in immature neurons is retained in regions of the brain where neuronal growth is known to persist. Additionally, the recapitulation of immature MAP expression occurs in regenerating neurons. These

Figure 47.

A model for the role of MAPs in axonal and dendritic development in brain.

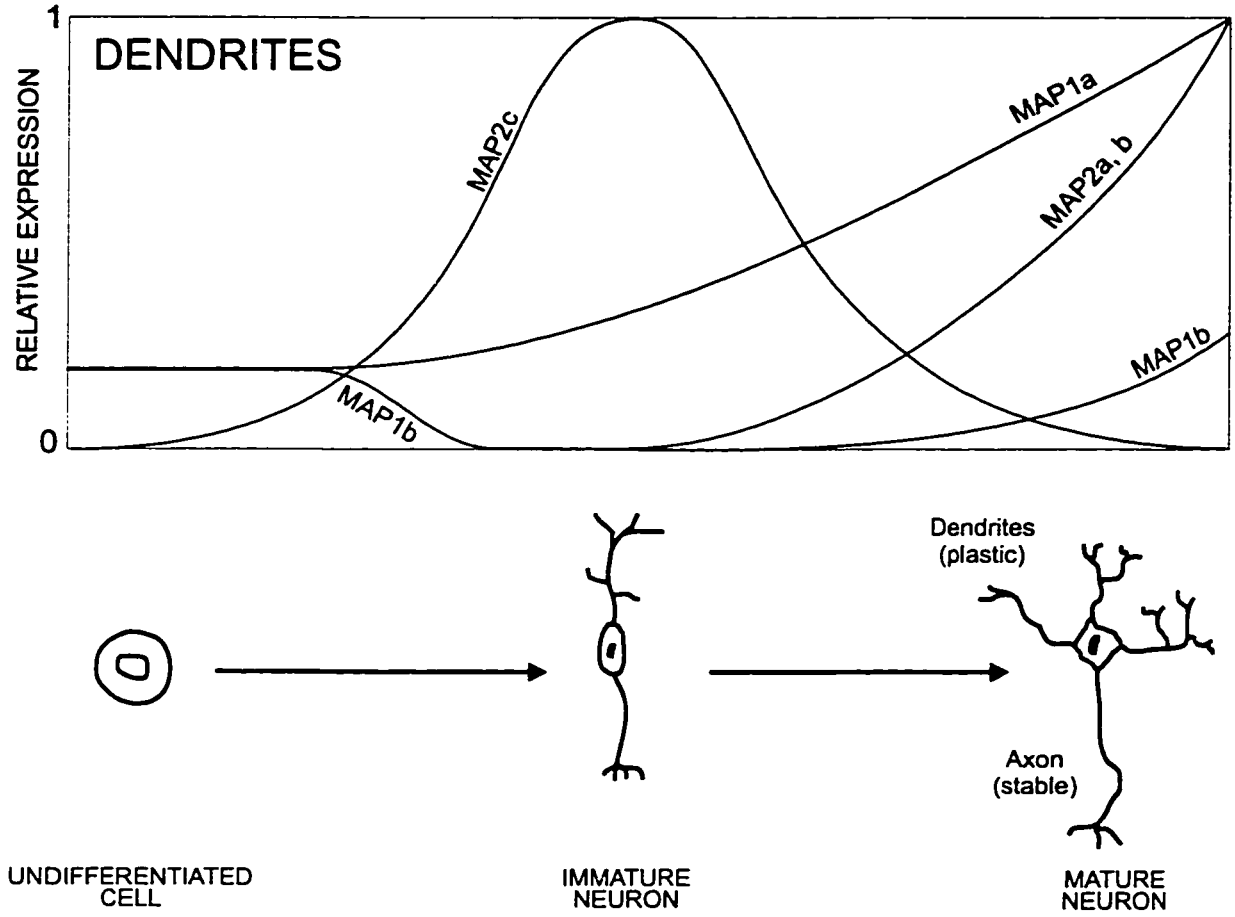
1
DENDRITES
RELATIVE EXPRESSION
MAP2c
MAP1a
MAP2a, b
MAP1b
MAP1b
0
Dendrites
(plastic)
Axon
(stable)
UNDIFFERENTIATED
CELL
IMMATURE
NEURON
MATURE
NEURON

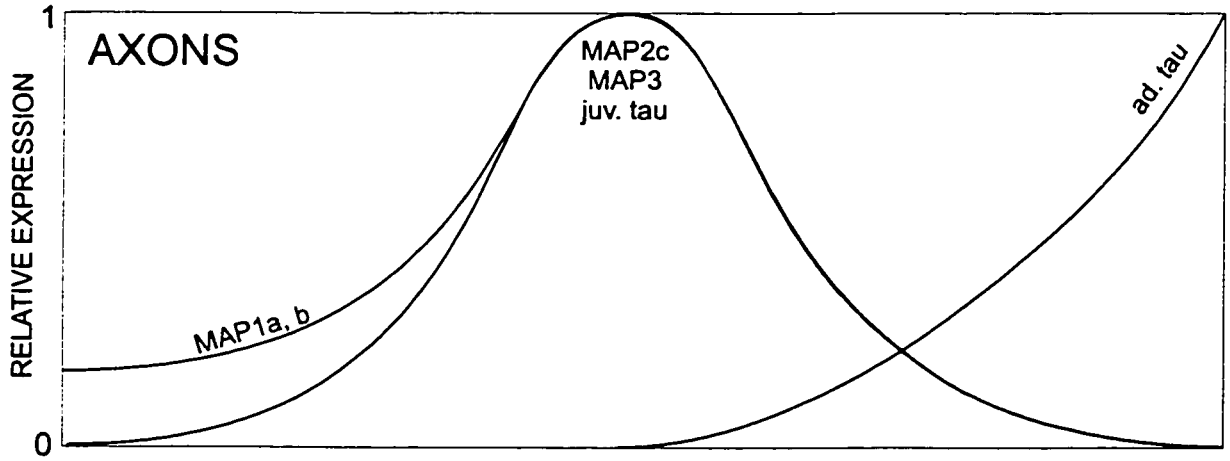
1
AXONS
RELATIVE EXPRESSION
MAP2c
MAP3
juv. tau
ad. tau
MAP1a, b
0

observations argue that the combinations of MAPs present in the immature neuron are essential for proper neuronal growth.

THE BIOCHEMISTRY OF THE MAP-MT INTERACTION

Data from this study and others reveals several patterns in the MT-binding domains of all MAPs. All contain two regions which bind MTs, a domain of basic repeats and a domain flanking these repeats (Aizawa et al., 1991; Lewis et al., 1988; Noble et al., 1989; Gustke et al., 1994). The MT-binding of MAP4 and tau is weakest with only the basic repeats, stronger with both flanking and repeat regions and strongest with only the flanking regions (Aizawa et al., 1991; Gustke et al., 1994). The weaker affinity for MAP1a with only the flanking regions compared to that in the presence of the basic repeats is consistent with this pattern. Additionally, although these flanking regions exhibit strong MT interactions, the normal function of the MAP is lost in the absence of the basic repeats (Aizawa et al., 1991; Trinczek et al.,1995), suggesting that in these MAPs, the basic repeats are important for normal MAP function. Gustke et al. (1994) have suggested a model for tau-MT interactions where the flanking regions serve as "jaws" forming the initial, high affinity MT-interaction, followed by a secondary interaction by the basic repeats. This mechanism may apply to all MAPs, with the flanking regions serving to target the MAPs to the MT surface and the basic repeats functioning as a "lock and key" mechanism which modulates the conformation of the tubulin molecule.

All MAPs interact at the c-terminus of β-tubulin (Littauer *et al.*, 1986; Aizawa *et al.*, 1987; Cross *et al.*, 1991) and this region is also involved in GTP binding (Burns and Farell, 1996). The basic repeats might affect the conformation of this region of the tubulin molecule, perhaps regulating GTP hydrolysis and MT disassembly. It is interesting to note that a correlation exists between the effect of a MAP on MT dynamics and the organization of its basic repeats. Stabilizing MAPs such as MAP2, tau and MAP4 all contain 3 – 5 basic repeats of 18 aa which are highly conserved among these MAP species (Lewis *et al.*, 1988; Aizawa *et al.*, 1989; Chapin and Bulinski, 1991). Weak stabilizers, like MAP1a and MAP1b, have small basic repeats of a KKE motif that is much more numerous (11 in MAP1a, 21 in MAP1b) (Noble et al., 1989; Langkopf et al., 1992). It is possible that the nature of

the basic repeats determines the conformation of the c-terminus of β-tubulin and hence the effect of a particular MAP on MT dynamics.

FUTURE PROSPECTS

THE BASIC REPEATS OF MAP1a

The obvious missing link in the data presented in this thesis is the absence of data for the basic repeats alone binding to MTs. Although analogous repeats can bind MTs in MAP1b this question still remains to be answered for MAP1a. PCR-amplification of the region of MAP1a containing the basic repeats and its insertion in to a plasmid vector has been accomplished. However, this fragment is highly unstable when inserted into plasmid vectors and despite numerous attempts using a variety of strategies, only one successfull insertion into pKJ1DF-6myc was obtained and this was out of frame. Attempts to insert small oligonucleotide linkers to bring the cDNA for the basic repeats in frame with the tag only resulted in the loss of all or part of the insert. Perhaps PCR-based ligation protocols will allow the successful insertion of this fragment into the expression vector and allow characterization of its effects on MTs.

Additionally, a deletion mutant of full length MAP1a in which only the basic repeats were deleted would be informative in determining domain function of MAP1a.

REAL TIME MT DYNAMICS OF MAP1a-BOUND MTs.

A direct measure of the real time MT dynamics (assembly, disassembly, catastrophe, rescue) in the presence of MAP1a and MAP1a fragments would allow for a more detailed assessment of the effects of individual domains. This could be done *in vivo* by establishing permanently transfected cell lines expressing MAP1a or MAP1a fragments. HeLa cells would be an ideal cell line, as they contain no endogenous MAP1a. MAP1a tagged with green fluorescent protein (GFP) would allow live monitoring of MAP1a expressing cells. The visualization of GFP-MAP1a localization in permanently transfected cells would demonstrate the MT binding of MAP1a in vivo. A comparison of MT dynamics could be made in cells expressing different fragments of MAP1a. These values could be correlated with MT dynamics

in untransfected cells by monitoring MT behaviour in cells microinjected with rhodamine labeled tubulin.

The effect of MAP1a and MAP1a fragments on MT dynamics could also be monitored *in vitro* by purifying MAP1a and MAP1a fragments expressed either in yeast, or in SF9 cells using the baculovirus system. The effects of these fragments on the dynamics of MTs assembled from phosphocelluose-purified tubulin could be monitored by differential interference contrast microscopy and turbidometry.

ANALYSIS OF MAP1a FUNCTION *IN VIVO*

Transgenic tau knockout mice, MAP1b mutant transgenic mice, and MAP2c overexpressing mice have been made. Analysis of the tau and MAP1b mice has hinted at MAP1a function, but no MAP1a transgenic mice have been made to date. Transgenic mice where MAP1a is knocked out or is missing the MT binding domain could reveal the *in vivo* function of this protein. Analysis of MAP1a knockout mice, particularly focusing on dendritic formation and plasticity would be a direct test of the above model for MAP1a function. MAP1a function could also be addressed in differentiating P19 EC cells by using the α1-tubulin promoter to drive over expression of MAP1a or inhibit expression by driving production of antisense mRNA for MAP1a. This promoter has been shown to drive developmentally upregulated, neuronal-specific expression in P19 EC cells (Rogers et al., 1995).

MAP1a / LC INTERACTIONS

LC1 and LC2 have been prepared that are tagged at the amino terminus with the hemagglutinin (HA) tag (Field *et al.*, 1988) however, due to time constraints, the LC3 construct was not completed and experiments were not conducted with these proteins. The HA tag is only 9 aa and only $1/10^{th}$ the size of the 6myc tag. It has been used successfully to tag the c-terminus of tubulin (Gonzalez-Garay and Cabral, 1995). This should preclude any steric or folding inhibition of normal LC function that could be occurring with the 6myc tag. It will also allow the detection of both LCs and myc-tagged MAP1a fragments in cotransfected cells. The transfection of P19 and HeLa cells with LCs should be repeated with HA-tagged LCs. Cotransfection experiments could also be performed with HA-tagged LCs and myc-tagged MAP1a

fragments. The interaction of LCs and MAP1a could also be tested in vitro using the MAP-binding assay developed. Results from these experiments could begin to answer many questions including:

1. Where are the binding site(s) for LCs?
2. Does LC2 allow MAP1a to stabilze MTs?
3. Does LC3 increase the affinity of MAP1a for MTs?
4. Is LC processing required for LC association.

Finally, the full-length n-terminal myc-tagged MAP1a could be tagged at the c-terminus with the HA-tag. This would allow the direct analysis of MAP1a/LC2 processing. For example, the presence of the pre-processed polypeptide (containing both tags) could be determined by western blotting with mAb 9E10 and a HA-tag Ab. Processing of this polypeptide could be monitored by the presence of separate, HA-tagged LC2 and myc-tagged MAP1a.

APPENDIX 1 – CHARACTERIZATION OF MAP1b mAb 6D4

The monoclonal IgG 6D4 was provided by Dr. L. Binder who in a personal communication suggested it was specific for MAP1b. However, aside from western blotting, no characterization of this mAb had been conducted. Before using this antibody to detect MAP1b, we characterized it by a variety of methods to ensure that it specifically recognized MAP1b and this recognition was not inhibited nor dependent on phosphorylation of MAP1b.

The first step was to localize 6D4 imunoreactivity (IR) in cryosections of post-natal and adolescent rat brain by immunofluorescence microscopy. In the neo-natal rat, regions of the presumptive cerebellum, spinal Tr trigeminal nerve, and facial nucleus all displayed intense IR, but at this stage of development no recognizable cellular structures could be discerned, preventing a specific localization from being determined (Fig. 48). In the adolescent rat brain, cerebellar organization more typical of a mature organism was seen. 6D4 IR was observed in Purkinje cell bodies and dendrites, in the molecular layer, and in parallel fibers (axons) (Fig 49 b, d). In a cross section of the spinal Tr trigeminal nerve, many axons were present and these displayed intense 6D4 IR (Fig. 49c). In the facial nucleus, 6D4 IR was observed in cell bodies and in neurites (Fig. 49e). In the granule cell layer of the cochlear nuclei (primarily axonal), 6D4 IR was observed in the mossy fibers (Fig. 49f).

Immunodetection of western blots of twice cycled bovine brain MT preparations (S3) by 6D4 revealed a single polypeptide of approximately 330 kDa. This polypeptide was smaller than the 350 kDa MAP1a polypeptide detected with mAb 1A-1 (Fig. 50A). Antigen profiles were then compared between 6D4 and 1B-4, a MAP1b specific antibody that is insensitive to MAP1b phosphorylation (Bloom *et al.*, 1985). Western blotting revealed identical patterns of 6D4 and 1B-4 IR was identical. A single 330 kDa polypeptide was observed which increased in abundance during differentiation, peaked between day 4 and day 6, and then dropped in abundance during the later stages of differentiation (Fig. 50B). Quantitative dot blotting also showed that the relative amounts of the 6D4 antigen and the 1B-4 antigen during differentiation were virtually identical (Fig. 51).

Figure 48

Detection of 6D4 immunoreactivity in neo-natal rat brain cryosections by immunofluorescence microscopy. a) 2° Ab control, b) presumptive cerebellum (low mag.), c) presumptive spinal tr trigeminal nerve, d) presumptive cerebellum (high mag.), e) presumptive facial nucleus. Scale bars = 80μm.

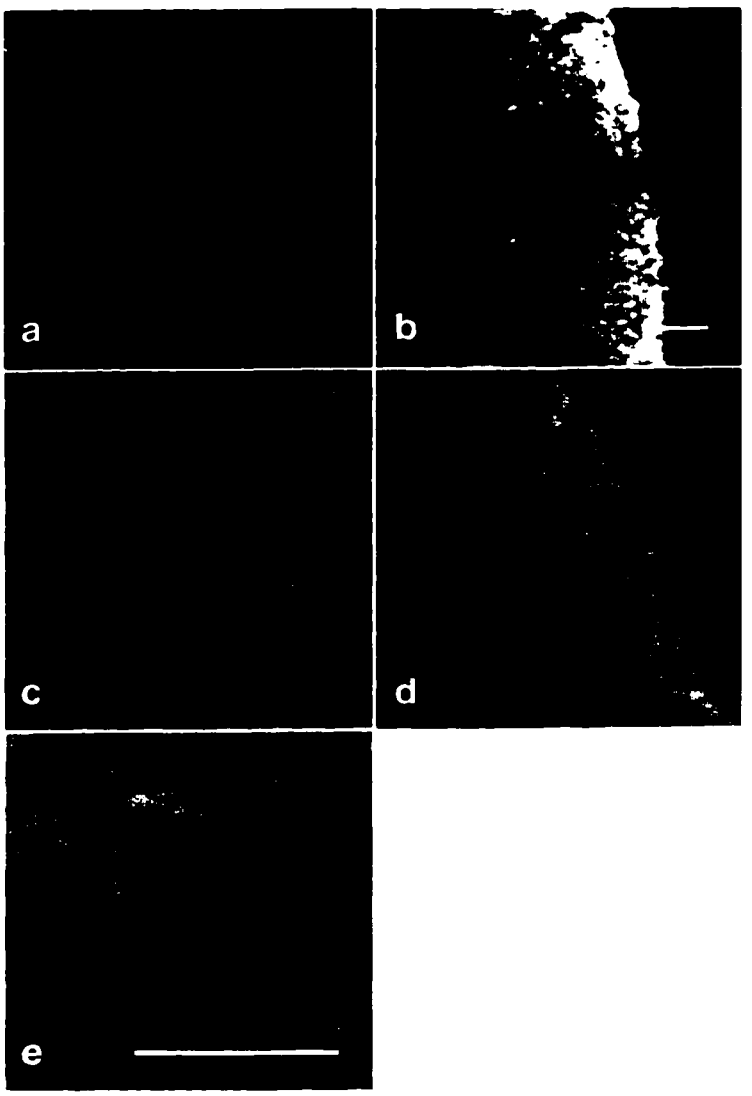
a
b
c
d
e

Figure 49

Detection of 6D4 immunoreactivity in adolescent (120g) rat brain cryosections by immunofluorescence microscopy. a) 2° Ab control, b) cerebellum (low mag.), c) spinal tr trigeminal nerve, d) cerebellum (high mag.), e) facial nucleus, f) granule cell layer of cochlear nucleus. Scale bars = 80μm.

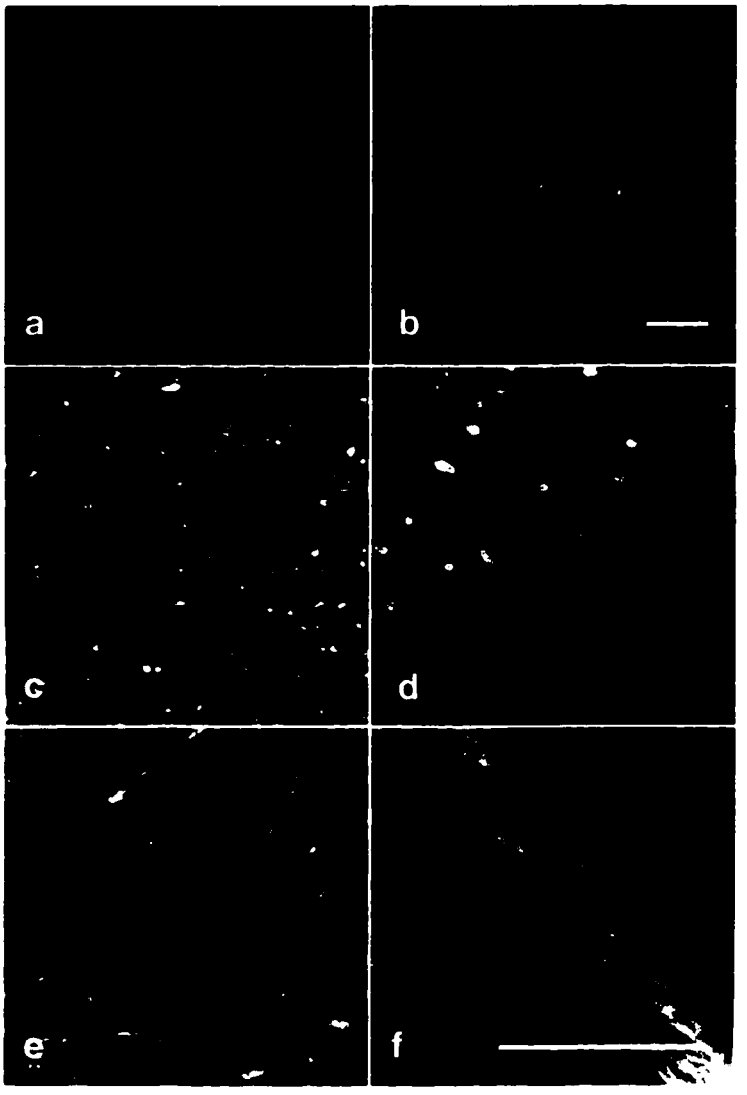
a
b
c
d
e
f

Figure 50

Characterization of 6D4 IR by western blotting. A) 2X cycled bovine brain MT (S3) extract was separated on a 4-15% gradient gel. Western blots were probed with 6D4. Immunodetection of MAP1A using mAb 1A-1 is provided for comparison. B) SDS-whole cell extracts from day 0 to 12 of differentiating P19 EC cells were separated on 7.5% gels. Western blots were probed with 6D4. Immunodetection of MAP1B using mAb 1B-4 is provided for comparison.

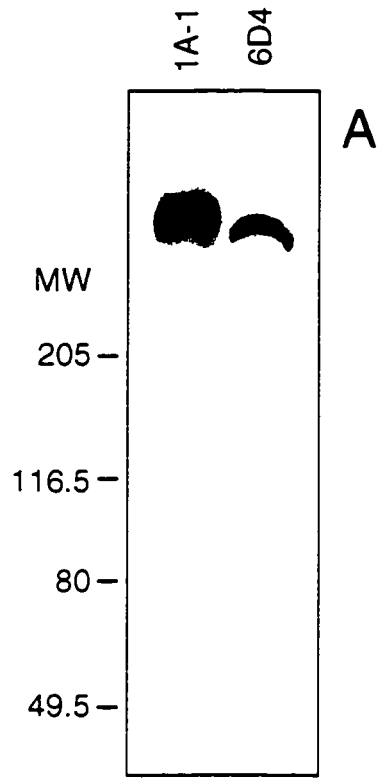
1A-1
6D4
A
MW
205
116.5
80
49.5

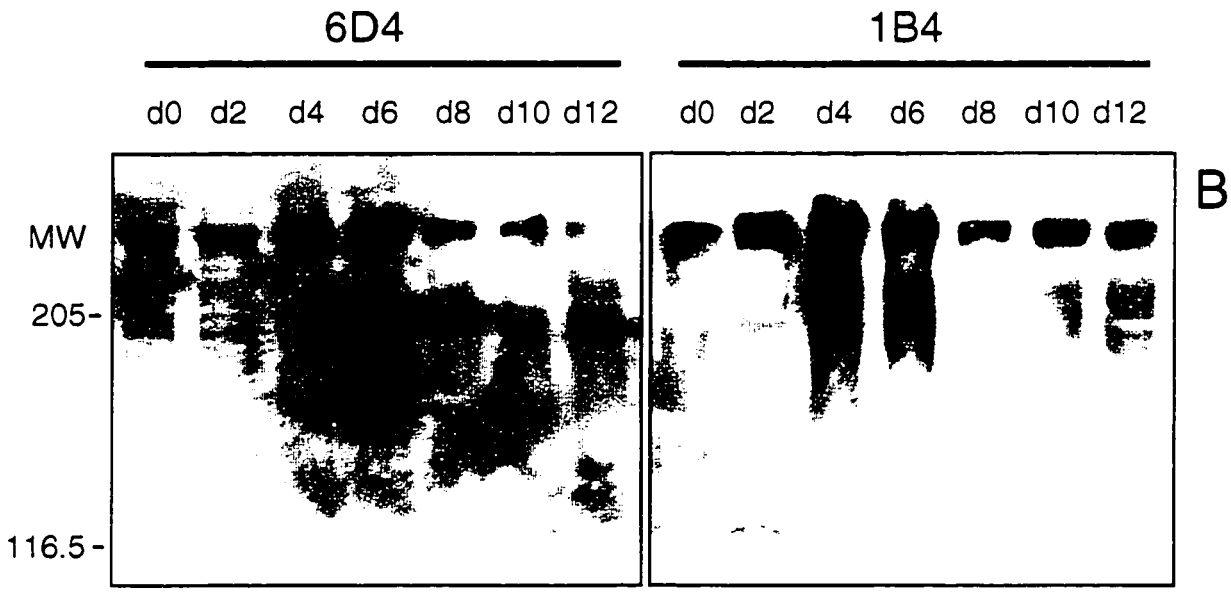
6D4
1B4
d0 d2 d4 d6 d8 d10 d12
d0 d2 d4 d6 d8 d10 d12
B
MW
205
116.5

Figure 51

Comparison of 6D4 and 1B-4 IR in differentiating P19 EC cells. Levels of the 6D4 antigen in SDS-whole cell extracts of day 0 to 12 from differentiating P19 EC cells were determined by quantitative dot blotting. Levels of MAP1b using mAb 1B-4 are provided for comparison. Error bars represent the standard error of the averages of three measurements from three independent experiments.

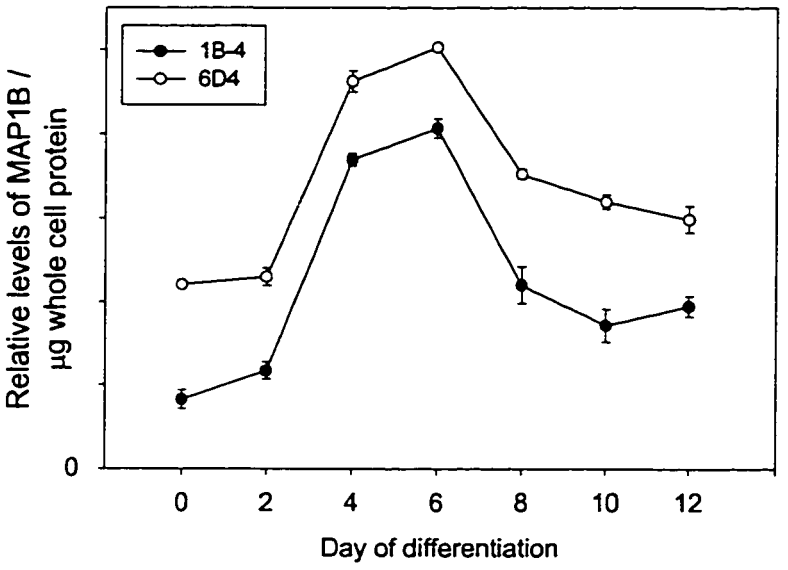
1B-4
6D4
Relative levels of MAP1B / µg whole cell protein
0
0
2
4
6
8
10
12
Day of differentiation

The 6D4 IR in rat brain demonstrates that 6D4 antigen is present early in development and is present in both axons and dendrites. The 6D4 IR in post-natal and developing brain resembles MAP1b localization in the developing brain (Schoenfeld *et al.*, 1989). The 6D4 antigen is a 330 kDa polypeptide that associates with MTs through 2 cycles of assembly and disassembly of MTs, indicating that it is a MAP. It is identical to the 1B-4 antigen in apparent molecular weight and expression in differentiating P19 EC cells, indicating that it is MAP1b. Additionally, the similar profile of 6D4 compared with that of 1B-4 in differentiating P19 EC cells suggests that the 6D4 antibody is not sensitive to phosphorylation. This characterization establishes that mAb 6D4 recognizes MAP1b independent of phosphorylation.

APPENDIX 2- HETEROLOGOUS EXPRESSION OF MAP1 LIGHT CHAINS

INTRODUCTION

MAP1 components (MAP1a and MAP1b) normally present in developing brain are composed of one heavy chain (traditionally known as MAP1a or MAP1b) and several light chains. The three different light chains (see introduction) associate at or near the MT-binding domains of the heavy chains. Due to their close proximity to the MT-binding domain, it has been suggested that these light chains play a role in either binding MAP1a or MAP1b to MTs or in modulating the effects of MAP1a and MAP1b on MT dynamics. This appendix includes preliminary experiments on light chain characterization and function. How light chains may impact MAP1 function during neuronal development is discussed.

RESULTS

EXPRESSION OF LC3 IN DIFFERENTIATING P19 EC CELLS

The expression of LC3 was compared with its heavy chains (MAP1a and MAP1b) in differentiating P19 EC cells. MAP1a, MAP1b and βIII-tubulin displayed the same patterns as previously described in this study. MAP1a and 1b levels rose to a peak at day 4 to 6 and fell with further differentiation. βIII-tubulin was undetectable in undifferentiated cells, but the amounts of βIII-tubulin present steadily increased during differentiation. In contrast to MAP1a and 1b, LC3 was detectable at low levels in undifferentiated cells and steadily increased during differentiation (Fig. 52A). Analysis of the relative levels of these four antigens by quantitative dot blotting confirmed these results. Peak levels of MAP1a and MAP1b occurred between day 4 and day 6 while LC3 and βIII-tubulin peaked much later. A drop in LC3 and βIII-tubulin levels was observed at day 12 (Fig. 52B).

MT STABILITY AND MT-BOUND MAPS

The resistance to depolymerization induced by colchicine was used as an indirect test for MT dynamics during differentiation. Absolute tubulin levels were determined by quantitative dot blotting of polymer extracts from differentiating P19

Figure 52

Accumulation of LC3 and its heavy chains during differentiation of P19 EC cells. A) SDS-whole cell extracts of cells from day 0 to 12 were separated by SDS-PAGE on 7.5 (MAP1a and 1b) and 15% (LC3 and βIII-tubulin) gels. MAPs were immunodetected on western blots using mAbs 1A-1 (MAP1a), 6D4 (MAP1b), LC3 (light chain 3) and TuJ1 (βIII-tubulin). B) Levels of MAP1a, MAP1b light chain 3 and βIII-tubulin in SDS-whole cell protein from day 0 to 12 were determined by quantitative dot blotting using the mAbs as described above. βIII-tubulin levels are provided for comparison. Error bars represent the standard error of the averages of three measurements from three independent experiments. Relative protein levels at days 2-8 (MAP1a), 2-12 (MAP1b), 4-12 (LC3) and 6-12 (βIII-tubulin) were significantly different from day 0 values ($p < 0.05$) as determined by the Student's t-test.

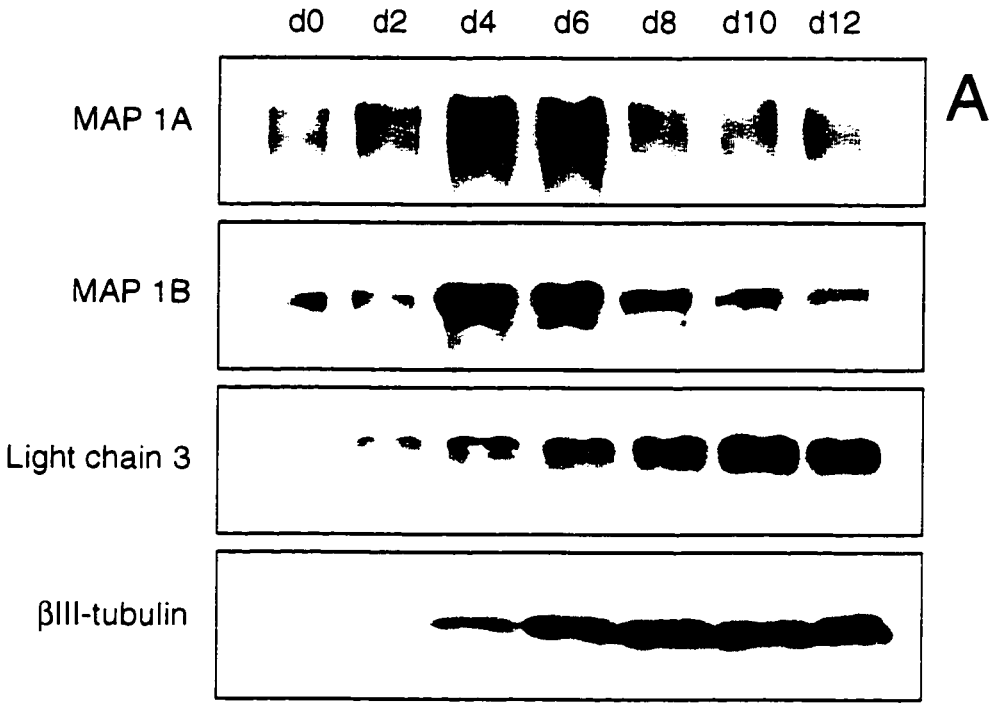
d0
d2
d4
d6
d8
d10
d12
MAP 1A
MAP 1B
Light chain 3
βIII-tubulin
A

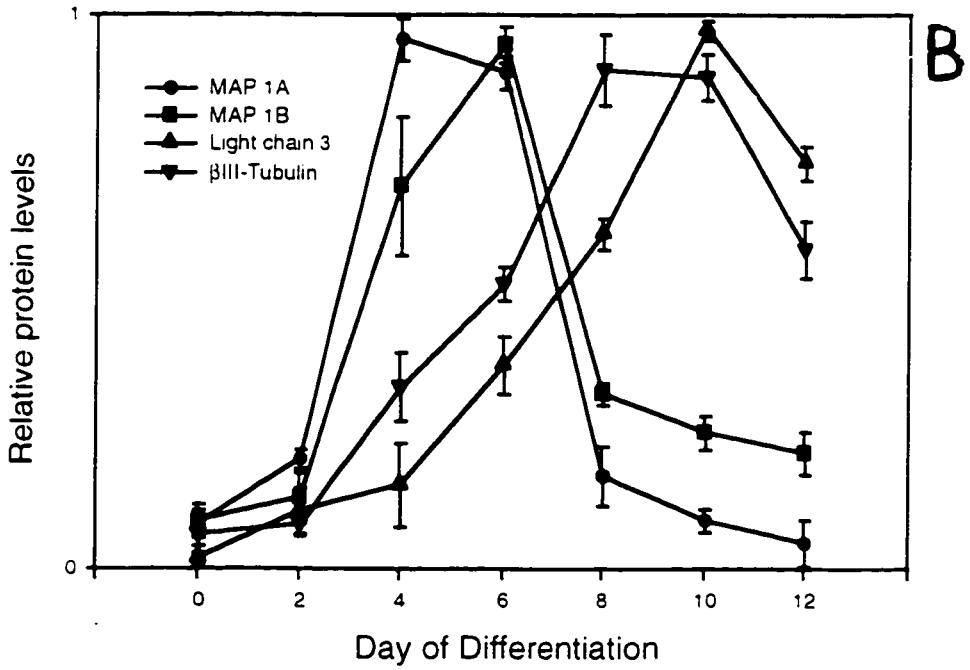
MAP 1A
MAP 1B
Light chain 3
βIII-Tubulin
Relative protein levels
1
0
0
2
4
6
8
10
12
Day of Differentiation
B

Figure 53

Colchicine stability of MTs during differentiation of P19 EC cells. Absolute tubulin levels per μg of total cellular protein in polymer were determined by quantitative dot blotting with mAb DM1B using phosphocellulose-purified tubulin as a standard. Extracts were taken from differentiating P19 EC cells from day 0 to 12 that were either untreated, treated for 15 min or treated for 30 min with 1mg / ml of colchicine (see graph legend). Error bars represent the standard error of three measurements.

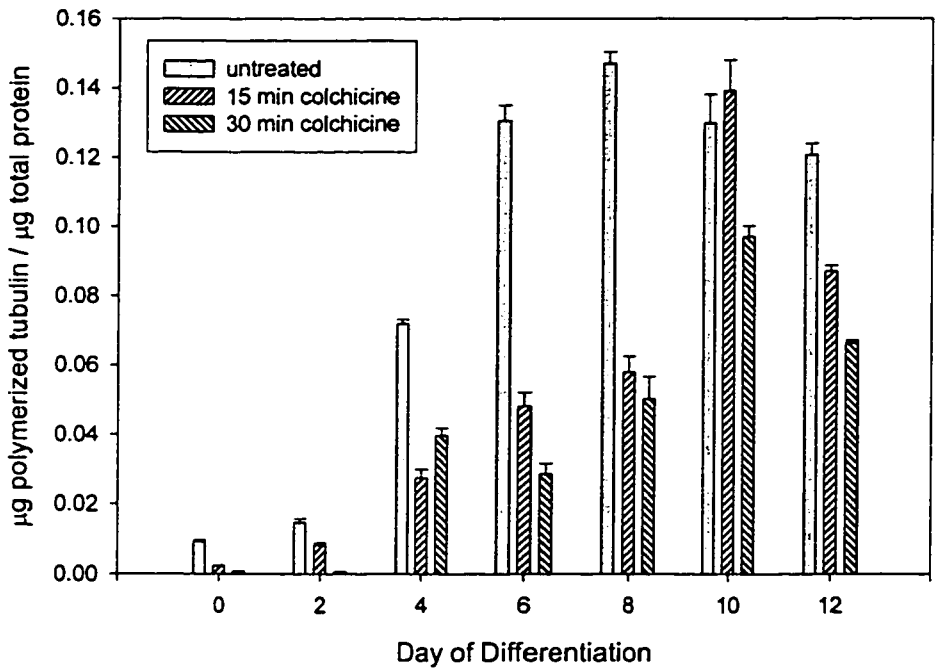
untreated
15 min colchicine
30 min colchicine
µg polymerized tubulin / µg total protein
0.16
0.14
0.12
0.10
0.08
0.06
0.04
0.02
0.00
0
2
4
6
8
10
12
Day of Differentiation

EC cells, using phosphocellulose-purified tubulin as a standard. Differentiating cultures were either untreated or treated for 15 or 30 min with 1mg / ml of colchicine.

As shown in Figure 53, undifferentiated P19 EC cells had a relatively small amount of polymerized tubulin that was almost completely depolymerized after 30 min of colchicine treatment. There was a slight increase in polymerized tubulin levels by day 2, but no significant increase in colchicine resistance was observed. By day 4 there was a large increase in tubulin levels in polymer and these MTs were more resistant to colchicine-induced depolymerization. Tubulin polymer levels continued to increase by day 6 and day 8, but no increase in the colchicine resistance was observed compared to day 4. However, by day 10 almost all the MTs present were resistant to colchicine-induced depolymerization. At day 12, the amount of polymerized tubulin was similar to day 10, but these MTs appeared to be less resistant to colchicine than at day 10.

The relative levels of MAP1a, MAP1b, MAP2 (HMW + LMW MAP2), LC3 and βIII-tubulin associated with total polymerized tubulin during differentiation were determined by quantitative dot blotting (Fig. 54). The amounts of βIII-tubulin incorporated into MTs continually increased during development. The levels of MT-bound MAP1a closely resembled the pattern of accumulation measured in whole cell extracts (Fig. 34), peaking at day 4 to day 6. MT-bound MAP1b was present in undifferentiated cells, but 2 days after induction there was a large decrease in the amount of MT-bound MAP1b. By day 4, there was a very large increase in MT-bound MAP1b that dropped by day 6 and MAP1b was not detectable at later days of differentiation. A small amount of MT-bound MAP2 was detected in undifferentiated cells, but none was detected by day 2. By day 4 there was a large increase in MT-bound MAP2 and the levels of MT-bound MAP2 increased to peak at day 8. MT-bound LC3 was undetectable at day 0 and day 2. From day 4 onwards the amounts of LC3 bound to MTs exhibited a biphasic pattern, with a small peak at day 6 followed by a much larger peak at day 12.

To compare the composition of MAPs along MTs, the relative levels of MT-bound MAPs (and βIII-tubulin) per unit length of MT (μg of polymerized tubulin) were calculated. These values were obtained by dividing the relative levels of MT-bound MAPs per μg of polymer protein by the amount tubulin present per μg of polymer

Figure 54

Levels of MT-bound MAPs and βIII-tubulin in differentiating P19 EC cells. Total levels of βIII-tubulin (mAb TuJ1), MAP1a (mAb 1A-1), MAP1b (mAb 6D4), MAP2 (LMW- + HMW-MAP2, mAb HM-2) and LC3 (pAb LC3) associated with polymerized MTs per μg of total cellular protein in differentiating P19 EC cells were determined by quantitative dot blotting. Error bars represent the standard error of the averages of three measurements from three independent experiments.

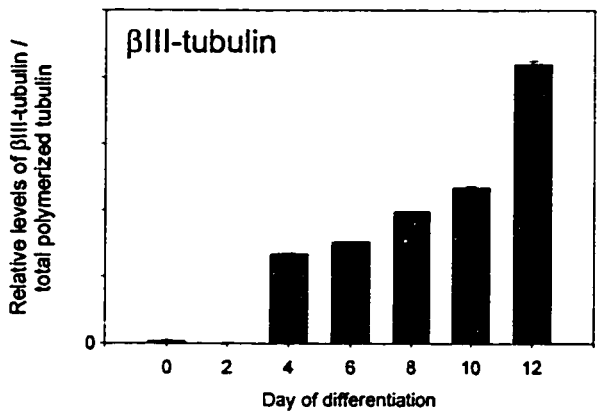
βIII-tubulin
Relative levels of βIII-tubulin / total polymerized tubulin
0
0 2 4 6 8 10 12
Day of differentiation

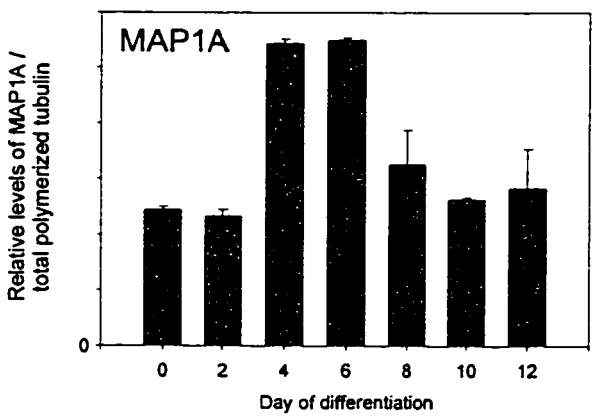
MAP1A
Relative levels of MAP1A / total polymerized tubulin
0
0 2 4 6 8 10 12
Day of differentiation

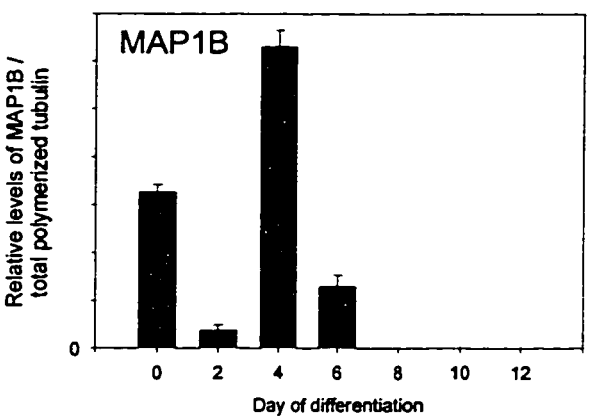
MAP1B
Relative levels of MAP1B / total polymerized tubulin
0
0 2 4 6 8 10 12
Day of differentiation

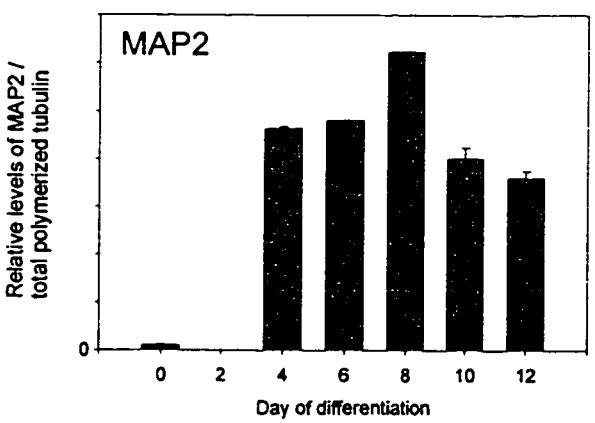
MAP2
Relative levels of MAP2 / total polymerized tubulin
0
0 2 4 6 8 10 12
Day of differentiation

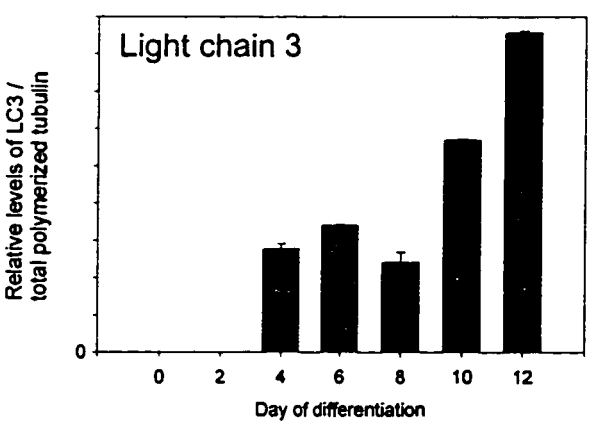
Light chain 3
Relative levels of LC3 / total polymerized tubulin
0
0 2 4 6 8 10 12
Day of differentiation

Figure 55

Density of MT-bound MAPs and βIII-tubulin in differentiating P19 EC cells. Levels of βIII-tubulin, MAP1a, MAP1b, MAP2 and LC3 associated per μg of polymerized tubulin in differentiating P19 EC cells were calculated by dividing levels of the above proteins associated with total polymerized tubulin by the amount of tubulin present per μg of whole cell protein for each time point analyzed. Error bars represent the standard error of the averages of three measurements from three independent experiments.

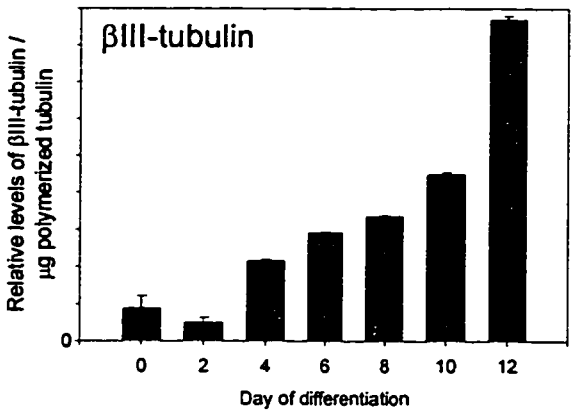
βIII-tubulin
Relative levels of βIII-tubulin / µg polymerized tubulin
0
0 2 4 6 8 10 12
Day of differentiation

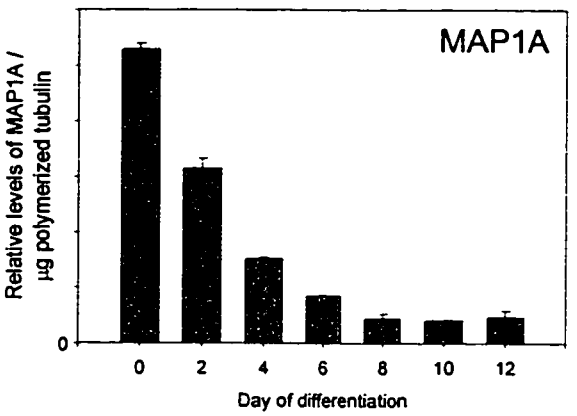
MAP1A
Relative levels of MAP1A / µg polymerized tubulin
0
0 2 4 6 8 10 12
Day of differentiation

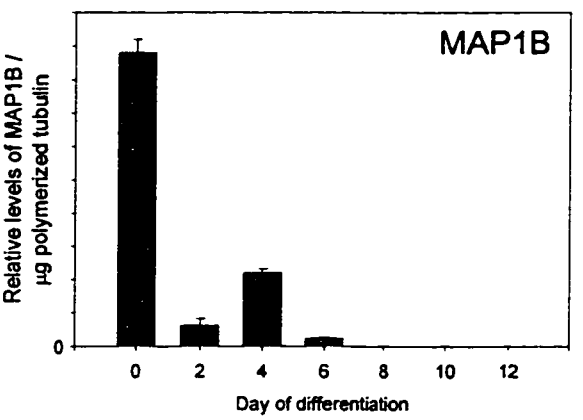
MAP1B
Relative levels of MAP1B / µg polymerized tubulin
0
0 2 4 6 8 10 12
Day of differentiation

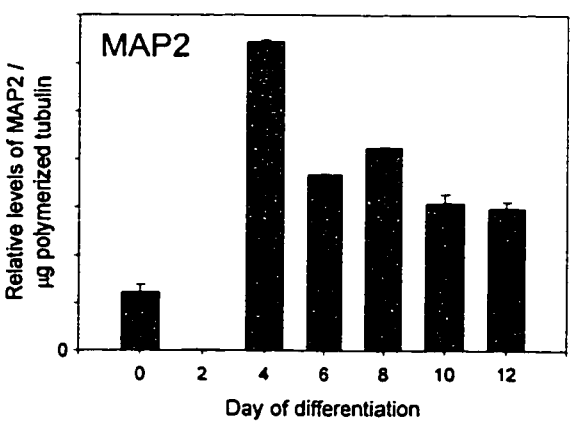
MAP2
Relative levels of MAP2 / µg polymerized tubulin
0
0 2 4 6 8 10 12
Day of differentiation

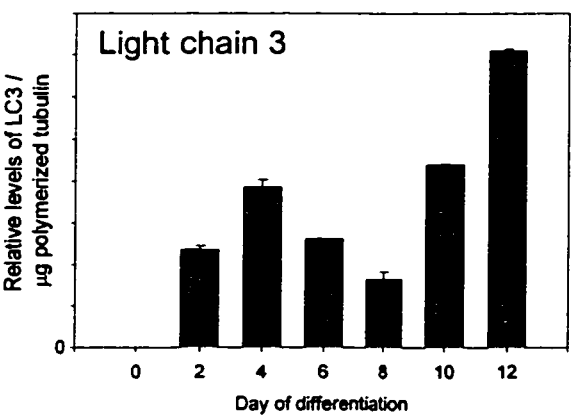
Light chain 3
Relative levels of LC3 / µg polymerized tubulin
0
0 2 4 6 8 10 12
Day of differentiation

protein from cells that had not been treated with colchicine (Fig. 55). The incorporation of βIII-tubulin per unit MT length increased as differentiation progressed. The levels of MAP1a per unit MT length were highest in undifferentiated cells, but continually decreased during differentiation until day 6, after which levels remained constant. MAP1b levels dropped even more dramatically than MAP1a during differentiation, with a sharp drop by day 2 followed by a slight increase by day 4 and by day 8 MT-bound MAP1b was undetectable. MT-bound MAP2 was detected in undifferentiated cells but was barely detectable by day 2. At day 4 there was a large increase in MT-bound MAP2. The amount of MT-bound MAP2 dropped significantly by day 6, increased slightly by day 8 and then dropped slightly by days 10 and 12. No MT-bound LC3 was detectable in undifferentiated cells, however MTs did have some bound LC3 by day 2. The amounts of MT-bound LC3 per unit MT length peaked at day 4 and then its presence on MTs decreased after day 4 until day 8. By day 10 MT-bound LC3 levels were equivalent to levels observed at day 4 and by day 12 there was a much larger amount of MT-bound LC3 per unit MT length than at any other day.

EXPRESSION OF LCs IN UNDIFFERENTIATED P19 EC AND HELA CELLS

To determine if LCs had any effect on MT organization, myc-tagged LCs were expressed in undifferentiated P19 EC and HeLa cells. PAbs raised against native LC1, 2 and 3 were used to detect LCs. Two of these pAbs, LC1 and LC2, had to be affinity purified to reduce non-specific interactions. The effect of affinity purification on the specificity of these pAbs is demonstrated in Figure 56. LC1 and LC2 were detected using either affinity purified (P-LC1, P-LC2) or unpurified (LC1, LC2) pAbs. Affinity purification removed almost all the non-specific reactivity from the serum. P-LC1 recognized a single 31 kDa polypeptide and P-LC2 recognized a single 27 kDa polypeptide. These apparent molecular masses are similar to those published for LC1 and LC2 (Kuznetsov *et al.*, 1987; Schoenfeld *et al.*, 1989).

The expression of various myc-tagged LC constructs (Fig. 57) was analyzed by SDS-PAGE (Fig. 58). In transfected P19 EC and HeLa cells the apparent molecular mass of all myc tagged fragments closely approximated their predicted molecular mass (Fig. 58*). 6mycLC1 and 6mycLC2 could also be detected by P-

Figure 56

Affinity purification of pAbs LC1 and LC2. SDS-whole cell extracts from undifferentiated P19 EC cells were separated by SDS-PAGE on 12% gels. Light chains were detected on western blots with anti-LC1, purified anti-LC1, anti-LC2 and purified anti-LC2. Molecular weight markers (MW) are in kD.

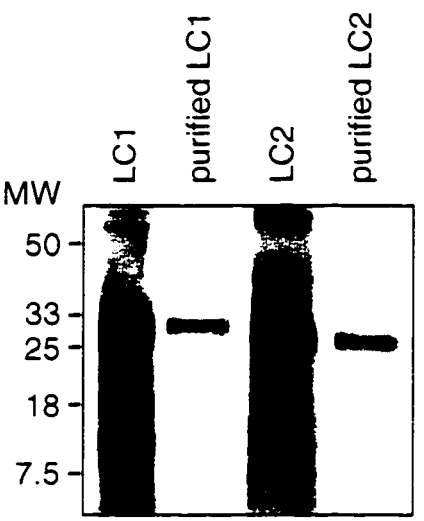
MW
LC1
purified LC1
LC2
purified LC2
50
33
25
18
7.5

Figure 57

Schematic showing the various 6myc-tagged LC expression constructs used in this study. The predicted molecular weights for each fragment are provided in kD.

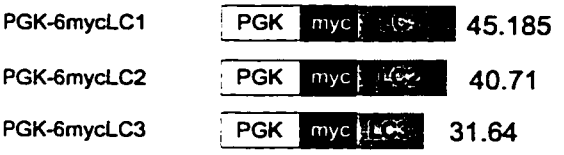
PGK-6mycLC1
PGK
myc
45.185
PGK-6mycLC2
PGK
myc
40.71
PGK-6mycLC3
PGK
myc
31.64

Figure 58

Expression of 6myc – tagged LCs in transfected P19 EC and HeLa cells. 20μg (P19) or 10μg (HeLa) of transfected whole cell extracts were separated by SDS-PAGE on 12% gels. 6myc-tagged LCs (*) were immunodetected on western blots using mAb 9E10. Endogenous LC expression (arrows) was detected using microaffinity purified pAbs anti-LC1 and anti-LC2 and pAb anti-LC3

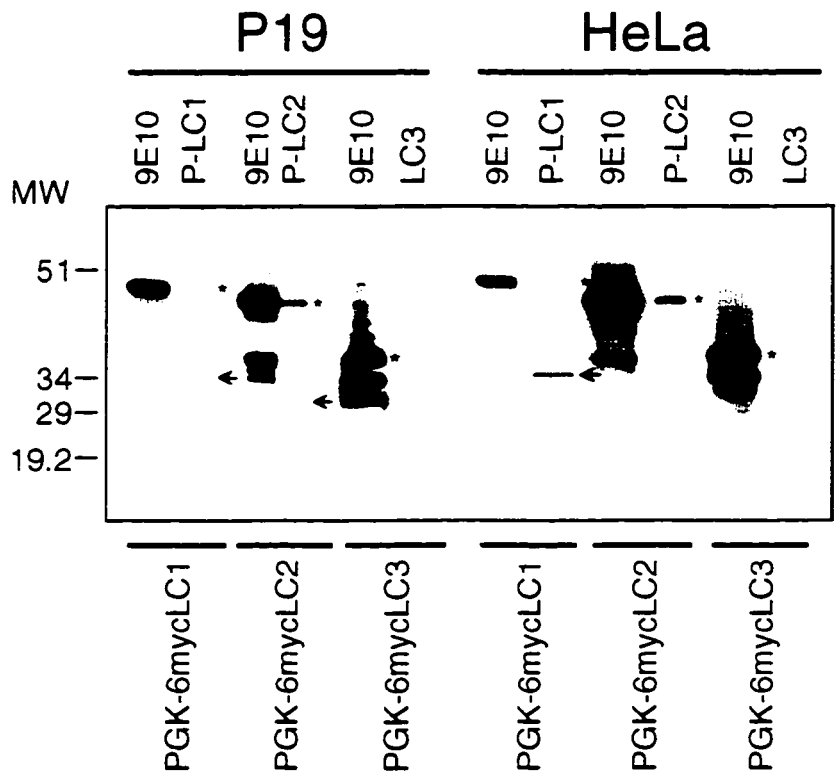
P19
HeLa
9E10
P-LC1
9E10
P-LC2
9E10
LC3
9E10
P-LC1
9E10
P-LC2
9E10
LC3
MW
51
34
29
19.2
PGK-6mycLC1
PGK-6mycLC2
PGK-6mycLC3
PGK-6mycLC1
PGK-6mycLC2
PGK-6mycLC3

Figure 59

Localization of tubulin (YOL1/34, a – l) and 6myc tagged LCs (mAb 9E10, a′ - l′) in transfected P19 EC (a – f′) and HeLa cells (g – l′) by digital immunofluorescence microscopy. Cells were fixed by precipitation (a – c′, g – l′) or by extraction / fixation (d – f′, j –l′). LCs expressed were LC1 (left column), LC2 (middle column) and LC3 (right column). Scale bar = 20μm.

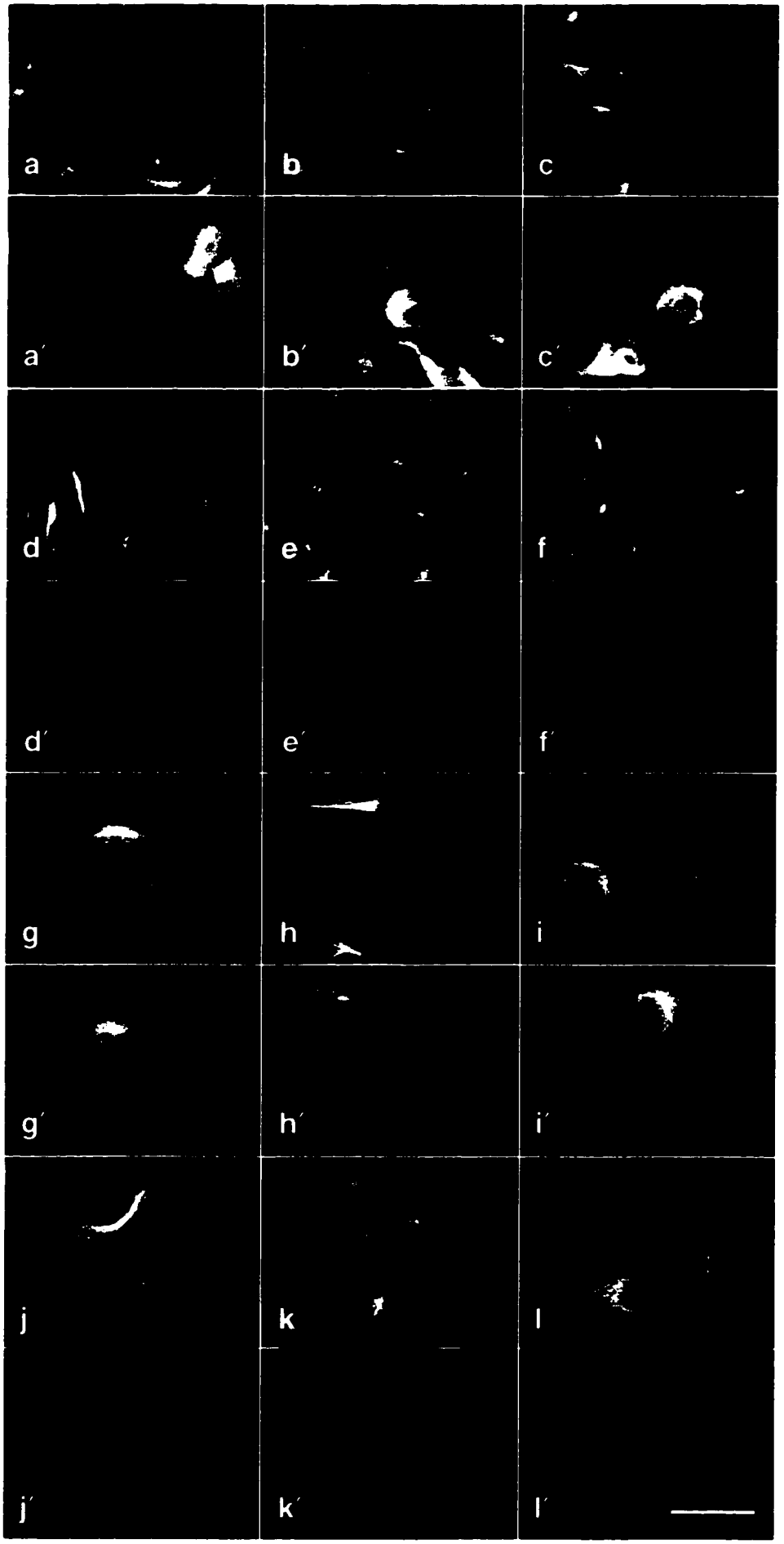
a
b
c
a′
b′
c′
d
e
f
d′
e′
f′
g
h
i
g′
h′
i′
j
k
l
j′
k′
l′

LC1 and P-LC2, but 6mycLC3 was not detected by LC3. P-LC1 and P-LC2 also detected endogenous LC1 and LC2 (Fig. 58, arrows). No LC2 was detected in HeLa cells. No endogenous LC3 was detected in either cell line.

The effect of expression of myc-tagged LCs on MT organization was characterized by digital immunofluorescence microcopy. In transfected P19 EC cells fixed by precipitation, 6mycLC1, 6mycLC2 and 6mycLC3 were detected in the cytoplasm of expressing cells (Fig. 59a′, b′, c′). No MT colocalization was observed and MTs in transfected cells had a similar distribution to MTs in untransfected cells (Fig. 59a - c′). Exogenously expressed LCs were never detected in transfected cells prepared by extraction / fixation (Fig. 59d – f′). These results were duplicated in HeLa cells (Fig. 59g – l′).

DISCUSSION

EXPRESSION OF LC3 IN DIFFERENTIATING P19 EC CELLS

The peak levels of MAP1a and 1b were observed during day 4 to 6 while the peak levels of LC3 occurred later in differentiation. Mann *et al.* (1996) also showed that the amount of LC3 increased during embryonic brain development. This suggests that the amount of LC3 bound to either MAP1a or MAP1b increases as differentiation increases. The increase in LC3 levels in differentiating P19 EC cells occurs concomitantly with an increase in MT stability, suggesting LC3 has its greatest effect on the role of MAP1a or MAP1b in MT dynamics during the later stages of differentiation when MTs are most stable.

MT STABILITY AND MT-BOUND MAPS

The profile of total polymerized tubulin, incorporation of βIII-tubulin into MTs, and MT stability in differentiating P19 EC cells is similar to that reported by Laferrière and Brown (1996). A comparison of the levels of MAP1a and 1b in SDS-whole cell extracts with the levels in total MT polymer, indicates that most of the MAP1a present during differentiation is MT-bound while most or all of the MAP1b present is not MT-associated after day 4. The peak in MAP1a levels in SDS-whole cell extracts is concomitant with the large increase in polymerized tubulin seen during the growth phase of differentiation. This suggests that there is some mechanism

acting to regulate the levels of MAP1a present on MTs during differentiation. It is possible that MAP1a expression is regulated by feedback inhibition in which cytosolic MAP1a prevents further synthesis of MAP1a. The increase in MT polymer would sequester MAP1a from the cytoplasm and this may stimulate increased MAP1a synthesis. Removal of MAP1a from MTs (perhaps by competition with other MAPs) would result in increased concentrations of cytosolic MAP1a, preventing further synthesis. Because the majority of MAP1a appears in the MT-bound fraction both in undifferentiated cells and in differentiating cells, the threshold for this feedback inhibition may be low.

The MAP1a peak seen during the growth phase is probably required to keep appropriate amounts of MAP1a bound to MTs so that they function properly during this period. The peak in bound MAP2 followed by lower, but similar levels from day 6 onward are probably due to the different expression patterns of HMW and LMW forms of MAP2 during differentiation. LMW-forms are present early in differentiation and then decrease later in differentiation while HMW-MAP2 continually increases during differentiation. LC3 associates with both MAP1a and 1b (Schoenfeld *et al.*, 1989). The biphasic pattern of MT-bound LC3 might be due to a loss of MT-bound MAP1b during early differentiation. The high levels of MT-bound LC3 later in differentiation probably represent LC3 associated with MAP1a. From this, it follows that the LC3 composition of MAP1a steadily increases during development.

LC3 FUNCTION

The steady increase in LC3 associated with MAP1a during differentiation is concomitant with an increase in MT stability. This might suggest that LC3 increases the ability of MAP1a to stabilize MTs. However, Pedrotti *et al.* (1994) showed that native MAP1a purified from adult brain has a weaker effect on MT dynamics compared to MAP2 and the MAP1a used in those experiments presumably was associated with LC3. We have shown that the LC3 present in undifferentiated P19 EC cells is not MT-bound while the majority of MAP1a is present in the cytoskeletal fraction (bound to MTs). This indicates that LC3 is incapable of associating with either MAP1a or 1b in undifferentiated cells. Overexpression of MAP1a fragments in the undifferentiated cells had a similar effect on MT dynamics compared to MAP2 as

obtained in vitro by Pedrotti *et al.* (1994) using LC3-associated MAP1a. This suggests the MT-stabilizing properties of MAP1a are not affected by LC3. LC3 might serve to increase the affinity of MAP1a and MAP1b for MTs. However, MAP1b in differentiating P19 EC cells, which presumably contains increasing amounts of LC3, is lost from MTs during later stages of differentiation. The dissociation of MAP1b from adult brain (also presumably LC3-associated) from MTs in the presence of MAP2 is greater than MAP1a (Pedrotti and Islam, 1993), suggesting that LC3-bound MAP1b is more weakly associated with MTs than LC3-bound MAP1a. LC3 may serve to increase the affinity of MAP1b for MTs during the early growth phase (day 2 – 4) of differentiation when MAP2 is present at low levels. MAP1a is found in the adult brain primarily in dendrites where it colocalizes with MAP2 on the same MTs (Shiomura and Hirokawa, 1987; Schoenfeld *et al.*, 1989). LC3 association with MAP1a may increase the affinity of MAP1a for MTs so that it is capable of competing with MAP2 for binding sites on mature neuronal MTs.

EXPRESSION OF LCs IN UNDIFFERENTIATED P19 EC AND HELA CELLS

While all three myc-tagged LCs could be detected in cells fixed by precipitation, none could be detected in untreated and taxol-treated cells (data not shown) prepared by the extraction / fixation method. In cells fixed by precipitation and in taxol-treated, extraction / fixation prepared cells, the respective MT colocalizations of MAP1b and 1a were observed. The fact the LC colocalization with MTs was not observed under either of these conditions suggests that exogenously expressed LCs can not associate with MAP1a or MAP1b. It is possible that the myc tag interfered with normal heavy chain / light chain interactions. Alternatively, it is possible that the region of the nascent MAP1 polypeptide containing LC1 or LC2 interacts with the heavy chain region prior to the processing event that results in the formation of endogenous LC1 and LC2 from the MAP1a/LC2 and MAP1b/LC1 polypeptides. Exogenously introduced LC1 or LC2 might not be competent to associate with heavy chains because it has already been "processed". LC3 could be detected in undifferentiated cultures, but no MT bound LC3 was detectable. Because LC3 is neuron specific, the association of LC3 with MAP1a or MAP1b (and

thus with MTs) might require neuronal-specific factors that are not present in undifferentiated cells.

NEURONAL-SPECIFIC ANTIGENS IN UNDIFFERENTIATED P19 EC CELLS

In undifferentiated P19 EC cells, we observed the presence of low levels of neuron-specific MAP2, LC3 and βIII-tubulin bound to MTs. 2 days after RA-induction, MT-bound MAP2 and LC3 were undetectable, but then both increased by day 4. MAP1b also exhibited a large decrease 2 days after RA-induction, but then also increased by day 4. The presence of neuron-specific proteins could be the result of very low levels of spontaneous differentiation occurring in undifferentiated cultures. The drop in expression of these proteins suggests that undifferentiated P19 EC cells are actually in a state of quasi-differentiation, aberrantly expressing neuronal proteins at very low levels. Induction of differentiation by RA might correct the regulation of expression of these neuronal proteins (including MAP1b) so that they follow the patterns of expression required for normal neurite growth and maturation. The absence of a drop in MAP1a levels following RA-induction suggests this MAP is required during the early stages of differentiation, perhaps to initiate process outgrowth.

APPENDIX 3 – OLIGONUCLEOTIDES USED IN THIS STUDY

TABLE 2. List of oligonucleotides used for sequencing.

OLIGONUCLEOTIDE	OLIGONUCLEOTIDE SEQUENCE (5′-3′)	POSITION ON MAP1A cDNA	PURPOSE
OLIGO-1	CTCTGGGGCTGAGGTCGAGA	2283	sequence Apa I joint
OLIGO-2	AGGTCAAAGGGGGATGGCAC	501	sequence Nco I joint
OLIGO-3	CCCTGTGTGGCTCTGGAATA	4479	sequence Eco RV joint
OLIGO-4	TACTGAGAAGATTGTGCGTG	1227	sequence Hind III joint
OLIGO-6	GAGAGCTTGGGCGACTCTACC	NA	check translation frame with 6myc tag
PCR-1	CGACGGTATCGATAAGCTATG	NA	construction of PGK-6mycN1A-2ΔBR
PCR-2	GGCCAGCTTGCTCACTGCTGT	985	"
PCR-3	GAGAGAGGTTTGCTGGCTGAA	1625	"
PCR-4	GTCGGGCCCAGCTCTGCTTCTCTC	2338	"
SEQ-1	TGCTCACACACATTGGGGCTG	257	sequence PGK-6mycN1A2ΔBR
SEQ-2	CACTGACCCTCTTCCACAAAA	557	"
SEQ-3	AGCTTCGGCACCTGGACTTTC	845	"
SEQ-4	GTGGAAAGGGAGAAAGAGGTA	1761	"
SEQ-5	GGTACTCTGTTCTCACCCTTC	NA	ensure proper translational termination in constructs where necessary
SEQ-6	GCAGGGAGTGGTTTCTCACCC	1681	sequence PGK-6mycN1A2ΔBR
SEQ-7	CAGAGCAGTGATGGAGGTCAG	750	"
SEQ-8	CGGTTTAAGTGCTGAAGAGTG	503	"
SEQ-9	ACAGCAAAGAGAGCAGAGTCC	164	"
SEQ-10	GGTGAGGTCGCCCAAGCTCTC	NA	"
SEQ-11	CCCGGCATTCTCGCACGCTTC	NA	"

Figure 60

MAP showing locations of the various oligonucleotides used in this study.

MAP1A cDNA

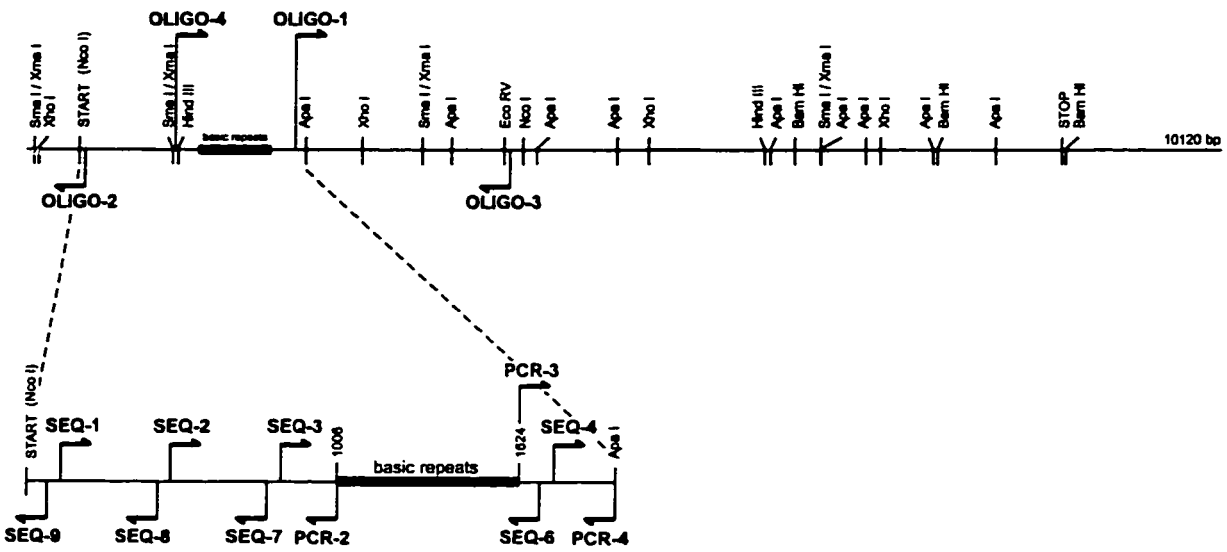

pKJ1ΔF-6myc

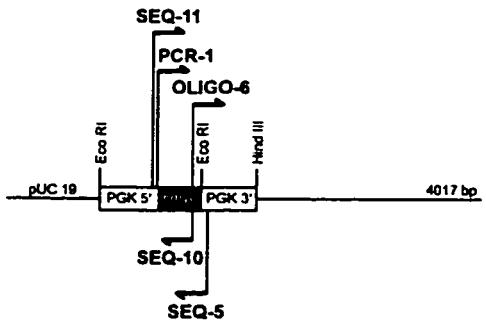

pPOP

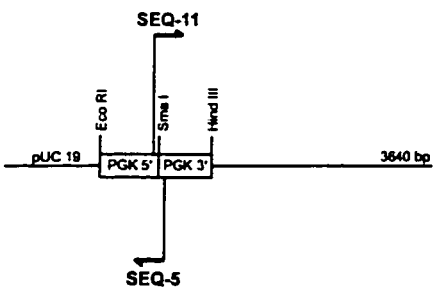

REFERENCES

Adavi, S., Murthy, N., Bramblett, G.T. and Flavin, M. 1985. The sites at which brain microtubule-associated protein 2 is phosphorylated *in vivo* differ from those accessible to cAMP-dependent kinase *in vitro*. *J. Biol. Chem.* **260**: 4364-4370.

Aizawa, H., Emori, Y., Mori, A., Mirofushi, H., Sakai, H. and Suzuki, K 1991. Functional analysis of the domain structure of microtubule-associated protein 4 (MAPU). *J. Biol. Chem.* **266**: 9841-9846.

Aizawa, H., Emori, Y., Morifushi, H., Kawasaki, H., Sakai, H, and Suzuki, K 1990. Molecular cloning of a ubiquitously distributed microtubule-associated protein with M_r 190,000. *J. Biol. Chem.* **265**: 13849-13855.

Aizawa, H., Kawaski, H., Murofushi, H., Kotani, S., Suzuki, K. and Sakai, H. 1989. A common amino acid sequence in 190 kDa microtubule-associated protein and tau for the promotion of microtubule assembly. *J. Biol. Chem.* **264**: 5885-5890.

Aizawa, H., Mirofushi, H., Kotani, S., Hisanaga, S., Hirokawa, N. and Sakai, H. 1987. Comparison of a major heat-stable microtubule-associated protein in HeLa cells and 190-kDa microtubule-associated protein in bovine adrenal cortex. *J. Biol. Chem.* **262**: 3782-3787.

Aletta, J.M., Lewis, S.A., Cowan, N.J., and Green, L.A. 1988. Nerve growth factor regulates both the phosphorylation and steady-state levels of microtubule-associated protein 1.2 (MAP1.2). *J. Cell Biol.* **106**: 1573-1581.

Andreadis, A., Wagner, B.K., Broderick, J.A. and Kosik, K.S. 1996. A tau promoter region without neuronal specificity. *J. Neurochem.* **66**: 2257-2263,

Arnold, S.E., Lee, V.M., Gur, R.E. and Trojanowski, J.Q. 1991. Abnormal expression of two microtubule associated proteins (MAP-2 and MAP-5) in specific subfields of the hippocampal formation in schizophrenia. *Proc. Natl. Acad. Sci. U.S.A.* **88**: 10850-10854.

Aoki, C. and Seikevitz, P. 1985. Ontogenetic changes in the cyclic adenosine 3' 5'-monophosphate-stimulatable phosphorylation of cat visual cortex proteins, particularly of microtubule-associated protein 2 (MAP-2): effects of normal and dark rearing and of the exposure to light. *J. Neurosci.* **5**: 2465-2483.

Asai, D.J., Thompson, W.C., Wilson, L., Dresden, C.F., Schulman, H. and Purich, D.L. 1985. Microtubule-associated proteins (MAPs): a monoclonal antibody to MAP1 decorates microtubules *in vitro* but stains stress fibers and not microtubules *in vivo*. *Proc. Natl. Acad. Sci. U.S.A.* **82**: 1434-1438.

Audebert, S., Desbruyères, E., Gruszczynski, C., Koulakoff, A., Gros, F., Denoulet, P. and Eddé, B. 1993. Reversible polyglutamylation of α- and β-tubulin and microtubule dynamics in mouse brain neurons. *Neuron* **8**: 831-842.

Audebert, S., Koulakoff, A., Berwald-Netter, Y., Gros, F., Denoulet, P. and Eddé, B. 1994. Developmental regulation of polyglutamylated α- and β-tubulin in mouse brain neurons. *J. Cell Sci.* **107**: 2313-2322.

Avila, J. 1991. Does MAP1b bind to tubulin through the interaction of α-helices. *Biochem. J.* **274**: 621-622.

Baas, P.W. and Ahmad, F.J. 1992. The plus ends of stable microtubules are the exclusive nucleating structures for microtubules in the axon. *J. Cell Biol.* **116**: 1231-1241.

Baas, P.W., Deitch, J.S., Black, M.M. and Banker, J.A. 1988. Polarity orientation of microtubules in hippocampal neurons: uniformity in the axon and nonuniformity in the dendrite. *Proc. Natl. Acad. Sci. U.S.A.* **85**: 8335-8339.

Bahr,B.A., Lam, N. and Lynch, G. 1994. Changes in the concentrations of tau and other structural proteins in the brains of aged mice. *Neurosci. Lett.* **175**: 49-52.

Banerjee, A., Roach, M.C., Wall, K.A., Lopata, M.A., Cleveland, D.W. and Ludueña, R.F. 1988. A monoclonal antibody against type II isotype of β-tubulin. Preparation of isotypically altered tubulin. *J. Biol. Chem.* **263**: 3029-3034.

Barlow, S., Gonzalez-Garay, M.L., West, R.R., Olmsted, J.B. and Cabral, F. 1994. Stable expression of heterologous microtubule-associated proteins (MAPs) in chinese hamster ovary cells: evidence for differing roles of MAPs in microtubule organization. *J. Cell Biol.* **126**: 1017-1029.

Berling, B., Wille, H., Röll, B., Mandelkow, E.M., Garner, C.C. and Mandelkow, E. 1994. Phosphorylation of microtubule-associated proteins MAP2a, b and MAP2c at Ser136 by proline-directed kinases in vivo and in vitro. *Eur. J. Cell Biol.* **64**: 120-130.

Bernhardt, R., Huber, G. and Matus, A. 1985. Differences in the developmental pattern of three microtubule-associated proteins in the rat cerebellum. *J. Neurosci.* **5**: 977-991.

Bigot, D. and Hunt, S.P. 1991. The effects of quisqualate and nocodazole on the organization of MAP2 and neurofilaments in spinal cord neurons in vitro. *Neurosci. Lett.* **131**: 21-26.

Binder, L.I., Frankfurter, A., Kim, H., Cáceres, A., Payne, M.R. and Rebhun, L.I. 1984. Heterogeneity of microtubule-associated protein 2 during rat brain development. *Proc. Natl. Acad. Sci. U.S.A.* **81**: 5613-5617.

Black, M.M. and Greene, L.A. 1982. Changes in colchicine susceptibility of microtubules associated with neurite outgrowth: studies with nerve growth factor-responsive PC12 pheochromocytoma cells. *J. Cell Biol.* **95**: 379-386.

Black, M.M., Slaughter, T. and Fischer, I. 1994. Microtubule-associated protein 1b (MAP1b) is concentrated in the distal region of growing axons. *J. Neurosci.* **14**: 857-870.

Black, M.M., Slaughter, T., Moshiach, S., Obrocka, M. and Fischer, I. 1996. Tau is enriched on dynamic microtubules in the distal region of growing axons. *J. Neurosci.* **16**: 3601-3619.

Bloom. G.S., Luca, F.C. and Vallee, R.B. 1984a. Widespread cellular distribution of MAP-1A (microtubule-associated protein 1A) in the mitotic spindle and on interphase microtubules. *J. Cell Biol.* **98**: 331-340.

Bloom, G.S., Luca, F.C. and Vallee, R.B. 1985. Microtubule-associated protein 1B: Identification of a major component of the neuronal cytoskeleton. *Proc. Natl. Acad. Sci. U.S.A.* **82**: 5404-5408.

Bloom, G.S., Schoenfeld, T.A. and Vallee, R.B. 1984b. Widespread distribution of the major polypeptide component of MAP1 (microtubule-associated protein 1) in the nervous system. *J. Cell Biol.* **98**: 320-330.

Bloom, G.S. and Vallee, R.B. 1983. Association of microtubule-associated protein 2 (MAP2) with microtubules and intermediate filaments in cultured brain cells. *J. Cell Biol.* **96**: 1523-1531.

Blose, S.H., Meltzer, D.I. and Feramisco, J.R. 1984. 10-nm filaments are induced to collapse in living cells microinjected with monoclonal and polyclonal antibodies against tubulin. *J. Cell Biol.* **98**: 847-858.

Bongiovanni, G., Barra, H.S. and Hallak, M.E. 1994. Some common properties between a brain protein that is modified by posttranslational arginylation and the microtubule-associated STOP protein. *J. Neurochem.* **63**: 2295-2299.

Bosc, C., Cronk, J.D., Pirollet, F., Watterson, D.M., Haiech, J., Job, D. and Margolis, R.L. 1996. Cloning, expression, and properties of the microtubule-stabilizing protein STOP. *Proc. Natl. Acad. Sci. U.S.A.* **93**: 2125-2130.

Boucher, D., Larcher, J.C., Gros, F. and Denoulet, P. 1994. Polygultamylation of tubulin as a progressive regulator of *in vivo* interactions between the microtubule-associated protein tau and tubulin. *Biochem.* **33**: 12471-12477.

Boyne, L.J., Martin, K., Hockfield, S. and Fischer, I. 1995. Expression and distribution of phosphorylated MAP1B in growing axons of cultured hippocampal neurons. *J. Neurosci. Res.* **40**: 439-450.

Brandt, R. and Lee, G. 1993. Functional organization of microtubule-associated protein tau. *J. Biol. Chem.* **268**: 3414-3419.

Brandt, R. and Lee, G. 1994. Orientation, assembly, and stability of microtubule bundles induced by a fragment of tau protein. *Cell Mot. Cytoskel.* **28**: 143-154.

Brugg, B. and Matus, A. 1988. PC12 cells express juvenile microtubule-associated proteins during nerve growth factor-induced neurite outgrowth. *J. Cell Biol.* **107**: 643-650.

Brugg, B. and Matus, A. 1991. Phosphorylation determines the binding of microtubule-associated protein 2 (MAP2) to microtubules in living cells. *J. Cell Biol.* **114**: 735-743.

Brugg, B., Reddy, D. and Matus, A. 1993. Attenuation of microtubule-associated protein 1B expression by antisense oligodeoxynucleotides inhibits initiation of neurite outgrowth. *Neurosci.* **52**: 489-496.

Bruckenstein, D.A., Lein, P.J., Higgins, D. and Fremeau, R.T. Jr. 1990. Distinct spatial localization of specific mRNAs in cultured sympathetic neurons. *Neuron* **5**: 808-819.

Bulinski, J.C. 1994. MAP4. In: Microtubules. Edited by J.S. Hyams and C.W. Lloyd. Wiley-Liss Inc. NY pp 167-182.

Bulinski, J.C. and Borisy, G.G. 1980a. Immunofluorescence localization of the HeLa cell microtubule associated protein in microtubules *in vitro* and *in vivo*. *J. Cell Biol.* **87**: 792-801.

Bulinski, J.C. and Borisy, G.G. 1980b. Widespread distribution of a 210000 molecular weight microtubule-associated protein in cells and tissues of primates. *J. Cell Biol.* **87**: 802-808.

Burgin, K.E., Ludin, B., Ferralli, J. and Matus, A. 1994. Bundling of microtubules in transfected cells does not involve an autonomous dimerization site on the MAP2 molecule. *Mol. Biol. Cell* **5**: 511-517.

Burns, R.G. and Farrell, K.W. 1996. Getting to the heart of β-tubulin. *Trends in Cell Biol.* **6**: 297-303.

Bush, M.S. and Gordon-Weeks, P.R. 1994. Distribution and expression of developmentally regulated phosphorylation epitopes on MAP1B and neurofilament proteins in the developing rat spinal cord. *J. Neurocytol.* **23**: 682-698.

Bush, M.S., Tonge, D.A., Woolf, C. and Gordon-Weeks, P.R. 1996. Expression of a developmentally regulated, phosphorylated isoform of microtubule-associated protein 1B in regenerating axons of the sciatic nerve. *Neurosci.* **73**: 553-563.

Cáceres, A., Binder, L.I., Payne, M.R., Bender, P., Rebhun, L. and Steward, O. 1984. Differential subcellular localization of tubulin and the microtubule-associated protein MAP2 in brain tissue as revealed by immunocytochemistry with monoclonal hybridoma antibodies. *J. Neurosci.* **4**: 391-410.

Cáceres, A. and Kosik, K.S. 1990. Inhibition of neurite polarity by tau antisense oligonucleotides in primary cerebellar neurons. *Nature* **343**: 461-463.

Cáceres, A., Mautino, J. and Kosik, K.S. 1992a. Supression of MAP2 in cultured cerebellar macroneurons inhibits minor neurite formation. *Neuron*: **9**: 607-618.

Cáceres, A., Potrebic, S. and Kosik, K.S. 1992b. The effect of tau antisense oligonucleotides on neurite formation of cultured cerebellar macroneurons. J. Neurosci. 11: 1515-1523.

Cadrin, M., Wasteneys, G.O., Jones-Villeneuve, E.M.V., Brown, D.L. and Reuhl, K.R. 1988. Effects of methlymercury on retinoic acid-induced neuroectodermal derivatives of embryonal carcinoma cells. *Cell Biol. Toxicol.* **4**: 61-80.

Calvert, R. and Anderton, B.H. 1985. A microtubule-associated protein which is expressed at elevated levels during development of the rat cerebellum. *EMBO J.* **4**: 1171-1176.

Chapin, S.J., and Bulinski, J.C. 1991. Non-neuronal 210X10^3 M_r microtubule-associated protein (MAP4) contains a domain homologous to the microtubule-binding domains of neuronal MAP2 and tau. *J. Cell Sci.* **98**: 27-36.

Chapin, S.J., Bulinski, J.C. and Gunderson, G.G. 1991. Microtubule bundling in cells. *Nature* **349**: 24.

Chapin, S.J., Lue, C.M., Yu, M.T. and Bulinski, J.C. 1995. Differential expression of alternatively spliced forms of MAP4: a repertoire of structurally different microtubule binding domains. *Biochem.* **34**: 2289-2301.

Charrière-Bertrand, C., Garner, C., Tardy, M. and Nuñez, J. 1991. Expression of various microtubule-associated protein 2 forms in the developing mouse brain and in cultured neurons and astrocytes. *J. Neurochem.* **56**: 385-391.

Chen, J., Kanai, Y, Cowan, N.J. and Hirokawa, N. 1992. Projection domains of MAP2 and tau determine spacings between microtubules in dendrites and axons. *Nature* **360**: 674-677.

Chen. C. and Okayama, H. 1987. High-efficiency transfection of mammalian cells by plasmid DNA. *Mol. Cell. Biol.* **7**: 2745-2752.

Chung, W.J., Kindler, S., Seidenbecher, C. and Garner, C.C. 1996. MAP2a, an alternatively spliced variant of microtubule-associated protein 2. *J. Neurochem.* **66**: 1273-1281.

Cleveland, D.W., Hwo, S.Y. and Kirschner, M.W. 1977. Purification of tau, a microtubule-associated protein that induced assembly of microtubules from purified tubulin. *J. Mol. Biol.* 116: 207-225.

Cravchik, A., Reddy, D. and Matus, A. 1994. Identification of a novel microtubule-binding domain in microtubule-associated protein 1A (MAP1A). *J. Cell Sci.* **107**: 661-672.

Coffey, R.L. and Purich, D.L. 1995. Non-cooperative binding of the MAP2 microtubule-binding region to microtubules. *J. Biol. Chem.* **270**: 1035-1040.

Collins, C.A. 1994. Dynein-based organelle movement. In: Microtubles. Edited by J.S. Hyams and C.W. Lloyd. Wiley-Liss Inc. NY pp 367-380.

Collins, C.A. and Vallee, R.B. 1987. Temperature-dependent reversible assembly of taxol-treated microtubules. *J. Cell Biol.* **105**: 2847-2854.

Correas, I., Radilla, R. and Avila, J. 1990. The tubulin-binding sequence of brain microtubule-associated proteins, tau and MAP-2, is also involved in actin binding. *Biochem J.* **269**: 61-64.

Couchie, D., Chabas, S., Mavilia, C. and Nuñez, J. 1996. New forms of HMW MAP2 are preferentially expressed in the spinal cord. *FEBS Lett.* **388**: 76-79.

Couchie, D., Mavilia, C., Georgieff, I.S., Liem, R.K.H., Shelanski, M.L. and Nuñez, J. 1992. Primary structure of high molecular weight tau present in the peripheral nervous system. *Proc. Natl. Acad. Sci. U.S.A.* **89**: 4378-4381.

Crandall, J.E. and Fischer, I. 1989. Developmental regulation of microtubule-associated protein 2 expression in regions of mouse brain. *J. Neurochem*, **53**: 1910-1917.

Cross, D., Dominguez, J., Maccioni, R.B. and Avila, J. 1991. MAP-1 and MAP-2 binding sites at the c-terminus of β-tubulin. Studies with synthetic tubulin peptides. *Biochem.* **30**: 4362-4366.

Cunningham, C.C., LeClerc, N., Flanagan, L.A., Lu, M., Janmey, P.A. and Kosik, K.S. 1997. Microtubule-associated protein 2c reorganizes microtubules and microfilaments into distinct cytological structures in an actin-binding protein-280 deficient cell line. *J. Cell Biol.* **136**: 854-857.

Dammerman, M., Yen, S.H. and Shafit-Zagardo, B. 1989. Sequence of a human MAP-2 region sharing epitopes with Alzheimer neurofibrillary tangles. *J. Neurosci. Res.* **24**: 487-495.

De Brabander, M., Bulinski, J.C., Geuens, G., De May, J. and Borisy, G.G. 1981. Immunoelectron microscopic localization of the 210000 molecular weight microtubule-associated protein in cultured cells of primates. *J. Cell Biol.* **91**: 438-445.

Denoulet, P., Filliatreau, G., deNéchaud, B., Gros, F. and Di Giamberardino, L. 1989. Differential axonal transport of isotubulins in the motor axons of the rat sciatic nerve. *J. Cell Biol.* **108**: 965-971.

Dewar, D. and Dawson, D.A. 1997. Changes in cytoskeletal protein immunostaining in myelinated fibre tracts after focal cerebral ischaemia in rat. *Acta Neuropathol.* **93**: 71-77.

Díaz-Nido and Avila, J. 1989. Quantitation of microtubule-associated protein MAP-1B in brain and other tissues. *Int. J. Biochem.* **21**: 723-730.

Díaz-Nido, J., Serrano, L., Hernández, M.A. and Avila, J. 1990. Phosphorylation of microtubule proteins in rat brain at different developmental stages: comparison with that found in neuronal cultures. *J. Neurochem.* **54**: 211-222.

Díaz-Nido, J., Serrano, L., López-Otin, C., Vandekerckhove, J. and Avila, J. 1990. Phosphorylation of the neuronal-specific β-tubulin isotype. *J. Biol. Chem.* **265**: 13949-13954.

Díaz-Nido, J., Serrano, L., Méndez, E. and Avila,J. 1988. A casein kinase-II related activity is involved in phosphorylation of microtubule-associated protein MAP-1B during neuroblastoma cell differentiation. *J. Cell Biol.* **106**: 2057-2065

Díez-Guerra, F.J. and Avila, J. 1995. An increase in phosphorylation of microtubule-associated protein 2 accompanies dendrite extension during the differentiation of cultured hippocampal neurons. *Eur. J. Biochem.* **227**: 68-77.

Di Tella, M., Feiguin, F., Morfini, G. and Cáceres, A. 1994. Microfilament-associated growth cone component depends upon tau for its intracellular localization. *Cell Mot. Cytoskel.* **29**: 117-130.

Dotti, C.G., Banker, G.A. and Binder, L.I. 1987. The expression and distribution of the microtubule-associated protein tau and microtubule-associated protein 2 in hippocampal neurons in the rat *in situ* and in cell culture. *Neurosci.* **23**: 121-130.

Doll, T., Meichsner, M., Reiderer, B.M., Honegger, P. and Mauts, A. 1993. An isoform of microtubule-associated protein 2 (MAP2) containing four repeats of the tubulin-binding motif. *J. Cell Sci.* **106**: 633-640.

Doll, T., Papandrikopoulou, A. and Matus, A. 1990. Nucleotide and amino acid sequences of embryonic rat MAP2c. *Nuc. Acids Res.* **18**: 361.

Domínguez, J.E., Buenida, B., López-Otín, C., Antony, C., Karsenti, E. and Avila, J. 1994. A protein related to brain microtubule-associated protein MAP1B is a component of the mammalian centrosome. *J. Cell Sci.* **107**: 601-611.

Drubin, D.G., Feintstein, S.C., Shooter, E.M. and Kirschner, M.W. 1985. . Nerve growth factor-induced neurite outgrowth in PC12 Cells involves the coordinate induction of microtubule assembly and microtubule assembly-promoting factors. *J. Cell Biol.* **101**: 1799-1807.

Drubin, D.G. and Kirschner, M.W. 1986. Tau protein function in living cells. *J. Cell Biol.* **103**: 2739-2746.

Dye, R.B., Fink, S.P. and Williams, R.C. Jr. 1993. Taxol-induced flexibility of microtubules and its reversal by MAP-2 and tau. *J. Biol. Chem.* **268**: 6847-6850.

Edson, K., Weisshaar, B. and Matus, A. 1993. Actin depolymerization induces process formation on MAP2-transfected non-neuronal cells. *Develop.* **117**: 689-700.

Edelmann, W., Zervas, M., Costello, P., Roback, L., Fischer, I., Hammarback, J.A., Cowan, N., Davies, P., Wainer, B. and Kucherlapati, R. 1996. Neuronal abnormalities in microtubule-associated protein 1B mutant mice. *Proc. Natl. Acad. Sci. U.S.A.* **93:** 1270-1275.

Esmaeli-Azad, B., McCarty, J.H. and Feinstein, S.C. 1994. Sense and antisense transfection analysis of tau function: tau influences net microtubule assembly, neurite growth and neuritic stability. *J. Cell Sci.* **107**: 869-879.

Evan, G.I., Lewis, G.K., Ramsay, G. and Bishop, J.M. 1985. Isolation of monoclonal antibodies specific for the human c-myc proto-oncogene product. *Mol. Cell Biol.* **5**: 3610-3616.

Falconer, M.M., Echeverri, C.J. and Brown, D.L. 1992. Differential sorting of beta-tubulin isotypes into colchicine-stable microtubules during neuronal and muscle differentiation of embryonal carcinoma cells. *Cell Mot. Cytoskel.* **21**: 313-325.

Falconer, M.M., Vaillant, A.R., Reuhl, K.R., Laferrière, N. and Brown, D.L. 1994. The molecular basis of microtubule stability in neurons. *Neurotoxicol.* **15**: 109-122.

Falconer, M.M., Vielkind, U. and Brown, D.L. 1989. Establishment of a stable, acetylated microtubule bundle during neuronal commitment. *Cell Mot. Cytoskel.* **12**: 169-180.

Fawcett, J.W., Mathews, G., Housden, E., Goedert, M. and Matus, A. 1994. Regenerating sciatic nerve axons contain the adult rather than the embryonic pattern of microtubule associated proteins. *Neurosci.* **61**: 789-804.

Fellous, A., Prasad, V., Ohayon, R., Jordan, M.A, and Ludueña, R.F. 1994. Removal of the projection domain of microtubule-associated protein 2 alters its interaction with tubulin. *J. Prot. Chem.* **13**: 381-391.

Ferhat, L., Represa, A., Bernard, A., Ben-Ari, Y. and Khrestchatisky, M. 1996. MAP2d promotes bundling and stabilization of both microtubules and microfilaments. *J. Cell Sci.* **109**: 1095-1103.

Ferralli, J., Doll, T. and Matus, A. 1994. Sequence analysis of MAP2 function in living cells. *J. Cell Sci.* **107**: 3115-3125.

Field, J., Nikawa, J., Broek, D., MacDonald, B., Rodgers, L., Wilson, I.A., Lerner, R.A. and Wigler, M. 1988. Purification of a RAS-responsive adenylyl cyclase complex from *Saccharomyces cerevisiae* by use of an epitope addition method. *Mol. Cell. Biol.* **8**: 2159-2165.

Fink, J.K., Jones, S.M., Esposito,C. and Wilkowski, J. 1996. Human microtubule-associated protein 1a (MAP1A) gene: genomic organization, cDNA sequence, and developmental and tissue specific expression. *Genomics* **35**: 577-585.

Fischer, B., Retchkiman, I., Bauer, J., Platt, D. and Popa-Wagner, A. 1995. Pentylenetetrazole-induced seizure upregulates levels of microtubule-associated protein 1B mRNA and protein in the hippocampus of the rat. *J. Neurochem.* **65**: 467-470.

Fischer, I., Konola, J. and Cochary, E. 1990. Microtubule-associated protein (MAP1B) is present in cultured oligodendrocytes and co-localizes with tubulin. *J. Neurosci. Res.* **27**: 112-124.

Fischer, I. and Romano-Clarke, G. 1990. Changes in microtubule-associated protein MAP1B phosphorylation during rat brain development. *J. Neurochem.* **55**: 328-333.

Frankfurter, A., Binder, L.I. and Rebhun, L. 1986. Limited tissue distribution of a novel β-tubulin isoform. *J. Cell Biol.* **103**: 273A

Frappier, T.F., Georgieff, I.S., Brown, K. and Shelanski, M.L. 1994. τ-regulation of microtubule-microtubule spacing and bundling. *J. Neurochem.* **63**: 2288-2294.

Frederich, P. and Asódi, A. 1991. MAP-2: a sensitive cross linker and adjustable spacer in dendritic architecture. *FEBS Lett.* **295**: 5-9.

Fujii, T., Watanabe, M. and Nakamura, A. 1996. Characterization of microtubule-associated protein 1-associated protein kinases from rat brain. *Neurochem. Int.* **28**: 535-544.

Fujii, T., Watanabe, M., Ogoma, Y., Kondo, Y. and Arai, T. 1993. Microtubule-associated proteins, MAP1A and MAP1B, interact with F-actin *in vitro*. *J. Biochem.* **114**: 827-829.

Gamblin, T.C., Nachmanoff, K., Halpain, S. and Williams, R.C. Jr. 1996. Recombinant microtubule-associated protein 2c reduced the dynamic instability of individual microtubules. *Biochem.* **35**: 12576-12586.

Gard, D.L. and Kirschner, M. 1985. A polymer-dependent increase in phosphorylation of β-tubulin accompanies differentiation of a mouse neuroblastoma cell line. *J. Cell Biol.* **100**: 764-774.

Garel, J.R., Job, D. and Margolis, R.L. 1987. Model of anaphase chromosome movement based on polymer-guided diffusion. *Proc. Natl. Acad. Sci. U.S.A.* **84**: 3599-3603.

Garner, C.C., Garner, A., Huber, G., Kozak, C. and Matus, A. 1990. Molecular cloning of microtubule-associated protein 1 (MAP1A) and microtubule-associated protein 5 (MAP1B): identification of distinct genes and their differential expression in developing brain. *J. Neurochem.* **55**: 146-154.

Garner, C.C. and Matus, A. 1988. Different forms of microtubule-associated protein 2 are encoded by separate mRNA transcripts. *J. Cell Biol.* **106**: 779-783.

Garner. C.C., Tucker, R.P. and Matus, A. 1988. Selective localization of messenger RNA for cytoskeletal protein MAP2 in dendrites. *Nature* **336**: 674-677.

Georgieff, I.S., Liem, R.K., Mellado, W., Nuñez, J. and Shelanski, M.L. 1991. High-molecular weight tau: preferential localization in the peripheral nervous system. *J. Cell Sci.* **100**: 55-60.

Goedert, M. and Jakes, R. 1990. Expression of separate isoforms of human tau protein: correlation with tau pattern in brain and effects on tubulin polymerization. *EMBO J.* **9**: 4225-4230.

Geodert, M., Jakes, R., Crowther, R.A., Six, J., Lübke, U., Vandermeeren, M., Trojanowski, C.P. and Lee, V.M. 1993. The abnormal phosphorylation of tau protein at serine 202 in Alzheimer's disease recapitulates phosphorylation during development. *Proc. Natl. Acad. Sci. U.S.A.* **90**: 5066-5070.

Geodert, M., Jakes, R., Spillantini, M.G. and Crowther, R.A. 1994. Tau protein and Alzheimer's disease. In: Microtubules. Edited by J.S. Hyams and C.W. Lloyd. Wiley-Liss Inc. NY pp 183-200.

Goedert, M., Spillantini, M.G. and Crowther, R.. 1992. Cloning of a big tau microtubule-associated protein characteristic of the peripheral nervous system. *Proc. Natl. Acad. Sci. U.S.A.* **89**: 1983-1987.

Goedert, M., Spillantini, M.G., Jakes, R., Rutherford, D. and Crowther, R.A. 1989a. Multiple isoforms of human microtubule-associated protein tau: sequences and localization in neurofibrillary tangles of Alzheimer's disease. *Neuron* **3**: 519-526.

Goedert, M., Spillantini, M.G., Potier, M.C., Ulrich, J. and Crowther, R.A. 1989b. Cloning and sequencing of the cDNA encoding an isoform of microtubule-associated protein tau containing four tandem repeats: differential expression of tau protein mRNAs in human brain. *EMBO J.* **8**: 393-399.

Gonzalez-Garay, M.I. and Cabral, F. 1995. Overexpression of an epitope-tagged β-tubulin in Chinese hamster ovary cells causes an increase in endogenous α-tubulin synthesis. *Cell. Mot. Cytoskel.* **31**: 259-272.

Goode, B.L. and Feinstein, S.C. 1994. Identification of a novel microtubule binding and assembly domain in the developmentally regulated inter-repeat region of tau. *J. Cell Biol.* **124**: 769-782.

Greenwood, J.A. and Johnson, G.V. 1995. Localization and *in situ* phosphorylation state of nuclear tau. *Exp. Cell Res.* **220**: 332-337.

Gustke, N., Trinczek, B., Biernat, J., Mandelkow, E.M. and Mandelkow, E 1994. Domains of τ protein and interactions with microtubules. *Biochem.* **33**: 9511-9522.

Hagestedt, T., Lichtenberg, B., Wille, H., Mandelkow, E.M. and Mandelkow, E. 1989. Tau protein becoms long and stiff upon phosphorylation: correlation between paracrystalline structure and degree of phosphorylation. *J. Cell Biol.* **109**: 1643-1651.

Hammarback, J.A., Obar, R.A., Hughes, S.M. and Vallee, R.B. 1991. MAP1B is encoded as a polyprotein that is processed to form a complex n-terminal microtubule-binding domain. *Neuron* **7**: 129-139.

Hanahan, D. 1983. Studies of transformation of *Escherichia coli* with plasmids. *J. Mol. Biol.* **166**: 557-580.

Harada, A., Oguchi, K., Okabe, S., Kuno, J., Terada, S., Ohshima, T., Sato-Yoshitake, R., Takei, Y., Noda, T. and Hirokawa, N. 1994. Altered microtubule organization in small-calibre axons of mice lacking tau protein. *Nature* **369**: 488-491.

Harrison, L., Cheetham, M.E. and Calvert, R.A. 1993. Investigation of the changes in neuronal distribution and phosphorylation state of MAP1X during development. *Dev. Neurosci.* **15**: 68-76.

Heidemann, S.R. 1996. Cytoplasmic mechanisms of axonal and dendritic growth in neurons. *Intl. Rev. Cytol.* **165**: 235-296.

Heidemann, S.R., Landers, J.M. and Hamborg, M.A. 1981. Polarity orientation of axonal microtubules. *J. Cell Biol.* **91**: 661-665.

Himmler, A., Dreschel, D., Kirschner, M.W. and Martin, D.W. Jr. 1989. Tau consists of a set of proteins with repeated c-terminal binding domains and variable N-terminal domains. *Mol. Cell. Biol.* **9**: 1381-1388.

Hirokawa, N., Funakoshi, T., Sato-Harada, R. and Kanai, Y. 1996. Selective stabilization of tau in axons and microtubule-associated protein 2c in cell bodies and dendrites contributes to polarized localization of cytoskeletal proteins in mature neurons. *J. Cell Biol.* **132**: 667-679.

Hirokawa, N., Hisanaga, S.I. and Shiomura, Y. 1988. MAP2 is a component of crossbridges between microtubules and neurofilaments in the neuronal cytoskeleton: quick-freeze, deep-etch immunoelectron microscopy and reconstitution studies. *J. Neurosci.* **8**: 2769-2779.

Hirokawa, N., Shiomura, Y. and Okabe, S. 1988. Tau proteins: the molecular structure and mode of binding on microtubules. *J. Cell Biol.* **107**: 1449-1459.

Huber. G., Alaimo-Beuret, D. and Matus, A. 1985. MAP3: characterization of a novel microtubule-associated protein. *J. Cell Biol.* **100**: 496-507.

Huber, G. and Matus, A. 1990. Microtubule-associated protein 3 (MAP3) expression in non-neuronal tissues. *J. Cell Sci.* **95**: 237-246.

Illenberger, S., Drewes, G., Trinczek, B., Biernat, J., Meyerm H., Olmsted, J.B., Mandelkow, E.M. and Mandelkow, E. 1996. Phosphorylation of microtubule-associated proteins MAP2 and MAP4 by the protein kinase $p110^{mark}$. *J. Biol. Chem.* **271**: 10834-10843.

Ingber, D.E. 1993. Cellular tensegrity: defining new rules of biological design that govern the cytoskeleton. *J. Cell Sci.* **104**: 613-627.

Joly, J.C. and Purich, D.L. 1990. Peptides corresponding to the second repeated sequence in MAP-2 inhibit binding of microtubule-associated proteins to microtubules. *Biochem.* **29**: 8916-8920.

Joly, J.C., Flynn, G. and Purich, D.L. 1989. The microtubule-binding fragment of microtubule-associated protein-2: location of the protease-accessible site and identification of an assembly-promoting peptide. *J. Cell Biol.* **109**: 2289-2294.

Jones-Villeneuve, E.M.V., McBurney, M.W., Rogers, K.A. and Kalnins, V.L. 1982. Retinoic acid induces embryonal carcinoma cells to differentiate into neurons and glial cells. *J. Cell Biol.* **94**: 253-262.

Joshi, H.C. and Baas. P.W. 1993. A new perspective on microtubules and axon growth. *J. Cell Biol.* **121**: 1191-1196.

Joshi, H.C, and Cleveland, D.W. 1989. Differential utilization of β-tubulin isotypes in differentiating neurites. *J. Cell Biol.* **109**: 663-673.

Kalcheva, N., Albala, J.S., Binder, L.I. and Shafit-Zagardo, B. 1994. Localization of specific epitopes on human microtubule-associated protein 2. *J. Neurochem.* **63**: 2336-2341.

Kalcheva, N., Weidenheim, M., Kress, Y. and Shafit-Zagardo, B. 1997. Expression of microtubule-associated protein-2a and other novel microtubule-associated protein-2 transcripts in human fetal spinal cord. *J. Neurochem.* **68**: 383-391.

Kanai, Y., Chen, J. and Hirokawa, N. 1992. Microtubule bundling by tau proteins *in vivo*: analysis of functional domains. *EMBO J.* **11**: 3953-3961.

Kanai, Y. and Hirokawa, N. 1995. Sorting mechanisms of tau and MAP2 in neurons: suppressed axonal transit of MAP2 and locally regulated microtubule binding. *Neuron* **14**: 421-432.

Kanai, Y., Takemura, R., Oshima, T., Mori, H., Ihara, Y., Yanagisawa, M., Masaki, T. and Hirokawa, N. 1989. Expression of multiple tau isoforms and microtubule bindle formation in fibroblasts transfected with a single tau cDNA. *J. Cell Biol.* **109**: 1173-1184.

Kenner, L., El-Shabrawi, Y., Hutter, H., Forstner, M., Zatloukal, K., Hoefler, G., Preisegger, K.H., Kurzbauer, R. and Denk, H. 1994. Expression of three- and four-repeat tau isoforms in mouse liver. *Hepatol.* **20**: 1086-1089.

Khan, I.A. and Ludueña, R.F. 1996. Phosphorylation of β_{III}-tubulin. *Biochem.* **35**: 3704-3711.

Kilmartin, J.V., Wright, B. and Milstein, C. 1982. Rat monoclonal antibodies derived by using a new nonsecreting rat cell line. *J.Cell Biol.* **93**: 576-582.

Kindler, S. and Garner, C.C. 1994. Four repeat MAP2 isoforms in human and rat brain. *Mol. Brn. Res.* **26**: 218-224.

Kindler, S., Schulz, B., Goedert, M. and Garner, C.C. 1990a. Molecular structure of microtubule-associated protein 2b and 2c from rat brain. *J. Biol. Chem.* **265**: 19679-19684.

Kindler, S., Schwanke, B., Schulz, B. and Garner, C.C. 1990b. Complete cDNA sequence encoding rat high and low molecular weight MAP2. *Nuc. Acids Res.* **18**: 2822.

Kirkpatrick, L.L. and Brady, S.T. 1994. Modulation of the axonal microtubule cytoskeleton by myelinating Schwann cells. *J. Neurosci.* **14**: 7440-7450.

Kirschner, M. and Mitchison, T. 1986. Beyond self-assembly: from microtubules to mophogenesis. *Cell* **45**: 329-342.

Kitagawa, K., Matsumoto, M., Niinobe, M., Mikoshiba, K., Hata, R., Veda, H., Handa, N., Fukunaqua, R., Isaka, Y., Kimura, K. and Kamada, T. 1989. Microtubule-associated protein 2 as a sensitive marker for cerebral ischemic damage: immunohistochemical investigation of dendritic damage. *Neurosci.* **31**: 401-411.

Knops, J., Kosik, K.S., Lee, G., Pardee, J.D., Cohen-Gould, L. and McConlogue, L. 1991. Overexpression of tau in a nonneuronal cell induces long cellular processes. *J. Cell Biol.* **114**: 725-733.

Knowles, R., LeClerc, N. and Kosik, K.S. 1994. Organization of actin and microtubules during process formation in tau-expressing SF9 cells. *Cell Mot. Cytoskel.* **28**: 256-264.

Kosik, K.S., Orecchio, L.D., Bakalis, S., Duffy, L. and Neve, R.L. 1988. Partial sequence of MAP2 in the region of a shared epitope with Alzheimer neurofibrillary tangles. *J. Neurochem.* **51**: 587-598.

Kosik, K.S., Orecchio, L.D., Bakalis, S. and Neve, R.L. 1989. Developmentally regulated expression of specific tau sequences. *Neuron* **2**: 1389-1397.

Kotani, S., Nishida, E., Kumagai, H. and Sakai, H. 1985. Calmodulin inhibits interaction of actin with MAP2 and tau, two major microtubule-associated proteins. *J. Biol. Chem.* **260**: 10779-10783.

Kreis, T.E. 1990. Role of microtubules in the organization of the golgi apparatus. *Cell Mot. Cytoskel.* **15**: 67-70.

Kuznetsov, S.A. and Gelfand, V.I. 1987. 18 kDa microtubule-associated protein: identification as a new light chain (LC-3) of microtubule-associated protein 1 (MAP-1). *FEBS Lett.* **212**: 145-148.

Kuznetsov, S.A., Rodionov, V.I., Nadezhdina, E.S., Murphy, D.B. and Gelfand, V.I. 1986. Identification of a 34-kD polypeptide as a light chain of microtubule-associated protein-1 (MAP-1) and its association with a MAP-1 peptide that binds to microtubules. *J. Cell Biol.* **102**: 1060-1066.

Laemmli, U.K. 1970. Cleavage of structural proteins during the assembly of the head of bacteriophage T4. *Nature* **227**: 680-685.

Laferrière, N.B. and Brown, D.L. 1996. Expression and posttranslational modification of class III β-tubulin during neuronal differentiation of P19 embryonal carcinoma cells. *Cell Mot. Cytoskel.* **35**: 188-199.

Laferrière, N.B., MacRae, T.H. and Brown, D.L. 1997. Tubulin synthesis and assembly in differentiating neurons. *Biochem. Cell Biol.* **75**: 7-21.

Langkopf, A., Guilleminot, J. and Nuñez, J. 1994. Two novel HMW MAP2 variants with four microtubule-binding repeats and different projection domains. *FEBS Lett.* **354**: 259-262.

Langkopf, A., Guilleminot, J. and Nuñez, J. 1995. τ and microtubule-associated protein 2c transfection and neurite outgrowth in ND 7/23 cells. *J. Neurochem.* **64**: 1045-1053

Langkopf, A., Hammarback, J.A., Müller, R., Vallee, R.B. and Garner, C.G. 1992. Microtubule-associated proteins 1A and LC2: Two proteins encoded in one messenger RNA. *J. Biol. Chem.* **267**: 16561-16566.

LeClerc, N., Baas, P.W., Garner, C.C. and Kosik, K.S. 1996. Juvenile and Mature MAP2 isoforms induce distinct patterns of process outgrowth. *Mol. Biol. Cell* **7**: 443-455.

LeClerc, N., Kosik, K.S.,Cowan, N., Pienkowski, T.P. and Baas, P.W. 1993. Process formation in SF9 cells induced by the expression of a microtubule-associated protein 2C-like construct. *Proc. Natl. Acad. Sci. U.S.A.* **90**: 6223-6227.

Ledesma, M.D., Bonay, P., Colaço, C. and Avila, J. 1994. Analysis of microtubule-associated protein tau glycation in paired helical filaments. *J. Biol. Chem.* **269**: 21614-21619.

Lee, G., Cowan, N. and Krischner, M. 1988. The primary structure and heterogeneity of tau protein from mouse brain. *Science* **239**: 285-288.

Lee, J.C., Tweedy, N. and Timasheff, S.N. 1978. *In vitro* reconstitution of calf brain microtubules: effects of macromolecules. *Biochem.* **17**: 2783-2790.

Lee, V.M., Balin, B.J., Otvos, L. and Trojanowski, J.Q. 1991. A68 – a major subunit of paired helical filaments and derivatized forms of tau. *Science* **251**: 675-678.

Lee, Y.C. and Wolff, J. 1984. Calmodulin binds to both microtubule-associated protein 2 and τ proteins. *J. Biol Chem.* **259**: 1226-1230.

Léger, J.G., Brandt, R. and Lee, G. 1994. Identification of tau protein regions required for process formation in PC12 cells. *J. Cell Sci.* **104**: 3403-3412.

Lewis, S.A. and Cowan, N.J. 1990. Microtubule bundling. *Nature* **345**: 674.

Lewis, S.A., Ivanov, I.E., Lee, G.H. and Cowan, N.J. 1989. Organization of microtubules in dendrites and axons is determined by a short hydrophobic zipper in microtubule-associated proteins MAP2 and tau. *Nature* **342**: 498-505.

Lewis, S.A., Villasante, A., Sherline, P. and Cowan, N.L. 1986. Brain-specific expression of MAP2 detected using a cloned cDNA probe. *J. Cell Biol.* **102**: 2098-2105.

Lewis, S.A., Wang, D. and Cowan, N.J. 1988. Microtubule-associated protein MAP2 shares a microtubule-binding motif with tau protein. Science 242: 936-939

Li, Y. and Black, M.M. 1996. Microtubule assembly and turnover in growing axons. *J. Neurosci.* **16**: 531-544.

Lim, S.S., Sammak, P.J. and Borisy, G.G. 1989. Progressive and spatially differentiated stability of microtubules in developing neuronal cells. *J. Cell Biol.* **109**: 253-263.

Litman, P., Barg, J., Rindzooksi, L. and Ginzburg, I. 1993. Subcellular localization of tau mRNA in differentiating neuronal cell culture: implications for neuronal polarity. *Neuron* **10**: 627-638.

Littauer, U.Z., Giveon, D., Thierauf, M., Ginzburg, I. and Ponstingl, H. 1986. Common and distinct tubulin binding sites for microtubule-associated proteins. *Proc. Natl. Acad. Sci. U.S.A.* **83**: 7162-7166.

Lloyd, R.A., Gentelmen, S. and Chader, G.J. 1994. Assay of tubulin acetyltransferase activity in subcellular tissue fractions. *Anal. Biochem.* **216**: 42-46.

Lo, M.M.S., Fieles, A.W., Norris, T.E., Dargis, P.G., Caputo, C.B., Scott, C.W., Lee, V. and Goedert, M. 1993. Human tau isoforms confer distinct morphological and functional properties to stably transfected fibroblasts. *Mol. Brn. Res.* **20**: 209-220.

Lopata, M.S. and Cleveland, D.W. 1987. *In vivo* microtubules are copolymers of available beta-tubulin isotypes: localization of each of six vertebrate beta-tubulin isotypes using polyclonal antibodies elicited by synthetic peptide antigens. *J. Cell Biol.* **105**: 1707-1720.

Lu, Q. and Wood, J.G. 1993. Characterization of fluorescently derivatized bovine tau protein and its localization and functions in cultured chinese hamster ovary cells. *Cell Mot. Cytoskel.* **25**: 190-200.

Ludin, B., Ashbridge, K., Fünfschilling, U. and Matus, A. 1996. Functional analysis of the MAP2 repeat domain. *J. Cell Sci.* **109**: 91-99.

Maccioni, R.B., Rivas, C.I. and Vera, J.C. 1988. Differential interaction of synthetic peptides from the carboxy-terminal regulatory domain of tubulin with microtubule-associated proteins. *EMBO J.* **7**: 1957-1963.

Maccioni, R.B., Serrano, L., Avila, J. and Cann, J.R. 1986. Characterization and structural aspects of the enhanced assembly of tubulin after the removal of its carboxy-terminal domain. *Eur. J. Biochem.* **156**: 375-381.

MacPherson, P. and McBurney, M.W. 1995. . P19 embryonal carcinoma cells: a source of cultured neurons amenable to genetic manipulation. In the neuronal cell lines edition of: Methods: a companion to methods in enzymology. A.F. Rousso and S.H. Green, editors. Academic Press Inc. San Diego, U.S.A. **7**: 238-252.

MacRae, T.H. 1997. Tubulin posttranslational modifications: enzymes and their mechanisms of action. *Eur. J. Biochem.* **244**: 265-278.

MacRae, T.H. and Langdon, C.M. 1989. Tubulin synthesis, structure and function: what are the relationships? *Biochem. Cell Biol.* **67**: 770-790.

Maniatis, T., Fritsch, E.F. and Sambrook, J. 1982. Molecular cloning: A laboratory manual. Cold Spring Harbour Press, NY.

Mandelkow, E.M., Drewes, G., Beirnat, J., Gustke, N., Van Lint, J., Vandenheede, J.R. and Mandelkow, E. 1992. Glycogen synthase kinase-3 and the Alzheimer-like state of microtubule-associated protein tau. *FEBS Lett.* **314**: 315-321.

Mandelkow, E.M. and Mandelkow, E. 1993. Tau as a marker for Alzheimer's disease. *TIBS.* **18**: 480-483.

Mangan, M.E. and Olmsted, J.B. 1996. A muscle-specific variant of microtubule-associated protein 4 (MAP4) is required in myogenesis. *Develop.* **122**: 771-781.

Mann, S.S, and Hammarback, J.A. 1994. Molecular characterization of light chain 3. *J. Biol. Chem.* 269 (15): 11492-11497.

Mann, S.S. and Hammarback, J.A. 1996. Gene localization and developmental expression of light chain 3: a common subunit of microtubule-associated protein 1A (MAP1A) and MAP1B. *J. Neurosci. Res.* **43**: 535-544.

Mansfield, S.G., Díaz-Nido, J., Gordon-Weeks, P.R. and Avila, J. 1992. The distribution and phosphorylation of the microtubule-associated protein MAP1B in growth cones. *J. Neurocytol.* **21**: 1007-1022.

Margolis, R.L. and Job, D. 1994. Microtubule stabilization. In: Microtubules. Edited by J.S. Hyams and C.W. Lloyd. Wiley-Liss Inc. NY pp 221-228.

Margolis, R.L., Job, D., Pabion, M. and Rauch, C.T. 1986a. Sliding of STOP proteins on microtubules: a model system for diffusion-dependent microtubule-motility. *Ann NY Acad. Sci.* **466**: 306-321.

Margolis, R.L.,Rauch, C.T. and Job, D. 1986b. Purification and assay of a 145-kDa protein ($STOP_{145}$) with microtubule-stabilizing and motility behaviour. *Proc. Natl. Acad. Sci. U.S.A.* **83**: 639-643.

Margolis, R.L., Rauch, C.T., Pirollet, F. and Job, D. 1990. Specific association of STOP protein with microtubules *in vitro* and with stable microtubules in mitotic spindles of cultured cells. *EMBO J.* **9**: 4095-4102.

Marsden, K.M., Doll, T., Ferralli, J., Botteri, F. and Matus, A. 1996. Transgenic expression of embryonic MAP2 in adult mouse brain: implications for neuronal polarization. *J. Neurosci.* **16**: 3265-3273.

Maruta, H., Greer, K. and Rosenbaum, J.L. 1986. The acetylation of alpha-tubulin and its relationship to the assembly and disassembly of microtubules. *J. Cell Biol.* **103**: 571-579.

Mary, J., Redeker, V., LeCaer, J.P., Rossier, J., and Schmitter, J.M. 1996. Posttranslational modifications in the c-terminal tail of axonemal tubulin from sea urchin sperm. *J. Biol. Chem.* **103**: 571-579.

Matus, A. 1988. Microtubule-associated proteins: their potential role in determining neuronal morphology. *Ann. Rev. Neurosci.* **11**: 29-44.

Matus, A. 1990a. Microtubule-associated proteins. *Curr. Op. in Cell Biol.* **2**: 10-14.

Matus, A. 1990b. Microtubule-associated proteins and the determination of neuronal form. *J. Physiol.* **84**: 134-137.

Matus,, A. 1994. Stiff microtubules and neuronal morphology. *Tr. Neurol. Sci.* **17**: 19-22.

McBurney, M.W. 1993. P19 embryonal carcinoma cells. *Int. J. Dev. Biol.* **37**: 135-140.

McBurney, M.W., Reuhl, K.R., Ally, A.I., Naspuri, S., Bell, J.C. and Craig, J. 1988. Differentiation and maturation of embryonal carcinoma-derived neurons in culture. *J. Neurosci.* **8**: 1063-1073.

McBurney, M.W., Jones-Villeneuve, E.M.V., Edwards, M.K.S. and Anderson, P.J. 1982. Control of muscle and neuronal differentiation in a cultured embryonal carcinoma cell line. *Nature* **299**: 165-167.

McBurney, M.W. and Rogers, B.J. 1982. Isolation of male embryonal carcinoma cells and their chromosome replication patterns. *Dev. Biol.* **89**: 503-508.

McKerracher, L., Vallee, R.B. and Aguayo, A.J. 1989. Microtubule-associated protein 1A (MAP1A) is a ganglion cell marker in adult rat retina. *Vis. Neurosci.* **2**: 349-356.

Meichsner, M., Doll, T., Reddy, D., Weisshaar, B. and Matus, A. 1993. The low molecular weight form of microtubule-associated protein 2 is transported into both axons and dendrites. *Neurosci.* **54**: 873-880.

Miller, F.D., Naus, C.C.G., Durand, M., Bloom, F.E. and Milner, R.J. 1987. Isotypes of α-tubulin are differentially regulated during neuronal maturation. *J. Cell Biol.* **105**: 3065-3073.

Mitchison, T. and Kirschner, M. 1984. Dynamic instability of microtubule growth. *Nature* **312**: 237-242.

Mitchison, T. and Kirschner, M. 1988. Cytoskeletal dynamics and nerve growth. *Neuron* **1**: 761-772.

Montejo de Garcini, E., de la Luna,S., Dominiguez, J.E. and Avila, J. 1994. Overexpression of tau protein in COS-1 cells results in the stabilization of centrosome-independent microtubules and extension of cytoplasmic processes. *Mol. Cell. Biochem.* **130**: 187-196.

Moody, S.A., Quigg, M.S. and Frankfurter, A. 1989. Development of peripheral trigeminal system in the chick revealed by an isotype-specific anti-β-tubulin monoclonal antibody. *J. Comp. Neurol.* **279**: 567-580.

Morassutti, D.J., Staines, W.A., Magnuson, D.S.K., Marshall, K.C. and McBurney, M.W. 1994. Murine embryonal carcinoma-derived neurons survive and mature following transplantation into adult rat striatum. *Neurosci.* **58**: 753-763.

Morishima-Kawashima, M. and Kosik, K.S. 1996. The pool of MAP kinase associated with microtubules is small but constitutively active. *Mol. Biol. Cell* **7**: 893-905.

Moritz, M., Braunfeld, M.B., Sedat, J.W., Alberts, B. and Agard, D.A. 1995. Microtubule nucleation by γ-tubulin-containing rings in the centrosome. *Nature* **378**: 638-640.

Murofushi, H., Kotani, S., Aizawa, H., Hisanaga, S., Hirokawa, N. and Sakai, H. 1986. Purification and characterization of a 190-kD microtubule-associated protein from bovine adrenal cortex. *J. Cell Biol.* **103**: 1911-1919

Murphy, D.B. and Borisy, G.G. 1975. Association of high molecular weight proteins with microtubules and their role in microtubule assembly *in vitro*. *Proc. Natl. Acad. Sci. U.S.A.* **72**: 2696-2700.

Murthy, A.S.N. and Flavin, M. 1983. Microtubule assembly using the microtubule-associated protein MAP-2 prepared in defined states of phosphorylation with protein kinase and phosphatase. *Eur. J. Biochem.* **137**: 37-46.

Niinobe, M., Maeda, N., Ino, H. and Mikoshiba, K. 1988. Characterization of microtubule-associated protein 2 from mouse brain and its localization in the cerebellar cortex. J. *Neurochem.* **51**: 1132-1139.

Noble, M., Lewis, S.A. and Cowan, S.J. 1989. The microtubule binding domain of microtubule-associated protein MAP1B contains a repeated sequence motif unrelated to that of MAP2 and tau. J. Cell Biol. 109: 3367-3376.

Nothias, F., Fischer, I., Murray, M., Mirman, S. and Vincent, J.D. 1996. Expression of a phosphorylated isoform of MAP1B is maintained in adult central nervous system areas that retain the capacity for structural plasticity. *J. Comp. Neurol.* **368**: 317-334.

Oakley, B.R. 1994. γ-tubulin. In: Microtubles. Edited by J.S. Hyams and C.W. Lloyd. Wiley-Liss Inc. NY pp 33-46.

Obar, R.A., Dingus, J., Bayley, H. and Vallee, R.B. 1989. The RII subunit of cAMP-dependent protein kinase binds to a common amino-terminal domain on microtubule-associated proteins 2a, 2b and 2c. *Neuron* **3**: 639-645.

Oblinger, M.M., Argasinski, A., Wong, J. and Kosik, K.S. 1991. Tau gene expression in rat sensory neurons during development and regeneration. *J. Neurosci.* **11**: 2453-2459.

Oblinger, M.M. and Kost, S.A. 1994. Coordinate regulation of tubulin and microtubule-associated proteins during development of hamster brain. *Dev. Br. Res.* **77**: 45-54.

Okabe, S. and Hirokawa, N. 1989. Rapid turnover of microtubule-associated protein MAP2 in the axon revealed by microinjection of biotinyated MAP2 into cultured neurons. *Proc. Natl. Acad. Sci. U.S.A.* **86**: 4127-4131.

Olesen, O.F. 1994. Expression of low molecular weight isoforms of microtubule-associated protein 2. *J. Biol. Chem.* **269**: 32904-32908.

Olmsted, J.B., Asnes, C.F., Parysek, L.M., Lyon, H.D. and Kidder, G.M. 1986. Distribution of MAP4 in cells and in adult and developing mouse tissues. *Ann. NY Acad. Sci.* **466**: 292-305.

Olson, K.R., McIntish, J.R. and Olmsted, J.B. 1995. Analysis of MAP4 function in living cells using green fluorescent protein (GFP) chimeras. *J. Cell Biol.* **130**: 639-650.

Ookata, K., Hisanaga, S., Bulinski,J.C., Murofushi, H., Aizawa, K., Itoh, T.J., Hotain, H., Okumura, E., Tachibana, K. and Kishimoto, T. 1995. Cyclin B interaction with microtubule-associated protein 4 (MAP4) targets $p34^{cdc2}$ kinase to microtubules and is a potential regulator of M-phase dynamics. *J. Cell Biol.* **128**: 849-862.

Padilla, R., Lopez, C., Otin, C., Serrano, L. and. Avila, J. 1993. Role of the carboxy terminal region of beta tubulin on microtubule dynamics through its interaction with the GTP phosphate binding region. *FEBS Lett.* **325**:173-176.

Pabion, M., Job, D. and Margolis, R.L. 1984. Sliding of STOP proteins on microtubules. *Biochem.* **23**: 6642-6648.

Panda, D., Miller, H.P., Banarjee, A., Ludueña, R.F. and Wilson, L. 1994. Microtubule dynamics *in vitro* are regulated by the tubulin isotype composition. *Proc. Natl. Acad. Sci. U.S.A.* **91**: 11358-11362.

Papandrikopoulou, A., Doll, T., Tucker, R.P., Garner, C.C. and Matus, A. 1989. Embryonic MAP2 lacks the cross linking sidearm sequences and dendritic targeting signal of adult MAP2. *Nature* **340**: 650-652.

Papasozomenos, S.C. and Binder, L.I. 1987. Phosphorylation determines two distinct species of tau in the central nervous system. *Cell Mot. Cytoskel.* **8**: 210-226.

Paturle-Lafanechère, L., Eddé, B., Denoulet, P., VanDorsselaer, A., Mazarquil, H., LeCaer, J.P., Wehland, J. and Job, D. 1991. Characterization of a major brain tubulin variant which cannot be tyrosinated. *Biochem.* **30**: 10523-10528.

Paturle-Lafanechère, L., Manier, M., Trigault, N., Pirollet, F., Mazarquil, H., and Job, D. 1994. Accumulation of delta 2-tubulin, a major brain tubulin variant that cannot be tyrosinated, in neuronal tissues and in stable microtubule assemblies. *J. Cell Sci.* **107**: 1529-1543.

Pedrotti, B., Francolini, M., Cotelli, F. and Islam, K. 1996a. Modulation of microtubule shape in vitro by high molecular weight microtubule associated proteins MAP1A, MAP1B and MAP2. *FEBS Lett.* **384**: 147-150.

Pedrotti, B., Colombo, R. and Islam, K. 1994a. Interactions of microtubule-associated protein MAP2 with unpolymerized and polymerized actin using a 96-well microtiter plate solid-phase immunoassay. *Biochem.* **33**: 8798-8806.

Pedrotti, B., Colombo, R. and Islam, K. 1994b. Microtubule associated protein MAP1A is an actin-binding and crosslinking protein. *Cell Mot. Cytoskel.* **29**: 110-116.

Pedrotti, B. and Islam. K. 1994. Purified native microtubule-associated protein MAP1A: kinetics of microtubule assembly and MAP1A / tubulin stoichiometry. *Biochem.* **33**: 12463-12470.

Pedrotti, B. and Islam, K. 1995a. Purification of microtubule-associated protein MAP1B from bovine brain: MAP1B binds to microtubules but not to microfilaments. *Cell Mot. Cytoskel.* **30**: 301-309.

Pedrotti, B. and Islam, K 1995b. Microtubule associated protein 1B (MAP1B) promotes efficient tubulin polymerization in vitro. *FEBS Lett.* **371**: 29-31.

Pedrotti, B. and Islam, K. 1995c. Purification of microtubule associated protein MAP1B from bovine brain: MAP1B binds to microtubules but not to microfilaments. *Cell Mot. Cytoskel.* **30**: 301-309.

Pedrotti, B. and Islam, K. 1996. Dephosphorylated but not phosphorylated microtubule associated protein MAP1B binds to microfilaments. *FEBS Lett.* **388**: 131-133.

Pedrotti, B., Soffientini, A. and Islam, K. 1993. Sulphonate buffers affect the recovery of microtubule-associated proteins MAP1 and MAP2: Evidence that MAP1A promotes assembly. *Cell Motil. Cytoskel.* **25**: 234-242

Pedrotti, B., Ulloa, L., Avila, J. and Islam, K. 1996b. Characterization of microtubule-associated protein MAP1B: phosphorylation state, light chains and binding to microtubules. *Biochem.* **35**: 3016-3023.

Pereira, A. and Goldstein, L.S.B. 1994. The kinesin superfamily. In: Microtubles. Edited by J.S. Hyams and C.W. Lloyd. Wiley-Liss Inc. NY pp 269-284.

Pierre, N. and Nuñez, J. 1983. Multisite phosphorylation of tau proteins from rat brain. *Biochem. Biophys. Res. Comm.* **115**: 212-219.

Piperno, G. and Fuller, M.T. 1985. Monoclonal antibodies specific for an acetylated form of α-tubulin recognize the antigen in cilia and flagella from a variety of organisms. *J. Cell Biol.* **101**: 2085-2094.

Pirollet, F., Derancourt, J., Haiech, J., Job, D., and Margolis, R.L. 1992. Ca++-calmodulin regulated effectors of microtuble stability in bovine brain. *Biochem.* **31**: 8849-8855.

Pirollet, F., Rauch, C.T., Job. D., and Margolis, R.L. 1988. Monoclonal antibody to microtubule-associated STOP protein: affinity purification of neuronal STOP activity and comparison of the antigen with activity in neuronal and non neuronal extracts. *Biochem.* **28**: 835-841.

Pratt, M.A.C., Langston, A.W., Gudas, L.J. and McBurney, M.W. 1993. Retinoic acid fails to induce expression of Hox genes in differentiation-defective murine embryonal carcinoma cells carrying a mutant gene for alpha retinoic acid receptor. *Differentiation* **53**: 105-113.

Przyborksi, S.A. and Cambray-Deakin, M.A. 1995. Developmental regulation of MAP2 variants during neuronal differentiation *in vitro*. *Dev. Brn. Res.* **89**: 187-201.

Quinlan, E.M. and Halpain, S. 1996. Postsynaptic mechanisms for bidirectional control of MAP2 phosphorylation by glutamate receptors. *Neuron* **16**: 357-368.

Raff, E.C. 1994. The role of multiple tubulin isoforms in cellular microtubule function. In: Microtubles. Edited by J.S. Hyams and C.W. Lloyd. Wiley-Liss Inc. NY pp 33-46.

Redeker, V., LeCaer, J.P., Rossier, J. and Promé, J.C. 1991. Structure of the polyglutamyl side chain posttranslationally added to α-tubulin. *J. Biol. Chem.* **266**: 23461-23466.

Redeker, V., Levilliers, N., Schmitter, J.M, LeCaer, J.P., Rossier, J., Adoutte, A. and Bré, M.H. 1994. Polyglycylation of tubulin: a posttranslational modification in axonemal microtubules. *Science* **266**: 1688-1691.

Riederer, B., Cohen, R. and Matus, A. 1986. MAP5: a novel brain microtubule-associated protein under strong developmental regulation. *J. Neurocytol.* **15**: 763-775.

Riederer, B. and Matus, A. 1985. Differential expression of distinct microtubule-associated proteins during brain development. *Proc. Natl. Acad. Sci. U.S.A.* **82**: 6006-6009.

Rivas, C.I., Vera, J.C. and Maccioni, R.B. 1988. Anti-idiotypic antibodies that react with microtubule-associated proteins are present in the sera of rabbits immunized with synthetic peptides from tubulin's regulatory domain. *Proc. Natl. Acad. Sci. U.S.A.* **85**: 6092-6096.

Robinson, J.M. and Vandré, D.D. 1995. Stimulus-dependent alterations in macrophage microtubules: increased tubulin polymerization and detyrosination. *J. Cell Sci.* **108**: 645-655.

Rogers, D., Gloster, A., Laferrière, N., Brown, D., Peterson, A. and Miller, F.D. 1995. Identification of cis-elements in the Tα1 promoter responsible for neuron-specific gene expression in transgenic mice. *Soc. Neurosci. Abstr.* **21**: 1522.

Rubino, H.M., Dammermann, M., Shafit-Zagardo, B., and Erlichman, J. 1989. Localization and characterization of the binding site for the regulatory subunit of type II cAMP-dependent protein kinase of MAP2. *Neuron* **3**: 631-638.

Safei, R. and Fischer, I. 1989a. Regulation of microtubule-associated protein 2 (MAP2) mRNA expression during rat brain development. *J. Mol. Neurosci.* **1**: 189-198.

Safei, R. and Fischer, I. 1989b. Cloning of a cDNA encoding MAP1B in rat brain: regulation of mRNA levels during development. *J. Neurochem.* **52**: 1871-1879.

Saito, N., Kawai, K. and Nowak, T.S. Jr. 1995. Reexpression of developmentally regulated MAP2c mRNA after ischemia: colocalization with hsp72 mRNA in vulnerable neurons. *J. Cereb. Blood Flow* **15**: 205-215.

Sato-Yoshitake, R., Shiomura, Y., Miyasaka, H. and Hirokawa, N. 1989. Microtubule-associated protein 1B: molecular structure, localization, and phosphorylation-dependent expression in developing neurons. *Neuron* **3**: 229-238.

Sattilaro, R.F. 1986. Interaction of microtubule-associated protein 2 with actin filaments. *Biochem.* **25**: 2003-2009.

Schoenfeld, T.A., McKerracher, L., Obar, R. and Vallee, R.B. 1989. MAP1A and MAP1B are structurally related microtubule-associated proteins with distinct developmental patterns in the CNS. *J. Neurosci.* **9**: 1712-1730.

Scholey, J.M. and Vale, R.D. 1994. Kinesin-based organelle transport. In: Microtubles. Edited by J.S. Hyams and C.W. Lloyd. Wiley-Liss Inc. NY pp 343-365.

Schulze, E. and Kirschner, M. 1986. Microtubule dynamics in interphase cells. *J Cell Biol.* **102:**1020-1031

Selden, S.C. and Pollard, T.D. 1983. Phosphorylation of microtubule-associated proteins regulates their interaction with actin filaments. *J. Biol. Chem.* **258**: 7064-7071.

Serrano, L., de la Torre, J., Maccioni, R.B. and Avila, J. 1984. Involvement of the carboxy-terminal domain of tubulin in the regulation of its assembly. *Proc. Natl. Acad. Sci. U.S.A.* **81**: 5989-5993.

Serrano, L., Díaz-Nido, J., Wandosell, F. and Avila, J. 1987. Tubulin phosphorylation by casein kinase II is similar to that found *in vivo*. *J. Cell Biol.* **105**: 1731-1739.

Serrano, L., Montejo de Garcini, E., Hernàndez, M.A. and Avila, J. 1985. Localization of the tubulin binding site for tau protein. *Eur. J. Biochem.* **153**: 595-600.

Shea, T.B. and Beermann, M.L. 1994. Respective roles of neurofilaments, microtubules, MAP1B, and tau in neurite outgrowth and stabilization. *Mol. Biol. Cell.* **5**: 863-875.

Shafit-Zagardo, B., Kalcheva, N., Dickson, D., Davies, P. and Kress, Y. 1997. Distribution and subcellular localization of high-molecular weight microtubule-associated protein-2 expressing exon 8 in brain and spinal cord. *J. Neurochem.* **68**: 862-873.

Sharma, N., Kress, Y. and Shafit-Zagardo, B. 1994. Antisense MAP-2 oligonucleotides induce changes in microtubule assembly and neuritic elongation in pre-existing neurites of rat cortical neurons. *Cell Mot. Cytoskel.* **27**: 234-247.

Shiomura, Y. and Hirokawa, N. 1987. Colocalization of microtubule-associated protein 1A and microtubule-associated protein 2 on neuronal microtubules *in situ* revealed with double-label immunoelectron microscopy. *J. Cell Biol.* **104**: 1575-1578.

Skerjanc, I.S., Slack, R.S., and McBurney, M.W. 1994. Cellular aggregation enhances myoD-directed skeletal myogenesis in embryonal carcinoma cells. *Mol. Cell Biol.* **14**: 8451-8459.

Smith, E.F. and Sale, W.S. 1994. Mechanisms of flagellar movement: functional interactions between dynein arms and the radial spoke-central apparatus complex. In: Microtubles. Edited by J.S. Hyams and C.W. Lloyd. Wiley-Liss Inc. NY pp 381-392.

Steffanini, M., DeMartino, C. and Zamboni, L. 1967. Fixation of ejaculated spermatozoa for electron microscopy. *Nature* **216**: 173-174.

Steiner, B., Mandelkow, E.M., Biernat, J., Gustke, N., Meyer, H.E., Schmidt, B., Mieskes, G., Söling, H.D., Dreschel, D., Kirschner, M.W., Goedert, M. and Mandelkow, E. 1990. Phosphorylation of microtubule-associated protein tau: identification of the site for Ca^{2+} -calmodulin-dependent kinase and the

relationship with tau phosphorylation in Alzheimer tangles. *EMBO J.* **9**: 3539-3544.

Sullivan, K.F. and Cleveland, D.W. 1986. Identification of conserved isotype-defining variable region sequences of four vertebrate β-tubulin polypeptide classes. *Proc. Natl. Acad. Sci. U.S.A.* **83**: 4327-4331.

Takemura, R., Okabe, S., Umeyama, T. and Hirokawa, N. 1995. Polarity orientation and assembly process of microtubule bundles in nocodazole-treated, MAP2c transfected COS cells. *Mol. Biol. Cell* **6**: 981-996.

Takemura, R., Okabe, S., Umeyama, T., Kanai, Y., Cowan, J. and Hirokawa, N. 1992. Increased microtubule stability and alpha tubulin acetylation in cells transfected with microtubule-associated proteins MAP1B, MAP2 or tau. *J. Cell Sci.* **103**: 953-964.

Tanaka, Y., Kawahata, K., Nakata, T. and Hirowawa, N. 1992. Chronological expression of microtubule-associated proteins (MAPs) in EC cell P19 after neuronal induction by retinoic acid. *Br. Res.* **596**: 269-278.

Theurkauf, W.E. and Vallee, R.B. 1983. Extensive cAMP-dependent and cAMP-independent phosphorylation of microtubule-associated protein 2. *J. Biol. Chem.* **258**: 7883-7886.

Thrower, D., Jordan, M.A. and Wilson, L. 1991. Quantitation of cellular tubulin in microtubules and tubulin pools by competitive ELISA. *J. Immunol. Meth.* **136**: 45-51.

Thurston, V.C., Zinkowski, R.P. and Binder, L.I. 1996. Tau as a nucleolar protein in human nonneuronal cells *in vitro* and *in vivo*. *Chromosoma* **105**: 20-30.

Trinczek, B., Biernat, J., Baumann, K.H., Mandelkow, E.M. and Mandelkow, E. 1995. Domains of tau protein, differential phosphorylation and dynamic instability of microtubules. *Mol. Biol. Cell* **6**: 1887-1902.

Tonge, D.A., Golding, J.P. and Gordon-Weeks, P.R. 1996. Expression of a developmentally regulated, phosphorylated isoform of microtubule-associated protein 1B in sprouting and regenerating axons *in vitro*. *Neurosci.* **73**: 541-551.

Towbin, H., Staehlin, T. and Gordon, J. 1979. Electrophoretic transfer of proteins from polyacrylamide gels to nitrocellulose sheets: procedure and some applications. *Proc. Natl. Acad. Sci. U.S.A.* **76**: 4350-4354.

Tsuyama, S., Branblett, G.T., Huang, K.P. and Flavin, M. 1986. Calcium / phospholipid-dependent kinase recognizes sites in microtubule-associated protein 2 which are phosphorylated in living brain and are not accessible to other kinases. *J. Biol. Chem.* **261**: 4110-4116.

Tucker, R. P., L. I. Binder, and A. I. Matus. 1988a. Neuronal microtubule-associated proteins in the embryonic avian spinal cord. *J. Comp. Neurol.* **271**:44-55.

Tucker, R.P. and Matus, A. 1988b. Microtubule-associated proteins characteristic of embryonic brain are found in the adult mammalian retina. *Dev. Biol.* **130**: 423-434.

Tucker, R.P., Viereck, C. and Matus, A. 1988c. The ontogeny and phylogenetic conservation of MAP2 forms. *Protoplasma* **145**: 195-199.

Ulloa, L., Avila, J. and Díaz-Nido, J. 1993a. Heterogeneity in the phosphorylation of microtubule-associated protein 1B during rat brain development. *J. Neurochem.* **61**: 961-972.

Ulloa, L., Díez-Guerra, F.J., Avila, J. and Díaz-Nido, J. 1993b. Localization of differentially phosphorylated isoforms of microtubule-associated protein 1B in cultured rat hippocampal neurons. *Neurosci.* **61**: 211-223.

Umeyama, T., Okabe, S., Kanai, Y. and Hirokawa, N. 1993. Dynamics of microtubules bundled by microtubule associated protein 2c (MAP2c). *J. Cell Biol.* **120**: 451-465

Vaillant, A.R. and Brown, D.L. 1995. Accumulation of microtubule-associated protein 1A (MAP1a) in differentiating P19 embryonal carcinoma cells. *Biochem. Cell Biol.* **73**: 695-702.

Vale, R.D., Coppin, C.M., Malik, F., Kull, F.J. and Milligan, R.A. 1994. Tubulin GTP hydrolysis influences the structure, mechanical properties and kinesin-driven transport of microtubules. *J. Biol. Chem.* **269**: 23769-23775.

Vallee, R.B. 1982. A taxol-dependent procedure for the isolation of microtubules and microtubule-associated proteins (MAPs). *J. Cell Biol.* **92**: 435-442.

Vallee, R.B. and Davis, S.E. 1983. Low molecular weight microtubule-associated proteins are light chains of microtubule-associated protein 1 (MAP 1). *Proc. Natl. Acad. Sci. U.S.A.* **80**: 1342-1346.

Vandecandelaere, A., Pedrotti, B., Utton, M.A., Calvert, R.A. and Bayley, P.M. 1996. Differences in the regulation of microtubule dynamics by microtubule-associated proteins 1B and MAP2. *Cell Mot. Cytoskel.* **35**: 134-146.

Viereck, C., Tucker, R.P., Binder, L.I. and Matus, A. 1988. Phylogenetic conservation of brain microtubule-associated proteins MAP2 and tau. *Neurosci.* **26**: 893-904.

Viereck, C., Tucker, R.P. and Matus, A. 1989. The adult rat olfactory system expresses microtubule-associated proteins found in the developing brain. *J. Neurosci.* **9**: 3547-3557.

Villasante, A., Wang, D., Dobner, P., Lewis, S.A. and Cowan, N.J. 1986. Six mouse α-tubulin mRNAs encode five distinct isotypes: testis-specific expression of two sister genes. *Mol. Cell Biol.* **6**: 2409-2419.

Voller, A., Bidwell, D.E. and Bartlett, A. 1979. The enzyme-linked immunosorbent assay (ELISA). *Dynatech Laboratories Inc.*, Alexandria, VA.

Wandosell, F., Serrano, L., Hernández, M.A. and Avila, J. 1986. Phosphorylation of tubulin by a calmodulin-dependent protein kinase. *J. Biol. Chem.* **261**: 10332-10339.

Wang, X.M., Peloquin, J.G., Zhai, Y., Bulinski, J.C. and Borisy, G.G. 1996. Removal of MAP4 from microtubles *in vivo* produces no observable phenotype at the cellular level. *J. Cell Biol.* **132**: 345-357.

Wang, Y., Loomis, P.A., Zinkowski, R.P. and Binder, L.I. 1993. A novel tau transcript in cultured human neuroblastoma cells expressing nuclear tau. *J. Cell Biol.* **121**: 257-267.

Webster, D.R., Wehland, J., Weber, L. and Borisy, G.G. 1990. Detyrosination of alpha-tubulin does not stabilize microtubules *in vivo*. *J. Cell Biol.* **111**: 113-122.

Weingarten, M.D., Lockwood, A.H., Hwo, S.Y. and Kirschner, M.W. 1975. A protein factor essential for microtubule assembly. *Proc. Natl. Acad. Sci. U.S.A.* **72**: 1858-1862.

Weisshaar, B., Doll, T. and Matus,A. 1992. Reorganization of the microtubular cytoskeleton by embryonic microtubule-associated protein 2 (MAP2c). *Develop.* **116**: 1151-1161.

Weisshaar, B. and Matus, A. 1993. Microtubule-associated protein 2 and the organization of cellular microtubules. *J. Neurocytol.* **22**: 727-734.

West, R.R., Tenbarge, K.M. and Olmsted, J.B. 1991. A model for microtubule-associated protein 4 structure. Domains defined by comparisons of human, mouse and bovine sequences. *J. Biol. Chem.* **266**: 21886-21896.

Wille, H., E.M. Mandelkow, Dingus, J., Vallee, R.B., Binder, L.I. and Mandelkow, E. 1992. Domain structure and antiparallel dimers of microtubule-associated protein 2 (MAP2). *J. Struct. Biol.* **108**: 49-61.

Wolf, A., Houdayer, M., Chillet, D., de Néchaud, B., and Denoulet, P. 1994. Structure of the polyglutamyl chain of tubulin: occurrence of alpha and gamma

linkages between glutamyl units revealed by monoreactive polyclonal antibodies. *Biol. Cell* **81**: 11-16

Xiang, H. and MacRae, T.H. 1995. Production and utilization of detyrosinated tubulin in developing *Artemia* larvae: Evidence for a tubulin-reactive carboxypeptidase. *Biochem. Cell Biol.* **71**: 673-685.

Yamamoto, H., Fukunaga, K., Tanaka, E. and Miyamoto, E. 1983. Ca2+ - and calmodulin-dependent phosphorylation of microtubule-associated protein 2 and τ factor, and inhibition of microtubule assembly. *J. Neurochem.* **41**: 1119-1125.

Yamamoto, H., Saitoh, Y., Fukunaga, K., Nishimura, H. and Miyamoto, E. 1988. Dephosphorylation of microtubule proteins by brain phosphatases 1 and 2A and its effect on microtubule assembly. *J. Neurochem.* **50**: 1614-1623.

Yamauchi, T. and Fujisawa, H. 1988. Regulation of the interaction of actin filaments with microtubule-associated protein 2 by calmodulin-dependent protein kinase II. *Biochem. Biophys. Acta* **968**: 77-85.

Ye, J., Yang, L., Del Bigio, M.R., Summers, R., Salerno, T.A. and Deslauriers, R. 1995. The effect of circulatory arrest and retrograde cerebral perfusion on microtubule-associated protein 2: an immunohistochemical study in pig hippocampus. *Neurosci. Lett.* **222**: 9-12.

Yin, H.S., Chou, H.C. and Chiu, M.M. 1997. Changes in the microtubule proteins in the developing and transected spinal cords of the bullfrog tadpole: induction of microtubule-associated protein 2c and enhanced levels of tau and tubulin in regenerating axons. *Neurosci.* **67**: 763-775.

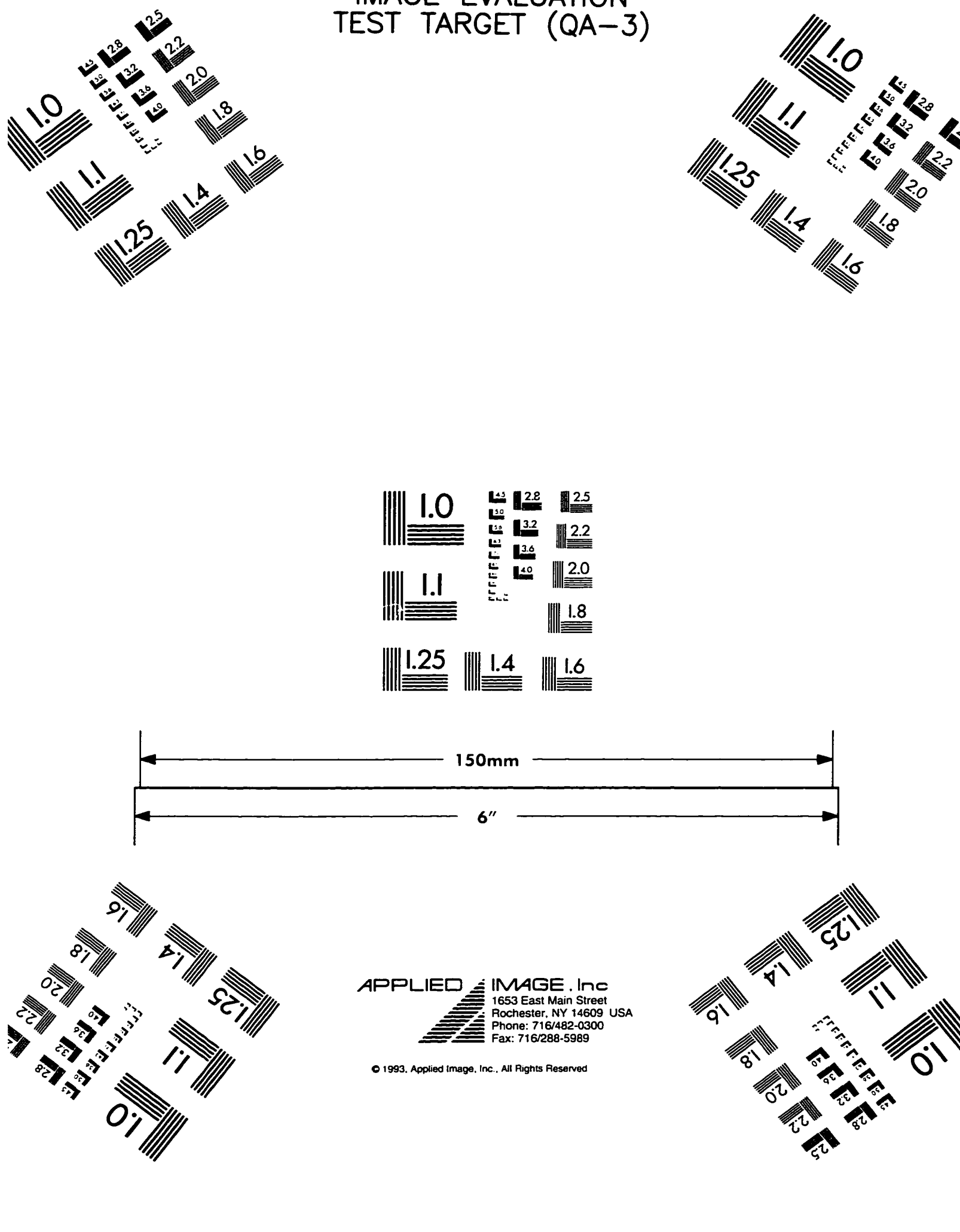
IMAGE EVALUATION
TEST TARGET (QA-3)
1.0
1.1
1.25
1.4
1.6
1.8
2.0
2.2
2.5
2.8
3.2
3.6
4.0
150mm
6"
APPLIED IMAGE, Inc
1653 East Main Street
Rochester, NY 14609 USA
Phone: 716/482-0300
Fax: 716/288-5989
© 1993, Applied Image, Inc., All Rights Reserved